Fall 2010

Corrosion resistance of enamel-coated steel reinforcement for concrete

Charles Robert Werner

CORROSION RESISTANCE OF ENAMEL-COATED STEEL REINFORCEMENT FOR CONCRETE

by

CHARLES ROBERT WERNER

A THESIS

Presented to the Faculty of the Graduate School of the

MISSOURI UNIVERSITY OF SCIENCE AND TECHNOLOGY

In Partial Fulfillment of the Requirements for the Degree

MASTER OF SCIENCE CIVIL ENGINEERING

2010

Approved by

Jeffery S. Volz, Advisor
Richard K. Brow
Genda Chen

ABSTRACT

Originally developed to enhance the bond between concrete and steel, reactive enamel coatings have shown great promise in protecting steel from corrosive environments. However, the corrosion resistance of the material has not yet been tested beyond 40 days. Moreover, when the material was tested, it was applied to smooth steel pins, not deformed steel bars which are commonly used in reinforced concrete structures. Therefore, this study focused on the corrosion resistance of three different enamel coatings, along with a standard epoxy coating, each of which were applied to both smooth and deformed steel bars and included both short-term and long-term test methods.

The three enamel coatings tested within this study were: reactive enamel, pure enamel, and double enamel. The reactive enamel was obtained by combining pure enamel with calcium silicate (cement) at a 1-to-1 ratio by weight. The double enamel was composed of an inner layer of pure enamel and an outer layer of reactive enamel. Each coating was subjected to a modified ASTM B117 salt spray test and a potentiostatic polarization test that followed the Accelerated Corrosion Test (ACT) Method. In addition to these two tests, the corrosion resistance of the reactive enamel coating was also evaluated through a modified AASHTO T-259 ponding test, which included periodic resistivity and half-cell measurements.

Results obtained from the tests revealed that the pure and double enamel coatings provided a superior amount of protection when compared to the 50/50 enamel coating. However, the overall performance of the pure and double enamel coatings was limited by the manufacturing process, which resulted in significant variations in coating thickness.

ACKNOWLEDGMENTS

First and foremost, I would like to thank my advisor, Dr. Jeffery S. Volz, for the time and effort in which he has spent in making this research endeavor as successful as it is today. Without his charismatic personality, unending patience, and expressed appreciation for the work that I have done, I sincerely believe that my time spent here at Missouri S&T would not have been as enjoyable as it was. I am thankful for the care and respect in which he has shown me throughout the time we have spent working together. I will always look upon him as being a great mentor and friend.

I would like to thank the Missouri Department of Transportation and the National University Transportation Center for financially supporting me, along with this project, throughout the past two years. I would also like to thank Michael Koenigstein for his hard work and dedication in supplying me with the necessary specimens that were required in order to complete this study.

I would like to thank the members of my committee, Dr. Genda Chen and Dr. Richard Brow, for their guidance and the time in which they had spent reviewing my thesis.

I would like to thank Dr. Matt O'Keefe, Dr. Signo Reis, Dr. William Pinc, Dr. Elizabeth Kulp, Simon Joshi, and Clarissa Wisner, for without them, a significant portion of this project may not have been possible.

I would like to thank Jason Cox, John Bullock, Benjamin Gliha, Angela Watts, Trevor Looney, Michael Lusher, Steve Gabel, and Dave Satterfield for their assistance in constructing, testing, and maintaining my test specimens when I was unable to do so. I would also like to thank Karen White for looking out for my academic well-being.

Last but not least, I would like to thank my parents, Carol and Charles, sisters, Devon, Brooke, and Brittany, and grandmothers Quinta and Margaret for the love and care they have shown me throughout my life, including that of which was shown by my dear friend Winston, who I greatly miss and will never forget.

Charles R. Werner

TABLE OF CONTENTS

LIST OF ILLUSTRATIONS

LIST OF TABLES

1 INTRODUCTION

1.1 BACKGROUND, PROBLEM, & JUSTIFICATION

During the 1960's, a majority of the state highway agencies began to practice "bare road policy." The policy involved the application of deicing salts upon state roads during the winter months. As a result, a large portion of reinforced concrete bridges began to show signs of deterioration, in the form of corrosion and spalling, within seven to ten years after the states had adopted the policy, which is still in practice today [Zemajtis et al., 1996].

According to the national bridge inventory, more than half of the registered bridges within the United States (U.S.) are made of reinforced concrete, most of which are susceptible to chloride induced corrosion [Hartt et al., 2004]. In 2001, a Federal Highway Administration (FHWA) sponsored study predicted that the U.S. will spend an estimated 8.3 billion dollars annually over the next ten years in an effort to repair or replace bridges exhibiting corrosion-related damage. Furthermore, the indirect costs associated with the repair or replacement of corroding bridges will amount to approximately ten times the direct costs [Koch et al., 2001].

Over the past 40 years, the FHWA, along with other state highway agencies, began to sponsor investigative studies into the development and evaluation of newly formulated, corrosion resistant, steel reinforcing bars in the hope of reducing the federal and state expenditures on bridge repair. Through these government funded studies, three well known types of corrosion resistant steel reinforcing bars have evolved. They are as follows: epoxy-coated rebar (ECR), galvanized steel rebar, and stainless steel rebar.

1.1.1 Epoxy-Coated Reinforcement. Originally developed in the 1970's, ECR is the most commonly used method in North America of protecting reinforced concrete structures and pavements from corrosive elements. Laboratorial studies have shown that the epoxy coating can provide exceptional corrosion protection to steel reinforcement by acting as a physical barrier that separates the underlying steel from corrosive environments. However, in the late 1980's, field surveys conducted by the Florida Department of Transportation (FDOT) discovered that ECR embedded within the substructure of several relatively new marine bridges had begun to exhibit signs of

corrosion. These discoveries lead to an extensive amount of government funded investigative studies, which were aimed at evaluating the condition of ECR embedded in concrete structures and pavements throughout the country [Broomfield, 2007].

By the mid 1990's, a consensus was formed about the field performance of damaged epoxy-coating reinforcement as a result of the information gathered from these investigative studies and further laboratorial experiments. The consensus was that when the coating is damaged, and ECR is continuously saturated with water, a loss in adhesion between the coating and the steel substrate will occur. As a result, the steel beneath the coating is no longer protected from corrosive elements, for the elements are now able to travel along the epoxy-steel interface. Although this consensus does exist, the significance of this phenomenon, in terms of the degree to which it affects the epoxy's ability of providing long-term corrosion protect, has not yet been fully established [Sohanghpurwaia, 2005].

1.1.2 Galvanized Steel Reinforcement. During the early 1980's, a FHWA sponsored study evaluating the corrosion performance of galvanized steel reinforcement was conducted by David Manning, Ed Escalante, and David Whiting in an effort to confirm whether or not the material was superior to ECR. The results obtained from the study suggested that galvanized steel was inferior to ECR. This conclusion was further supported by an additional study conducted in the 1990's. However, after a recent re-evaluation of the material's performance throughout the previous three decades, Stephen R. Yeomans concluded that galvanized steel reinforcement may be more effective in combating the degradation of steel than what was originally asserted [Broomfield, 2007].

Unlike ECR, defects or breaks within the protective zinc coating will not reduce the corrosion performance of galvanized steel reinforcement to any great degree, for the zinc surrounding the defect will sacrificially corrode prior to the degradation of the underlying steel. Because of this property, a great deal of attention must be paid when using both uncoated (bare) steel rebar and galvanized steel rebar within a structure, for an accelerated depletion of a galvanized steel bar's zinc coating may occur when it comes into contact with an uncoated steel bar. This coupling affect would lead to a significant reduction in the long term corrosion performance of galvanized steel rebar [Broomfield, 2007].

1.1.3 Stainless Steel Reinforcement. A structure reinforced with stainless steel is estimated to have a service life that is considerably longer than that of a structure containing either ECR or galvanized steel reinforcement. The one major drawback in stainless steel reinforcement is the price. In an attempt to reduce the price, while maintaining a large portion of its corrosion resistance, the stainless steel industry developed stainless steel clad reinforcement. However, the price of stainless steel clad reinforcement is still more than twice that of ECR or galvanized steel reinforcement [Koch et al., 2001].

With regard to its performance, pitting has been known to form along stainless steel reinforcement when improper grades of stainless steel are used. Therefore, steps should be taken in order to assure that either a pure or clad stainless steel rebar consists of the proper grade. Similar to galvanized steel reinforcement, when placing stainless steel reinforcement within a structure that also possesses uncoated reinforcement, preventative measures should be in place to avoid contact between stainless and non-stainless steel bars. If a stainless steel bar comes into contact with an uncoated steel bar, the uncoated steel bar may corrode in an accelerated fashion [Broomfield, 2007].

1.1.4 Enamel-Coated Reinforcement. Recent studies conducted by the U.S. Army Corps of Engineers have shown that a newly developed enamel composition holds great promise in protecting concrete reinforcing steel from corrosive environments. The newly developed enamel incorporates calcium silicate particles that are dispersed throughout the coating's thickness, with a portion of the particles partially exposed along the coating's exterior surface. The coating is referred to as "reactive enamel" due to the chemical reaction that occurs shortly after the enamel has been placed within freshly batched concrete.

Exposed calcium silicate particles along the surface of the enamel react with available water molecules within concrete to form a dense layer of calcium silicate hydrate (CSH). As a result of this reaction, the bond between the concrete and the embedded reinforcement increases while the permeability of the coating-concrete interface subsequently decreases and further protects the reinforcement from corrosive elements. Testing has also shown that cement particles embedded within the reactive enamel are capable of sealing cracks within the coating when presented with a sufficient

amount of moisture. This showed that not only does the reactive enamel protect the steel from corrosion, but that it also has the ability to heal itself when slightly damaged [Weiss, 2009].

Although the reactive enamel has already been subjected to several investigative studies conducted by the U.S. Army Corps of Engineers, a large portion of their studies have focused upon the bonding aspect of the reactive enamel as opposed to the corrosion performance of the material. Moreover, when they did conduct tests that were specifically focused upon the evaluation of the material's corrosion resistance, the tests were short term (less than two months) and the coating was often applied to smooth steel pins, not deformed steel bars which are commonly used in reinforced concrete structures.

1.2 OBJECTIVES & SCOPE OF WORK

The main objective of this study is to characterize the relative corrosion resistance of three enamel coatings that have been applied to both smooth and deformed steel reinforcing bars through a non-electrostatic dipping process.

The following scope of work was implemented in an effort to attain this objective: (1) review applicable literature; (2) develop a research plan; (3) evaluate the relative corrosion performance of the newly developed reactive enamel coating when embedded within a highly alkaline environment through designing, constructing, and monitoring of several reinforced concrete ponding specimens; (4) evaluate the relative corrosion performance of the three enamel coatings when placed within a humid, sodium chloride (NaCl) contaminated environment with an elevated air temperature; (5) quantify each coating's overall ability to postpone the onset of corrosion when placed within a corrosion cell; (6) conduct a forensic investigation upon the reinforced concrete ponding specimens; (7) analyze the information gathered throughout the testing to develop findings, conclusions, and recommendations; and (8) prepare this thesis in order to document the information obtained during the study.

1.3 RESEARCH PLAN

The research plan entailed monitoring the corrosion performance of the three enamel coatings that were applied to both smooth and deformed steel bars through a non-

electrostatic dipping process, as described in Section 2.3.2. The three enamel coatings that were under evaluation were referred to as: pure enamel, 50/50 enamel and double enamel. The pure enamel coating was composed of a single, alkali resistant, enamel coating. The 50/50 enamel coating, on the other hand, consisted of a single coat that was composed of 50 percent pure enamel and 50 percent calcium silicate (or cement) by weight. Production of the 50/50 enamel was the same as that of the pure enamel except for the addition of the calcium silicate, which was added to the enamel slurry prior to the dipping process. A two-coat, two-fire process was used in the development of the double enamel coating. The first coat (or ground coat) of the double enamel coating consisted of pure enamel, while the second coat (or cover coat) consisted of the 50/50 enamel. Preparation of the steel surface followed that of conventional enameling techniques, as did the firing process. Further information about these techniques and procedures may be found in Section 2.3.2

Ponding specimens were constructed to evaluate the corrosion resistance of the 50/50 enamel coating within a cementitious environment. As a baseline for comparison, both uncoated and epoxy-coated steel reinforcement were also tested. The test consisted of subjecting a total of 25 ponding specimens to a continuous two week wet / one week dry cycle, for a period of 54 weeks. Concrete resistivity and half-cell potential readings were carried out every 6 weeks over the course of the testing period. Upon completion of the test, each reinforced specimen was then forensically evaluated.

A salt spray test was used to rapidly assess the relative corrosion performance of the three enamel coatings along with a standard epoxy coating. The test consisted of subjecting a total of 64 specimens to a series of wet/dry cycles for a period of twelve weeks. After testing, the uniformity of each coating, as well as the steel-coating bond along both the deformed and smooth bars, was evaluated through visual and microscopic cross-sectional examination.

The accelerated corrosion test (ACT) method was used to quantify the overall ability of each enamel coating, along with the standard epoxy coating, to resist the onset of corrosion. The test consisted of placing a specimen within a corrosion cell that contained a NaCl solution. A specimen consisted of a single segment of coated or uncoated steel reinforcement that was either grouted or non-grouted. While situated

within the corrosion cell, a constant potential was applied to the specimen and the resulting current was measured over time. The test was completed upon the onset of intense corrosion, which is detected by an abrupt increase in the monitored electric current. In general, these tests run between 300 and 1500 hours, not including sample preparation.

The benefit of the ACT is that the applied potential will force the chloride ions to attack the coated rebar. This test will thus expose any material or processing defects in the coating that would allow the transport of chloride ions to the steel surface and allow initiation of corrosion. The test will also partially determine whether the enamel coating has the ability to heal itself through hydration of the embedded calcium-silicate.

1.4 OUTLINE

This thesis consists of six sections and three appendices. Section 1 briefly explains the costs associated with deteriorating U.S. bridges, metallic and non-metallic coatings used to protect steel reinforcement from corrosive environments, the study's objective, and the manner in which the objective was attained.

Section 2 summarizes the process by which steel corrodes within concrete, methods that are commonly used to evaluate the condition of the steel embedded in concrete, the background associated with both epoxy-coated reinforcement and enameled steel, and tests that may be used to evaluate the corrosion resistance of either a cementitious material or protective steel coating.

Sections 3 through 5 pertain to the ponding test, salt spray test, and accelerated corrosion test, respectively. Each section contains a section that describes the test's layout, procedure, results, and findings.

Section 6 restates the findings that were established during the course of the study, which inevitably lead to the conclusions and recommendations presented therein.

There are three appendices, with one for each of the three test methods. Appendix A contains additional information, test data, and photographs associated with the ponding test. Appendix B contains a series of photographs along with a drawing that is associated with the salt spray test. Appendix C contains all test data that is associated with the accelerated corrosion test.

2 LITERATURE REVIEW

When unprotected and exposed to atmospheric conditions, steel will corrode. Steel corrodes under these conditions, for as a material, steel is unstable due to the process in which it is made. Processing steel requires large amounts of energy in order to extract iron from ore. In doing so, the iron is placed within an elevated energy state that results in the material being unstable when stored within an atmospheric condition [Carino, 1999]. The iron will react naturally with its surrounding environment to reach a lower, more stable, energy state such as iron oxide or rust [Smith, 1977]. In an effort to prevent this reaction from occurring, protective epoxy and enamel coatings are commonly applied to steel. Indirectly, steel is also protected from corrosion when placed within concrete.

2.1 CORROSION OF STEEL IN CONCRETE

When embedded in concrete, steel reinforcement is protected from corrosion by a dense impermeable film known as a "passive" layer. The "passive" layer is developed and maintained in highly alkali environments, such as concrete. Concrete is an alkaline material, for it possesses high concentrations of hydroxides within its pore solution. The hydroxides are produced when the high concentrations of soluble calcium, sodium, and potassium oxides, contained within the concrete, interact with water. The passive layer is thought to be a combination of metal oxide/hydroxide and minerals that are present within portland cement [Broomfield, 2007]. Although the passive layer is impenetrable, it is still susceptible to damage, which can lead to corrosion of the underlying steel. Destruction of the passive layer occurs when a sufficient amount of chlorides accumulate at the steel-concrete interface and/or when the concrete at a depth equal to that of the embedded steel becomes carbonated.

2.1.1 Carbonation. Carbonation is the reaction between carbonic acid (H_2CO_3) and the hydroxides (OH^-) contained in concrete pore solution. Carbonic acid is formed when a front of carbon dioxide gas (CO_2) diffuses through concrete and dissolves within its pore solution:

$$CO_2 + H_2O \rightarrow H_2CO_3 \quad (1)$$

The diffusion of carbon dioxide through concrete closely follows Fick's first law of diffusion and can be approximated by:

$$\frac{dx}{dt} = \frac{D_o}{x} \quad (2)$$

where x is the distance to the surface, t is time, and D_o is a diffusion coefficient that accounts for the quality of the concrete [Broomfield, 2007]. Once created, carbonic acid then reacts with the available calcium hydroxide ($Ca(OH)_2$) within the pore solution to form calcium carbonate ($CaCO_3$):

$$H_2CO_3 + Ca(OH)_2 \rightarrow CaCO_3 + 2H_2O \quad (3)$$

This reaction subsequently reduces the pH of the pore solution, which is typically between 12 and 13. In an attempt to combat this reduction in pH, additional calcium hydroxide within the concrete dissolves into the surrounding pore solution. However, only a limited amount of calcium hydroxide is contained within concrete and with time the pH will eventually fall to a value where the passive layer can no longer be sustained. With the passive layer unable to sustain itself, the underlying steel is then susceptible to corrosion.

2.1.2 Chloride Attack. Chlorides are most commonly introduced to concrete through external sources, such as seawater and deicing salts. However, at times chlorides may intentionally be added to a concrete mixture through the use of seawater and/or calcium chloride ($CaCl_2$), a chemical admixture used to accelerate the hydration of portland cement. A large portion of the chlorides that are intentionally added to a batch of concrete will react with tricalcium aluminate ($Ca_3Al_2O_6$ or C_3A), a compound within portland cement, to form chloroaluminates. This reaction removes chloride ions from the concrete's pore solution that would have otherwise been able to contribute towards the destruction of the passive layer. However, carbonation of concrete is known to break

down these chloroaluminates, which in turn releases the bound chlorides into the concrete's pore solution [Broomfield, 2007]. Now the chlorides, which were once bound, are free to diffuse through the concrete and attack the passive layer, similarly to the chlorides that were externally introduced to the concrete.

Transport of externally generated chlorides through concrete is commonly carried out by three specific mechanisms. Those three mechanisms are: absorption/capillary action, permeation, and diffusion. When saltwater is placed upon dry concrete, the chlorides within the water are immediately transported several millimeters below the concrete's surface by way of absorption. If an accumulation of water is present upon the surface of the concrete the chlorides may then permeate further into the concrete due to hydraulic pressure. When a chloride gradient exists within the concrete and pore solution is present, chloride ions may then diffuse through the concrete following Fick's second law of diffusion, which is represented by Broomfield (2007) as:

$$\frac{C_{max} - C_d}{C_{max} - C_{min}} = \text{erf}\left(\frac{x}{\sqrt{4D_c t}}\right) \tag{4}$$

where variables within the error function (erf) correspond to the depth of C_d (x), time (t), and the diffusion coefficient of chlorides in concrete (D_c). Variables C_{max} and C_{min} relate to the maximum and baseline chloride concentrations within the concrete, respectively. Variable C_d corresponds to the chloride concentration within the concrete at a certain distance (x) from the surface.

Chloride attack begins when unbounded chloride ions reach the passive layer of an embedded bar and promote the release of ferrous (Fe^{2+}) ions by forming an iron-chloride complex ($FeCl_2$):

$$Fe^{2+} + 2Cl^- \rightarrow (FeCl_2) \tag{5}$$

As the complex migrates away from the steel, it reacts with water (H_2O) molecules contained in the concrete's pores:

$$(FeCl_2) + 2H_2O \rightarrow Fe(OH)_2 + 2H^+ + 2Cl^- \quad (6)$$

Ferrous hydroxides ($Fe(OH)_2$) are formed during this reaction along with hydrogen (H^+) ions that locally reduce the pH of the pore solution surrounding the embedded bar, aiding in the destruction of the passive layer [Song et al., 2010]. The chloride ions that are responsible for the initiation of this reaction are then released back into the pore solution. Now free within the pore solution, the chloride ions are available to return to the steel where the two, chemical reactions (equations 5 and 6) may once again be carried out. However, as researched by Delbert A. Hausmann [Hausmann, 1967], the hydroxide ions within the concrete continually counteract the chlorides' attempt in the destruction of a passive layer.

Through mathematical calculations and laboratorial experiments involving bare steel bars contained in a simulated porous, chloride contaminated, concrete environment, Hausmann discovered that the chlorides' success in breaking down a passive layer depended upon the ratio of chloride ions to hydroxide ions at the steel-concrete interface. He concluded that the ratio of chloride ions to hydroxide ion had to be greater than 0.6 in order for the bar to actively corrode. This ratio corresponds to 0.4 percent chlorides by weight of cement when the chlorides are cast into the concrete during batching. This percentage decreases by 50 percent when the chlorides are introduced to the concrete through external sources [Broomfield, 2007].

2.1.3 Corrosion Process. Once an embedded steel bar's passive layer has been damaged, the bar is susceptible to corrosion. The actual degradation of a bar takes place at an area known as the anode. At this location ferrous ions are released into the surrounding concrete while the two electrons ($2e^-$) generated during this reaction are consumed elsewhere.

$$Fe \rightarrow Fe^{2+} + 2e^- \quad (7)$$

The site at which the electrons are consumed is known as the cathode. The cathode utilizes the electrons, along with water and oxygen (O_2), to create hydroxyl ions (OH^-):

$$2e^- + H_2O + \frac{1}{2}O_2 \rightarrow 2OH^- \quad (8)$$

Once formed, the hydroxyl ions flow through the concrete, back to a location near the anode, to react with the ferrous ions and initiate the formation of rust. When in contact with one another, the ferrous and hydroxyl ions react to form ferrous hydroxide ($Fe(OH)_2$):

$$Fe^{2+} + 2OH^- \rightarrow Fe(OH)_2 \quad (9)$$

Two additional reactions are required before the commonly seen red rust is created. First, the newly formed ferrous hydroxide reacts with water and oxygen to form ferric hydroxide ($Fe(OH)_3$):

$$4Fe(OH)_2 + O_2 + 2H_2O \rightarrow 4Fe(OH)_3 \quad (10)$$

The ferric hydroxide then reconfigures itself into hydrated ferric oxide ($Fe_2O_3 \bullet H_2O$ or red rust) while water molecules are formed:

$$2Fe(OH)_3 \rightarrow Fe_2O_3 \cdot H_2O + 2H_2O \quad (11)$$

Hydrated ferric oxide is known to have a volume that is typically six times that of the iron which it replaces [Broomfield, 2007]. The volume relationship between iron and other various forms of its oxides may be seen in Figure 2.1.

Due to this increase in volume at the steel-concrete interface, tensile stresses will form within the concrete and cracks will begin to appear along the surface of the structure. In some cases, spalling of the concrete may be observed. At times black rust (Fe_3O_4) may form instead of the typical red rust and as a result no visual signs of cracking may be seen along the concrete surface. This is due to the fact that black rust is less expansive than red rust, as shown in Figure 2.1.

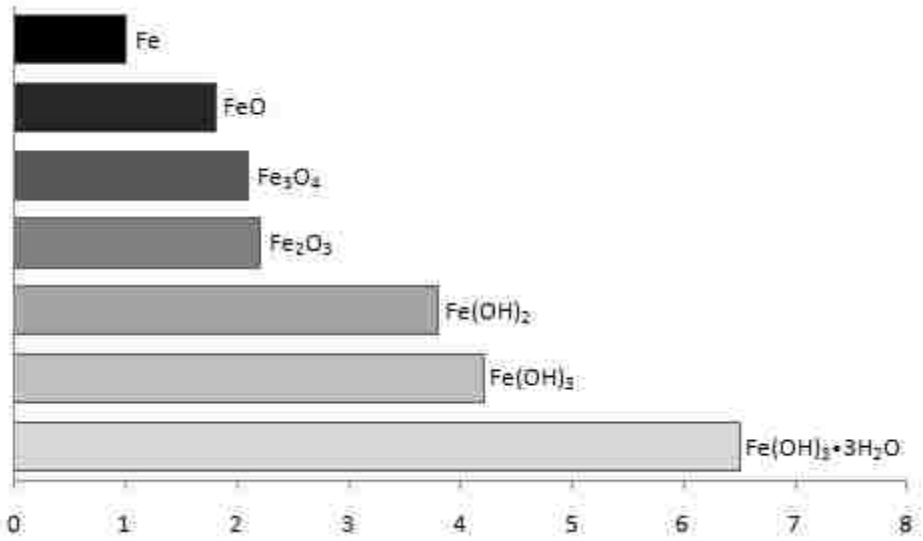

Figure 2.1: Volumes of various iron oxides relative to iron [Broomfield, 2007].

Black rust is developed when the anode becomes deprived of oxygen and the cathode, which is required in order for the corrosion process to proceed, is located several inches away from the anode [Broomfield, 2007]. A lack of oxygen within the concrete may be caused by damaged waterproofing membranes placed along the surface of the concrete. Black rust may also appear along steel bars embedded within marine structures that happen to be continuously saturated.

A steel bar embedded within a moist, chloride contaminated, concrete environment, may also be susceptible to macrocell corrosion. Macrocell corrosion is represented by a small anode, one or two inches in length, that is supported by a large cathode of several feet in size [Broomfield, 2007]. Macrocell corrosion is commonly seen within moist, chloride contaminated concrete, where together the two conditions create an electrolyte that is capable of reducing the electrical resistance of the concrete surrounding the embedded bar. A concrete with a lower resistance allows for further and faster transport of hydroxyl ions from the cathode to the anode.

2.2 CONDITION EVALUATION

This section addresses three procedures that are commonly used to evaluate the corrosion condition of steel embedded in concrete. Factors capable of affecting the results and/or interpretation of each test are also discussed within this section.

2.2.1 Concrete Resistivity. A concrete's electrical resistance may be measured in an attempt to quantify the rate at which a bare, depassivated steel bar, embedded within the concrete, corrodes. As mentioned in the previous section, the corrosion process is dependent upon the ability of charged ions, such as hydroxyl ions (OH^-), to flow from the cathode to the anode. The quicker the ions can flow from the cathode to the anode, the quicker the corrosion process may proceed, provided that the cathode is supplied with a sufficient amount of oxygen and water. The transport of electricity through concrete closely resembles that of ionic current, therefore it is possible to classify the rate of corrosion of a bar embedded within concrete by quantifying the electrical resistance of the concrete surrounding it [Whiting and Nagi, 2003].

Currently, concrete resistivity measurement may be carried out in the field using one of three methods: single-electrode method, two-probe method, or the four-probe method. Of the three methods, the two-probe is the least accurate and at times the most labor intensive [Broomfield, 2007]. The inaccuracy of the two-probe method may be due to the manner in which the equipment operates. The two-probe resistivity meter operates by measuring the potential between two electrodes while an alternating current is passed from one electrode to the other. Error within a measurement can develop when one of the two probes is placed directly over a piece of coarse aggregate. It has been stated that the two-probe resistivity meter only measures an area of the concrete, surrounding the electrode, that is equal to ten times that of the contact area between the electrode and the concrete [Whiting and Nagi, 2003]. With a typical aggregate having a resistance that is 100 times that of cement paste, inaccurate resistivity values can be reported. In an attempt to achieve a more accurate reading, the two electrodes may be placed within shallow pre-drilled holes [Broomfield, 2007], making the two-probe method more labor intensive.

The single-electrode method is a newer, more advanced method in measuring a concrete's resistivity. The single-electrode incorporates the steel reinforcing cage within

the concrete as one electrode while a portable, second electrode (or "single" electrode), is placed along the concrete surface. This method specifically measures the resistance of the concrete cover by applying the following equation:

$$\text{Resistivity } (\Omega\,\text{cm}) = 2RD \tag{12}$$

where R is the iR drop between the rebar cage and the surface electrode and D is the diameter of the surface electrode. This method is susceptible to contact resistance problems and is most accurate when the surface electrode is placed between embedded bars as opposed to directly over them [Broomfield, 2007].

Originally developed in 1916 by Frank Wenner, the four-probe method was initially designed for geophysical studies. The method was later adopted for the evaluation of concrete by Richard Stratfull in 1957 during a field investigation of San Francisco's San Mateo-Hayward Bridge [Sengul and Gjørv, 2009]. Today the four-probe method (or Wenner method) is the most widely used and researched method for in-situ evaluation of concrete resistivity.

The four probe resistivity meter, also known as the Wenner probe, contains four equally spaced electrodes that are positioned along a straight line. The two outer electrodes send an alternating current through the concrete while the inner electrodes measure the drop in potential. The resistivity is then calculated using the following equation:

$$\rho = \frac{2\pi sV}{I} \tag{13}$$

where ρ is the resistivity (Ωcm) of the concrete, s is the spacing of the electrodes (cm), V is the recorded voltage (V), and I is the applied current (A).

As the applied current passes through the concrete it travels in a hemispherical pattern as shown in Figure 2.2. The depth at which the current travels within the concrete is a function of the electrode spacing. The further apart the electrodes are spaced, the deeper the applied current travels [Sengul and Gjørv, 2009]. Therefore, the distance at

which the electrodes are spaced becomes crucial when acquiring an accurate resistivity value for concrete. This is especially true when evaluating thin and/or reinforced concrete members.

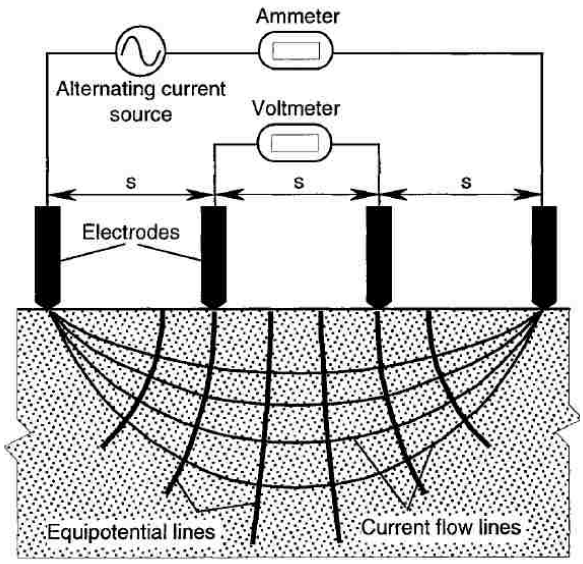

Figure 2.2: Schematic representation of the four-probe resistivity method.

Research has shown that when a Wenner probe's electrodes are spaced at a distance greater than that of the concrete cover, a reduction in the concrete's resistivity may be reported. This is attributed to a "short circuiting" effect which occurs when the applied current reaches a depth equal to that of the reinforcement. This effect is commonly seen when readings are taken parallel and directly over the embedded steel. It is therefore recommended that measurements should be taken perpendicular to the direction of the reinforcement when interference with the steel cannot be avoided [Broomfield, 2007].

A study, conducted by Sengul and Gjørv (2009), found that an electrode spacing to cover ratio equal to 0.6 provided an accurate reading even if the Wenner Probe was positioned parallel and directly above an embedded bar. However, as the electrode

spacing to cover ratio increased beyond 0.6, a decrease in the concrete's resistance was reported. When the Wenner probe was placed perpendicular to the embedded bar and the electrode spacing to cover ratio varied in values greater than 0.6, a slight increase in the concrete's resistivity was observed. The researchers also examined the so-called "boundary affect," which is caused when resistivity readings are conducted near the edge of a specimen or when the electrode spacing to specimen thickness ratio exceeds a certain value.

The "boundary affect" has been known to increase the reported resistivity of a concrete, since the resistivity values gathered from using a four-probe resistivity meter are calculated using equation (13), which assumes the readings were conducted upon a semi-infinite volume of material. However, this assumption is not true when the Wenner probe approaches an edge of a specimen, for the flow of current through the concrete becomes constricted and subsequently an increase in resistivity is reported. Therefore, it has been recommended that the electrode spacing along a probe should be less than or equal to ¼ of the minimum dimension of the specimen [Whiting and Nagi, 2003]. Sengul and Gjørv further confirmed this recommendation through their previously mention study. Nonetheless, if the electrode spacing becomes too small an inaccurate resistivity value may be reported as well.

With concrete being a non-homogeneous material, it has been recommended that the electrode spacing to maximum aggregate size ratio be greater than or equal to 1½ in order to obtain a representative value for a concrete's resistivity. A ratio less than 1½ can result in the test being influenced by a piece of coarse aggregate, which would lead to a highly inaccurate concrete resistivity value. As stated earlier, coarse aggregate that is commonly used and accepted in current practice is known to have an electrical resistance that is greater than 100 times that of a typical portland cement paste [Whiting and Nagi, 2003].

Electrical resistivity of concrete is also highly dependent upon the quality and quantity of its paste. The more paste a concrete has, the easier it is for charged ions to bypass the more impermeable aggregate. The permeability of a concrete's paste is greatly dependent upon the water-to-cement ratio used during the batching process. As a concrete's water-to-cement ratio decreases so does its porosity. This decrease in porosity

reduces the ease to which charged ions may travel through the paste and in turn increases the overall resistivity of a concrete. In fact, a study found that when a concrete's water-to-cement ratio increased from 0.40 to 0.55, its resistivity decreased by 50 percent [Whiting and Nagi, 2003].

In 1987, Langford and Broomfield first published a relationship between the corrosion rate for a depassivated steel bar embedded within a concrete of known resistivity, as may be seen in Table 2.1. Since then Broomfield further claimed that a concrete resistivity greater than 100 kΩcm will essentially prevent any steel reinforcement from corroding [Broomfield, 2007]. The information gathered by Richard Stratfull, during his 1957 field investigation of San Francisco's San Mateo-Hayward Bridge, was compared alongside additional information that was collected while monitoring the bridge after his initial study. The results showed that areas along the structure which reported resistivity values between 50 and 70 kΩcm possessed reinforcement that was corroding at a very low (almost negligible) rate [Sengul and Gjørv, 2009]. Today, Table 2.1 has been widely accepted as a quick and approximate way to correlate the rate at which a depassivated steel bar corrodes in a concrete of known resistivity.

2.2.2 Corrosion Potential Measurements. As was stated earlier, the corrosion process is dependent upon the ability of steel to dissolve into the surrounding concrete along with the availability of oxygen and water at the steel-concrete interface. When these criteria are met, the anodic and cathodic reactions may proceed. In electrochemistry, each of the two reactions are said form a single half-cell. When the two half-cells are connected by an electrical conductor (steel) and a semi-permeable membrane (concrete), a corrosion cell is formed, where electrical and ionic current is transferred from one half-cell to the other. The flow of electrons from one half-cell to the other is an indication of the cell corrosion potential, or the susceptibility of the anodic reaction to occur. Therefore, by measuring the corrosion potential of a steel bar embedded within concrete, its risk of dissolving into the surround concrete (or corroding) may be assessed.

Table 2.1: Correlation between concrete resistivity and the rate of corrosion for a depassivated steel bar embedded within the concrete [Broomfield, 2007].

Concrete Resistivity	Rate of Corrosion
> 20 kΩcm	Low
10-20 kΩcm	Low to Moderate
5-10 kΩcm	High
< 5 kΩcm	Very High

The corrosion potential of a bare steel bar embedded in concrete may be measured using an external half-cell (or reference electrode) and a high impedance voltmeter (≥10 MΩ). A typical reference electrode consists of a metal rod submerged within a known concentrated solution of its own ions. Commonly used electrodes are made of metal having a higher nobility than that of steel; such as, copper, silver, and platinum. Therefore, when a reference electrode is connected to an embedded steel bar using a high impedance voltmeter, along with a series of wires (as shown in Figure 2.3), the reference electrode becomes the half-cell where the cathodic (or reduction) reaction occurs, while the embedded steel bar becomes the half-cell where the anodic (or oxidation) reaction occurs. Connection of the two half-cells is completed when the reference electrode, which contains a semi-permeable membrane in the form of a porous plug/sponge along its end, comes into contact with the concrete surface directly above the embedded bar. Now with an established corrosion cell, the ferrous ions may be released into the concrete, while the electrons created during the reaction are free to travel to the reference electrode (via wiring) where a reduction reaction may occur.

As electrons travel from the steel to the reference electrode, a voltage is read by the voltmeter. According to Broomfield (2007), if the section of steel beneath a copper/copper sulphate electrode (CSE) is still protected by the passive layer, a voltage reading above -200 mV will be displayed. If the passive layer is damaged or has begun to breakdown, a voltage reading between -200 mV and -350 mV will be observed. A voltage reading below -350 mV corresponds to a depassivated steel bar that is actively

corroding within the concrete [Broomfield, 2007]. Through field and laboratory studies conducted in the 1970's, an empirical relationship between a bar's potential (mV) and its risk of corrosion was developed and is shown in Table 2.2. However, care should be taken when interpreting results, for the correlation between a bar's true corrosion risk and that of its potential may not necessarily agree with the relationship shown in Table 2.2. This may be due to a number of factors such as, but not limited to: oxygen concentration, carbonation/concrete resistance, and protective steel coatings [Gu and Beaudoin, 1998].

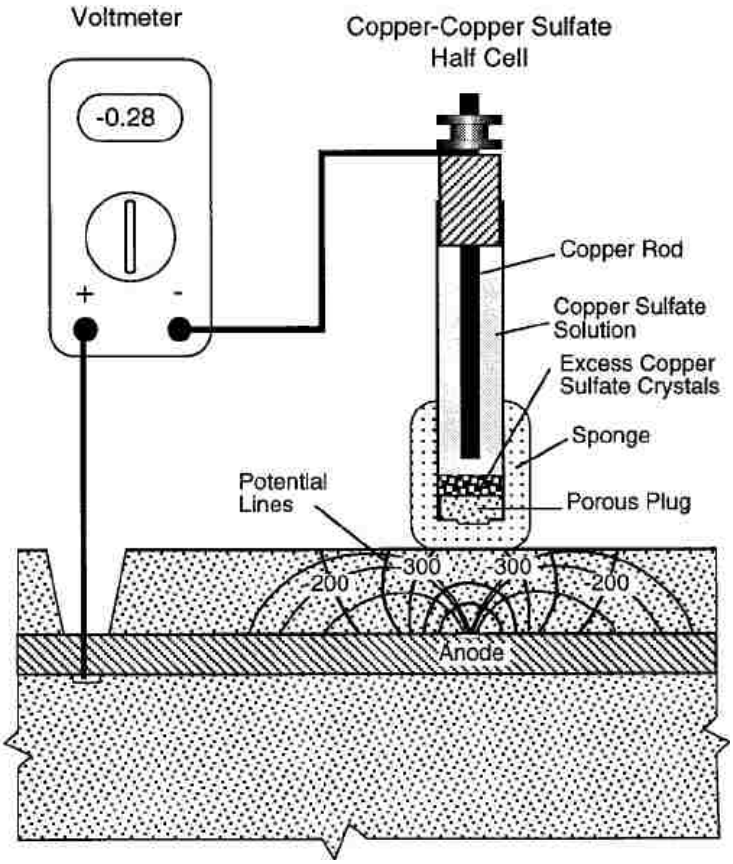

Figure 2.3: Schematic representation of the equipment and procedure used when conducting a half-cell potential measurement.

Table 2.2: Correlation between the corrosion potential of a steel bar embedded within concrete and risk of corrosion [Broomfield, 2007].

Potential (CSE)	**Corrosion Risk**
> -200 mV	Low (< 10%)
-200 to -350 mV	Intermediate
-350 to -500 mV	High (> 90%)
< -500 mV	Severe

A steel bar placed within an environment lacking in oxygen is capable of generating highly negative potentials that may reach beyond -350 mV. According to Table 2.2, this low potential corresponds to a 90 percent probability that the steel is corroding. However, with a lack of oxygen, the cathodic reaction may not be established. Therefore, although a bar may report a highly negative potential, without oxygen (or the cathodic reaction) the corrosion process may not proceed.

When conducting corrosion potential readings upon bars embedded within carbonated concrete, a bar's reported potential may be more positive than its actual value. A more positive potential value may be attributed to the dry nature of carbonated concrete as well as the formation of calcium carbonate within the concrete's pore structure. These two factors are known to increase a concrete's resistance , which in turn increases (more positive) a bar's reported potential as may be seen within the following equation:

$$V_{measured} = V_{actual} \times \frac{\Omega_{voltmeter}}{\Omega_{voltmeter} + \Omega_{concrete}} \quad (14)$$

where $V_{measured}$ is the reported potential of the bar, V_{actual} is the actual potential of the bar, $\Omega_{voltmeter}$ is the resistance of the voltmeter, and $\Omega_{concrete}$ is the resistance of the concrete. Dry carbonated concrete also causes a bar to corrode in a uniform fashion, where the anodic (active) and cathodic (non-active) areas along the bar are closely

spaced. Therefore, the potential of a uniformly corroded bar tends to be more positive, due to the averaging of the active and non-active sites along the bar.

Galvanized steel bars, commonly coated with zinc, are known to report potentials greater than that of uncoated steel bars [Broomfield, 2007]. This is due to the fact that zinc is lower in the galvanic series than steel and as a result a greater potential is created when connected to a more noble metal, such as copper. Therefore, Table 2.2 may be of no use when interpreting potential measurements gathered from testing galvanized steel bars. The effectiveness of conducting potential measurements upon epoxy-coated steel bars has also been questioned, mostly due to the epoxy's ability to insulate a single bar from that of the entire reinforcing cage embedded within the concrete structure. Therefore, the equipment (reference electrode and voltmeter) must be directly attached to each individual piece of epoxy-coated bar embedded within the structure to achieve an accurate assessment of the steel corrosion risk [Gu and Beaudoin, 1998].

2.2.3 Chloride Content Analysis. As was discussed earlier in this section, chlorides are known to attack the passive layer protecting a steel bar from corrosion. However, a sufficient amount of chlorides needs to be present at the steel-concrete interface in order to effectively destroy the passive layer. Therefore, chloride analyses are conducted on reinforced concrete structures to determine whether a sufficient amount of chlorides are present at a depth equal to that of embedded steel and/or how quickly the chlorides are diffusing through the concrete.

To assist in the calculation of the rate at which chloride ions diffuse through a concrete element, chloride profiles are commonly developed. A chloride profile represents the chloride concentration at various depths within the concrete. In order to obtain an accurate representation of the chloride distribution within the concrete, Broomfield (2007) recommends that a chloride profile have a minimum of four data points. These data points may then be used, along with Equation (4) in Section 2.1.2 of this section, to determine the rate at which the chlorides diffuse through the concrete. The diffusion rate can be used to approximate the time at which a sufficient amount of chlorides may reach a depth equal to that of the reinforcement and thereby predict the time at which the embedded bars may begin to corrode.

Currently, the American Society for Testing and Materials (ASTM) International publishes a standard procedure for testing the acid-soluble (ASTM C1152) and water-soluble (ASTM C1218) chloride concentrations within concrete. The results obtained from the acid-soluble chloride test corresponds to the concentration of both the bound and free chlorides contained within the concrete, whereas the water-soluble chloride test measures the concentration of only the unbound (free) chlorides contained within the concrete. It's the free chlorides that are capable of contributing toward the destruction of a bar's passive layer. Therefore, ASTM standard C1218 is considered to be more informative than the ASTM C1152 standard; however, the results obtained from the water-soluble test are known to be less accurate and difficult to reproduce. Both standards are commonly carried out in a lab and involve subjecting a concrete powder sample to an acid which is then followed by titration. Results from the acid-soluble (total) test can then be correlated to the values shown in Table 2.3 so that the corrosion risk of the embedded bars may be classified [Broomfield, 2007].

Table 2.3: Correlation between percent chloride by mass of concrete and corrosion risk [Broomfield, 2007].

% Cl by Mass of Concrete	Corrosion Risk
< 0.03	Negligible
0.03-0.06	Low
0.06-0.14	Moderate
> 0.14	High

Over the years chloride testing kits have been developed so that quick and accurate chloride analyses may be conducted within the field. Included within a kit is a chloride-ion selective electrode. The electrode measures the potential (mV) of a solution bearing chloride ions, which may then be compared to that of potentials gathered from solutions of known chloride concentrations. This method has been widely studied and

was found to correlate well with that of the ASTM standards as well as the American Association of State Highway and Transportation Official's (AASHTO) T260 standard. The method was also found to be more accurate than Quantab strips, which is an alternative method for conducting chloride analysis in the field.

Concrete powders are normally collected from drillings or the pulverization of cores. An overall sample size of 20 grams is required when following most standards. Both the ASTM and AASHTO standards require the test sample to be 10 grams in size and capable of passing a No. 20 (850 µm) or No. 50 (300 µm) sieve, respectively. When collecting a powder sample from a specimen at a fitted depth, multiple drilling locations are encouraged. Mixing of the powder collected from multiple locations will increase the statistical accuracy of the results as well as eliminate the likelihood that a piece of aggregate dominated the sample. An effort should be made to avoid losing a sample's fine powder, which is known to possess high chloride concentrates. A sample may become contaminated when handled with bare hands and therefore contact between exposed skin and that of the sample shall be held to a minimum [Broomfield, 2007].

2.3 PROTECTIVE COATINGS

The following section contains a brief summary of information that pertains to the history and development of both epoxy-coated steel reinforcement and enameled steel.

2.3.1 Fusion Bonded Epoxy. Under the Federal Highway Administration's (FHWA) National Experimental and Evaluation Program (Project No. 16), epoxy-coated steel reinforcement (ECR) was first implemented within a bridge deck located in West Conshohocken, Pennsylvania in 1973. During the years that followed, the program continued to sponsor the use of ECR in bridge decks throughout the country. By 1976 a total of 40 bridge decks throughout 18 states, along with the District of Columbia, contained ECR [Pyć et al., 2000]. According to the Concrete Reinforcing Steel Institute (CRSI), in 2008 over 60,000 bridges listed within the National Bridge Inventory contained ECR.

The process of manufacturing ECR was originally adopted from the piping industry and involves an electrostatic procedure. Before a steel bar is coated, it first must be cleaned to a near-white finish through a blasting process. During this stage any pre-

existing rust or mill scale, along with contaminants, are removed from the surface of the steel. Blasting also increases the surface roughness of the steel, which promotes adhesion between the steel and the applied epoxy. Once clean, the bar is then electrically grounded and preheated to a temperature of around 450 °F (230 °C). After the bar has been properly heated, it is then sprayed with a dry, electrically charged, epoxy powder which rapidly melts to form a continuous coating around the bar. Within a period of less than one minute after its application, the epoxy coating cures to a hardened state. Once the epoxy has hardened, the bar is then quenched using water. The quenching process typically lasts until the bar reaches a temperature that allows for it to be safely handled by hand. After the bar has been quenched, it is then transferred to a storage facility (or yard) where it remains until it is shipped [Pyć, 1998].

Although the process of epoxy coating steel reinforcing bars has evolved throughout the past four decades, to a point where the coating can be rapidly applied in a consistently uniform manner, defects within the coating may still develop. Therefore, standard quality assurance procedures are commonly carried out within the industry to assure that defects within the applied coating remain low and that an effective steel-epoxy bond is continually developed.

In 1981, ASTM International issued ASTM A775/A775M, a standard specification for epoxy-coated straight steel bars that may be fabricated (bent/cut) after the coating process. Fourteen years later (1995) ASTM published a second standard designated as ASTM A934/A934M, describing the proper requirements for epoxy-coated pre-fabricated steel bars [Gustafson, 1999]. Currently, both standards contain the same or similar requirements in terms of the expected quality and performance of the epoxy coating. Today, an epoxy coating is required to be 7 to 16 mil thick (175 to 400 µm) while possessing no more than one holiday per linear foot, on average. The epoxy coating is also expected to withstand a flexibility test without showing signs of cracking and/or debondment. These tests are required to be carried out several times throughout an eight hour production period. Each eight hour production period shall also include one cathodic debondment test in order to examine the bond between the steel and the epoxy coating.

According to both standards, properly coated bars may be stored outdoors, in an unprotected manner, for a period of only two months. After two months, actions must be taken in order to protect the bars from further degradation. All areas along a bar's coating that exhibit signs of damage should be repaired prior to concrete placement. However, when the extent of damaged exceeds two percent of the coated area within any one foot segment of the bar, the bar should be rejected from use.

In an effort to promote higher quality standards within the industry, CRSI developed a voluntary certification program for facilities manufacturing ECR in 1991. The certification requirements are said to be more stringent than that of the ASTM specifications and each facility registered in the program is susceptible to an unannounced inspection at least once a year [Gustafson, 1999]. Currently, CRSI recognizes a total of 37 certified facilities located in North America.

Laboratorial studies have shown that the epoxy coating is capable of protecting steel by acting as both a physical and electrochemical barrier. As a physical barrier, the epoxy coating prevents the steel from interacting with aggressive chloride ions, along with other corrosive elements, which would lead to the deterioration of the steel. The coating has also shown the ability to reduce macrocell corrosion by limiting both the size and the number of locations along a bar where the cathodic reaction can occur. Field surveys of ECR structures have further confirmed these laboratory findings [Gustafson, 1999 and Lee, 2004]. However, a large portion of these surveys have also discovered significant amounts of debondment between the epoxy coating and the steel, specifically at locations where the concrete is consistently saturated with water [Pyć et al., 2000].

Between 1986 and 1993, the Florida Department of Transportation (FDOT) began to report significant deterioration of ECR embedded within the substructure of five major marine bridges [Sagüé et al., 1994]. These discoveries concerned the FDOT, for the bridges were less than ten years old and from previous experience in dealing with similar structures built with uncoated reinforcement, these five structures should have lasted at least 12 years (on the average) before showing any signs of corrosion related issues.

With ECR having been a relatively new material, but was already incorporated within 300 bridges throughout the state of Florida, the FDOT decided to fund an investigative study that focused upon the state of their ECR bridges. The study involved

the evaluation of ECR embedded in the substructures of 25 large bridges located within a highly corrosive environment. Cores were taken from each structure in an effort to obtain a representative sample of the ECR embedded within the 25 bridges. Analysis of the cores revealed that the chloride concentration within many of the selected bridges was lower than that of the established threshold required to initiate corrosion. Further evaluation of each bridge lead to the conclusion that no bridge within the study showed any signs of severe corrosion; however, the ECR embedded within each bridge did show significant signs of debondment [Sagüé et al., 1994].

In 1989, the Oregon Department of Transportation (ODOT) forensically evaluated a concrete beam that was partially submerged in the Yaquina Bay near Newport, Oregon [Griffith and Laylor, 1999]. The beam was vertically positioned in the bay for a period of nine years and was reinforced with ECR. Visual examination of the reinforcement located at an elevation along the beam coinciding with the bay's tidal zone revealed that several of the stirrups, along with half the longitudinal bars, showed signs of corrosion. Following the visual examination, the coating's adhesion to the steel was evaluated. During the evaluation, it was discovered that the coating was thinly applied and permeable, while the steel beneath the coating exhibited a low blast profile. These three properties were thought to have contributed towards the poor adhesion seen between the epoxy and the steel.

Nine years later the test was repeated with a second beam that was stored within the bay for a period of 18 years. This time transverse cracks were detected along the beam's surface at locations that coincided with stirrups embedded within the concrete. The coating along a majority of the reinforcement removed from the beam showed some signs of debondment. Bars showing the most severe signs of debondment were removed from the segment of the beam that was situated within the bay's tidal zone. It was within this location that the majority of the corrosion was seen. Although the results obtained from autopsying the two beams were similar, the blast profile of the steel embedded in the second beam was within today's acceptable range [Griffith and Laylor, 1999].

In the mid 90's, the Pennsylvania Department of Transportation (PennDOT) took part in a joint venture with the New York State Department of Transportation (NYSDOT) in an effort to survey and evaluate the performance of ECR bridge decks scattered

throughout each state. Three cores, each containing two pieces of ECR, were removed from a total of 80 bridges surveyed within the study. Half of the bridges were located in Pennsylvania while the remaining 40 bridges were location in New York. Chloride analysis of the cores revealed that approximately 80 percent of the decks did not contain a sufficient amount of chlorides required to initiate corrosion of the embedded steel. Of the 473 pieces of ECR removed from the cores, 409 exhibited no signs of corrosion, 62 showed pin sized areas of corrosion, while the remaining 2 showed significant amounts of corrosion. Further examination was conducted upon selected bars. This additional examination revealed that seven percent of the selected bars showed that corrosion had taken place beneath the applied coating. A loss in adhesion between the epoxy coating and the steel was seen in 53 percent of the 473 pieces of ECR collected during the study. The coating along 13 percent of the bars showed a complete loss in adhesion. Conclusions made as a result of the study suggested that over 50 percent of the ECR embedded within the bridge decks throughout the two states experienced some degree of debondment. This loss in adhesion was believed to have occurred within the first six to ten years of a bar's service life. However, the extent of debondment seen along a piece of ECR was no indication of the bar's deterioration due to corrosion [Sohanghpurwaia, 2005].

An epoxy coating's ability to prevent steel from corroding is highly dependent upon the degree to which it is adhered to the steel when a sufficient amount of chlorides reach a depth within the concrete equal to that of the ECR. Factors known to affect the epoxy-steel bond include: excessive outdoor exposure, environmental conditions within the concrete, concrete pore solution, thickness and permeability of the coating, defects within the coating, and the surface properties of the steel substrate such as roughness.

Laboratory studies have shown that potassium (K) and sodium (Na) ions, which reside in concrete pore solution, can expedite the debonding process, especially when breaks within the coating exist [Sagüé et al., 1994]. Research has also discovered that the rate of debondment increases as the relative humidity within the concrete, at a depth equal to that of the embedded ECR, reaches 60 percent or higher. As a means for reference, concrete located in the state of Virginia typically has a relative humidity of greater than 80 percent [Pyć et al., 2000].

Although the number of breaks within an epoxy coating can significantly influence the degree to which the coating becomes debonded from the steel, it is not the only deciding factor. Debondment can also occur near thinly coated and/or highly permeable areas along a bar.

Since epoxy is an organic material, it is unable to prevent the permeation of water and oxygen. Since ECR is commonly embedded in concrete having a high relative humidity, water and oxygen diffuse through the coating towards the underlying steel. As water reaches the interface between the coating and the steel it tends to accumulate within debonded areas. These areas of debondment may be attributed to impurities that were present along the steel surface during the coating process. It is thought that this gathering of water molecules further invokes the debonding process through either a chemical or mechanical process. During the progressive debondment of the coating, a blister may form and the underlying steel may begin to corrode [Pyć, 1998].

Once the epoxy coating has debonded from the steel, the steel is no longer protected from corrosion. Corrosion of the steel located beneath the debonded epoxy typically proceeds in an oxygen-reduced environment where ferrous ions dissociate from the steel and react with water molecules to form ferrous hydroxide and hydrogen ions:

$$Fe^{2+} + 2H_2O \rightarrow Fe(OH)_2 + 2H^+ \quad (15)$$

The production of hydrogen ions accelerates the corrosion process by attracting negatively charged chloride ions while at the same time creating an acidic environment [Pyć et al., 2000].

Although a consensus exists with respect to the epoxy's susceptibility of debonding from a steel substrate, the significance of this, in terms of the degree to which it affects the epoxy's ability of providing long term corrosion protect, has not yet been fully established [Sohanghpurwaia, 2005].

2.3.2 Enamel. Through the discovery of Mycenaean artifacts, believed to have been created over 3,000 years ago, enamel has displayed and continues to display an exceptional ability to withstand harsh environments [Andrews, 1961]. Today, enamel is commonly applied to steel surfaces to protect the material from corrosive environments.

This application is widely seen in household appliances, such as microwaves, ovens/stove tops, washing machines, hot-water heaters, etc. Enamel-coated steel has also been successfully incorporated into the construction industry in the form of interior and exterior cladding along buildings and tunnels [Arcelor, 2008]. Recently, a new form of enamel has been developed that is specifically designed for steel reinforcing bars embedded within concrete.

The newly developed enamel incorporates calcium silicate particles that are dispersed throughout the coating's thickness, with a portion of the particles partially exposed along the coating's exterior surface. The enamel is referred to as "reactive enamel" due to the chemical reaction that occurs shortly after the enamel has been placed within freshly batched concrete. Exposed calcium silicate particles along the surface of the enamel react with available water molecules within concrete to form hydration products such as calcium silicate hydrate (CSH). This reaction increases the bond between the concrete and the embedded reinforcement while protecting the steel from corrosive elements that may accumulate within the concrete over the lifetime of the structure [Weiss et al., 2009].

Enamel is typically comprised of the following four constituents: refractories, fluxes, adhesion agents, and opacifiers. Silica (SiO_2) is the main constituent in enamel and is commonly found in quartz, feldspar, clay, and mica. Adjusting the quantities of the four materials will alter the properties of the enamel; such as the enamel's melting point, coefficient of expansion, and adhesiveness [Arcelor, 2008].

Refractories help in the development of the enamel's structure. Alumina (Al_2O_3) is a common refractory oxide that increases the enamel's resistance to temperature, chemical attack, and abrasion.

Fluxes are used to react with the refractories, which in turn lowers the enamel's melting point and increases its coefficient of expansion. Many fluxes used in the production of enamel are in the form of alkaline oxides, such as sodium (Na_2O), potassium (K_2O), lithium (Li_2O), calcium (CaO), magnesium (MgO), and boron oxide (B_2O_3). Fluorine (F_2) is also a fluxing agent and is often used in the production of enamel [Andrews, 1961].

Adhesion agents, in the form of metal oxides, are added to an enamel to promote the adhesion between the enamel and the steel. Typical adhesion agents include nickel (NiO), molybdenum (MoO_2), cobalt (Co_3O_4), cupric (CuO), manganese (MnO_2) and chromic oxide (Cr_2O_3).

Opacifiers serve in the development of enamel's visual qualities. Commonly used opacifiers include titanium dioxide (TiO_2), antimony oxide (Sb_2O_5), zirconium oxide (ZrO_2), and tin oxide (SnO_2).

Manufacturing of enamel may involve fusing up to 15 different types of materials that have been precisely weighed out in an effort to create an enamel with a specific coefficient of expansion, melting point, and adhesiveness. The fusion process consists of melting the mixture of constituents and then rapidly cooling the molten material using water. The rapid cooling of the material is essential to avoid any phase separation. After the material is cooled, it is crushed to form what is commonly referred to as "frit."

Prior to using frit in the enameling process it first must be ground down further and then mixed with floating (suspension) agents, coloring agents, electrolytes, and additional refractories and opacifiers. Water is then added to the mix to form a slurry. The slurry may then be applied to the steel through a spraying or dipping process. However, the frit may also be applied to the steel through a dry (spraying) process.

When the dry method of enameling is used, grinding of the frit into a powder is required. Once the frit has been ground, the powder is then sieved and passed through a magnetic field to remove any iron particles within the powder. If the iron were to remain within the powder, holes would develop within the enamel during the firing process and would remain thereafter. After processing the powder, the grains are then coated with silicon to enhance the temporary bond between the frit and the steel prior to firing.

Currently, single-layer or double-layer enamel is commonly applied to steel. The first layer of double-layer enamel is referred to as the "ground-coat." The ground-coat contains high amounts of metal oxides that react with the steel to form alloys. This reaction promotes the highly desired chemical bond between the enamel and the steel. Because of this bond, the ground-coat is considered to contribute greatly toward the corrosion resistance of a double-layer enamel. While the second layer (cover-coat) of double-layer enamel contains negligible amounts of adhesive agents, but helps in the

development of the enamel's aesthetic look and chemical resistance. Enamel's resistance toward alkali environments (washing machines, concrete, etc.) can be enhanced with the addition of zirconium oxide (ZrO_2).

Preparation of the steel surface is an important part of the enameling process. Before steel can be enameled it first needs to be degreased, neutralized, and dried. If the steel was hot rolled, shot blasting may be required prior to degreasing. After degreasing, rinsing, pickling, acid rinsing, nickelling, and an additional rinsing may be required, especially if the applied enamel contains small amounts of adhesion agents.

Shot blasting is used as a means of cleaning the steel surface. Blasting also roughens the surface of the steel and thereby increases its surface area. An increase in surface area promotes a stronger steel-enamel bond by providing the enamel a larger contact surface to react with. After the steel has been blasted, it is then degreased using a detergent.

Once degreased, the steel may then be subjected to a single hot water rinse or a series (hot, cold, and demineralising) of rinses depending on whether the surface of the steel will be further treated. If pickling of the steel surface will be conducted, then a single rinse may be sufficient.

Pickling of the steel is conducted once the hot water rinse has been completed. Pickling is the act of subjecting the steel to an acid (sulphuric acid) to increase the micro-roughness of the steel surface. Similar to that of shot blasting, increasing the micro-roughness of the steel surface through pickling will in turn strength the steel-enamel bond. Pickling of steel tends to result in the steel surface having a pH of lower than 2.8. This low pH will have an adverse affect upon the nickelling process, since nickelling of steel is most effective when the pH of the steel surface is at a value of 2.8. Therefore, acid rinsing is conducted in order to increase the pH of the steel surface.

Once the steel surface has reached the proper pH, nickel is then deposited along the surface of the steel. Nickelling is especially important when an enamel, containing an minimal amount of adhesion agents, is used as the ground coat. The quantity of nickel required to achieve proper adherence of the enamel to the steel is a function of the quantity of iron lost during the pickling process.

The final rinse and neutralization of the steel are carried out after the nickelling process in order to gradually remove any remaining acid along the surface of the steel. Drying of the steel is then conducted to prevent the steel from corroding prior to the application of the enamel.

As mentioned earlier, enamel may be applied to a steel surface through a wet or dry process. The wet process consists of either spraying enamel slurry upon the surface of the steel or dipping the steel into a vat containing enamel slurry, which is commonly referred to as a "slip." With the proper setup and equipment, both applications (spraying and dipping) can impart negative charges upon the enamel particles, which would result in a uniform distribution of the enamel coating. This method would also grant the enameller more control over the thickness of the applied coating. However, the wet process of applying enamel is often conducted in a manner that does not involve electrostatics, which can lead to a coating that is non-uniformly applied (variations in thickness).

The dry enameling process is carried out in a similar manner to that of the wet electrostatic spraying method, except that the enamel particles are not contained within a slurry but are instead typically coated with silicon to prevent the particles from hydrating. If the particles were permitted to hydrate, a reduction in electrical resistance would result and the distribution of the enamel upon the steel surface would be affected.

Once applied, the enamel is then fired at a temperature between 1436 - 1562°F (780 - 850°C). The actual temperature at which the enamel is fired is a function of atmospheric conditions within the oven, as well as the properties of the enamel and the substrate (steel). A higher firing temperature produces an enamel of higher quality; however, too high of a temperature can alter the phase of the steel. Thickness of the steel must also be taken into account when determining the duration of the firing.

During the firing process, a bond between the steel and the enamel is created through a series of chemical reactions. This series of reactions begin as the temperature approaches 1022°F (550°C). It is near this temperature that the steel starts to oxidize as oxygen and moisture from the atmosphere within the furnace travel through the porous (unfused) enamel. While the steel is oxidizing, atomic hydrogen is generated and diffuses into the steel where molecular hydrogen (H_2) is subsequently formed. As the

temperature continues to rise from 1022°F (550°C) to 1526°F (830°C), the oxidation of the steel begins to slow down, for the enamel has now begun to melt. During this period the iron oxide, which had formed earlier, begins to dissolve into the surrounding enamel where it reacts with the metal oxides contained within the enamel along with the carbon at the surface of the steel to form Fe-Ni-Co alloys. It is during this period when the bond between the enamel and the steel is developed. Both carbon dioxide (CO_2) and carbon monoxide (CO) are also formed at the steel-enamel interface during this period and begin to travel outwardly through the molten enamel in order escape into the surrounding atmosphere. Once the firing is complete, the enamel begins to solidify while molecular hydrogen is expelled from within the steel, where it then becomes trapped beneath the enamel. When an excessive amount of hydrogen becomes trapped beneath the enamel, the enamel will break away from the steel and a defect along the surface of the coating will appear. This defect is commonly referred to as a "fishscaling," for the pieces of enamel that break away from the steel closely resemble that of a fish's scale.

Enamel is an electrically insulating material that has a typical resistivity of 1×10^{14} Ωcm at room temperature [Andrews, 1961]. Therefore, when steel is properly coated with enamel, it becomes corrosion resistant. Moreover, when the enamel coating is damaged and the exposed steel is subjected to a corrosive environment, corrosion will only occur within the damaged area, for the chemical bond between the enamel and the steel prevents corrosive elements from traveling beneath the protective coating. As an impermeable material, enamel is extremely resistant to environmental conditions including ultra-violet light. It also can withstand sudden changes in temperature and has a high resistance to fire [Arcelor, 2008]. A recent study, conducted by the United States (US) Army Corps of Engineers, reported that the newly developed reactive enamel can increase the bond strength between steel and mortar by over 400 percent. The study also reported that when steel was coated with either pure or reactive enamel, the corrosion resistance of the material increased [Weiss, 2009].

The study conducted by the US Army Corps of Engineers involved placing six coated and three uncoated smooth steel pins in sand that was saturated with a 3 percent salt-water solution for a period of 40 days. The environment was designed to mimic a carbonated concrete contaminated with chlorides. Each of the nine pins were ¼ in. (0.64

cm) in diameter and 3 in. (7.6 cm) long. Half of the six coated pins were coated with pure enamel while the remaining three were coated with reactive enamel. The reactive enamel was composed of 50 percent portland cement and 50 percent pure enamel. The average thickness of the two coatings was 31 mils (800 µm). Using a drill, a defect was created at a single point along the length of each of the six coated pins. The defect was less than one millimeter in diameter and extended through the thickness of the coating. After 40 days of testing, the only signs of corrosion along the six enameled pins was seen at the intentionally damaged areas; whereas the uncoated pins exhibited severe signs of corrosion. Under further investigation, it was discovered that the actively corroding area along each of the enameled pins was confined and unable to penetrate beneath either of the enamel coatings.

Through additional testing, it was also discovered that the cement particles embedded within the reactive enamel were capable of sealing cracks that were deliberately created along the surface of the coating. This showed that not only does the reactive enamel protect the steel from corrosion, but it also possessed a "self-healing" ability [Weiss, 2009].

2.4 TESTING METHODS

Corrosion is a complex and highly unpredictable process which is often affected by numerous factors. These factors are often difficult to quantify and/or account for, which makes classifying and understanding a material's corrosion resistance extremely difficult. Therefore, when trying to characterize a material's ability to postpone the corrosion process, it may be beneficial to conduct a series of tests in hope that the results may lead to a clear and indisputable conclusion. This section describes the three tests which were used to study the corrosion resistance of various protective coatings. They are: the AASHTO T259 ponding test, the ASTM B117 salt spray test, and the accelerated corrosion test method.

2.4.1 Ponding Test. Understanding a concrete's resistance toward the ingress of destructive chloride ions is highly beneficial when attempting to design a durable reinforced concrete structure. Many factors within the concrete's design, along with the environmental in which the concrete is placed, must be taken into account when trying to

quantify a concrete's ability to resist the ingress of chlorides. Therefore, a standard concrete ponding test has been developed by both the American Association of State Highway and Transportation Official's (AASHTO) and ASTM International.

Both the AASHTO T259 and ASTM C1543 standard involve the casting and curing of several concrete slabs made of the same concrete that are capable of retaining a 3 percent saltwater solution upon their surface for a predetermined period of time. Depending upon which standard is used, a minimum of two (ASTM C1543) or four (AASHTO T259) slabs must be cast for each concrete under investigation with each slab having a thickness of approximately 3 in. (7.6 cm). The surface area of each slab shall be at least 28 in.^{2} (175 cm^2) or 46 in.^{2} (300 cm^2) in order to satisfy the AASHTO T259 or ASTM C1543 standard, respectively.

Once casting is complete, both standards require the slabs to be moist-cured for 14 days, at which time the slabs are to be air dried for two weeks (14 days) at a temperature of 73 ± 4°F (23 ± 2°C) and relative humidity of 50 ± 5 percent. Drying of the specimens is a critical step within both standards, as the concrete's ability to absorb the initial saltwater solution can be significantly altered when the slabs are not properly dried in accordance with the standards. Therefore, the procedures conducted after removing the slabs from the moist room and before initiating ponding must be closely followed.

After the saltwater has been placed within a slab's reservoir, a glass plate or a piece of polyethylene sheeting may be used to cover the specimen in order to prevent evaporation of the saltwater; however, the bottom surface of each slab shall remain unobstructed to promote air-flow around the specimen. The slabs are to be stored in this arrangement until the completion of the test, which may be for 90 days (AASHTO T259) or up to several years (ASTM C1543). However, once the test has been completed, the saltwater shall be removed promptly to promote drying of the specimens.

Once dry, a wire brush shall be used to remove any salt that may have crystallized along the surface of a slab's reservoir. After the surface has been cleaned, chloride analysis upon the slabs may be performed. The AASTHO T259 standard requires that the acid soluble (total) chloride content be determined upon concrete powder that was collected from depth ranges of 0.063 to 0.5 in. (0.16 to 1.3 cm) and 0.5 to 1.0 in. (1.3 to

2.5 cm). The ASTM C1543 standard requires that the acid soluble chloride content be determined from four concrete powder samples collected from the following depth ranges: 0.4 to 0.8 in. (1.0 to 2.0 cm), 1.0 to 1.4 in. (2.5 to 3.5 cm), 1.6 to 2.0 in. (4.0 to 5.0 cm), and 2.2 to 2.6 in. (5.5 to 6.5 cm).

As clearly stated within each standard, this test is meant to provide information pertaining to a concrete's ability to slow down or prevent the ingress of chlorides when an adjustment has been made to the mix design. The test is not, however, intended to provide a quantitative value for the lifespan of a reinforced concrete structure.

2.4.2 Salt Spray. Originally proposed in 1914 by J. A. Capp and later adopted by the National Institute of Standards and Technology (NIST), salt spray testing has become a widely recognized method for examining the corrosion resistance of protective coatings. In 1939, ASTM International developed ASTM B117, a standard salt spray test method specifically designed to evaluate the relative corrosion resistance of various metals and/or coatings. Today, salt spray chambers are designed according to the ASTM B117 standard and are automated to maintain a specified environment within the chamber [Doppke and Bryant, 1983].

A schematic representation of the ASTM B117 salt spray test is shown in Figure 2.4. As shown within the figure, a salty fog is injected into the enclosed chamber through a nozzle (or atomizer) centrally located along the chamber's floor. The atomizer is continually supplied with a 5 percent saltwater solution, that is stored within a reservoir positioned along one side of the chamber, and a steady stream of clean compressed air. The distribution of the salt fog throughout the chamber shall have a fallout rate such that 0.034 to 0.068 fl-oz. of solution (1.0 to 2.0 mL) is collected upon a horizontal surface measuring 12.4 $in.^2$ (80 cm^2). Temperature within the chamber shall be maintained (via heaters) at 95 ± 3°F (35 ± 2°C). The lid of the chamber shall be sloped to prevent any solution that has accumulated along the inner surface of the lid from falling upon the specimens lying below. Specimens within the chamber shall be oriented at an angle of 15° to 30° from the vertical and positioned in such a manner that prevents the specimens from contacting one another. A specimen's exposure to the salt fog shall be unobstructed. Solution that accumulates inside the chamber may be disposed of through a drain positioned within the chamber's floor. Prior to opening the chamber, a ventilating

system may be used to expel any salt fog lingering within the chamber; however, opening of the chamber shall be held to a minimum.

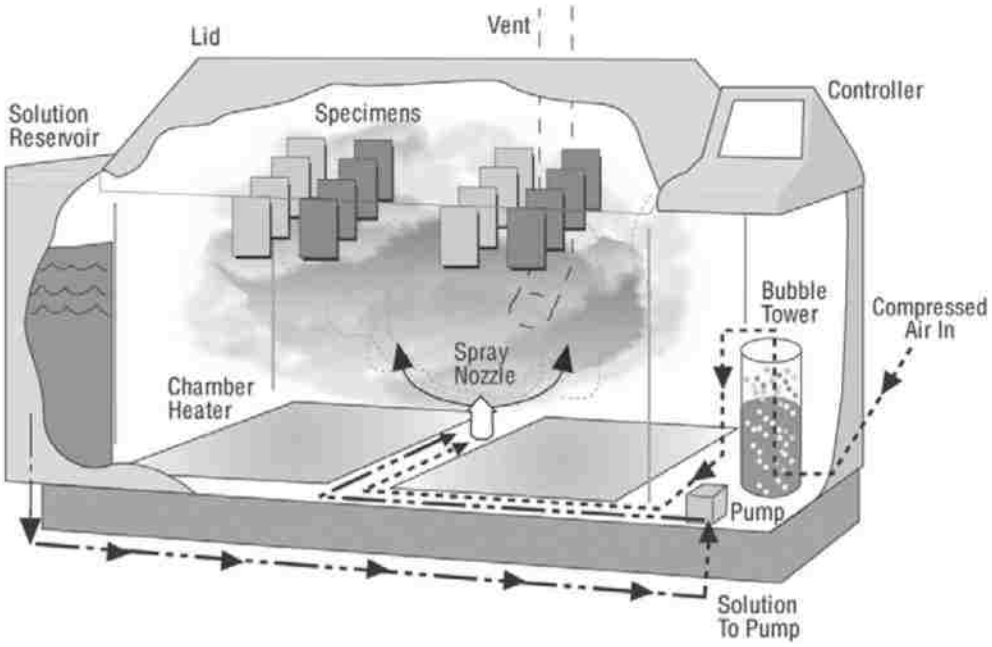

Figure 2.4: A schematic representation a salt spray chamber (Courtesy of the Q-Lab Corporation).

Although the test has been standardized and today's cabinets are designed to operate in accordance with the ASTM standard, variations within test results may be reported when testing identical specimens in multiple chambers. This phenomenon has been widely studied throughout the standard's existence, in large part by the American automotive industry, and although information gathered from these studies may have led to adjustments within the standard, the issue still exists today. Even though the test is flawed for some applications, it still has the ability to detect faults that may have resulted from the coating process. Such faults may include thinly coated areas, uniformity issues, and/or pores that are present within the coating. The validity of the test may also be

established by examining standard test specimens, of known performance, alongside specimens whose performance has not yet been established [Doppke and Bryant, 1983].

2.4.3 Accelerated Corrosion Test Method. The accelerated corrosion test (ACT) method was first created in 1992 during a Federal Highway Administration (FHWA) sponsored study conducted by Thompson, Lankard, and Sprinkel. Based off of the potentiostatic polarization test method, the ACT method was originally developed to evaluate the corrosion resistance of post-tensioning grouts. Shortly after its conception, the ACT method rapidly evolved through research conducted at The University of Texas at Austin [Pacheco, 2003] and has recently been used to evaluate the corrosion resistance of protective steel coatings [Volz et al., 2008].

Incorporated within an ACT specimen is a 7-wire prestressing steel strand centrally positioned within a cementitious grout. The steel strand shall be of Grade 270 and have a nominal diameter of ½ in. (1.3 cm). After the strand has been cut to the proper length of 14 in. (36 cm) and both of its ends have been beveled, the entire strand is cleaned using acetone.

Prior to grouting the strand, a polyvinyl chloride (PVC) mold is constructed. The mold shall consist of three pieces of PVC piping that have been cut to the following lengths: 6 in. (15 cm), 3.5 in. (8.9 cm), and 2.4 in. (6.1 cm). Each piece shall also have an inner diameter of 1 in. (2.5 cm). Two longitudinal slits are cut along the outer edge of the piece measuring 3.5 in. (8.9 cm) in length. After the three sections of PVC piping have been rinsed with water and dried, they are connected in the order shown in Figure 2.5 using silicone and duct tape. Once the silicone has vulcanized, the end of the mold containing the 2.4 in. (6.1 cm) long segment of PVC piping is capped, using a properly sized PVC cap. Before grouting, the mold shall be examined for leaks by filling the mold with water. If a leak is detected within the mold, the defect shall be corrected prior grouting.

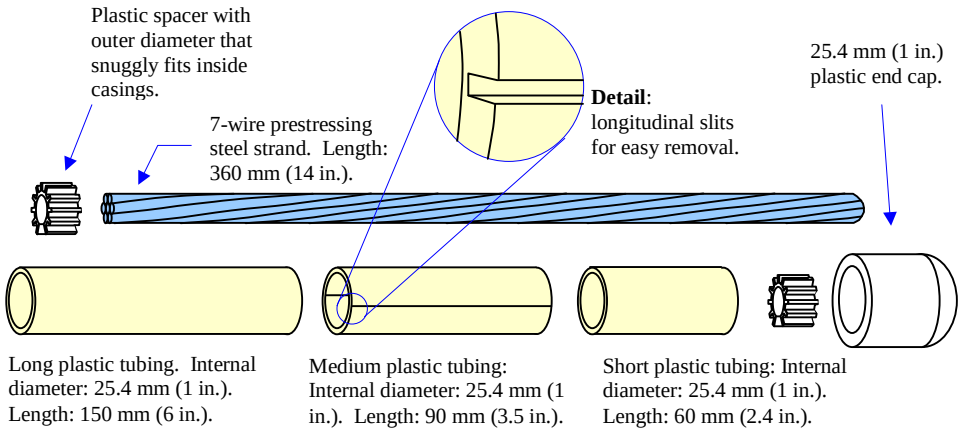

Figure 2.5: Breakdown of materials needed to construct a standard ACT specimen, excluding the grout [Pacheco, 2003].

Grouts subject to investigation are then prepared using distilled or deionized water following ASTM C938 for proportioning grout mixtures. While the strand is centrally positioned along the bottom of the mold (via a spacer) the bar is subsequently grouted in three equal lifts. After each lift, the grout is consolidated by slowly twisting the embedded strand while the mold is gently tapped. At no time during the casting process shall the strand be removed from the mold. Once casting is complete, the specimen is transferred to a curing chamber where it remains for period of 28 days. However, if fly ash has been used, a 56 day cure may be permitted. While curing, the end of the strand protruding out from the grout may be covered to prevent an excessive amount of rust from forming along the exposed steel surface.

Once the specimen has been properly cured, it may then be removed from the curing chamber and the 3.5 in. (8.9 cm) long section of the mold, containing the two longitudinal slits, is removed. Immediately after exposing the grout, the specimen shall be rinsed with water and then quickly placed within a beaker containing three liters of an electrolyte. The electrolyte consists of 5 percent sodium chloride (NaCl) and distilled (or deionized) water. After the specimen has been placed within the electrolyte, the construction of the corrosion cell may then be completed.

The corrosion cell contains three electrodes that are partially submerged within the saltwater solution. As shown in Figure 2.6, the specimen is labeled as the working electrode and is centrally located between the counter and reference electrode. The counter electrode shall be made of platinum or graphite, while a saturated calomel electrode (SCE) is used as the reference electrode. A distance of 4.8 in. (12 cm) shall be maintained between the centroids of the counter and reference electrodes. Once properly positioned within the corrosion cell, the electrodes are then connected to a multiplexer; which, in turn, is connected to a potentiostat.

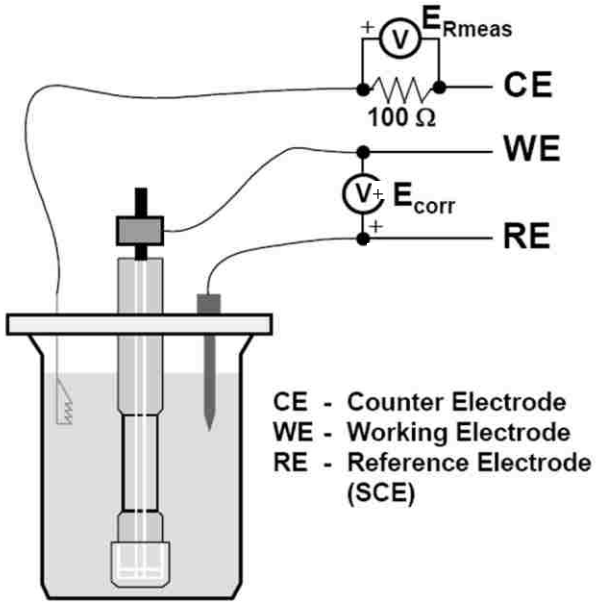

Figure 2.6: Accelerated corrosion test setup [Pacheco, 2003].

Before the test is initiated, a specimen's corrosion potential (E_{corr}) is determined using the reference electrode. After a specimen's E_{corr} has been determined, the multiplexer and potentiostat are then used to create a potential between the counter and working electrode of +400 mV_{SCE} above E_{corr}. This applied potential subsequently drives the negatively charged chloride ions (Cl^-) within the saltwater through the grout towards

the embedded steel. When the chlorides reach the steel-grout interface, they destroy the passive layer protecting the steel and the corrosion process is initiated. It is at this moment that the test is complete.

The initiation of corrosion is detected by an abrupt increase in the specimen's corrosion current (i_{corr}). A specimen's i_{corr} is recorded every 30 minutes throughout the duration of the test and is measured across a 100 Ω resistor that is in line with the counter electrode, as indicated in Figure 2.6. Upon completion of the test, the amount of time (usually expressed in hours) in which the specimen was able to postpone the onset of corrosion is recorded. This value is referred to as the specimen's (or grout's) time-to-corrosion (t_{corr}). In order to obtain a representative t_{corr} for a particular grout, a minimum of six specimens should be tested.

The benefit of the ACT method is that it can rapidly provide information about a grout's ability to resist the ingress of chlorides. The test can also expose any material or processing defects in a protective steel coating within a matter of hours. However, one drawback is that the test is sensitive to grouting defects, which can significantly alter a test result. Therefore, testing of grouted specimens that exhibit signs of defects should be avoided.

3 PONDING TEST

3.1 INTRODUCTION

Using both the AASHTO T259 and ASTM C1543 standard as guidelines, ponding specimens were constructed to evaluate the corrosion resistance of the 50/50 enamel coating within a cementitious environment. As a baseline for comparison, both uncoated and epoxy-coated steel rebar were also tested.

The test consisted of subjecting a total of 20 reinforced and 5 unreinforced concrete ponding specimens to a continuous two week wet / one week dry cycle, for a period of 54 weeks. The 20 reinforced concrete ponding specimens were divided into five groups, with four specimens to each group. The five groups were: uncoated, "perfect" epoxy, damaged epoxy, "perfect" 50/50 enamel, and damaged 50/50 enamel. The name of each group corresponded to the type of coated reinforcing bars embedded within a group's four specimens. The five unreinforced specimens were constructed as control specimens for concrete resistivity measurements.

The control specimens were used to obtain a "representative" concrete resistivity value for the overall set of specimens. Concrete resistivity and half-cell potential readings were carried out every 6 weeks over the course of the testing period. Upon completion of the test, chloride profiles were developed from randomly selected specimens. After developing the chloride profiles, specimens contained within each group were then forensically evaluated.

3.2 SPECIMEN DETAILS & MATERIALS

The specimens measured 18 in. x 18 in. (46 cm x 46 cm) in plan and 3½ in. (8.9 cm) in height. Each specimen contained a 15-in.-square (38 cm) by 1-in.-deep (2.5 cm) reservoir along its surface, as shown in Figure 3.1.

3.2.1 Steel Reinforcement. Four, 21-in.-long (53 cm), segments of deformed No. 4 (No. 13), Grade 60 rebar were embedded within each of the 20 reinforced specimens. Two of the four bars were positioned in the longitudinal direction and were given ½ in. (1.3 cm) of cover with respect to the surface of the reservoir. The remaining

two bars were positioned directly beneath and in contact with the two longitudinal bars, but in the transverse direction. The bars were spaced in plan as shown in Figure 3.1.

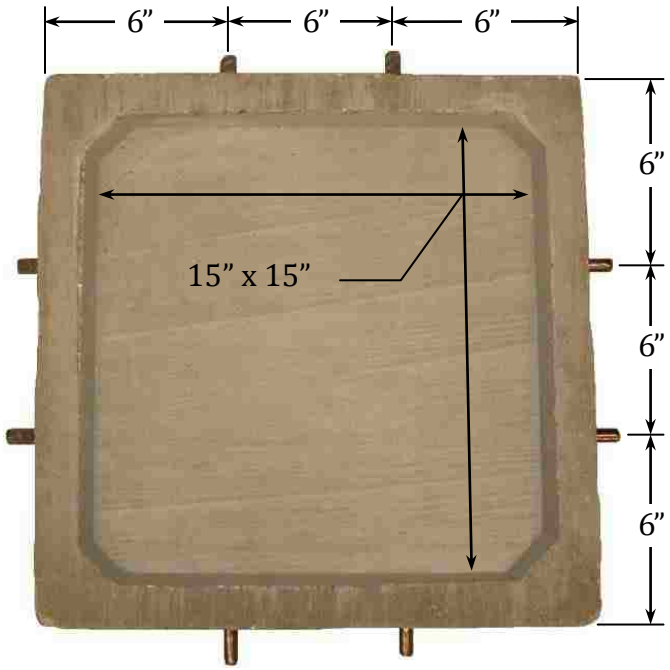

Figure 3.1: Typical reinforced ponding specimen.

After cutting the bars to a length of 21 in. (53 cm), half of the epoxy and enamel-coated bars were intentionally damaged. Each bar was damaged at three locations along one of its sides. With respect to either end of a bar, the three locations were at distances of 4½ in. (11 cm), 10½ in. (27 cm), and 16½ in. (42 cm). The three areas of damage along each bar were created using the same level of impact energy. Subjecting the two coatings to the same level of energy assured that the bars were prepared under the same condition while accounting for the ductility of each coating. The impact energy was created using an apparatus design based on ASTM specification G14.

The apparatus for intentionally damaging the coated bars is shown in Figure 3.2. The apparatus consists of a 2-lb. (0.91 kg) steel tup with a hemispherical head, a vertical

section of hollow aluminum tubing to guide the tup, and a horizontal section of steel angle to position the rebar. The bars were secured to the steel angle with clamps, and the tup was dropped from a height of 36 in. (91 cm) to damage the coatings. As shown in Figure 3.3, the 50/50 enamel coating exhibited an average area of damage that was approximately 3/8 in. x 1/2 in. (1.0 cm x 1.3 cm), whereas the epoxy coating showed an average area of damage that was approximately 1/16 in. x 1/8 in. (0.16 cm x 0.32 cm).

(a) (b)

Figure 3.2: Apparatus used to damage coated bars. (a) Overall view. (b) Tip of the tup aligned within the hollow aluminum tube.

(a) (b)

Figure 3.3: Representative view of an average intentionally damaged area along the two tested coatings. (a) 50/50 enamel. (b) epoxy.

Final preparation of the bars involved a thorough cleaning. First, a wire brush was used to remove any rust from the uncoated bars. Next, the uncoated and epoxy-coated bars were cleaned with a mild soap and water. After cleaning the bars, the epoxy and 50/50 enamel-coated bars were examined for unintentionally damaged areas. Any area along a bar that was unintentionally damaged received two coats of Rebar Green Epoxy Paint. The paint was manufactured by Aervoe Industries, Inc. and met ASTM D3963. The second coat was applied approximately one hour after the application of the first coat. After applying the second coat, each bar was set aside for a minimum period of 72 hours prior to being placed within the forms.

Both uncoated and "perfectly" coated bars were randomly oriented within the forms. Bars that were intentionally damaged were oriented with the side containing the three areas of damage facing downward towards the bottom of the form, which would eventually become the top surface of the specimens. In an effort to prevent any rotation and/or movement of the bars during casting, plastic zip ties were used to connect the bars running perpendicular to one another, as shown in Figure 3.4.

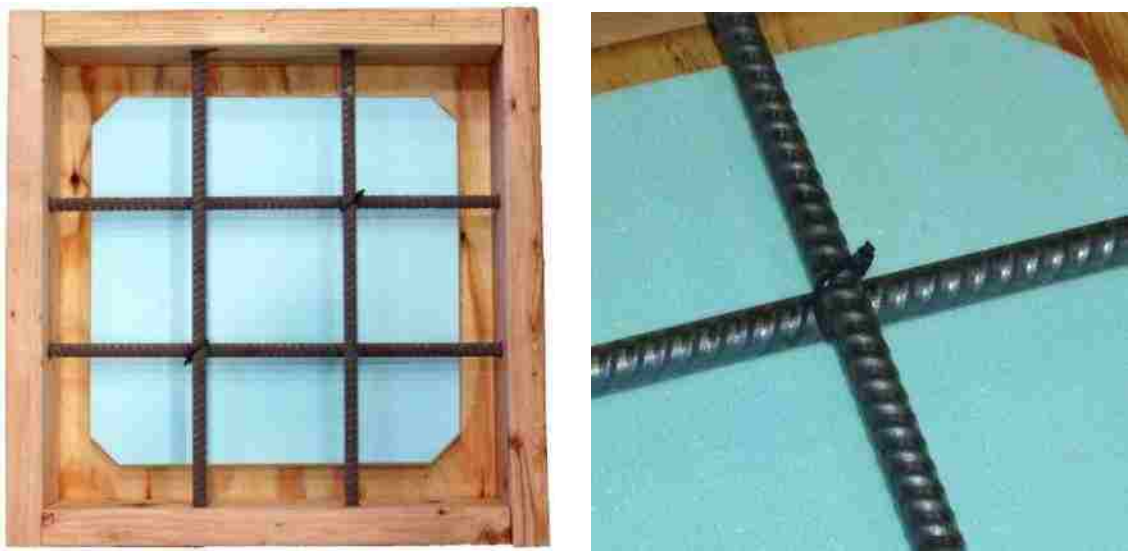

(a) (b)

Figure 3.4: Positioning and arrangement of reinforcement in a form prior to casting. (a) Overall view. (b) Connection of perpendicular bars.

3.2.2 Formwork. The forms used to cast the specimens were constructed of lumber and 1-in.-thick (2.5 cm) polyisocyanurate foam. The walls of each form were made of four pieces of 1½-in. x 3½-in. (3.8 cm x 8.9 cm) lumber. Two ⅝-in.-diameter (1.6 cm) holes were drilled through each of the walls at locations that conformed to the rebar locations. A 21-in. x 21-in. x ¾-in. (53 cm x 53 cm x 1.9 cm) section of plywood was used as the bottom of each form. Centrally located on the top of the plywood was a 15-in. x 15-in. x 1-in. (38 cm x 38 cm x 2.5 cm) section of polyisocyanurate foam. The foam was secured to the plywood using Polyurethane Premium Construction Adhesive manufactured by Henkel Corporation. Prior to using the forms, the interior surface of each form was coated with a layer of release agent that was manufactured by Dayton Superior. A typical form may be seen in Figure 3.4. A drawing of a typical form is shown in Figure A - 1.

3.2.3 Concrete. A standard 4000 psi (27.5 MPa) concrete was used for each of the 25 specimens. The mix had a 0.50 water-to-cement ratio and incorporated no chemical or mineral admixtures. Coarse and fine aggregate used within the mix consisted of ⅜-in. (1.0 cm) pea gravel and Jefferson City sand, as listed below in Table 3.1.

Batching of the concrete took place at a local ready-mix plant and was delivered to the lab where it was then placed indoors.

Table 3.1: Concrete constituents by weight.

Type I Cement	658	lbs.
⅜-in. Pea Gravel	1562	lbs.
Sand (Jefferson City)	1562	lbs.
Water	329	lbs.

Casting of the 25 specimens was broken up into three pours which occurred on three separate days over the course of a 7 month period. The first pour was on December 9, 2008 with the casting of the first and second specimen within each of the five groups containing reinforcement. Casting of the third and fourth specimen, within each of the five groups, occurred on February 2, 2009. The third and final pour took place on May 22, 2009 and consisted of casting the five unreinforced control specimens.

For each of the three pours, a total of five test cylinders, measuring 6 in. x 12 in. (15 cm x 31 cm), were cast alongside the ponding specimens. After each casting, plastic sheeting was used to cover the specimens and plastic caps were placed over the cylinders. The cylinders and specimens were moist cured for seven days. After curing, the specimens were demolded, labeled, and transported to the room in which they were stored during the 54 weeks of testing. However, before transporting the epoxy and 50/50 enamel specimens, the coating along one end of each of the four exposed bars was removed through grinding to provide the electrical connection necessary for the subsequent half-cell readings.

The 7 and 28-day compressive strengths of each pour were determined using four of the five cylinders that were cast and cured alongside the specimens. Before testing, the ends of each cylinder were capped following ASTM C617. All cylinders were tested in accordance with ASTM C39. The 7 and 28-day strengths were determined through

testing 1 and 3 cylinders, respectively. The average 28-day compressive strength of the three cylinders, along with the 7-day compressive strength based on one cylinder, for each of the three pours may be found in Table 3.2 below. Using the guidelines established by Committee 318 of the American Concrete Institute (ACI), the concrete used within the ponding test can be accepted as a 4000 psi concrete. For the average compressive strength of the three pours (4202 psi) was greater than the specified design strength (f'_c) of 4000 psi and the average compressive strength of each individual pour was not lower than f'_c by more than 500 psi.

Table 3.2: Compressive strength of concrete used in ponding test.

POUR	SLUMP (in.)	COMPRESSIVE STRENGTHS (psi)			
		7-Day	28-Day		
		Test Value	*Test Value*	*Average*	*Std. Dev.*
1	4-1/2	2147	4483 4252 4342	4359	116
2	6-1/2	2729	4431 4494 4213	4379	147
3	7-1/2	2724	3662 3672 4273	3869	350

3.3 TESTING & PROCEDURE

During the 54 weeks of testing, specimens were stored within a room that had an average ambient temperature of 68°F (20°C) and a relative humidity of 40 to 60 percent. Specimens were placed upon shelves in an elevated position that measured approximately

1 in. (2.5 cm) above the underlying shelf. In this position, the specimens were subjected to a series of 18 consecutive wet/dry cycles.

The wet phase of a wet/dry cycle lasted for a total of two weeks and consisted of placing ½ gallon (2 liters) of saltwater within a specimen's reservoir. The saltwater remained within a specimen's reservoir during the entire two weeks and consisted of distilled water with 5 percent ACS grade sodium chloride (NaCl) by weight. To prevent any evaporation of the saltwater, each specimen was covered with plastic sheeting that was held down with an elastic band. An image of a typical specimen during the wet phase of testing may be seen in Figure 3.5.

(a) (b)

Figure 3.5: Typical ponding specimen during either the wet or dry phase of testing. (a) Wet phase. (b) Dry phase.

The dry phase of a wet/dry cycle began when the saltwater contained within the specimen's reservoir was removed with the use of a vacuum. Removing the saltwater from a specimen involved positioning the hose of the vacuum along the front right corner of the specimen's reservoir and slowly lowering it into the saltwater. The hose remained within the front right corner of the specimen's reservoir until the majority of the saltwater was removed. The hose was then removed from the specimen's reservoir and the

specimen was then permitted to air dry, as shown in Figure 3.5 above, for a period of one week.

The wet/dry cycling of the specimens began directly after collecting the baseline resistivity and corrosion potential measurements for each specimen. Baseline readings were conducted within the first week after a group of specimens had reached an age of 28 days. Once the baseline measurement had been recorded the first wet/dry cycle began. Concrete resistivity and corrosion potential readings were then performed after every two consecutive wet/dry cycles (6 weeks).

3.3.1 Concrete Resistivity Measurements. The resistivity of each specimen was measured every six weeks with the use of a Canin^{+}, a corrosion analyzing instrument manufactured by Proceq. Canin^{+} incorporated the use of a Wenner Probe, also known as a four probe resistivity meter, which had a fixed electrode spacing of 2 in. (5.1 cm) and a nominal alternating current (AC) output of 180 μA at a frequency of 72 Hz. The equipment had an impedance of 10 MΩ and an operating range of 0 to 99 kΩcm with a 1 kΩcm resolution. The equipment was portable and required six AA batteries.

Resistivity measurements began immediately after a wet phase of testing had been completed. The saltwater retained within a specimen was first removed using the same procedure that was discussed in Section 3.3. Once the majority of the saltwater had been removed from the specimen, the remaining surface water was given time to evaporate. After approximately 30 minutes, the specimen began to reach a saturated-surface-dry (SSD) condition. The SSD condition was when the entire surface of a specimen's reservoir was visibly saturated, but did not possess any available saltwater. Paper towels were used to absorb any excess amounts of saltwater that may have accumulated within an area along the surface of a specimen's reservoir. However, this was only carried out when other areas along the surface the specimen's reservoir began to dryout. After removing the excess water, a squirt bottle, containing distilled water, was then used to re-saturate the dry areas along the specimen's surface. Once re-saturated, a template, made from ¼-in.-thick (0.64 cm) plexiglass, was then used to cover the surface of the specimen's reservoir. The template contained six set of four holes that were evenly spaced throughout its surface. A schematic layout of these holes is shown in Figure 3.6.

The holes were of the same diameter and were slightly larger than that of the Wenner Probe's four electrodes.

(a) (b)

Figure 3.6: Concrete resistivity equipment and the locations along a specimen where resistivity measurements were taken. (a) Canin^{+} equipment and Wenner Probe. (b) Locations where resistivity measurements were taken.

Preparation of the Wenner Probe consisted of removing the four sponges, partially inserted within the probe's electrodes, and letting them soak within distilled water. The sponges remained within the distilled water until the surface of the first specimen had reached the SSD condition. After the template was properly position within the specimen's reservoir, the sponges were then reinserted into the Wenner Probe's four electrodes. The Wenner Probe was then attached to the Canin^{+} and the resistivity of the specimen was measured.

A specimen's resistivity was measured at the six locations that may be seen in Figure 3.6. While conducting the measurements, any accumulation of water beneath the template was removed using paper towels. A measurement was deemed complete the moment the Canin^{+} continually reported a value to within 0.2 kΩcm. After completing

the first three measurements along a specimen, the four sponges located at the ends of the Wenner Probe's four electrodes, were re-saturated with distilled water through a dipping process. Once the sponges had been re-saturated the three remaining measurements were then taken.

3.3.2 Corrosion Potential Measurements. The corrosion potential of the rebar embedded within a specimen was measured immediately after the specimen's resistivity readings were recorded. Using the Canin^{+} equipment, which had an operating range of ±999 mV and incorporated a copper/copper sulfate half-cell, the corrosion potential at three locations along the length of each embedded bar was measured. These locations were spaced 6 in. (15 cm) on center and were offset a distance 3 in. (7.6 cm) from a specimen's side. A schematic layout of the locations in which potential readings were taken along the surface of a specimen may be seen in Figure 3.7 below.

(a) (b)

Figure 3.7: Corrosion potential equipment and the locations along a specimen where corrosion potential measurements were taken. (a) Canin^{+} equipment with copper/copper sulfate half-cell. (b) Locations along a specimen where corrosion potential measurements were taken.

Prior to conducting the baseline corrosion potential measurements of the first set of 10 specimens, the half-cell was prepared in accordance with the operating manual. The half-cell's cap, which contained a wooden plug underneath a sponge, was removed and placed within distilled water for approximately one hour. While soaking the wooden plug, the copper sulfate solution was prepared. The solution required a 10 to 4 ratio (by weight) of distilled water to copper sulfate crystals, plus an additional ½ teaspoon of copper sulfate crystals. Following the 10 to 4 ratio, the solution was prepared using 1.16 oz (33.0 g) of distilled water and 0.47 oz (13.2 g) of copper sulfate crystals. The solution was then transferred to the half-cell where an additional 0.14 oz (4.0 g) of copper sulfate crystals were added to the solution. The half-cell was then closed using the cap containing the saturated wooden plug. During the weeks when the half-cell was not in use, the end of the cell containing the wooden plug was capped to prevent the plug from drying out.

Before measuring the corrosion potential of an embedded bar contained within a specimen, the exposed steel along one end of the bar was cleaned. Cleaning of the steel was considered complete the moment a bright metal to bright metal connection between the bar and the voltmeter (or Canin^{+}) was achieved. The connection between the positive terminal of the voltmeter and the bar was made through the use of an alligator clip, as shown in Figure 3.7. After securely connecting the voltmeter to the bar, the half-cell was then connected to the voltmeter's negative terminal. The sponge attached to the end of the half-cell was then dipped into distilled water until it became fully saturated. Once the sponge was saturated, the three points, as can be seen in Figure 3.7, corresponding to the bar that was currently connected to the voltmeter were located with the use of a ruler. Measurements were then carried out by gently placing the half-cell upon each of the three locations. The recorded values were based on the Canin^{+}'s ability to automatically acquire a value once a reading had become stable. After the three values were recorded, the sponge was then re-saturated and the corrosion potential values for the three remaining bars embedded within the specimen were obtained using the same procedure.

3.3.3 Forensic Evaluation. Upon completion of the 54-week-long ponding test, a forensic evaluation was conducted on each group of specimens. The forensic evaluation involved a visual examination of the reinforcing bars embedded within a

specimen after they were carefully removed from the concrete. When it was deemed necessary, areas along selected bars were cross-sectioned and examined microscopically to further understand the coating's characteristics. Prior to the removal of the reinforcement, cores were taken from a portion of the selected specimens and the chloride profiles were developed.

3.3.3.1 Chloride content analysis. Among the 25 specimens, three specimens were chosen to undergo a chloride content analysis. Of the three specimens, one contained epoxy-coated rebar, one contained 50/50 enamel-coated rebar, and one contained uncoated rebar. The chloride analysis conducted upon these specimens involved determining the water soluble chloride content within multiple samples of concrete powder. The samples of powder were collected at various locations along the depth of a core. A core was removed from the middle of each specimen's reservoir and an additional core was taken from the corner of one of the three specimens.

Before a core was taken from a specimen, a concrete powder sample was collected from the surface of the specimen's reservoir at the location in which a core was going to be removed. Using a file, approximately 0.035 oz (1.0 g) of concrete paste, in a flower like state, was gathered from a 3-in. x 3-in. (7.6 cm x 7.6 cm) area along the surface of the specimen's reservoir. Additional powder was obtained from within the same area while using a drill and a ⅝-in.-diameter (1.6 cm) concrete drill bit. As the drill was running, it was slowly lowered onto the concrete surface and remained there for approximately two seconds. This procedure was then repeated multiple times until approximately 0.07 to 0.10 oz (2.0 to 3.0 g) of concrete powder was obtained. The penetration of the drill bit into the concrete was less than 0.1 in. (0.25 cm) and did not occur twice at any one location. After the powder was collected and placed within a labeled plastic bag, the coring location was marked on the bottom of the specimen, as shown in Figure 3.8.

Cores were obtained using a 3-in.-diameter (7.6 cm), water-cooled, diamond core bit. Each core was labeled along its bottom according to the specimen from which it was removed, followed by the letter "M" or "C" to indicate whether the core was from the specimen's middle or corner. After a core had been labeled, it was immediately placed within a plastic bag and then stored in a dry environment.

(a) (b)

Figure 3.8: Coring of a ponding specimen. (a) Coring locations. (b) Equipment used.

Before collecting concrete powder samples from a core, elevations along its height were marked using a pin. The marks indicated the elevations at which the concrete powder samples were to be collected. Those elevations were at distances of ¼ in. (0.64 cm), ¾ in. (1.9 cm), 1½ in. (3.8 cm), and 2 in. (5.1 cm) from the top surface, as shown in Figure 3.9. The top of the core was considered to be the area in which the surface powder sample was collected prior to coring. After the core was properly marked, it was placed within a vise that was securely attached to a drill press. As can be seen in Figure 3.9, a steel disk was positioned between the top of the core and the vise. This was done so to prevent any spalling of the core while collecting the powder sample located at a distance of ¼ in. (0.64 cm) from the top of the core. The alignment of the vise and the platform of the drill press were then adjusted so that the ¼ in. (0.64 cm) mark coincided with the ⅜-in.-diameter (0.95 cm) concrete drill bit. Once the mark was in line with the drill bit, a portion of the core's outer edge was removed by drilling to a depth of approximately ¼ in. (0.64 cm). This initial amount of powder was removed with compressed air. A paper plate was then attached to the perimeter of the core using scotch tape, as shown Figure 3.9. The drill bit was then reinserted into the ¼-in. (0.64

cm) deep hole that was previously drilled and 0.05 to 0.07 oz (1.5 to 2.0 g) of concrete powder was collected by drilling to a depth of approximately 2 in. (5.1 cm). The powder sample was then placed within a labeled plastic bag and the surrounding surfaces were cleaned using compressed air. This procedure was then repeated until concrete powder samples were collected from each of the four elevations marked along the depth of a core.

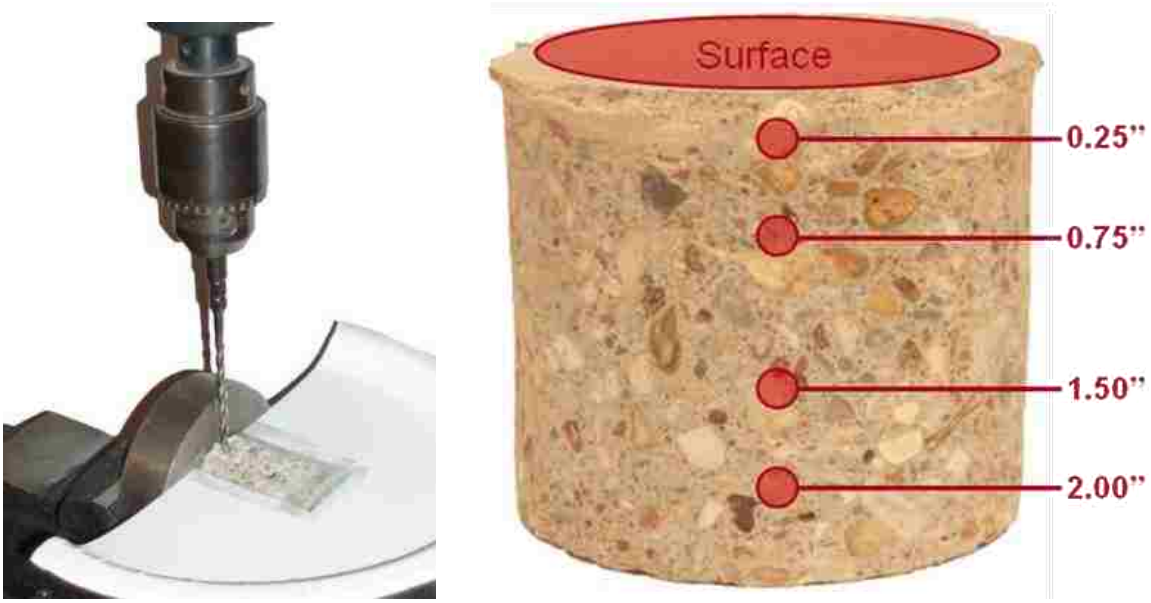

(a) (b)

Figure 3.9: Gathering of concrete powder samples. (a) Drilling procedure. (b) Locations along a core where concrete powder samples were collected.

Using Rapid Chloride Testing (RCT) equipment manufactured by Germann Instruments, Inc., the concentration of water soluble chlorides contained within each powder sample was determined. Using the graduated ampoule and compression pin that were included in the RCT kit, 0.053 oz (1.5 g) of concrete powder, from a single location along the height of a core, was measured. The powder was then transferred to a vial containing 0.304 fl-oz (9 mL) of an extraction liquid that was composed of 96 percent deionized water and 4 percent hydrogen peroxide (H_2O_2). The vial was then shaken for a

period of 5 minutes. After a vial had been shaken, the contents within the vial were then filtered into a vial containing 0.034 fl-oz (1 mL) of a buffer solution. The buffer solution consisted of 24 percent hepes ($C_8H_{18}N_2O_4S$) and 76 percent deionized water. While filtering the contents from one solution to the other, the chloride selective electrode was prepped and calibrated according to the directions provided by the manufacturer.

Prepping of the electrode consisted of filling it with a wetting agent that contained 2 percent potassium nitrate (KNO_3), 3 percent potassium chloride (KCl), and 95 percent deionized water. Any air bubbles entrapped within the electrode were removed by gently taping the exterior surface of the electrode with a finger. Once prepped, the electrode was then connected to a voltmeter and inserted into one of four vials containing a solution with a known chloride concentration. The four calibration liquids included within the RCT kit contained chloride concentration levels of 0.005, 0.020, 0.050, and 0.500 percent. Those four chloride concentrations produced voltage readings of approximately 100 mV, 72 mV, 49 mV, and -5 mV respectively. After removing the electrode from a vial, it was rinsed off using distilled water and then blotted dry with a tissue. The recorded voltage readings were then plotted upon a log chart that contained units of voltage in the x-axis and percent chlorides by weight of concrete in the y-axis. The four points were then connected by three straight lines which were drawn with the use of a straight edge. A data sheet containing this log chart may be seen in Figure A - 7.

After successfully filtering the solution from one vial to the other, the solution was then quickly shaken for 1 to 2 seconds. The calibrated electrode was then inserted into the vial and remained there until the voltage reading stabilized to within 0.2 mV. Once stable, the voltage reading was then recorded and the chloride content was determined by using the log chart that contained the data which was previously obtained from the calibration liquids. The electrode was then removed from the vial, rinsed with distilled water and blotted dry with a tissue.

3.3.3.2 Removal of reinforcement. Removal of reinforcing bars from a specimen was achieved by dividing the specimen into nine sections. The layout of the nine sections may be seen in Figure 3.10. The removal of a specimen's nine sections was done in a systematic order while using an air chisel that was oriented in either a 90° or 45° position, as shown in Figure 3.11.

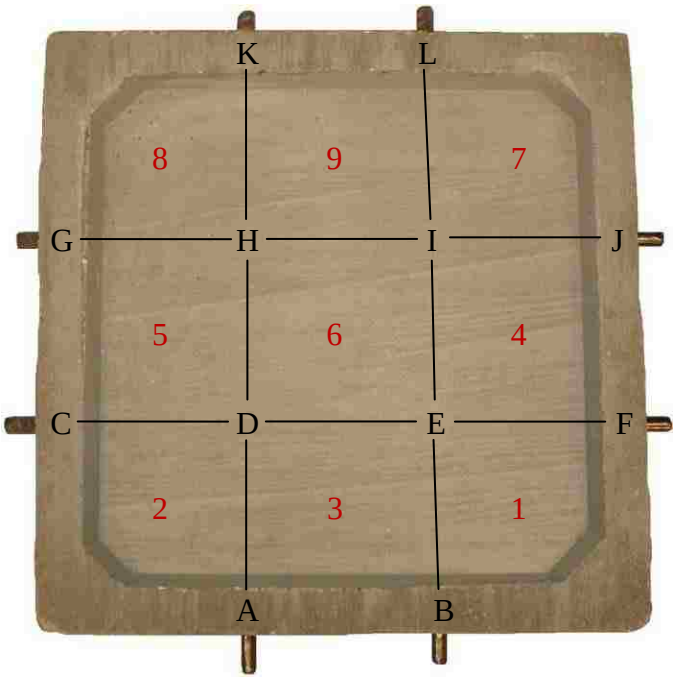

Figure 3.10: The nine sections of a ponding specimen.

Before removing the first section of a specimen, the 1-in.-high (2.5 cm) retaining wall surrounding the specimen's reservoir was removed using the air chisel. The nine sections were then removed in the order in which they are labeled in Figure 3.10. The three sections lying left of line AK and right of line BL were removed by chiseling in the 90° position along the black lines bordering each individual section. As the chisel began to approach the underlying reinforcement, it was then forced into the 45° position, which drove the chisel inward towards the section being removed. The chisel remained in this position until the section was removed from the overall specimen.

Section 3 was removed by chiseling along line DE and two additional lines that ran parallel to lines AD and BE. These two lines were located approximately 1 in. (2.5 cm) away from the edge of the section. Chiseling along these lines began in the 90° position until a groove was formed. Once a groove was constructed, the chisel was then placed in 45° position which drove the chisel towards the embedded reinforcement. As the chisel approached the reinforcement, wedges of concrete were jarred free and

removed. After carefully exposing the entire top half of the embedded reinforcement lying beneath lines AE and BE, the chisel was then placed along line DE. Chiseling along line DE began in the 90° position and was then switched to the 45° position once the chisel approached the underlying reinforcement. The section was then removed by hand along with the rebar lying beneath line CF. Section 6 was removed from the specimen using the same procedure that was used to remove section 3, while section 9 was removed using minimal effort.

Any loose material along the length of each of the four reinforcing bars was removed by hand. Afterwards, each bar was visually examined and photographed.

(a) (b)

Figure 3.11: Positioning of the air chisel. (a) 90° position. (b) 45° position.

3.3.3.3 Cross-sectional examination. In addition to visual examination, microscopic cross-sectional examination was used to evaluate the steel-coating interface at the intentionally damaged areas along a portion of the epoxy-coated reinforcing bars.

When a cross-section of a selected specimen was taken, the specimen was first cut into two pieces at a location that was approximately ½ in. (1.3 cm) from an area of interest. Depending upon availability or maintenance issues, the saw used to cut the

specimens was either a band-saw or a diamond-bladed chop-saw that incorporated the use of water during the cutting process. If the chop-saw was used, the two remaining pieces of the specimen were immediately dried upon the completion of the cut with the use of paper towels. The piece of the specimen containing the area of interest was then mounted within an epoxy.

Mounting of the specimens involved a PVC mold and a low viscosity, clear epoxy. The epoxy used during this process was manufactured by Allied High Tech Products, Inc. and required a resin to hardener ratio of 10 to 3, by weight. A polyvinyl chloride (PVC) cap, with an inner diameter of 1 in. (2.5 cm), was used to form the epoxy around the selected specimen. Prior to casting the epoxy, a thin uniform layer of petroleum jelly was applied along the mold's inner surface to act as a bond breaker. The epoxy and rebar specimen were then placed into the PVC mold and allowed to cure for at least 12 hours. Once cured, the specimen was removed from the PVC mold and cleaned. A slice of the specimen was then taken across the area of interest using one of the two saws previously mentioned. The slice was then labeled according to the specimen from which it was taken and then subsequently polished.

Polishing consisted of holding the face of the exposed steel against an 8-in.-diameter (20 cm) rotating platform that contained polishing paper. An assortment of five polishing papers, all of different grit, was used during the polishing process. The order of the five grits used, starting with the coarsest and ending with the finest was 180, 320, 600, 800, and 1200. The polishing papers were made with silicon carbide grit and were manufactured by Allied High Tech Products, Inc. A steady stream of water was used to continually saturate the surface of the polishing paper fixed upon the rotating platform. Once polishing was complete, the specimen was removed from the platform and carefully wiped dry with a Kimwipe tissue. Polishing of a specimen was deemed complete the moment a smooth transition zone between the coating and the steel was obtained. Examination of a finished cross-section was then conducted using a Hirox digital microscope.

3.4 RESULTS

3.4.1 Concrete Resistivity Measurements. The resistivity for each specimen group over the course of the 54 weeks of testing is shown in Figure 3.12. Each data point in the figure is an average value that represents the overall resistance of a specimen group during the 54 weeks of testing. Error bars, representing a 95 percent confidence interval for each data point, are also shown in Figure 3.12. A data point's confidence interval was developed using the standard error of a set's mean value (SEM) (ASTM G16, 1995). A data set consisted of four individual sets of six resistivity values which were gathered from the four specimens contained within each specimen group. Therefore, a data point's SEM was equal to the standard deviation of these 24 resistivity values divided by the square root of 24. A table of the resistivity values pertaining to a specific specimen within a specimen group may be found in Appendix A, starting with Table A - 2. Details about the procedure and equipment used while monitoring the resistivity of each specimen may be found in Section 3.3.1.

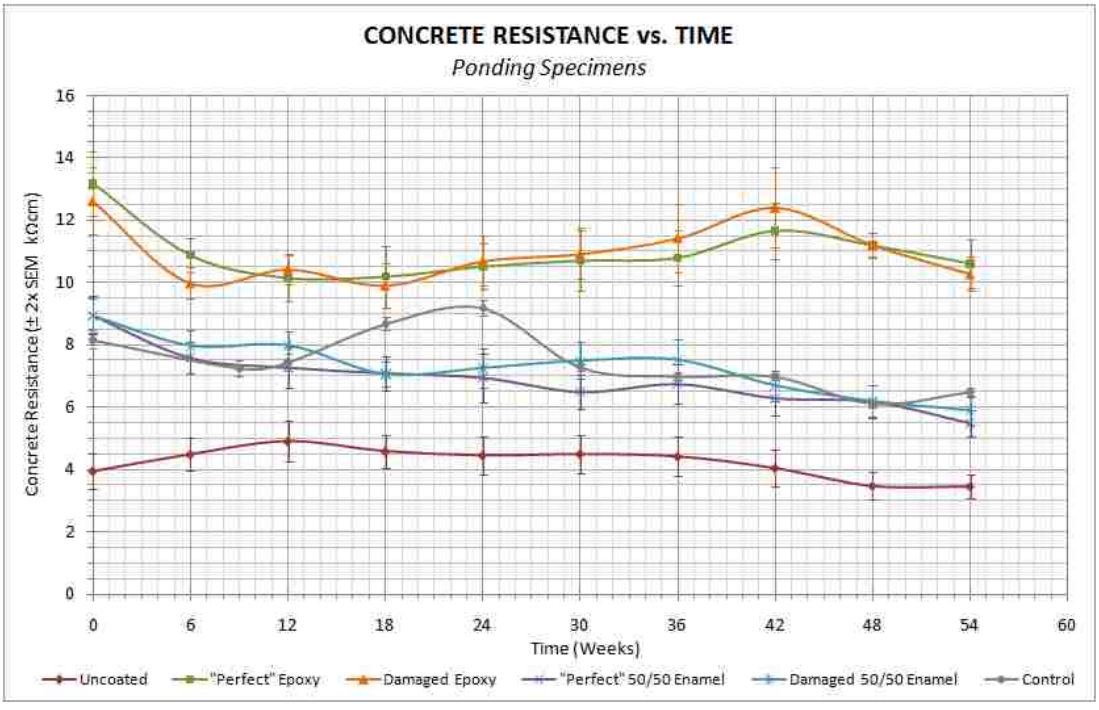

Figure 3.12: The trend in the average resistance for each specimen type during the 54 weeks of testing.

As shown in Figure 3.12, the resistivity for each group of specimens remained relatively constant during the testing period. Both the "perfect" and damaged 50/50 enamel specimens shared approximately the same resistance throughout the 54 weeks of testing. The same can be said about the specimens containing epoxy-coated rebar. Both the "perfect" and damaged epoxy groups reported equivalent overall resistance values of 11.0 kΩcm. A specimen group's overall resistance was calculated by averaging the group's ten data points shown within Figure 3.12. The overall resistance for each of the six groups of specimens, along with the 95 percent confidence interval corresponding to each value, is shown in Figure 3.13.

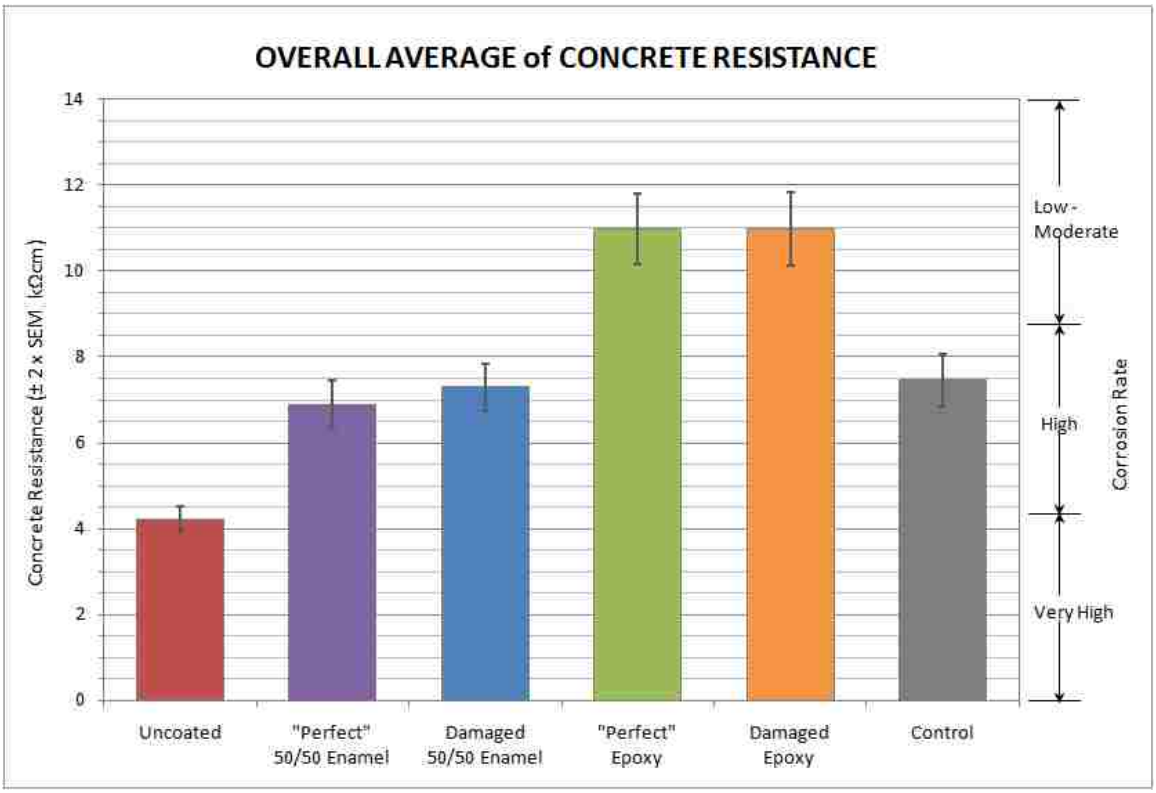

Figure 3.13: The overall average resistance of each specimen type throughout the testing period.

Using Table 2.1 and the overall resistance values reported in Figure 3.13, the corrosion rate of the reinforcing bars contained within each specimen group was generalized assuming that the bars were depassivated. With an overall resistance value of 4.2 kΩcm, the uncoated specimens exhibited the lowest resistance out of the six specimen groups. This low resistance correlated to a "very high" corrosion rate of the uncoated reinforcement. As stated earlier, both groups containing 50/50 enamel-coated reinforcement reported similar resistivity values throughout the testing period. The average overall resistance of the two groups was 7.1 kΩcm, which correlated to a "high" corrosion rate of the 50/50 enamel-coated bars. The highest overall resistance was reported by the two groups containing epoxy-coated rebar. Both groups reported an overall resistance value of 11.0 kΩcm, which correlated to a "low to moderate" corrosion rate of the epoxy-coated reinforcement. As a basis for comparison, the group containing unreinforced specimens reported an overall resistance of 7.5 kΩcm.

3.4.2 Corrosion Potential Measurements. Corrosion potential measurements for the five groups of reinforced specimens is shown in Figure 3.14. Each data point within the plot represents an average potential value for the four specimens contained within each group. Error bars, representing a 95 percent confidence interval for each data point, are also shown in Figure 3.14. A data point's confidence interval was developed using the standard error of a data set's mean value (SEM). A data set consisted of four individual sets of twelve potential measurements which were gathered from the four specimens contained within each specimen group. Therefore, a data point's SEM was equal to the standard deviation of these 48 potential measurements divided by the square root of 48. A table of potential measurements pertaining to a specific specimen within a specimen group may be found in Appendix A, starting with Table A - 13. Details about the procedure and equipment used while conducting the measurements may be found in Section 3.3.2.

As shown in Figure 3.14, all five groups follow a similar trend in corrosion resistance, which decreases over time. However, there are relative differences between the groups. Throughout the 54 weeks of testing, the two groups containing epoxy-coated bars reported the greatest corrosion resistance (more positive half-cell potential) of the five groups, while the lowest corrosion resistance (more negative half-cell potential) was

reported by the uncoated group. The two 50/50 enamel groups reported a corrosion resistance (half-cell potential) between the epoxy and uncoated specimens. Furthermore, the two enamel groups reported similar potential values throughout the test, with the "perfect" 50/50 enamel group consistently reporting the lower (more negative) of the two potential values.

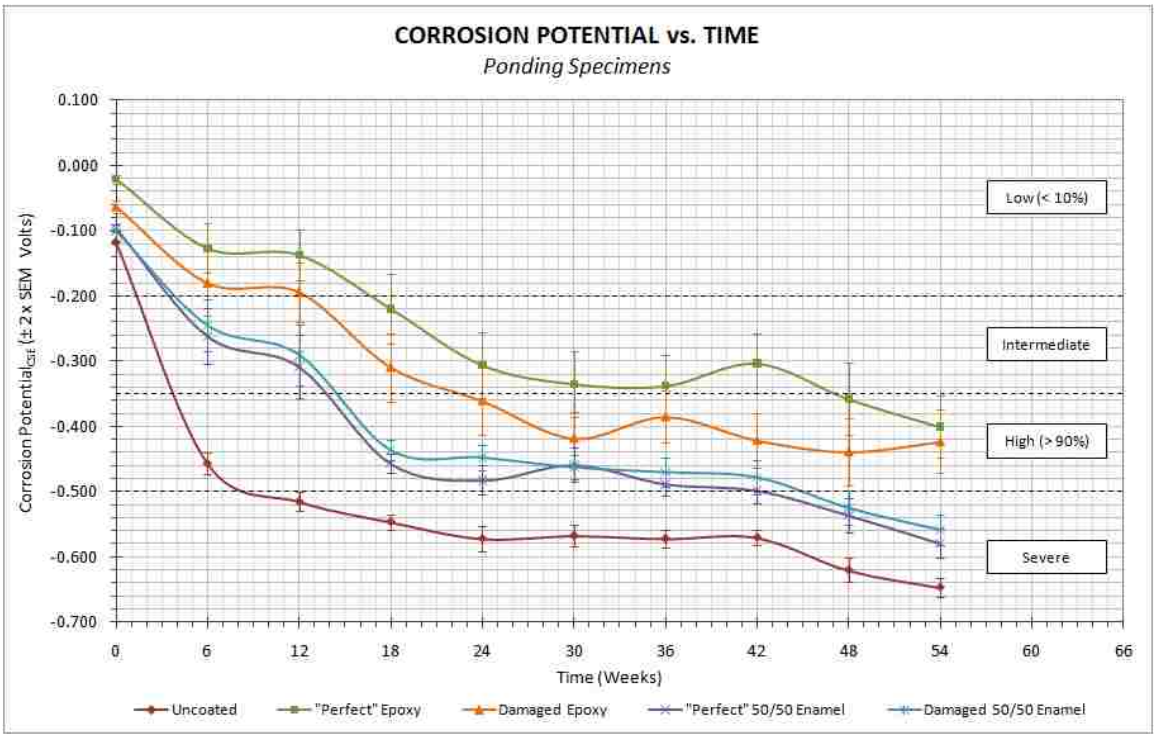

Figure 3.14: The trend of the average corrosion potential of each specimen group during the 54 weeks of testing.

As shown in Figure 3.14, the average potential for each specimen group changed significantly within the first 24 weeks of testing. During the 30 weeks that followed, the potential of each specimen group gradually decreased and by week 54 each group reported an average potential of less than -350 mV, which would indicate a high probability of corrosion. The final potential value for each specimen group is shown in Figure 3.15. The average potential values stated in the figure were calculated using the

final potential measurements collected from each specimen contained within a specimen group. Using error bars, the standard error within a specimen group's final potential value is also shown in Figure 3.15. Of the five groups, both the "perfect" epoxy group and damaged epoxy group reported the greatest distribution in potential measurements; whereas the potential measurements collected from the uncoated group showed the smallest distribution.

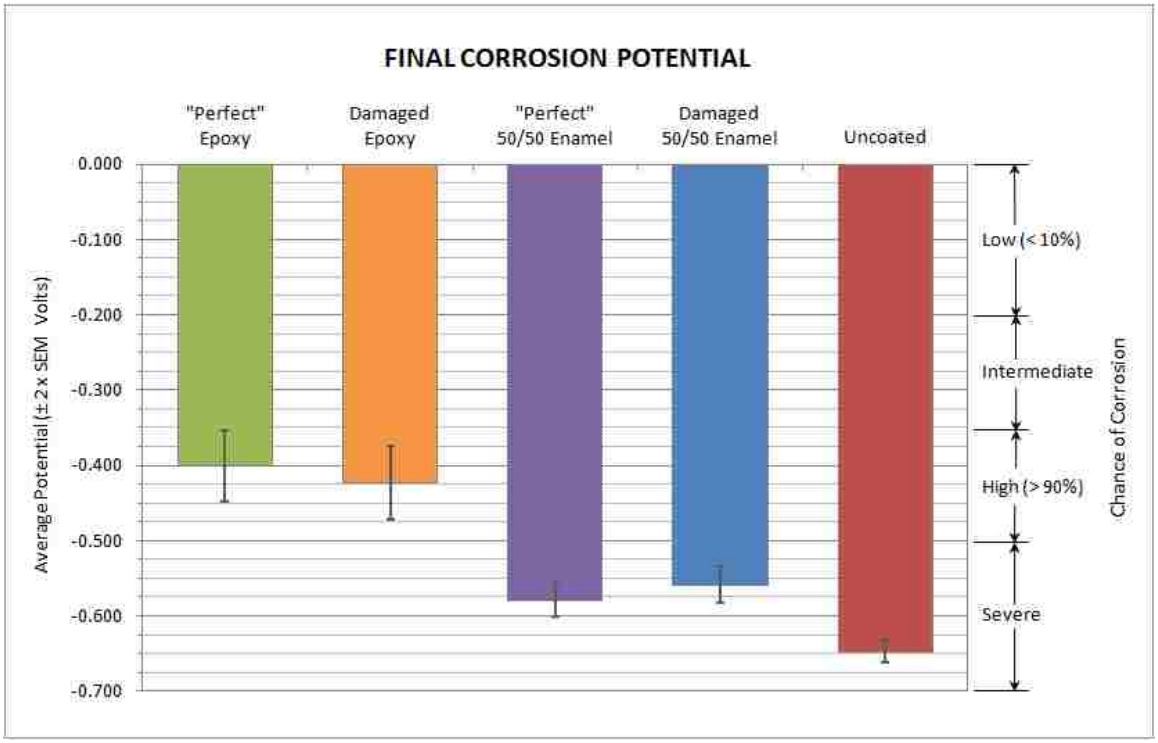

Figure 3.15: An average representation of the final corrosion potential of each specimen group at week 54.

Using Table 2.2 and the average potential values shown in Figure 3.15, the probability of the bars corroding within each specimen group was determined at the end of the testing period. Of the five specimen groups, the "perfect" 50/50 enamel group, damaged 50/50 enamel group, and the uncoated group reported final average potential values of less than -550 mV. Within those three groups, no individual specimen reported

an average corrosion potential of greater than -500 mV. This indicted a "severe" chance that each of the four specimens included within the three groups contained reinforcement that had begun to corrode. The two remaining groups, "perfect" epoxy and damaged epoxy, had final average potential values of -400 mV and -425 mV, respectively. This correlated to a "high (> 90%)" chance that a specimen belonging to either of those two groups contained corroding reinforcement. Moreover, the average potential of each of the four individual specimens contained within those two groups varied significantly, as each group contained one specimen that possessed a "severe" chance of corrosion and another specimen that possessed an "intermediate" chance of corrosion.

3.4.3 Forensic Evaluation. Included within this section are the results of the chloride-ion analysis and the visual examination of the reinforcing bars contained within each ponding specimen.

3.4.3.1 Chloride-ion analysis. Chloride profiles for three reinforced specimen groups are shown in Figure 3.16. As expected, a large concentration of water soluble chlorides was discovered along the surface of each specimen that was tested. The chloride concentration within each core dropped significantly from around 0.9 percent at the surface to approximately 0.35 percent at a depth of ¼ in. (0.64 cm). The chloride concentration then decreased further to a value of approximately 0.05 percent at a depth of 2.0 in. (5.1 cm). However, the chloride concentration within the core that was taken from the specimen containing uncoated reinforcement began to increase at some point between the depths of ¾ in. (1.9 cm) and 1½ in. (3.8 cm). As shown within Figure 3.16, the chloride concentration within this core continued to increase to a value of 0.6 percent at a depth of 2.0 in. (5.1 cm). Details about the procedure and equipment used while conducting the chloride-ion analysis may be found in Section 3.3.3.1.

Using the chloride profiles that were developed for the epoxy and 50/50 enamel specimen, as shown in Figure 3.16, the average chloride concentration at depths of ½ in. (1.3 cm) and 1½ in. (3.8 cm) were approximately 0.29 and 0.15 percent, respectively. It was within that depth range that the reinforcement for each specimen was located. Using the two chloride concentrations, along with the information provided in Table 2.3, the reinforcement embedded within the 20 specimens was considered to be under a "high" risk of corrosion.

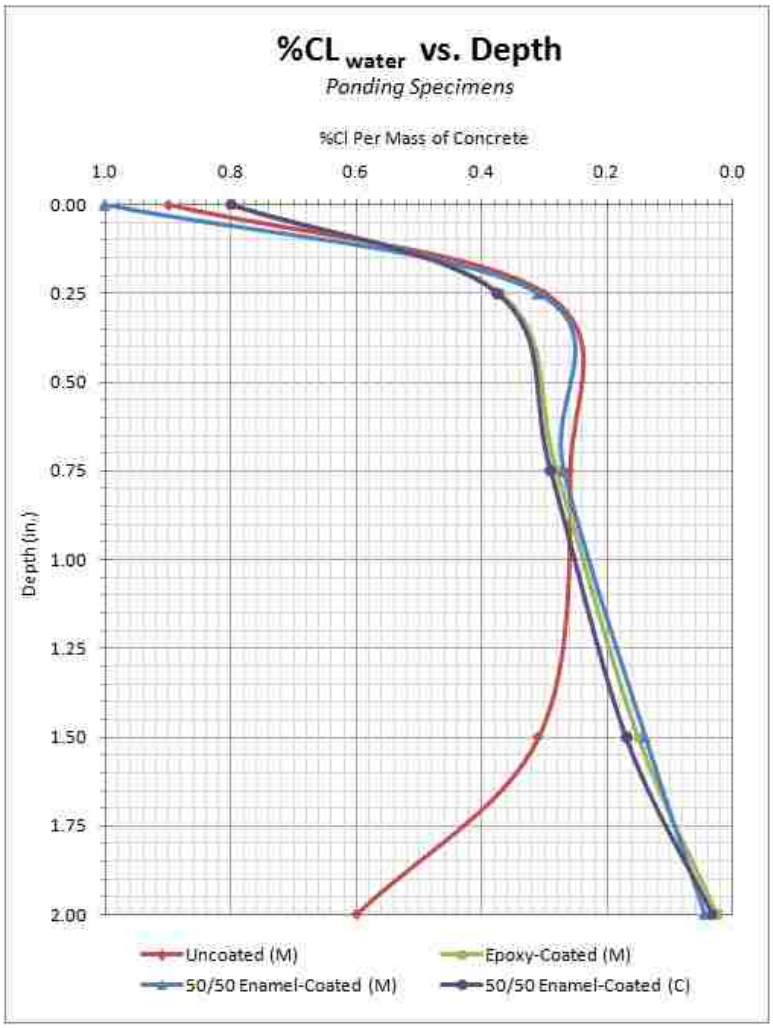

Figure 3.16: Typical chloride profiles for the 25 ponding specimens.

3.4.3.2 Uncoated bars. Within the first 8 weeks of testing, a portion of the specimens containing uncoated reinforcement began to show hairline cracks along the surface of their reservoir. The cracks were located directly above the reinforcement that had a cover of ½ in. (1.3 cm). By the 17th week, the cracks were fully developed and half of the specimens began to show signs of leaking from the reservoir. The leaking of a specimen was attributed to the crack penetrating through the thickness of a specimen's reservoir wall. Each wall that showed signs of leaking was patched with one layer of Loctite's Aquamarine Epoxy. During the weeks that followed, the cracks continued to

grow and by week 40, a portion of the cracks reappeared within the previously epoxied sections of a specimen's reservoir wall. A second layer of Aquamarine Epoxy was then applied to the newly formed cracks. An image of a typical crack that formed along the surface of a specimen's reservoir is shown in Figure 3.17.

Figure 3.17: Cracking along the surface of the specimens containing uncoated rebar.

The forensic evaluation of the uncoated group of specimens revealed that each of the four bars contained within a specimen exhibited signs of corrosion. Of the four bars contained within a specimen, the two located closest to the surface of the specimen's reservoir showed significant signs of corrosion, whereas the two bars lying furthest from the surface showed moderate signs of corrosion. This can be seen in Figure 3.18, which shows a typical set of four bars that were removed from a specimen that reported a maximum average potential of -662 mV at 54 weeks and an average resistance of 3.5 kΩcm throughout the testing period. The two bars labeled "3" and "4" in Figure 3.18 were positioned closest to the surface of the specimen's reservoir. Notice how bars "3" and "4" show more significant signs of corrosion than bars "1" and "2," which were position furthest away from the surface of the specimen's reservoir.

Figure 3.18: A typical set of uncoated reinforcing bars after being removed from a ponding specimen.

The reason for the widespread corrosion along bar "4" was due to a crack that was located directly above the bar. The crack was fully developed by the 17th week of testing and extended the entire width of the specimen. This crack was either caused by or exacerbated by the buildup of corrosion along the bar. The local areas of corrosion seen along the three remaining bars are most likely due to the low concrete resistance and the high levels of chlorides that were observed within the specimen. Images of uncoated bars that were contained within the group's three remaining specimens are shown in Appendix A, starting with Figure A - 9.

3.4.3.3 50/50 enamel bars. During the forensic evaluation of the specimens containing 50/50 enamel-coated rebar, a significant amount of the 50/50 enamel coating was unintentionally removed from each bar during the forensic examination. On average, a typical bar lost approximately 50 percent of its coating while being removed from a specimen. The majority of the coating that was detached from a bar was well adhered to the surrounding concrete. Portions of the coating that was attached to the concrete indicated red rust stains along its inner surface, as shown in Figure 3.19.

Figure 3.19: Red rust observed along the inner surface of a segment of 50/50 enamel that remained attached to a section of concrete.

The condition of the "perfect" and damaged 50/50 enamel-coated reinforcing bars was identical. Similarly to the uncoated specimens, both the "perfect" and damaged 50/50 enamel-coated specimens contained two bars that showed significant signs of corrosion (bars "3", "4", "7", and "8" in Figure 3.20), whereas the two remaining bars included within each specimen exhibited moderate signs of corrosion (bars "1", "2", "5", and "6"). A typical set of "perfect" and damaged 50/50 enamel-coated bars may be seen in Figure 3.20. The four "perfectly" coated bars shown in Figure 3.20(a) were removed from a specimen that reported a maximum average potential of -589 mV at 54 weeks and an average resistance of 6.0 kΩcm throughout the testing period. The four damaged 50/50 enamel-coated bars shown in Figure 3.20(b) were removed from a specimen that reported a maximum average potential of -575 mV at 54 weeks and an average resistance of 6.8 kΩcm throughout the testing period. Images of "perfect" and damaged 50/50 enamel-coated bars that were removed from the three remaining specimens contained within each specimen group are shown in Appendix A, starting with Figure A - 13.

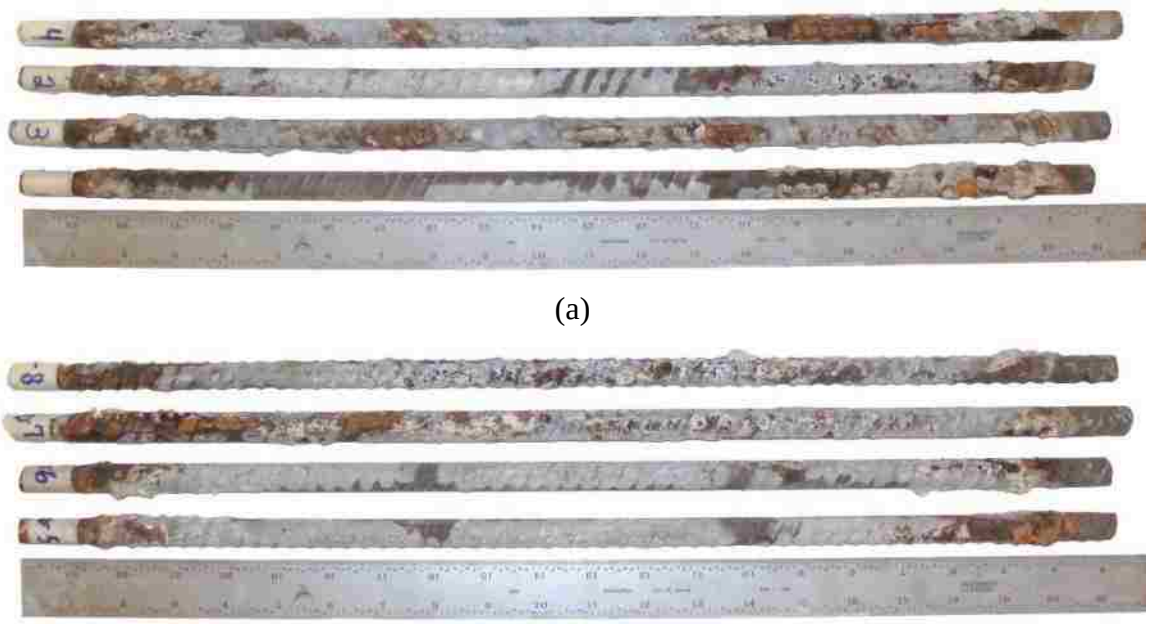

(a)

(b)

Figure 3.20: A typical set of "perfect" 50/50 enamel-coated and intentionally damaged 50/50 enamel-coated bars after being removed from a specimen. (a) "perfect" 50/50 enamel-coated bars. (b) Intentionally damaged 50/50 enamel-coated bars.

3.4.3.4 Epoxy bars. While visually examining the "perfect" epoxy-coated reinforcing bars, no significant signs of corrosion were observed. However, a typical bar did show minor signs of corrosion within damaged areas that appeared to have been pre-existing. As stated in Section 3.2.1, two layers of Rebar Green Epoxy Paint were applied to all pre-existing areas of damage along each epoxy-coated bar prior to testing. However, while removing the epoxy-coated bars from the specimens, the Rebar Green Epoxy Paint adhered to the concrete and as a result a portion of the pre-existing areas of damage were re-exposed, as shown in Figure 3.21(a). An overall view of a typical set of "perfectly" epoxy-coated bars may be seen in Figure 3.21(b). The bars shown within Figure 3.21(b) were removed from a specimen that reported an average potential of -316 mV at 54 weeks and an average resistance of 9.9 kΩcm throughout the testing period. Images of "perfect" epoxy-coated bars that were removed from the three remaining

specimens contained within the specimen group are shown in Appendix A, starting with Figure A - 21.

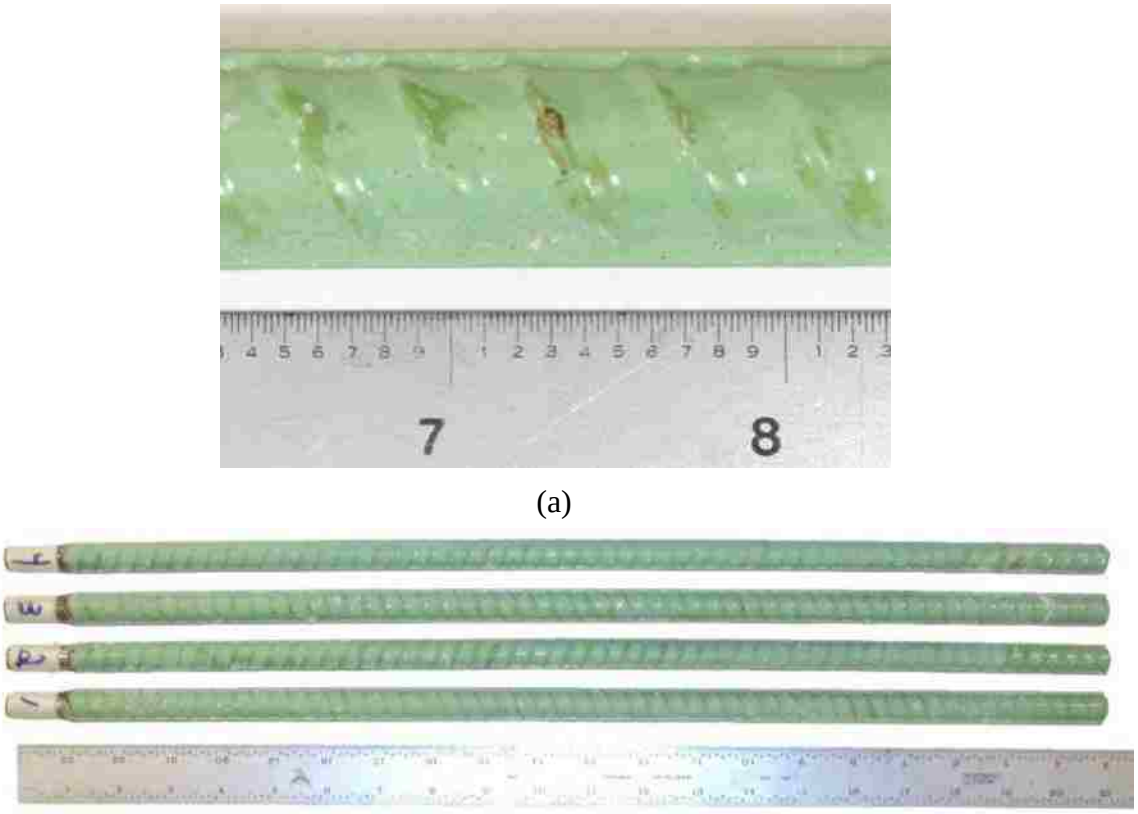

(a)

(b)

Figure 3.21: The condition of a typical set of "perfect" epoxy-coated bars after being removed from a specimen. (a) A re-exposed area of damage. (b) Overall condition of a typical set of "perfect" epoxy-coated bars.

Similarly to what was observed along the "perfect" epoxy-coated bars was also seen along the intentionally damaged epoxy-coated bars. Each intentionally damaged epoxy-coated bar exhibited areas of pre-existing damage that were re-exposed while the bar was removed from the specimen in which it was embedded. On average, one of five intentionally damaged areas (as shown in Figure 3.22(a)) exhibited significant signs of

corrosion, as can be seen in Figure 3.22(b). When a cross-section was taken through an area of damage that showed signs of corrosion, rust was observed beneath the coating as shown in Figure 3.22(c). However, a cross-section through an area of damage which exhibited no signs of corrosion revealed that the epoxy was well adhered to the steel and no rust was present beneath the coating. An overall view of a typical set of intentionally damaged epoxy-coated bars is shown in Figure 3.22(d). The bars were removed from a specimen that reported a maximum average potential of -440 mV at 54 weeks and an average resistance of 9.7 kΩcm throughout the testing period. Images of intentionally damaged epoxy-coated bars that were removed from the three remaining specimens contained within the specimen group are shown in Appendix A, starting with Figure A - 29. Also included in Appendix A, starting with Figure A - 33, are additional cross-sectional images that were taken through areas along selected bars that showed signs of damage.

(a) (b)

Figure 3.22: The condition of a typical set of intentionally damaged epoxy-coated bars after being removed from a specimen. (a) An intentionally damaged area along an epoxy-coated bar prior to testing. (b) The same area as shown in Part a of this figure after testing.

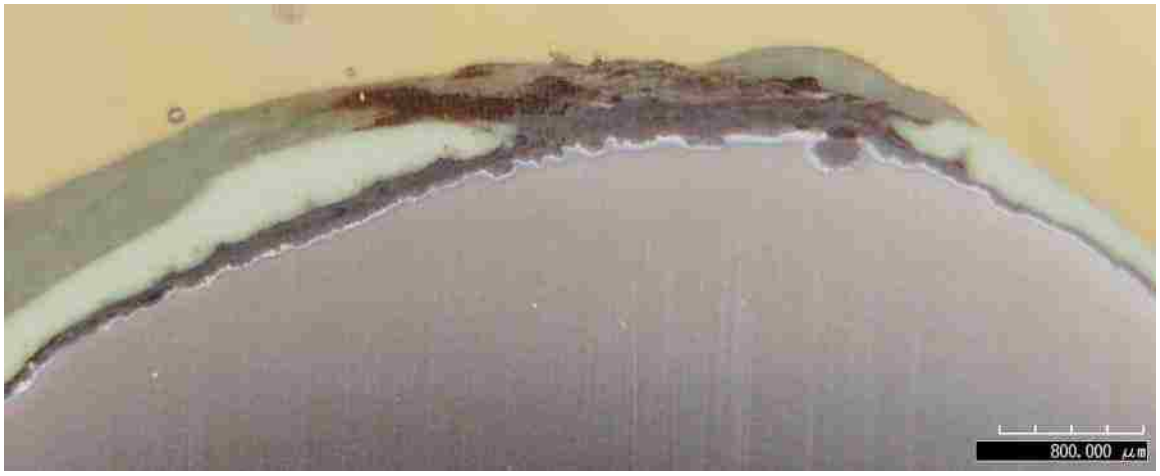

(c)

(d)

Figure 3.22 (cont.): The condition of a typical set of intentionally damaged epoxy-coated bars after being removed from a specimen. (c) A cross-sectional view of the intentional damaged area after testing. (d) Overall condition of a typical set of intentionally damaged epoxy-coated bars.

3.5 FINDINGS

3.5.1 Concrete Resistivity Measurements. After evaluating the concrete resistivity results, it was determined that the concrete resistance of a reinforced specimen was a function of the type of coating that was applied to the specimen's reinforcement. It was also determined that the resistance of a damaged epoxy or 50/50 enamel specimen was unaffected by the intentionally damaged areas along the specimen's reinforcement. On average, a specimen containing either "perfect" or damaged epoxy-coated reinforcement reported a resistance that was 1.47 times that of an unreinforced specimen's resistance. On average, specimens belonging to either the "perfect" or damaged 50/50 enamel group reported similar resistivity values to that of an unreinforced

specimen. The group containing uncoated reinforcement reported an average resistance that was 44 percent lower than the average resistance of an unreinforced specimen.

The significance of these values is as a relative indication of the corrosion resistance of the concrete/rebar system for each coating type. With the reinforced specimens having been constructed with the same concrete and steel reinforcement, the discrepancy within the resistivity readings is most likely attributed to the coating applied to the embedded reinforcement. This result would indicate that the epoxy coating provided the greatest resistance to the applied electrical current, while the uncoated bar provided the least resistance. The 50/50 enamel-coated bars provided a degree of resistance between that of the epoxy and uncoated bars.

3.5.2 Corrosion Potential Measurements. Figure 3.14 offers some very valuable information on the corrosion resistance of the coatings as a function of time when exposed to a high chloride environment. Although the trends are very similar for each group, the relative locations of the plots indicate the relative corrosion resistance of each coating. The epoxy coating provides the greatest degree of resistance, while the uncoated bars offer the least. The 50/50 enamel-coated bars offer a degree of resistance between that of the epoxy and uncoated bars.

However, when examining similar coatings, there are some noticeable differences. For instance, as shown in Figure 3.14, a 28 percent decrease in corrosion resistance was observed, on average, when comparing the damaged epoxy group to that of the "perfect" epoxy group throughout the duration of the test. An average 4 percent increase in corrosion resistance was seen when comparing the damaged 50/50 enamel group to that of the "perfect" 50/50 enamel group throughout the course of the 54-week-long test. To further verify these findings, paired t-tests were conducted upon the corrosion potential data gathered from both the 50/50 enamel specimens and the epoxy specimens. The p-values obtained from the two t-tests indicate that a significant difference does exist between the results obtained from the damaged 50/50 enamel and "perfect" 50/50 enamel specimens (p-value of 0.003) along with the results collected from the damaged epoxy and "perfect" epoxy specimens (p-value of 0.00004). Taking into account these results, it was found that the corrosion protection provided by the epoxy coating was jeopardized when damaged, while the corrosion protection provided

by the 50/50 enamel was unaltered when damaged. Although the corrosion protection of the 50/50 enamel coating was unaffected by the areas of damage, the coating consistently provided a lower level of protection when compared to that of the intentionally damaged epoxy-coated bars.

The final set of corrosion potential measurements indicated a "high (> 90%)" probability that the reinforcement contained within each specimen group was actively corroding. With a severe chance that the reinforcement contained within the two 50/50 enamel groups and the uncoated group had begun to corrode.

3.5.3 Chloride-ion Analysis. Through chloride-ion analysis, it was determined that a chloride profile, similar to the one labeled "uncoated" in Figure 3.16, can develop when cracks form along the surface of a specimen's reservoir. However, only four out of the 25 specimens in this study showed signs of cracking along the surface. A typical chloride profile developed from a specimen that exhibited no visible signs of cracking showed high levels of chlorides near the surface and a low concentration at a depth of around 2.0 in. (5.1 cm). A typical chloride profile is shown in Figure 3.16. Most importantly, the chlorides penetrated the concrete to the depth of the reinforcement in sufficient concentration to attack the passive layer and initiate corrosion.

3.5.4 Forensic Evaluation. Forensic evaluation of the specimens revealed significant variation in the condition of the four bars contained within a specimen that belonged to the uncoated group or either of the two 50/50 enamel groups. The reinforcing bars located closest to the surface of a specimen's reservoir exhibited significant signs of corrosion, while the two remaining bars, which were positioned at a lower elevation within the specimen, showed moderate signs of corrosion. On the other hand, the condition of the four reinforcing bars contained within a specimen belonging to either the "perfect" or damaged epoxy group were found to be substantially identical and exhibited only very limited corrosion.

A loss in adhesion between the epoxy coating and the steel was observed within a portion of the cross-sections that were taken through locations in which the epoxy coating was intentionally damaged. When a loss of adhesion was observed, the steel beneath the coating indicated signs of corrosion.

It was also observed that when a typical 50/50 enamel-coated reinforcing bar was removed from a specimen, half of the coating was detached from that bar. The portion of the coating that was unintentionally removed from a 50/50 enamel-coated bar was found to be securely attached to the surrounding concrete.

4 SALT SPRAY TEST

4.1 INTRODUCTION

A modified ASTM B117 salt spray test was used to assess the corrosion resistance of three enamel coating configurations along with a standard epoxy coating. The twelve weeks of testing began on August 26, 2009 and ended on November 20, 2009. The test consisted of subjecting a total of 64 specimens to a series of wet/dry cycles. Half of the 64 specimens were coated smooth steel bars while the remaining 32 specimens were coated deformed steel bars. Each group of 32 specimens contained 8 50/50 enamel-coated bars, 8 double enamel-coated bars, 8 pure enamel-coated bars, and 8 epoxy-coated bars. After testing, the uniformity of each coating, as well as the steel-coating bond along both the deformed and smooth bars, was evaluated through visual and microscopic cross-sectional examination.

4.2 SPECIMEN DETAILS & MATERIALS

Each specimen was approximately 11 in. (28 cm) in length and was made from either ½-in.-diameter (1.3 cm) smooth steel dowels or No. 4 (No. 13) deformed bars, with all steel conforming to ASTM A615 Grade 60. After the specimens were sectioned to the proper length, the ends were beveled and two layers of Loctite's Aquamarine Epoxy were uniformly applied along the ends of each specimen, as shown in Figure 4.1. The first layer of epoxy was cured a minimum of 12 hours prior to application of the second layer. While applying the second layer of epoxy, specimens were examined for areas of damage, similar to those shown in Figure 4.2(a), which may have been caused through handling and/or transporting of the specimens. During this process, a layer of epoxy was applied to each area exhibiting signs of damage. A layer of epoxy was also applied to any rare imperfections that were observed within each coating. These areas of imperfections were deemed as manufacturing defects and were seen within each type of coating. An area that would have been deemed as a manufacturing defect is shown in Figure 4.2(b) below. Before starting the test, the second layer of epoxy was cured a minimum of 48 hours.

Figure 4.1: A typical smooth and deformed salt spray specimen prior to testing.

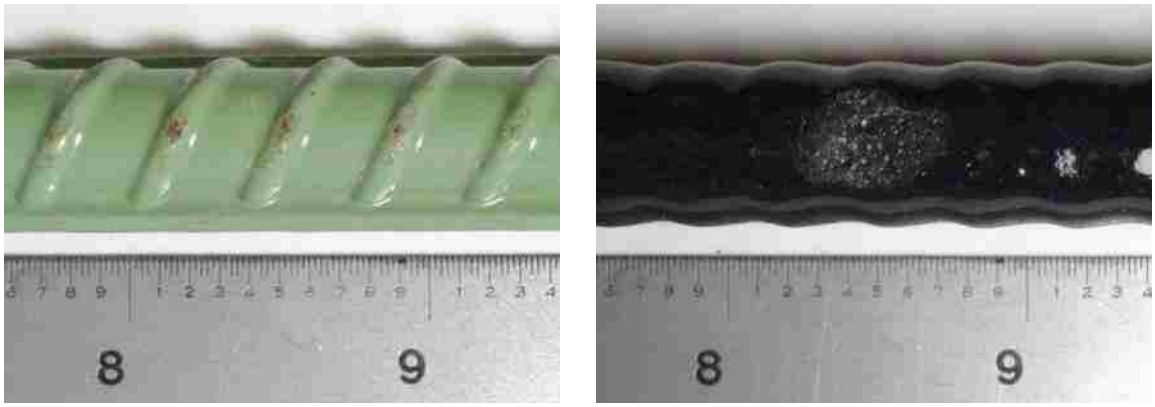

(a) (b)

Figure 4.2: Vulnerable areas along a coated specimen. (a) Damage due to handling and/or transporting of an epoxy-coated specimen. (b) Manufacturing defect along a pure enamel-coated specimen.

Prior to testing, one end of each specimen was labeled with black lettering and a number ranging from 1 to 8. The number corresponded to a specific specimen within a sample set; whereas the lettering represented the type of coating applied to that specific specimen. Letters "D," "F," "P," and "EP" indicated whether a specimen was coated with double enamel, 50/50 enamel, pure enamel, or epoxy, respectively. The sides and back of each specimen were also labeled using red lettering. In relation to a specimen's label, a letter "A" was placed along the specimen's right side while its back and left side were labeled with a "B" and "C," respectively. This labeling system was used to

systematically reposition each specimen within the salt spray chamber throughout the twelve weeks of testing.

4.3 TESTING & PROCEDURE

During the twelve weeks of testing, the set of 64 specimens was broken up into two groups of 32 specimens. Group 1 contained all of the deformed bars, and Group 2 contained all of the smooth bars. Each specimen remained within its assigned group throughout the entire testing period.

During the course of testing, the two groups were subjected to wet and dry environments at alternate times. For example, while the deformed specimens were subjected to the dry condition, the smooth specimens would have been subjected to the wet condition, or vice versa. The two groups of specimens were transferred from one condition to the other on Monday, Wednesday, and Friday of each week.

The total duration of the salt spray test was 2000 hours with each of the two groups spending half of the time in a dry environment and the remaining 1000 hours in a salty fog (wet) environment. With the two groups of specimens being transferred from one environment to the other on Monday, Wednesday, and Friday of each week, the typical duration of the wet or dry phase of testing was approximately 48 or 72 hours long. After a group had spent 72 hours within the wet environment, the group would spend the following 72 hour phase in the dry environment. This cycling was maintained throughout the 2000 hours of testing and resulted in each group spending an equal amount of time in both the wet and dry environments.

4.3.1 Repositioning of the Specimens. Specimens were repositioned within the salt spray chamber in a systematic order after every wet/dry cycle. This repositioning of the specimens ensured that each specimen received an equivalent amount of exposure to the corrosive environment by the time the test had been completed.

As shown in Figure 4.3, four holding racks, spaced 6 in. (15 cm) on center, were located within the chamber. Each holding rack supported a total of eight specimens that were spaced approximately 4 in. (10 cm) from each other. The eight specimens contained along a holding rack were coated with the same coating. The holding rack in which each of the four groups of specimens were designated depended upon where the

specimens were positioned during the previous wet phase. For instance, using the coordinate system show in Figure 4.3, specimens that were previously located along holding racks "A," "B," "C," and "D" would have been relocated to holding racks "D," "A," "B," and "C," respectively. Along with relocating the four groups of specimens within the chamber, the order of the specimens within each group was also changed. Specimens previously positioned in row 1 would be placed in row 8, while the remaining 7 specimens along each rack would move up one row from their previous position. Finally, the 32 specimens within the chamber were rotated 90 degrees clockwise along their longitudinal axis. After each specimen was rotated a full 360 degrees, they were then placed upside-down within the chamber. When the specimens returned to their original position, the procedure was then repeated until completion of the test.

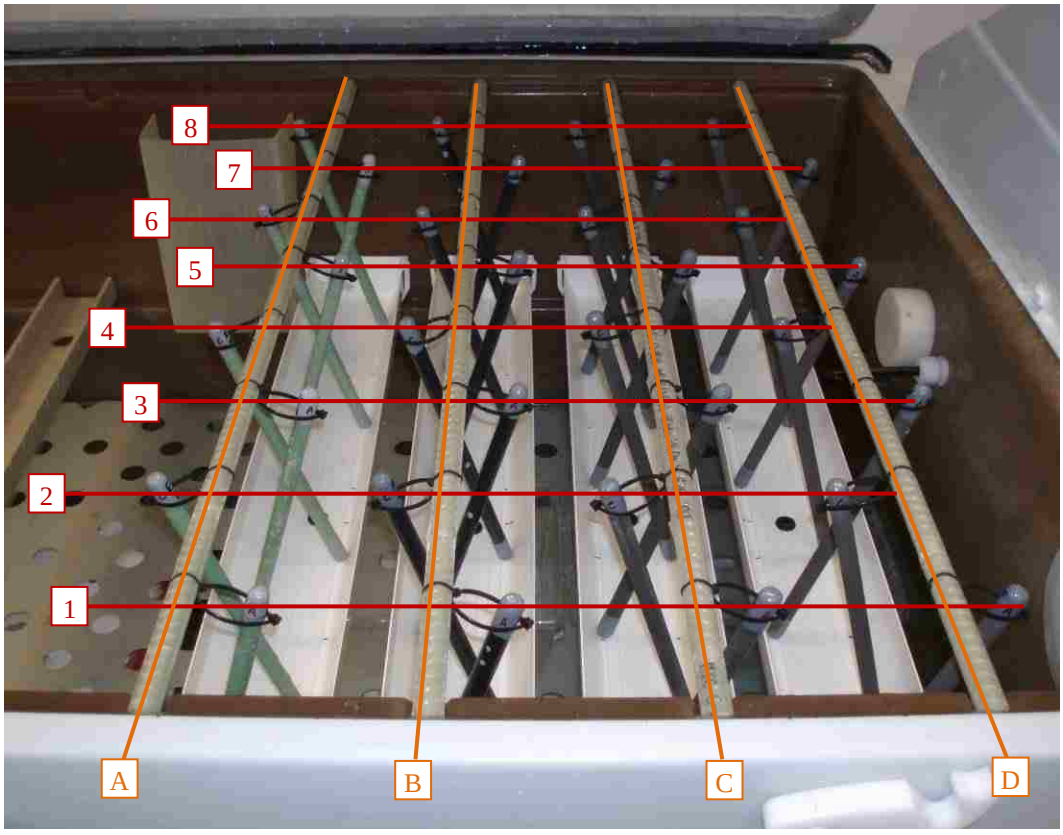

Figure 4.3: Specimen layout within the salt spray chamber.

4.3.2 Wet Phase. During the wet phase, specimens were supported by vinyl trays that spanned the width of the salt spray chamber and plastic zip-ties which were spaced every 4 in. (10 cm) along the lengths of the fiberglass rods, as shown in Figure 4.3. The fiberglass rods were spaced 6 in. (15 cm) on center from one another and were offset 4 in. (10 cm) from the chamber's side wall. Each specimen within the chamber was oriented at an angle of approximately 15 degrees from vertical in accordance with ASTM B117. A minimum distance of 3 in. (7.6 cm) was maintained between the walls of the chamber and the specimens. At no time during the test were any two specimens in contact with one another and a specimen never obstructed another specimen's exposure to the salt fog.

An atomizer located at the center of the chamber's floor was used to generate the salt fog that was constantly distributed throughout the chamber. While testing, the fallout rate of the salt fog was continually checked by positioning a plastic 3.38 fl-oz (100 mL) graduated cylinder between racks "B" and "C" in Figure 4.3 and approximately 10 in. (25 cm) from the front wall of the chamber. A 4-in.-diameter (10 cm) funnel was placed along the top of the graduated cylinder so that a greater amount of fog was collected over a standard period of time. On average, approximately 2.4 fl-oz (70 mL) of solution was collected every 48 hours during the test. The solution used throughout the testing period was composed of distilled water and 5 percent USP grade sodium chloride (NaCl) by weight. The temperature within the salt spray chamber was maintained at 95 ± 3 °F (35 ± 2 °C) during the twelve weeks of testing.

4.3.3 Dry Phase. The dry phase of the test consisted of placing 32 specimens in a dry environment with an average ambient temperature of 68 °F (20 °C) and a relative humidity of 40 to 60 percent. Racks constructed of wood and two carbon rods, as shown in Figure 4.4(a), were used to support the ends of each specimen. The racks suspended each specimen approximately ½ in. (1.3 cm) above the underlying shelf on which they were stored. The specimens were stored in an elevated position in order to enhance the flow of air around each specimen. A total of eight specimens, each spaced 1 in. (2.5 cm) on center, were distributed along the width of each rack. The eight specimens assigned to a rack were all of the same type and corresponded to the grouping within the salt spray chamber. At no time during the course of testing were any of the specimens in contact

with each other or any foreign object other than the wooden portion of the rack within which it resided. Figure 4.4(b) shows a representative view of how the 32 specimens were stored during the dry phase of the test.

(a) (b)

Figure 4.4: Specimen layout during the dry phase of testing. (a) Rack used to support a set of salt spray specimens. (b) Overall layout.

4.4 RESULTS

The results discussed within this section are based on visual observations during the course of the salt spray testing, as well as microscopic examination of sections taken at the conclusion of the test period. Values stated within this section are approximate unless otherwise noted. Photographs indicating the overall condition of each specimen are contained in Appendix B.

4.4.1 50/50 Enamel. The deformed 50/50 enamel-coated specimens performed relatively well up until the 6th week of testing, with each specimen only showing minor amounts of "pin sized" areas of corrosion that can be seen in Figure 4.5(a). However, during the 6 weeks of testing that remained, each specimen gradually began to show increased amounts of corroded areas along both the transverse and longitudinal ribs. By the 10^{th} week, the 50/50 enamel coating began to crack along a portion of the transverse ribs that had previously shown signs of corrosion. This cracking of the coating is shown

in Figure 4.5(b) below. When the test was complete, it was determined that most, if not all, of the visible corrosion had taken place along the transverse and longitudinal ribs of each specimen. On average, 57 percent of a specimen's transverse ribs and 12 percent of its longitudinal ribs showed signs of corrosion.

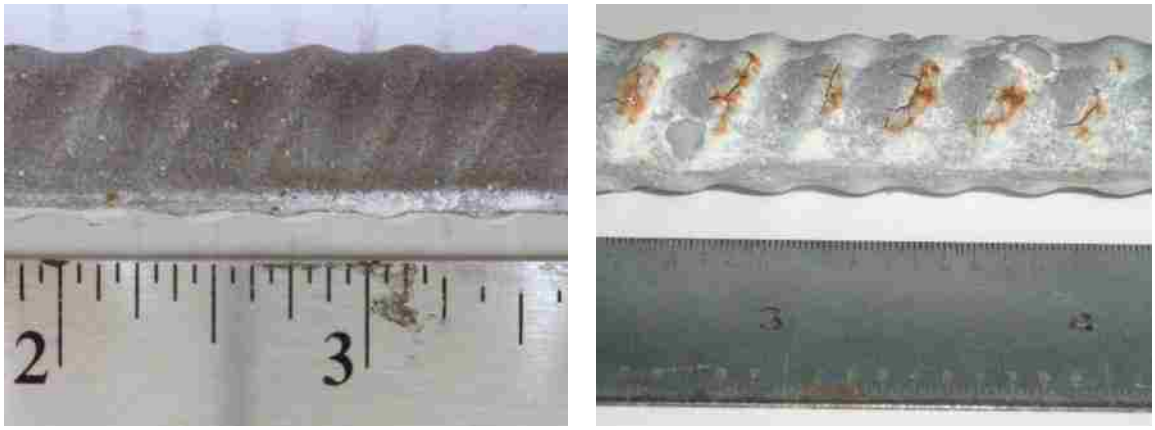

(a) (b)

Figure 4.5: The condition of a typical deformed 50/50 enamel-coated specimen after the fifth and twelfth week of testing. (a) Fifth week. (b) Twelfth week.

Similarly to the deformed specimens, the smooth 50/50 enamel-coated specimens appeared to have performed well up until the 8th week of testing. Prior to the 8th week, specimens only exhibited minor "pin sized" areas of corrosion that were spread out uniformly along the length of each specimen. It wasn't until the 10th week of testing when the severity of each specimen's condition began to show. During the 10th week of testing, the 50/50 enamel coating began to show signs of spalling around the areas that exhibited earlier signs of corrosion. When the test was completed two weeks later, 42 percent of the coating along an average specimen showed signs of spalling. When the coating along a spalled area was removed, an extensive amount of corrosion was seen along the surface of the underlying steel bar, which is shown in Figure 4.6(a). Figure 4.6(b) indicates a typical piece of the 50/50 enamel coating that shows "pin sized" areas

of corrosion along its surface while having an extensive amount of rust throughout its inner surface.

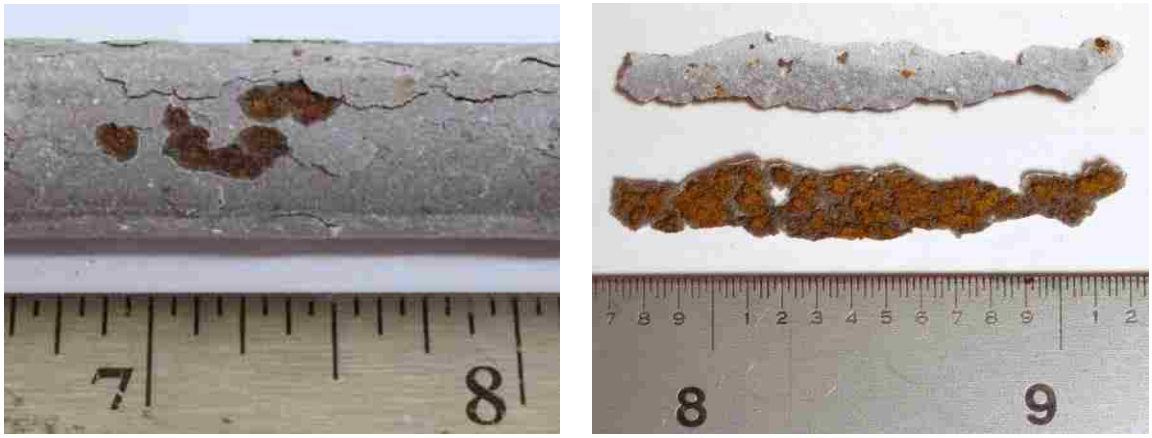

(a) (b)

Figure 4.6: The condition of the 50/50 enamel coating along a smooth specimen after twelve weeks of testing. (a) Spalling of the 50/50 enamel coating. (b) The top and bottom view of a typical piece of the 50/50 enamel coating that had fallen off of a smooth specimen shortly after completion of the testing.

Cross-sectional examination of the 50/50 enamel-coated specimens revealed that the thickness of the coating along a smooth specimen was between 8 and 12 mils (200 and 300 µm); whereas the thickness of the coating along a deformed specimen ranged from 8 and 30 mils (200 to 750 µm). This variation within the coating thickness was seen near transverse and longitudinal ribs, as shown in Figure 4.7.

The 50/50 enamel coating, throughout each cross-section, exhibited a grainy texture, which is shown in Figure 4.7(b), and a grayish brown color. However, at locations where the steel had begun to corrode, the color of the coating resembled that of red rust. This rusty-red coloring was not always uniform throughout the thickness of the coating. At times the outer surface of the coating would maintain its original grayish brown color while the inner surface of the coating became rusty-red, as shown in Figure 4.7(c).

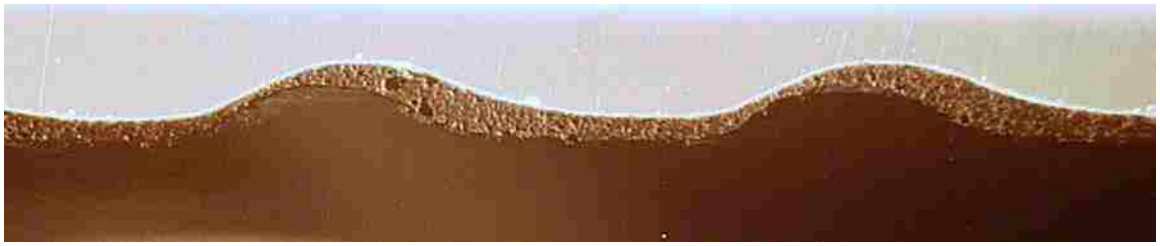

(a)

(b)

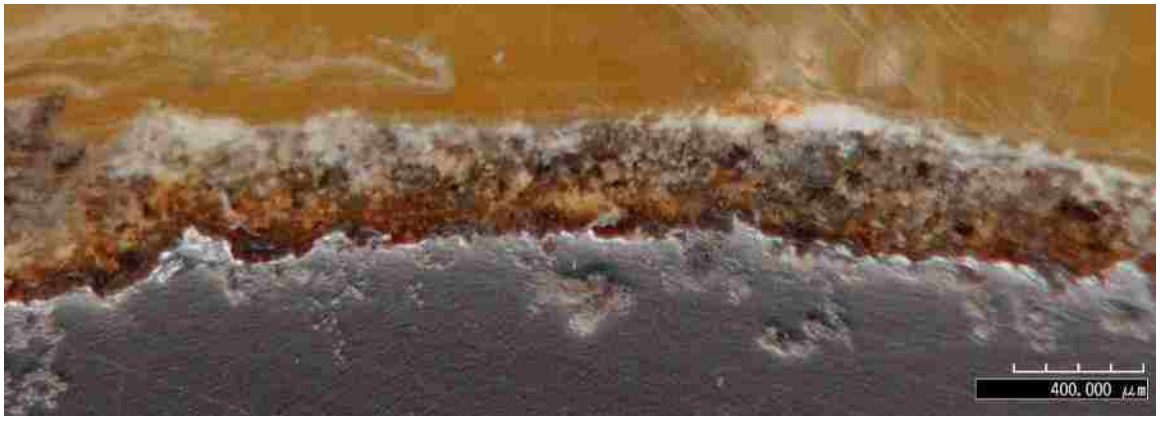

(c)

Figure 4.7: Cross-sectional views of the 50/50 enamel coating along smooth and deformed specimens. (a) A typical longitudinal view of the 50/50 enamel coating distributed along a deformed specimen. (b) A representative view of the 50/50 enamel's granular texture. (c) The color gradient seen within the thickness of the 50/50 enamel coating along a corroded section of a smooth specimen.

4.4.2 Double Enamel. The deformed double enamel-coated specimens showed "minor" signs of corrosion along a random portion of the transverse ribs within the first four weeks of testing. These areas of corrosion became more significant over the course

of the remaining eight weeks. By the time the test was complete, 18 percent of the transverse ribs along an average specimen exhibited "moderate" signs of corrosion and 31 percent showed "minor" signs of corrosion. Therefore, after the twelve weeks of testing, a total of 49 percent of an average specimen's transverse ribs showed either "minor" or "moderate" signs of corrosion. The difference between "minor" and "moderate" signs of corrosion along a corroding rib may be seen in Figure 4.8. The longitudinal ribs of each specimen showed minimal signs of corrosion with only one or two "pin sized" areas throughout each rib.

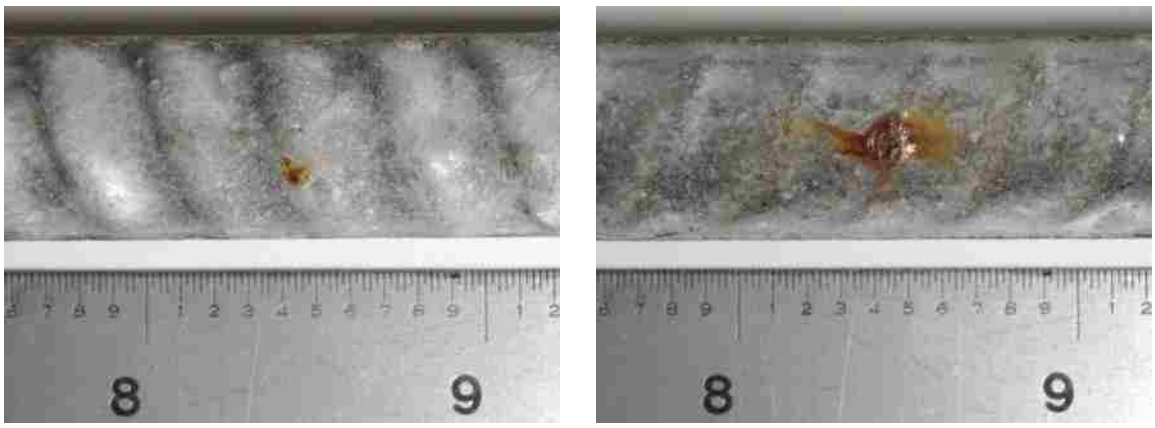

(a) (b)

Figure 4.8: Areas along a deformed double enamel-coated specimen showing various amounts of corrosion. (a) "Minor." (b) "Moderate."

The smooth double coated enamel specimens showed little signs of corrosion throughout the twelve weeks of testing. When the test was complete, each of the eight specimens had, on average, a total of eight areas that exhibited signs of corrosion. Areas that showed signs of corrosion were classified as either "minor" or "moderate." A typical "minor" and "moderate" area of corrosion may be seen in Figure 4.9. On average, three out of the eight areas that showed signs of corrosion were classified as "moderate."

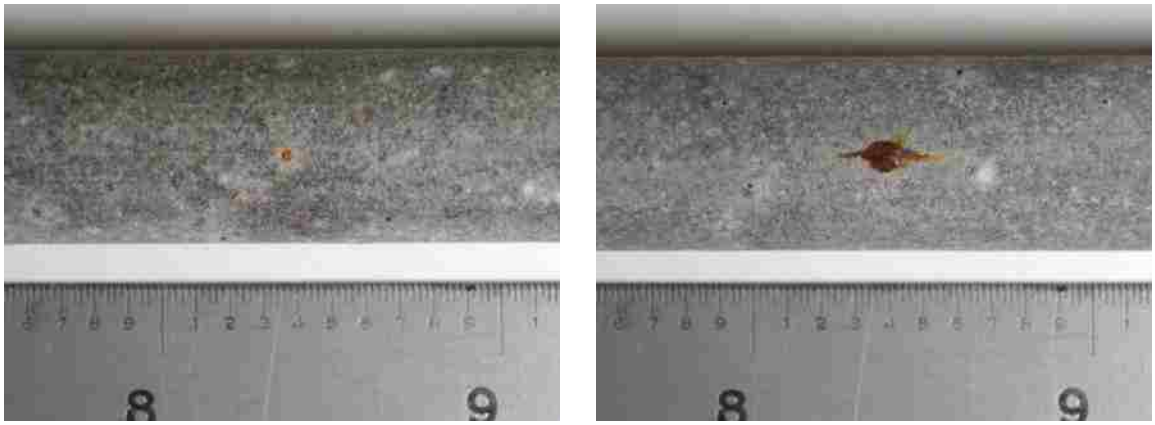

(a) (b)

Figure 4.9: Areas along a smooth double enamel-coated specimen showing various amounts of corrosion. (a) "Minor." (b) "Moderate."

The cross-sectional evaluation of the double coated enamel specimens revealed that a boundary between the first and second applied coating was maintained during the second round of firing and that only a minor amount of calcium silicate from the 50/50 enamel outer coating had percolated through the surface of the inner coating.

The double enamel coating was uniformly distributed along the lengths of each smooth specimen, which resulted in a coating thickness of around 16 mils (400 µm), as can be seen in Figure 4.10. However, the thickness of the coating along a deformed specimen fluctuated from 6 to 30 mils (150 to 750 µm). This fluctuation within the thickness of the coating was seen along the transverse ribs of the deformed specimens. At the locations where the coating was 30 mils (750 µm) thick, the boundary between the two layers was easily seen; whereas at locations along a specimen where the coating was thin, the boundary did not exist. When the boundary did not exist, the coating mainly consisted of a combination of the two applied coatings with a varying amount of calcium silicate. A typical distribution of the double enamel coating along a deformed specimen is shown in Figure 4.10.

(a)

(b)

(c)

Figure 4.10: Cross-sectional views of the double enamel coating along smooth and deformed specimens. (a) A typical longitudinal view of the double enamel coating distributed along a deformed specimen. (b) A thick portion of the double enamel coating that shows a distinct boundary between the two applied layers. (c) A thin portion of the double enamel coating showing no distinct boundary between the two applied layers.

(d)

Figure 4.10 (cont.): Cross-sectional views of the double enamel coating along smooth and deformed specimens. (d) A typical cross-sectional view of a smooth double enamel-coated specimen.

4.4.3 Pure Enamel. Within the first three days of testing, three out of the eight deformed pure enamel-coated specimens showed moderate signs of corrosion. By the second week, it was evident which of the eight specimens were performing well and which ones were not. A visual comparison between a specimen that had performed well and one that performed poorly may be seen in Figure 4.11.

Of the three specimens that showed a poor performance throughout the test, 83 percent of their transverse ribs showed signs of either "minor" or "significant" corrosion after the test was finished. The difference between "minor" and "significant" corrosion for the deformed black enamel-coated specimens is shown in Figure 4.12. An average of 58 percent of the transverse ribs that exhibited signs of corrosion along the three specimens were labeled as "significant" and 31 percent of the area along the specimens' longitudinal ribs showed extensive signs of corrosion. On average, 7 percent of the transverse ribs along the five remaining specimens showed "minor" signs of corrosion while 2 percent of the longitudinal ribs showed "significant" signs of corrosion. Among these five specimens, the average longitudinal rib showed corrosion along 3 percent of its length.

Figure 4.11: A visual comparison between a deformed pure enamel-coated specimen that performed well and one that performed poorly.

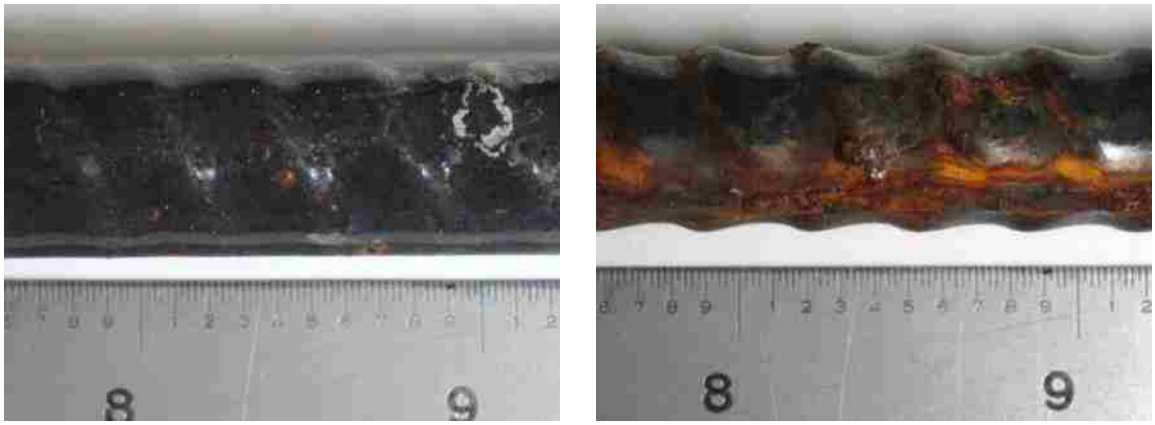

(a) (b)

Figure 4.12: Areas along a deformed pure enamel-coated specimen showing various amounts of corrosion. (a) "Minor." (b) "Significant."

The set of smooth pure enamel-coated specimens performed well throughout the twelve weeks of testing. When the test was complete, minor signs of corrosion were seen along the length of each specimen. Figure 4.13, shows a typical representation of the surface condition along a smooth pure enamel-coated specimen after testing.

Cross-sections of the smooth and deformed pure enamel-coated specimens revealed similar coating distribution patterns as those seen within the cross-sections of the 50/50 enamel-coated and double enamel-coated specimens. The coating was uniformly distributed along the smooth specimens and was approximately 10 mils (250 µm) thick; whereas, depending upon which of the eight deformed specimens were being examined, the thickness of the coating along an individual specimen ranged from 2 to 18 mils (50 to 450 µm) or 8 to 40 mils (200 to 1,000 µm), as shown in Figure 4.14(a) and

(b). Figure 4.14(c) and (d) are images along a portion of a cross-section that includes an area within the coating that was damaged. As shown in the two images, the bond between the enamel coating and the steel was maintained and only the exposed steel was corroded (i.e., no undercutting of the enamel coating occurred).

Figure 4.13: A typical representation of the surface condition along a smooth pure enamel-coated specimen after the salt spray test.

(a)

Figure 4.14: Cross-sectional views of the pure enamel coating along smooth and deformed specimens. (a) A longitudinal view of the pure enamel coating distributed along a deformed specimen that had performed well during the test.

(b)

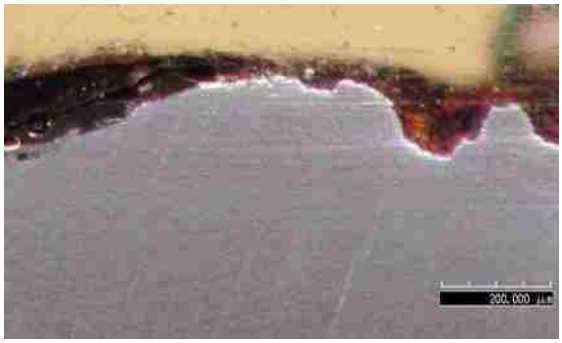

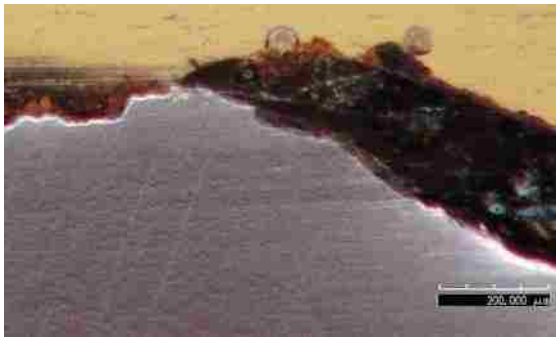

(c) (d)

(e)

Figure 4.14 (cont.): Cross-sectional views of the pure enamel coating along smooth and deformed specimens. (b) A representative view of the variation within the thickness of the pure enamel coating along a deformed specimen. (c) and (d) No undercutting of the coating was observed even after the pure enamel coating had been significantly damaged. (e) A typical cross-sectional view of a smooth pure enamel-coated specimen.

4.4.4 Epoxy. Both the deformed and smooth epoxy-coated specimens performed well throughout the duration of the test. After testing, each specimen showed minor spots of corrosion that were between 2 and 16 mils (50 and 400 µm) in diameter. Typically these spots were uniformly distributed throughout the length of each specimen, as shown in Figure 4.15, with an average deformed and smooth specimen having approximately 50 and 65 spots, respectively. The spots tended to increase in quantity and size along areas of the coating that appeared to have been degraded by excessive light exposure, as shown in Figure 4.15(c) below.

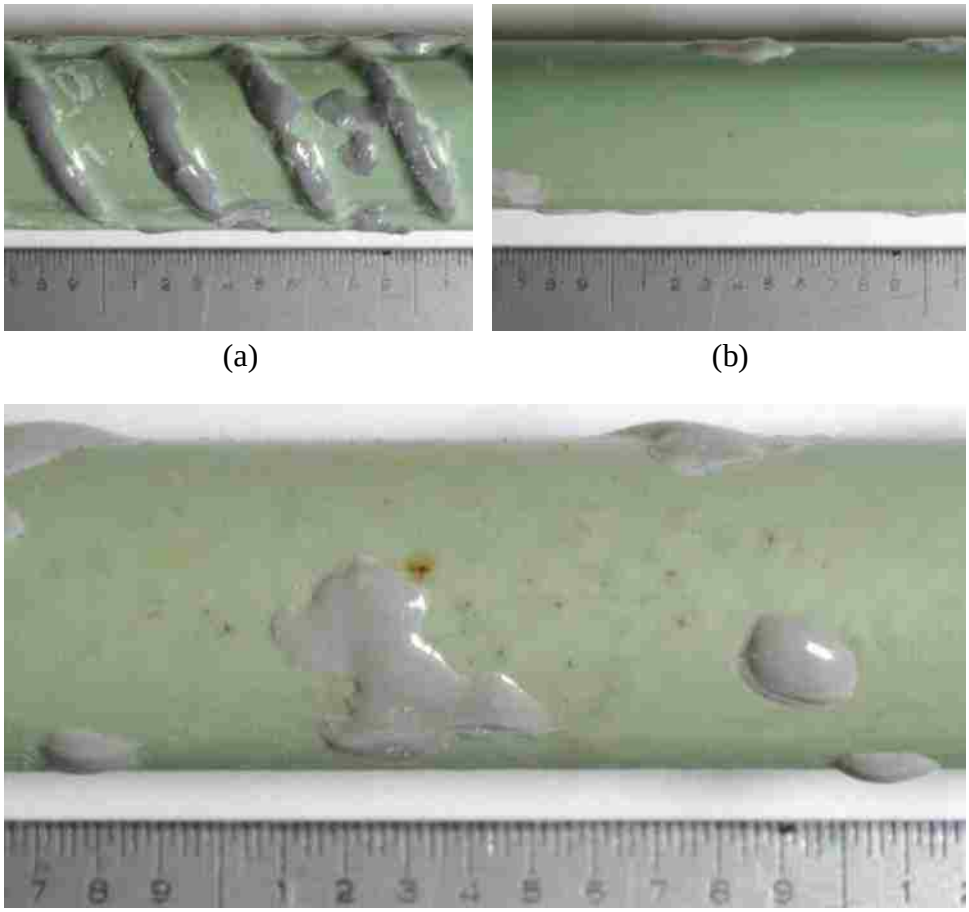

(a) (b)

(c)

Figure 4.15: Typical spots of corrosion along deformed and smooth epoxy-coated specimens. (a) Deformed specimen. (b) Smooth specimen. (c) Smooth specimen showing signs of degradation within the epoxy coating.

Cross-sections of the epoxy-coated specimens indicated a uniformly distributed coating along the lengths of both the smooth and deformed specimens. The thickness of the coating ranged from 8 to 14 mils (200 to 350 µm) and when intact, appeared to be well bonded to the steel, as shown in Figure 4.16. However, at locations along a specimen where the coating was breached, a separation between the coating and the steel was observed and the underlying steel had begun to corrode. This undercutting of the coating is shown in Figure 4.16(b).

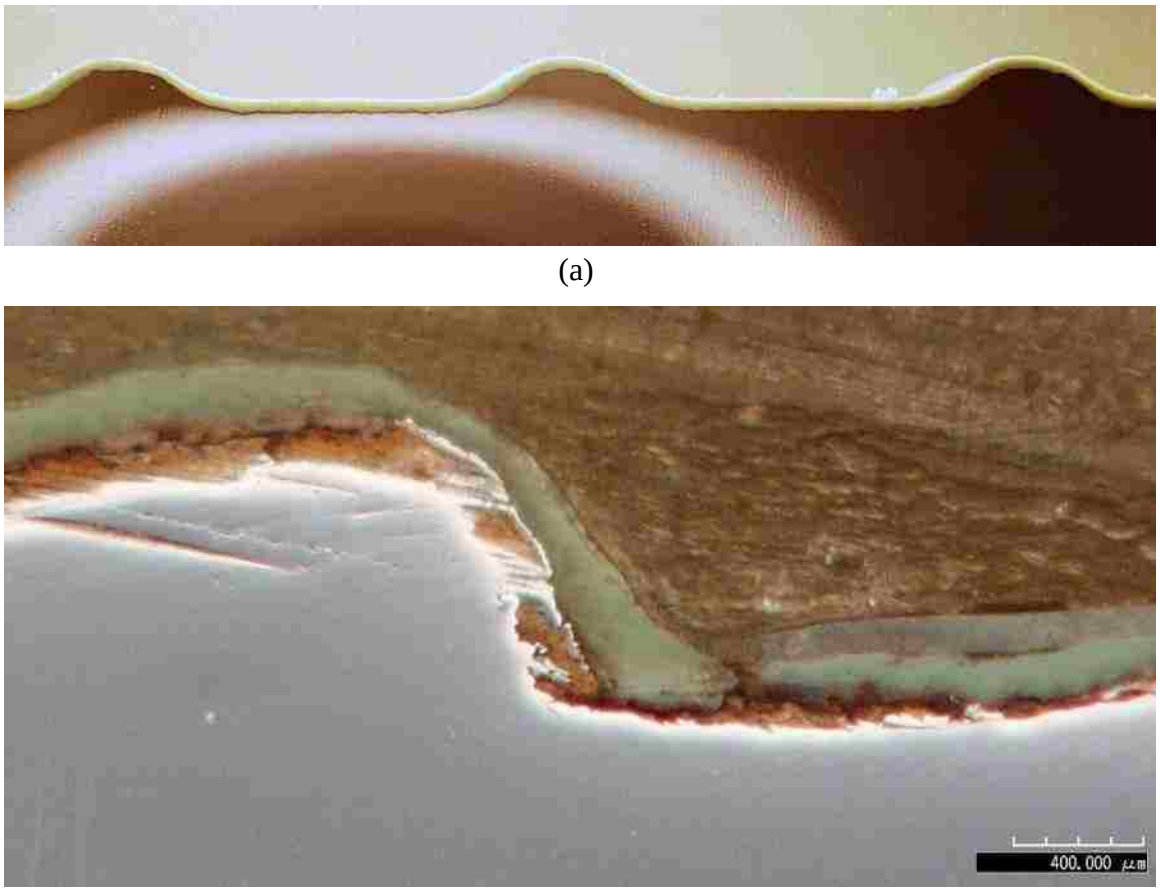

(a)

(b)

Figure 4.16: Cross-sectional views of the epoxy coating along smooth and deformed specimens. (a) A longitudinal view of the epoxy coating distributed along a deformed specimen. (b) Steel corroding underneath a slightly damaged section of the epoxy coating after testing.

(c)

Figure 4.16 (cont.): Cross-sectional views of the epoxy coating along smooth and deformed specimens. (c) A typical cross-sectional view of a smooth epoxy-coated specimen after testing.

4.5 FINDINGS

It was found that the performance of the three enamel coatings largely depended upon the coating's thickness and the concentration of calcium silicate within the coating. The uniformly coated smooth specimens, with an average coating thickness of around 8 to 16 mils (200 to 400 µm), outperformed the inconsistently coated deformed specimens that possessed thinly coated areas along their transverse and longitudinal ribs. However, although the 50/50 enamel-coated specimens shared similar coating distribution patterns as the pure and double enamel-coated specimens, it was seen that the deformed specimens outperformed the smooth specimen. This can best be explained by the large quantity of calcium silicate within the coating.

When a large quantity of calcium silicate is added to a pure enamel mixture and then fired to create 50/50 enamel, a porous material is created. The pores throughout the 50/50 enamel, as shown in Figure 4.7(b), provide pathways for oxygen, moisture, and chlorides to reach the steel. The iron oxide formed during the corrosion process then slowly begins to outwardly diffuse toward the exterior surface of the coating, as shown in Figure 4.7(c). Therefore, the time it takes for a 50/50 enamel specimen to show any significant signs of corrosion is a function of the coating's thickness and the rate of diffusion of both the corrosive elements and the iron oxide. This would explain why the inconsistently coated, deformed, 50/50 enamel specimens outperformed the uniformly

coated, smooth, 50/50 enamel specimens and why the overall performance of the smooth specimens decreased dramatically between the 8th and 10th week of testing.

The pure enamel, double enamel, and epoxy specimens all performed relatively well throughout the testing period. However, the deformed double enamel-coated specimens did show areas of weakness along a portion of their transverse ribs. These areas of weakness were thinly coated with what appeared to be an amalgamation of the two applied coatings. This mixing of the two coatings would, at times, lead to large concentrations of calcium silicate within the thinly coated sections of the coating. As a result, the coating along these sections exhibited similar properties to that of the 50/50 enamel.

The performance of a deformed pure enamel-coated specimen directly correlated to the minimum thickness of the applied coating along that specimen. The three specimens that performed poorly during the test had a minimum coating thickness of 2 mils (50 µm); whereas the five specimens that performed well during the test had a minimum coating thickness of 8 mils (200 µm). When damaged, the pure enamel coating maintained its bond with the steel and no undercutting was observed.

Both the deformed and smooth epoxy-coated specimens were uniformly coated and no significant signs of corrosion were observed along the surface of the specimens. However, when the coating showed signs of degradation in the form of discoloration, an increase in the amount of "pin-sized" areas of corrosion were observed. Undercutting of the coating was also observed along a section of a specimen that had a breach in the coating.

A summary of the results and findings obtain from the salt spray test may be found in Table 4.1 on the following page.

Table 4.1: Summary of results obtained from the salt spray test.

COATING:	BAR TYPE:	COATING THICKNESS:	RESULT:
50/50 Enamel	Deformed	8-30 mils *(200 - 750 µm)*	On average, 57 percent of a specimen's transverse ribs and 12 percent of its longitudinal ribs showed signs of corrosion (Figure 4.5).
	Smooth	8-12 mils *(200 - 300 µm)*	On average, 42 percent of a specimen's coating showed signs of corrosion induced spalling (Figure 4.6).
Double Enamel	Deformed	6 - 30 mils *(150 - 750 µm)*	On average, 18 percent of a specimen's transverse ribs exhibited "moderate" signs of corrosion and 31 percent showed "minor" signs of corrosion (Figure 4.8).
	Smooth	16 mils *(400 µm)*	On average, a specimen contained 5 "minor" and 3 "moderate" areas of corrosion (Figure 4.9).
Pure Enamel	Deformed	2 - 40 mils *(50 - 1000 µm)*	Of the eight specimens, three specimens performed poorly with 83% of the transverse ribs along an specimen showing either "minor" or "significant" signs corrosion (Figure 4.12). On average, 7% of the transverse ribs along the five remaining specimens showed "minor" signs of corrosion.
	Smooth	10 mils *(250 µm)*	Minor signs of corrosion were seen along the length of each specimen, as shown in Figure 4.13.
Epoxy	Deformed	8 - 14 mils *(200 - 350 µm)*	On average, a specimens displayed approximately 50 spots of corrsion (Figure 4.15) that ranged from 2 to 16 mils (50 to 400 µm) in diameter.
	Smooth	8 - 14 mils *(200 - 350 µm)*	On average, a specimens displayed approximately 65 spots of corrsion (Figure 4.15) that ranged from 2 to 16 mils (50 to 400 µm) in diameter.

5 ACCELERATED CORROSION TEST

5.1 INTRODUCTION

In the accelerated corrosion test (ACT) method, a constant potential is applied to the specimen and the resulting current is measured over time. The test is completed at the onset of intense corrosion, which is detected from an abrupt increase in the monitored electric current. Initially developed as a test to evaluate the corrosion resistance of post-tensioning grouts [Thompson et al., 1992], the ACT method has been extended to evaluating the corrosion resistance of steel coatings [Volz et al. 2008]. Typically, the samples consist of cylindrically cast elements, each containing a single reinforcing bar, which are then placed into a 5 percent by weight NaCl electrolyte corrosion cell. The length of time to complete this test depends on the ability of the system to resist the onset of corrosion. In general, these tests run between 300 and 1500 hours, not including sample preparation.

The benefit of the ACT is that the applied potential will force the chloride ions to attack the coated rebar. This test will thus expose any material or processing defects in the coating that would allow the transport of chloride ions to the steel surface and allow initiation of corrosion. The test will also examine the corrosion resistance of reactive enamel coatings while placed within a cementitious (high alkaline) environment.

Indirectly, the test also examined the ability to effectively coat a deformed bar through the dipping process used for the enamel coatings. This was accomplished by testing both smooth and deformed coated bars. As a basis for comparison, both uncoated and epoxy-coated bars were included within this study.

Testing began on August 11, 2009 and was completed on September 11, 2010. During that time, a total of 144 specimens were tested. Of the 144 specimens, 80 were grouted and 64 were non-grouted. Sixty-four out of the 80 grouted specimens contained bars that were coated with one of the four coatings examined within this test. The four coatings tested were: 50/50 enamel, double enamel, pure enamel, and epoxy. Half of the remaining 16 grouted specimens contained a smooth uncoated steel bar while the remaining eight specimens contained a deformed uncoated steel bar. The 64 coated specimens, included within each of the two sets, were divided into four specimen groups.

Each specimen group consisted of eight smooth and eight deformed bars that were coated with one of the four coating compositions previously mentioned.

5.2 SPECIMEN DETAILS & MATERIALS

A specimen consisted of one, 15-in.-long (38 cm), coated or uncoated steel bar that was either grouted or non-grouted. Depending upon the specimen, the bar was either a ½-in.-diameter (1.3 cm) smooth dowel or a No. 4 (No. 13), grade 60, deformed bar. Each bar used within the test conformed to ASTM A615 and was coated following ASTM A775 or as stated in Section 1.3. After the bars were coated, they were then sectioned to the proper length and a portion of their coating was removed. The removal of a bar's coating occurred along a ¾-in-long (1.9 cm) section that was located at one end of the bar, as shown in Figure 5.1. This section was located above the electrolyte of the corrosion cell and provided the electrical connection necessary for the test. While preparing the epoxy-coated bars, two additional steps were taken: beveling the end of the bar that was still partially coated and then cleaning the bar with soap and water.

Figure 5.1: A typical smooth and deformed coated bar prepared for the ACT method.

Two layers of Loctite's Aquamarine Epoxy were uniformly applied along the beveled end of each specimen, as shown in Figure 5.1. The first layer of epoxy was cured a minimum of 12 hours to prior to application of the second layer. While applying the second layer of epoxy, specimens were examined for areas of damage, similar to those shown in Figure 4.2(a), which may have been caused through handling and/or

transporting of the specimens. During this process, a layer of epoxy was applied to each area exhibiting signs of damage. A layer of epoxy was also applied to any rare imperfections that were detected in each coating. These areas of imperfections were deemed as manufacturing defects and were seen in each type of coating. An area that would have been deemed as a manufacturing defect may be seen in Figure 4.2(b). Before a specimen was grouted or tested, the second layer of epoxy was cured a minimum of 48 hours.

Bars were grouted within polyvinyl chloride (PVC) molds that were constructed using three pieces of PVC piping. The three pieces measured 5.9 in. (15 cm), 3.5 in. (8.9 cm), and 2.4 in. (6.1 cm) in length, as shown in Figure 5.2. Prior to constructing the molds, two longitudinal slits were cut along each 3.5-in.-long (8.9 cm) section of PVC. Constructing a mold involved connecting the three pieces of PVC, in the order shown in Figure 5.2, with silicone and duct tape. After securely connecting the three pieces of PVC, any silicone that had accumulated along the interior surface of the mold was removed with the use of paper towels. The partially completed mold was then set aside for a period of approximately 24 hours. After the silicone had cured, each mold was then capped using a properly sized PVC cap and PVC cement. When completed, a mold measured approximately 12.2 in. (31 cm) in length and had an inner diameter of 1¼ in. (3.2 cm). Before grouting a set of bars, each mold was filled with tap water and examined for leaks. Any mold that showed signs of leaking was either immediately fixed with use of additional duct tape or replaced by another mold.

Casting a set of specimens involved grouting a total of nine specimens in what is commonly referred to as a "neat grout." A batch of grout was prepared using approximately 10 lbs. (4.5 kg) of Type II portland cement and a water-to-cement ratio of 0.45. The grout was batched within a 2 gallon (7.6 liter) container using a high-shear mixer. After the grout had been thoroughly mixed, half of the grout was transferred to a pitcher. A plastic spacer and the epoxy-coated end of a bar were then placed within the mold. The plastic spacer was used to centrally position the bar along the bottom of the mold. Any bar that was coated with 50/50 or double enamel was first doused with deionized water using a squirt bottle. Dousing a bar with deionized water was considered complete the moment the entire coating of the bar had been saturated and excess water

began to drip from the epoxy-coated end of the bar. Once a bar was properly positioned within a mold, the mold was then filled with grout in three equally sized lifts. After each lift the bar was slowly twisted while the mold was tapped. Once fully grouted, the bar was then centrally positioned along the top of the mold using a second plastic spacer. A plastic baggie was then placed over the top of the specimen and secured with a rubber band. The specimen was then transferred to a curing chamber where it remained for a period of 28 days. The same procedure was then repeated for the remaining eight specimens within the set. After successfully casting two consecutive specimens, the grout contained within the pitcher was then poured back into the 2 gallon (7.6 liter) container where the grout was then remixed for a period of approximately one minute.

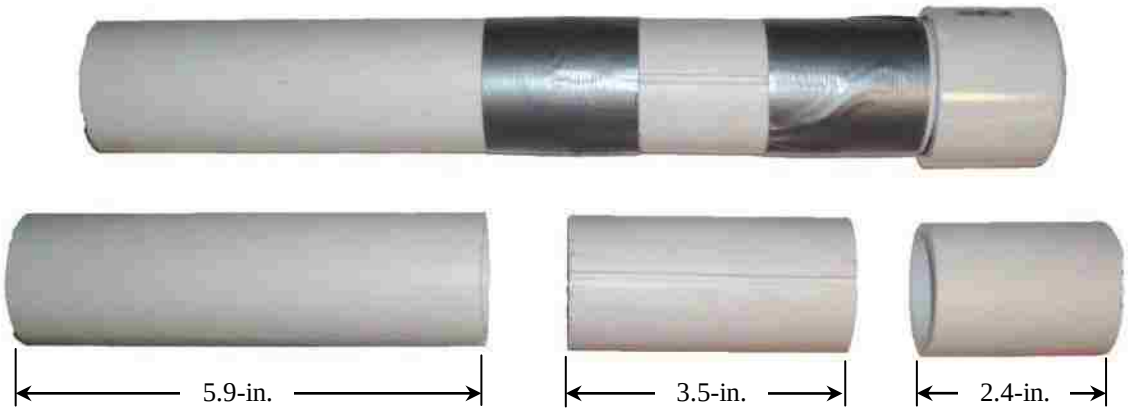

Figure 5.2: Three sections of PVC piping alongside a completed mold which was used during the casting of a grouted ACT specimen.

5.3 TESTING PROCEDURE

5.3.1 Non-Grouted Specimens. Pretest preparations varied slightly depending on the particular specimen coating. Testing a set of eight, non-grouted specimens began at least 48 hours after the last specimen within the set had received its final coat of Aquamarine Epoxy. To allow the calcium silicate to react prior to the test, each reactive-enamel specimen was first placed within a pitcher that contained deionized water for a

period of three days. After three days of soaking, the specimen was then permitted to air-dry for a minimum of 24 hour prior to initiating the test, as shown in Figure 5.3. Specimens containing no calcium silicate within their coating, such as the pure enamel-coated and epoxy-coated specimens, were cleaned with soap and water before they were tested.

(a) (b)

Figure 5.3: Preparation of non-grouted reactive enamel-coated specimens prior to testing. (a) Stored within deionized water for three straight days. (b) Permitted to air-dry for 24 hours prior to testing.

After prepping a set of specimens, each specimen was then placed in a corrosion cell, as shown in Figure 5.4(a). The corrosion cell consisted of a glass beaker that contained 0.8 gallons (3 liters) of electrolyte. The electrolyte was composed of deionized water and 5 percent ACS grade sodium chloride (NaCl) by weight. Before batching the solution, the deionized water was given a minimum of 24 hours to reach an ambient temperature of approximately 68°F (20°C). Once a bar was positioned within the solution, a plexiglass top was placed over the beaker. A brass grounding clamp was then attached to the exposed steel located at the top of the specimen. Both the counter and

reference electrodes were then partially inserted into the solution. The centroids of the counter and reference electrodes were equally spaced at a distance of approximately 2.4 in. (6.1 cm) from the center of the specimen (the working electrode). As shown in Figure 5.4, the counter and reference electrodes were supported by the plexiglass top and were located on opposite sides of the specimen. The counter electrode, supported approximately ½ in. (1.3 cm) above the bottom of the beaker, was made of a ½-in.-diameter (1.3 cm) graphite rod that was 12 in. (30 cm) in length. The graphite rod, manufactured by Graphtek LLC, was a grade GM-10. A gel-filled saturated calomel electrode (SCE), manufactured by Fisher Scientific, was used as the reference electrode and was positioned at a depth of approximately 3½ in. (8.9 cm) within the solution. After the electrodes were partially immersed within the solution, they were then individually connected to an eight-channel ECM8 multiplexer which was attached to a Series G300 potentiostat. Both the multiplexer and the potentiostat were manufactured by Gamry Instruments.

After properly connecting each of the eight corrosion cells to the multiplexer, the open circuit (OC) potential of each specimen was measured using the potentiostat and a computer that contained Gamry Instruments Framework software, Version 5.50. The accuracy of the potentiostat in measuring the OC potential of a specimen was within ±1 mV of its actual value. Once the OC potential of each specimen had been measured, a constant +400 mV_{OC} potential was applied to each specimen. The accuracy of the potentiostat in applying a potential to a specimen was within ±2 mV of the specified value. Depending upon the type of coating being tested, the corrosion current of each specimen was recorded every 5 or 30 minutes. The accuracy of the potentiostat in measuring the corrosion current of a specimen was to within ±50 pA. Testing of a specimen was considered complete when a continuous and/or substantial increase in a specimen's corrosion current was reported. When the testing of a specimen was complete, the specimen was disconnected and removed from the corrosion cell in which it resided.

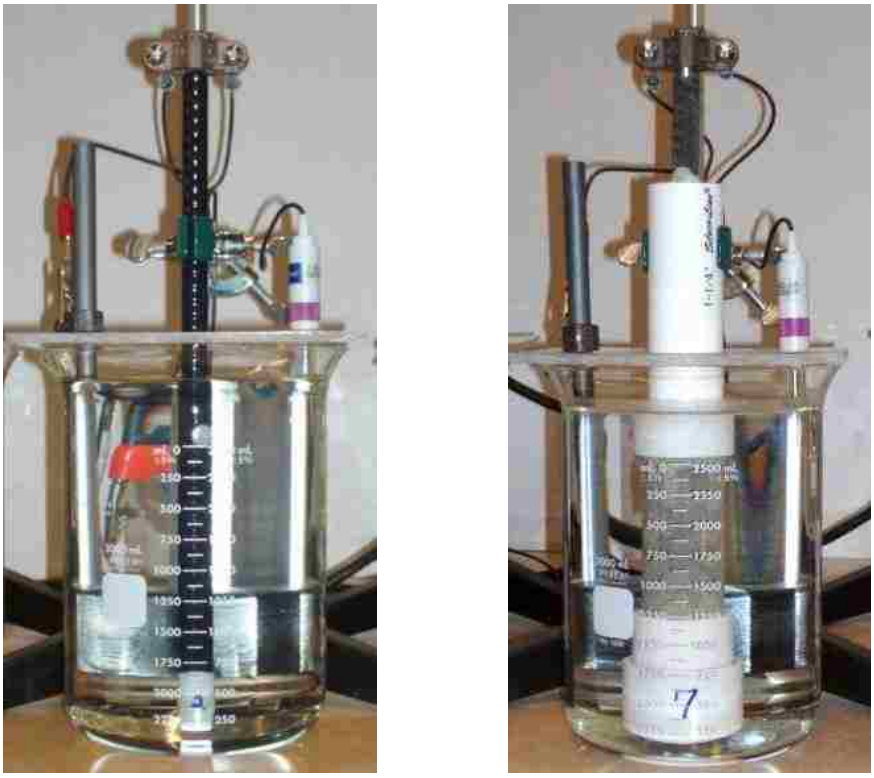

(a) (b)

Figure 5.4: A corrosion cell containing either a non-grouted or grouted ACT specimen. (a) Non-grouted. (b) Grouted.

5.3.2 Grouted Specimens. Pretest preparations were identical for all specimen types. Testing a set of grouted specimens began at least 28 days after the set was grouted. After removing the nine specimens from the curing chamber, they were immediately placed within a 5 gallon (18.9 liter) container partially filled with tap water. The two portions of duct tape used to connect the three sections of PVC were removed and the exterior surface of each specimen was cleaned using tap water. Using sandpaper, any rust that had gathered along the end of the specimen which contained the ¾-in.-section (1.9 cm) of exposed steel was removed. After the surface of each specimen was cleaned, the 3.5-in.-long (8.9 cm) section of PVC containing two longitudinal slits was removed from each specimen. Any silicone that remained along the surface of the freshly exposed grout was removed while the grout was inspected for voids and/or defects. Any specimen containing a void larger than that shown in Figure 5.5 was

omitted from the test. If no individual specimen exhibited any detrimental defects within its grout, eight randomly selected specimens were chosen for the test.

Figure 5.5: A void considered to be detrimental to the grouted specimen's performance in the ACT test.

After prepping a set of specimens, each specimen was then placed within a corrosion cell, as shown in Figure 5.4(b). After the eight specimens were selected, they were removed from the 5 gallon (18.9 liter) container and were each placed within a glass beaker. Each beaker contained 0.8 gallons (3 liters) of electrolyte which was batched using deionized water and 5 percent ACS grade NaCl. A plexiglass top was then placed over each beaker and a brass grounding clamp was attached to each individual specimen. The counter and reference electrodes were then placed within each corrosion cell and were then connected to the ECM8 multiplexer. Using a Series G300 potentiostat, the OC potential for each specimen was measured. After the OC potentials were measured, a +400 mV_{OC} potential was applied to each specimen. While testing, each specimen's corrosion current was recorded every 30 minutes. Testing of a specimen was considered

complete the moment a continual and/or substantial increase in a specimen's corrosion current was reported. When the testing of a specimen was complete, the specimen was disconnected and removed from the corrosion cell in which it resided.

5.4 RESULTS

The following section is a summary of the ACT results. The complete results for each individual specimen are contained within Appendix C. The ACT results are typically reported as the average of the time-to-corrosion (t_{corr}) values for a set of eight specimens of the same type. When a t_{corr} value corresponding to a single specimen fell outside the range of two standard deviations above or below the set's mean t_{corr} value, the specimen was discarded from the calculation as an outlier. Moreover, if a grouted specimen reported erratic corrosion current readings within the first 24 hours of testing, the result obtained from that specimen was excluded from the calculation. Of the 18 specimen sets, three sets contained a specimen that was excluded from the calculation of the set's average t_{corr}. Those three sets were: grouted deformed uncoated, grouted deformed 50/50 enamel-coated, and non-grouted deformed 50/50 enamel-coated. However, although normally reported as an average of eight specimens, the ACT testing protocol allows for a minimum of six specimens to represent t_{corr} for a set.

In some cases, there is a degree of judgment on determining the t_{corr} for a particular specimen. Three commonly observed test results are shown in Figure 5.6. The result labeled "A" in Figure 5.6 was commonly seen while testing a typical non-grouted specimen; the results labeled "B" and "C" were commonly seen while testing grouted specimens. When a test result for a non-grouted specimen resembled that of "A," the specimen received a t_{corr} value of zero (0) hours. The justification for assigning a t_{corr} value of 0 hours is that a significant level of corrosion current was reported throughout the duration of the test and visible signs of corrosion were seen along the specimen shortly after the test was initiated. Conversely, a specimen that produced a result similar to that which is labeled "B" in Figure 5.6 would have received a t_{corr} value that was measured from the start of the test to the moment when the well defined spike in corrosion current first appeared. For example, the specimen that produced the result labeled "B" in Figure 5.6 received a t_{corr} value of 530 hours. If a specimen exhibited a

minor increase in corrosion current over a long period of time that was then followed by a more significant increase in corrosion current, the t_{corr} value for that specimen would have been measured from the start of testing to the point at which the first significant increase in corrosion current was first detected. For instance, the specimen that produced the result labeled "C" in Figure 5.6 was assigned a t_{corr} value of 690 hours. The overall results for each specimen set may be found within Appendix C.

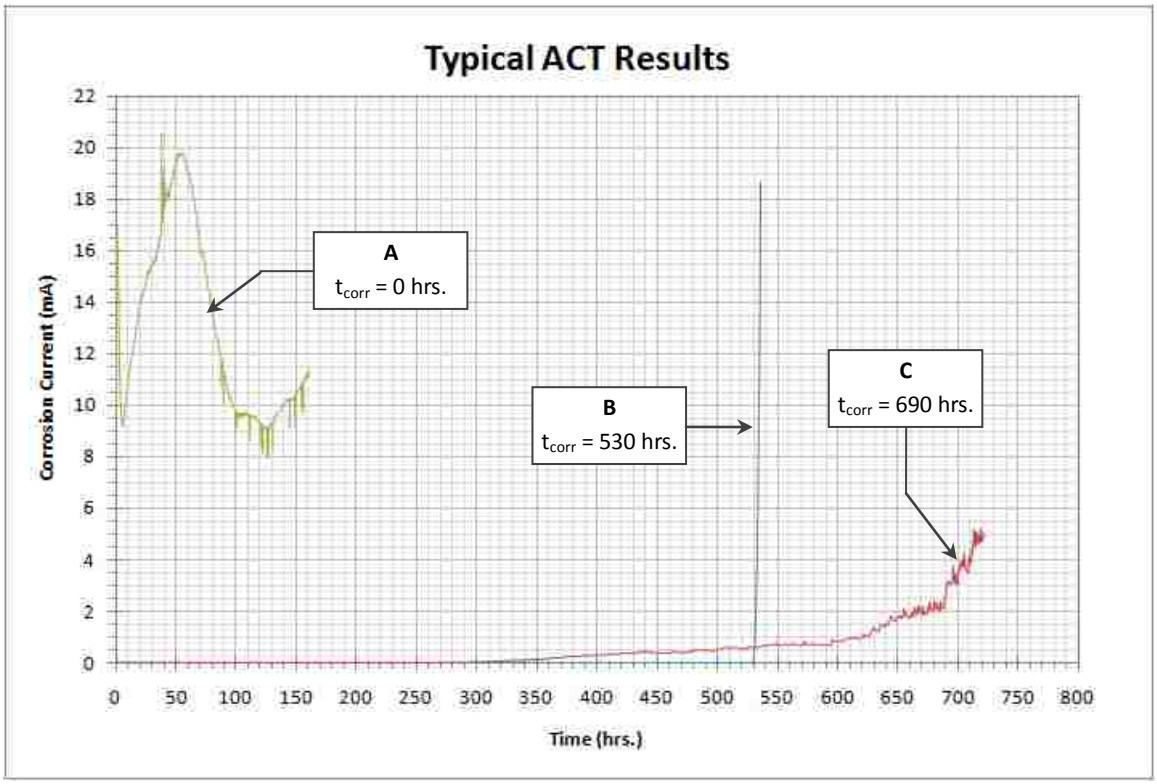

Figure 5.6: Three test results commonly seen during the ACT.

5.4.1 Non-Grouted Specimens. A summary of the ACT results for the non-grouted specimens is shown in Figure 5.7. The 95 percent confidence interval for each set's average t_{corr} is also included within the figure. A set's confidence interval was developed using the standard error of a set's mean value (SEM). The SEM for a set of

specimens was calculated by dividing the standard deviation of the sample set by the square root of the number of specimens used in deriving the set's average t_{corr} value.

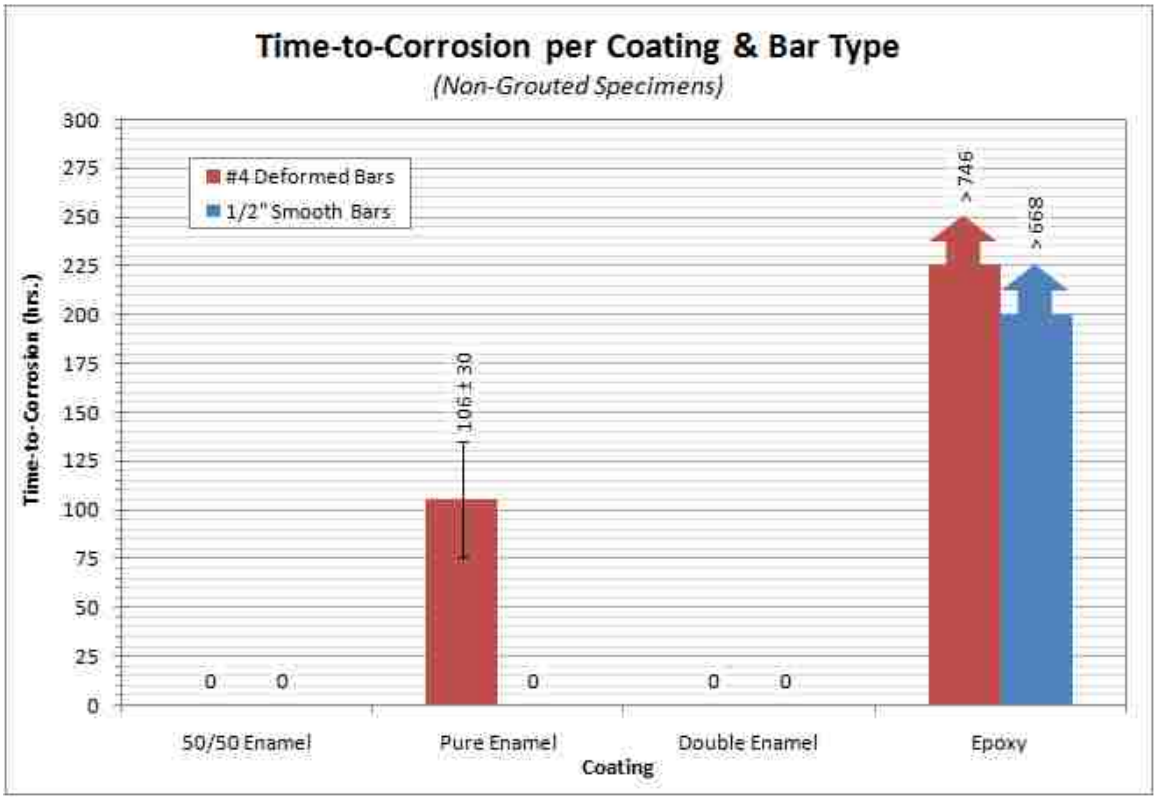

Figure 5.7: Test result summary for the non-grouted specimens.

Of the eight non-grouted specimen sets, only three sets managed to postpone the onset of corrosion for a measurable period of time. Those three sets included deformed pure enamel-coated bars and both smooth and deformed epoxy-coated bars. As shown in Figure 5.7, the deformed pure enamel-coated bars reported an average t_{corr} of 106 hours, whereas both the smooth and deformed epoxy-coated bars exhibited no visible signs of corrosion after 668 and 746 hours of testing, respectively. Testing of the epoxy-coated specimens ended prematurely, so to avoid any complication with the scheduling of the remaining tests.

5.4.2 Grouted Specimens. A summary of the ACT results for the grouted specimens is shown in Figure 5.8. The 95 percent confidence interval for each set's average t_{corr} is also included within the figure. A set's confidence interval was developed using the standard error of a set's mean value (SEM). The SEM for a set of specimens was calculated by dividing the standard deviation of the sample set by the square root of the number of specimens used in deriving the set's average t_{corr} value.

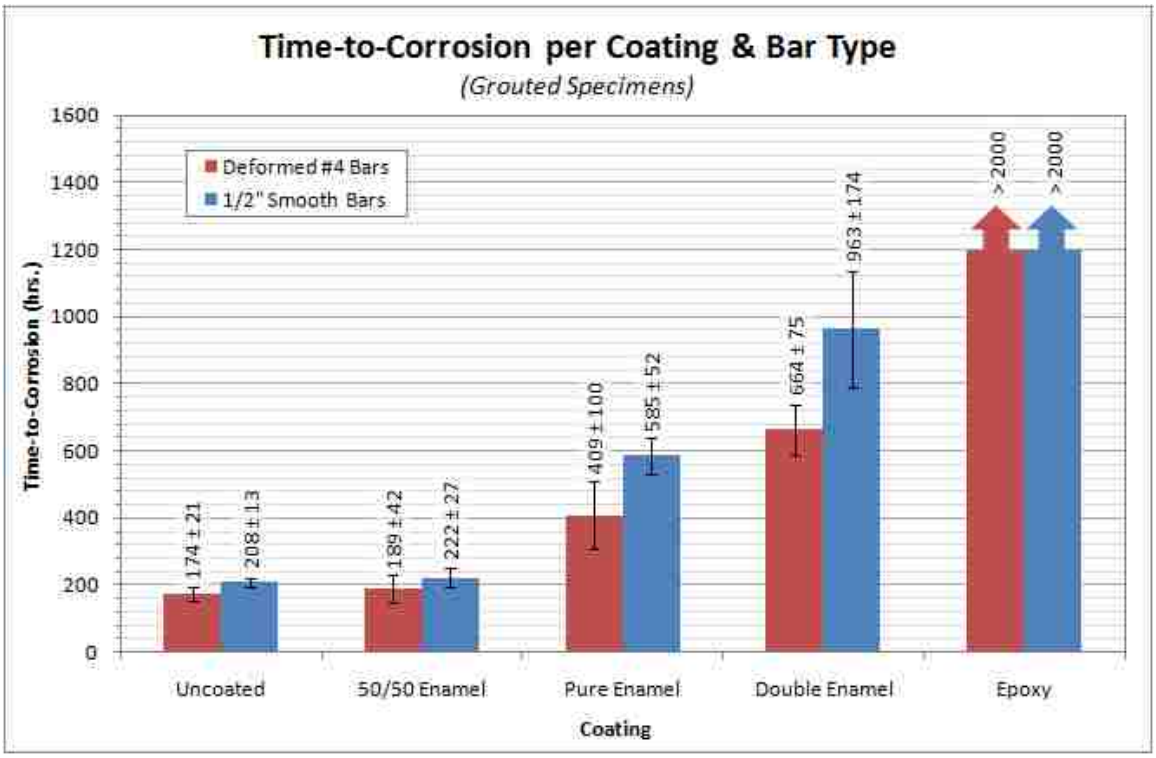

Figure 5.8: Test result summary for the grouted specimens.

The plot clearly indicates the relative ability of each of the coating types to protect the underlying steel. Also, in general, the smooth bars exhibited a longer t_{corr} value than the deformed bars, with the difference becoming more pronounced as the relative coating performance improved. A minor difference was observed between the average t_{corr} values obtained for both the grouted uncoated and grouted 50/50 enamel-coated

specimens. The average t_{corr} values for the grouted pure and double enamel-coated specimens, on the other hand, were approximately 2.4 and 4.0 times greater than that of the grouted 50/50 enamel coated specimens, respectively.

Among the pure and double enamel-coated specimens, the average t_{corr} for the deformed specimens varied significantly from that of the smooth specimens. Paired t-tests were conducted to further verify the differences within the t_{corr} values obtained for both the smooth and deformed pure enamel-coated specimens along with the smooth and deformed double enamel-coated specimens. The p-values obtained from the two t-tests suggest that a significant difference does exist between the t_{corr} values associated with the smooth and deformed pure enamel-coated specimens (p-value of 0.016) along with t_{corr} values associated with the smooth and deformed double enamel-coated specimens (p-value of 0.013). As shown in Figure 5.8, the average t_{corr} values for the deformed and smooth pure enamel-coated specimens were 409 and 585 hours, respectively. These two values corresponded to a 43 percent difference in t_{corr}. However, using the 95 percent confidence interval, the difference between those two values may vary from as low as 5 percent to as high as 106 percent. The coating that reported the greatest difference between the average t_{corr} of the smooth and deformed specimens was the double enamel-coating. Using a 95 percent confidence interval, the difference between the grouted smooth and deformed double enamel-coated specimens may varying from as low as 7 percent to as high as 193 percent. As indicated in Figure 5.8, the deformed double enamel-coated specimens reported an average t_{corr} value of 664 hours, which was 31 percent lower than that of the smooth double enamel-coated specimens.

Of the grouted specimens, the highest t_{corr} value was reported by both the smooth and deformed epoxy-coated specimens. The testing of both sets lasted for a period of approximately 2000 hours. Similarly to the testing of the non-grouted epoxy-coated specimens, testing of the grouted epoxy-coated specimens was completed prematurely due to deadlines within the study.

5.5 FINDINGS

Testing of the non-grouted, enamel-coated bars revealed that two out of three enamel compositions were unable to protect the underlying steel for any measureable

amount of time. The enamel coating that was able to postpone the onset of corrosion was the pure enamel coating as applied to the deformed bars. The exterior surface of each of the eight deformed pure enamel-coated specimens appeared identical to one another and resembled that of the specimen shown in Figure 4.12(a). Following the procedure stated in Section 3.3.3.3, a cross-section was developed from one of the eight bars. The cross-section revealed a coating thickness that ranged from approximately 8 to 40 mils (200 to 1,000 µm) and was similar to that which is shown in Figure 4.14(a).

Testing of the grouted specimens revealed a definite trend in the corrosion resistance of the different coatings. The uncoated specimen groups reported the lowest t_{corr} values, which were slightly lower than the values obtained from testing the 50/50 enamel-coated specimens. A significant increase in corrosion resistance of a specimen was observed when the 50/50 enamel coating was replaced by pure enamel. The corrosion resistance of the pure enamel coating increased by approximately 64 percent when a second coating composed of 50/50 enamel was applied to the exterior surface of the coated bar to form double enamel. Although the double enamel coating provided a great deal of corrosion protection to the underlying steel bar, the greatest t_{corr} values were reported by both groups containing epoxy-coated bars.

It was found that, on average, the pure and double enamel coatings were capable of increasing a smooth bar's corrosion resistance by approximately 180 and 360 percent, respectively, when grouted. However, those percentages decreased by approximately 24 percent when the smooth bar was replaced by a deformed bar. This decrease in t_{corr} may best be explained by the cross-sectional examination that was conducted upon the specimens that were included within the salt spray test. As shown in Figure 4.10 and Figure 4.14, the deformed double and pure enamel-coated bars were inconsistently coated and contained thinly coated areas near the transverse ribs, while the smooth double and pure enamel-coated bars were uniformly coated and possessed a coating thickness that was greater than the minimum coating thickness seen along the deformed bars containing similar coating compositions. Although the 50/50 enamel-coated bars shared identical coating distribution patterns to that of the double and pure enamel-coated bars, the thinly coated areas along a deformed bar appeared to have had little effect upon the reported t_{corr} values. In fact, the 50/50 enamel coating increased the t_{corr} value of an uncoated bar by

only 8 percent, on average. The inability of the 50/50 enamel coating to provide a substantial amount of protection may best be explained by the semipermeable calcium silicate particles embedded within the coating and the network of voids seen throughout the coating's thickness, as shown in Figure 4.7.

The epoxy coating showed an exceptional ability in protecting both smooth and deformed steel bars from corrosion when either grouted or non-grouted. Each non-grouted specimen withstood a minimum of 664 hours of testing without showing any signs of corrosion. The grouted specimens showed no signs of corrosion after being tested for a period of 2000 hours.

6 FINDINGS, CONCLUSIONS, & RECOMMENDATIONS

6.1 FINDINGS

6.1.1 Ponding Test. After evaluating the concrete resistivity results, it was determined that the concrete resistance of a reinforced specimen was a function of the type of coating that was applied to the specimen's reinforcement. It was also determined that the resistance of an epoxy or 50/50 enamel specimen was unaffected by the presence of intentionally damaged areas along the specimen's reinforcement. On average, a specimen containing either "perfect" or damaged epoxy-coated reinforcement reported a resistance that was 1.47 times that of an unreinforced specimen's resistance. On average, specimens belonging to either the "perfect" or damaged 50/50 enamel group reported similar resistivity values to that of an unreinforced specimen. While the group containing uncoated reinforcement reported an average resistance that was 44 percent lower than the average resistance of an unreinforced specimen.

The significance of these values is a relative indication of the corrosion resistance of the concrete/rebar system for each coating type. With the reinforced specimens having been constructed with the same concrete and steel reinforcement, the discrepancy within the resistivity readings is most likely attributed to the coating applied to the embedded reinforcement. This result would indicate that the epoxy coating provided the greatest resistance to the applied electrical current, while the uncoated bar provided the least resistance. The 50/50 enamel-coated bars provided a degree of resistance between that of the epoxy and uncoated bars.

Figure 3.14 offers some very valuable information on the corrosion resistance of the coatings as a function of time when exposed to a high chloride environment. Although the trends are very similar for each group, the relative locations of the plots indicate the relative corrosion resistance of each coating. The epoxy coating provides the greatest degree of resistance, while the uncoated bars offer the least. The 50/50 enamel-coated bars offer a degree of resistance between that of the epoxy and uncoated bars.

However, when examining similar coatings, there are some noticeable differences. For instance, as shown in Figure 3.14, a 28 percent decrease in corrosion resistance was observed, on average, when comparing the damaged epoxy group to that

of the "perfect" epoxy group throughout the duration of the test. An average 4 percent increase in corrosion resistance was seen when comparing the damaged 50/50 enamel group to that of the "perfect" 50/50 enamel group throughout the course of the 54-week-long test. To further verify these findings, paired t-tests were conducted upon the corrosion potential data gathered from both the 50/50 enamel specimens and the epoxy specimens. The p-values obtained from the two t-tests indicate that a significant difference does exist between the results obtained from the damaged 50/50 enamel and "perfect" 50/50 enamel specimens (p-value of 0.003) along with the results collected from the damaged epoxy and "perfect" epoxy specimens (p-value of 0.00004). Taking into account these results, it was found that the corrosion protection provided by the epoxy coating was jeopardized when damaged, while the corrosion protection provided by the 50/50 enamel was unaltered when damaged. Although the corrosion protection of the 50/50 enamel coating was unaffected by the areas of damage, the coating consistently provided a lower level of protection when compared to that of the intentionally damaged epoxy-coated bars.

The final set of corrosion potential measurements indicated a "high (> 90%)" probability that the reinforcement contained within each specimen group was actively corroding, with a severe chance that the reinforcement contained within the two 50/50 enamel groups and the uncoated group had begun to corrode.

Through chloride-ion analysis, it was determined that a chloride profile, similar to the one labeled "uncoated" in Figure 3.16, can develop when cracks form along the surface of a specimen's reservoir. However, only four out of the 25 specimens contained within this study showed signs of cracking along the surface. A typical chloride profile developed from a specimen that exhibited no visible signs of cracking showed high levels of chlorides near the surface and a low concentration at a depth of around 2.0 in. (5.1 cm). A typical chloride profile is shown in Figure 3.16. Most importantly, the chlorides penetrated the concrete to the depth of the reinforcement in sufficient concentration to attack the passive layer and initiate corrosion.

Forensic evaluation of the specimens revealed significant variation in the condition of the four bars contained within a specimen that belonged to the uncoated group or either of the two 50/50 enamel groups. The reinforcing bars located closest to

the surface of a specimen's reservoir exhibited significant signs of corrosion, while the two remaining bars, which were positioned at a lower elevation within the specimen, showed moderate signs of corrosion. On the other hand, the condition of the four reinforcing bars contained within a specimen belonging to either the "perfect" or damaged epoxy group were found to be substantially identical and exhibited only very limited corrosion.

A loss in adhesion between the epoxy coating and the steel was observed within a portion of the cross-sections that were taken through locations in which the epoxy coating was intentionally damaged. When a loss in adhesion was observed, the steel beneath the coating indicated signs of corrosion.

It was also observed that when a typical 50/50 enamel-coated reinforcing bar was removed from a specimen, half of the coating was detached from that bar. The portion of the coating that was unintentionally removed from a 50/50 enamel-coated bar was found to be securely attached to the surrounding concrete.

6.1.2 Salt Spray Test. It was found that the performance of the three enamel coatings largely depended upon the coating's thickness and the concentration of calcium silicate within the coating. The uniformly coated smooth specimens, with an average coating thickness of around 8 to 16 mils (200 to 400 µm), outperformed the inconsistently coated deformed specimens that possessed thinly coated areas along their transverse and longitudinal ribs. However, although the 50/50 enamel-coated specimens shared similar coating distribution patterns as the pure and double enamel-coated specimens, it was seen that the deformed specimens outperformed the smooth specimen. This can best be explained by the large quantity of calcium silicate within the coating.

When a large quantity of calcium silicate is added to a pure enamel mixture and then fired to create 50/50 enamel, a porous material is created. The pores throughout the 50/50 enamel, as shown in Figure 4.7(b), provide pathways for oxygen, moisture, and chlorides to reach the steel. The iron oxide formed during the corrosion process then slowly begins to diffuse outwardly toward the exterior surface of the coating, as shown in Figure 4.7(c). Therefore, the time it takes for a 50/50 enamel specimen to show any significant signs of corrosion is a function of the coating's thickness and the rate of diffusion of both the corrosive elements and the iron oxide. This would explain why the

inconsistently coated, deformed, 50/50 enamel specimens outperformed the uniformly coated, smooth, 50/50 enamel specimens and why the overall performance of the smooth specimens decreased dramatically between the 8th and 10th week of testing.

The pure enamel, double enamel, and epoxy specimens all performed relatively well throughout the testing period. However, the deformed double enamel-coated specimens did show areas of weakness along a portion of their transverse ribs. These areas of weakness were thinly coated with what appeared to be an amalgamation of the two applied coatings. This mixing of the two coatings would, at times, lead to large concentrations of calcium silicate within the thinly coated sections of the coating. As a result, the coating along these sections exhibited similar properties to that of the 50/50 enamel.

The performance of a deformed pure enamel-coated specimen directly correlated to the minimum thickness of the applied coating along that specimen. The three specimens that performed poorly during the test had a minimum coating thickness of 2 mils (50 µm); whereas the five specimens that performed well during the test had a minimum coating thickness of 8 mils (200 µm). When damaged, the pure enamel coating maintained its bond with the steel and no undercutting was observed.

Both the deformed and smooth epoxy-coated specimens were uniformly coated and no significant signs of corrosion were observed along the surface of the specimens. However, when the coating showed signs of degradation in the form of discoloration, an increase in the amount of "pin-sized" areas of corrosion were observed. Undercutting of the coating was also observed along a section of a specimen that had a breach in the coating.

6.1.3 Accelerated Corrosion Test. Testing of the non-grouted, enamel-coated bars revealed that two out of three enamel compositions were unable to protect the underlying steel for any measureable amount of time. The enamel coating that was able to postpone the onset of corrosion was the pure enamel coating as applied to the deformed bars. The exterior surface of each of the eight deformed pure enamel-coated specimens appeared identical to one another and resembled that of the specimen shown in Figure 4.12(a). Following the procedure stated within Section 3.3.3.3, a cross-section was developed from one of the eight bars. The cross-section revealed a coating thickness

that ranged from approximately 8 to 40 mils (200 to 1,000 µm) and was similar to that which is shown in Figure 4.14(a).

Testing of the grouted specimens revealed a definite trend in the corrosion resistance of the different coatings, as shown in Figure 5.8. The uncoated specimen groups reported the lowest t_{corr} values, which were slightly lower than the values obtained from testing the 50/50 enamel-coated specimens. A significant increase in corrosion resistance of a specimen was observed when the 50/50 enamel coating was replaced by pure enamel. The corrosion resistance of the pure enamel coating increased by approximately 64 percent when a second coating composed of 50/50 enamel was applied to the exterior surface of the coated bar to form double enamel. Although the double enamel coating provided a great deal of corrosion protection to the underlying steel bar, the greatest t_{corr} values were reported by both groups containing epoxy-coated bars.

It was found that, on average, the pure and double enamel coatings were capable of increasing a smooth bar's corrosion resistance by approximately 180 and 360 percent, respectively, when grouted. However, those percentages decreased by approximately 24 percent when the smooth bar was replaced by a deformed bar. This decrease in t_{corr} may best be explained by the cross-sectional examination that was conducted upon the specimens that were included within the salt spray test. As shown in Figure 4.10 and Figure 4.14, the deformed double and pure enamel-coated bars were inconsistently coated and contained thinly coated areas near the transverse ribs, while the smooth double and pure enamel-coated bars were uniformly coated and possessed a coating thickness that was greater than the minimum coating thickness seen along the deformed bars containing similar coating compositions. Although the 50/50 enamel-coated bars shared identical coating distribution patterns to that of the double and pure enamel-coated bars, the thinly coated areas along a deformed bar appeared to of had little effect upon the reported t_{corr} values. In fact, the 50/50 enamel coating increased the t_{corr} value of an uncoated bar by only 8 percent, on average. The inability of the 50/50 enamel coating to provide a substantial amount of protection may best be explained by the semipermeable calcium silicate particles embedded within the coating and the network of voids seen throughout the coating's thickness, as shown in Figure 4.7.

The epoxy coating showed an exceptional ability in protecting both smooth and deformed steel bars from corrosion when either grouted or non-grouted. Each non-grouted specimen withstood a minimum of 664 hours of testing without showing any signs of corrosion. The grouted specimens showed no signs of corrosion after being tested for a period of 2000 hours.

6.2 CONCLUSIONS

Based on the previously stated findings, the following conclusions can be drawn in reference to both the corrosion resistance and properties of the three enamel coatings when applied to smooth steel dowels or deformed steel reinforcing bars through a non-electrostatic dipping process:

1. The 50/50 enamel coating is more susceptible to impact damage than that of the epoxy coating.
2. When embedded in concrete, the 50/50 enamel coating can reduce the electrical conductivity of a steel bar. However, the insulating properties of the coating are lower than that of an epoxy coated steel bar.
3. When embedded in chloride contaminated concrete, the 50/50 enamel coating can reduce the occurrence of the anodic reaction; however, not to the same extent as that of an epoxy coated steel bar.
4. An area of damage, measuring approximately 0.2 $in.^2$ (1.3 cm^2) in size, will have no influence upon a 50/50 enamel-coated bar's performance during a ponding test.
5. Of the three enamel coatings, the 50/50 enamel coating provides the least amount of protection to the underlying steel, while the double enamel provides the highest amount of protection, and the pure enamel provides a degree of protection between the double and 50/50 enamel coatings.
6. Applying each of the three enamel coatings to a deformed bar, through a non-electrostatic dipping process, results in a coating that contains large variations within its thickness, with the coating being thinnest near the bar's transverse ribs. However, when using the same manufacturing process, each of the three enamel coatings can be uniformly applied to a smooth steel bar.

7. When the double enamel coating is applied to a deformed bar, the two separately applied layers of enamel may mix with one another to form what appears to be a single layer of reactive enamel that contains a substantial amount of calcium silicate throughout its thickness. This phenomenon occurs when the coating is thinly applied and will typically occur near a bar's transverse rib.
8. The overall performance of the three enamel coatings depended significantly the minimum thickness of each coating.
9. The excellent bond created between the steel reinforcement and both pure and double enamel coatings actively prevents corroding areas from traveling along the steel-coating interface (*i.e.*, no undercutting); whereas, the epoxy coating is unable to do so.
10. When undamaged and properly applied, both pure and double enamel coatings can protect steel reinforcement from chloride induced corrosion; whereas, the 50/50 enamel coating cannot.

6.3 RECOMMENDATIONS

Based on the findings and conclusions stated in the previous sections, the following recommendations were derived in regards to the future development and usage of enamel-coated steel reinforcement for concrete:

1. When attempting to protect a reinforced concrete structure or pavement from chloride induced corrosion, the 50/50 enamel coating is not recommended. However, the pure enamel and double enamel coatings show great promise provided a method of production exists that results in a more uniform coating thickness.
2. To obtain the maximum corrosion resistance of a reactive enamel coating, the calcium silicate included within the coating should be located as far away from the steel surface as possible.
3. To increase the overall efficiency of the enameling process (*i.e.*, least material waste), while at the same time improving the corrosion performance of enamel-coated, deformed steel reinforcement, the coating should be applied to the steel

through a manufacturing process that results in a uniform thickness, such as an electrostatic procedure.

4. An additional ponding test should be conducted in order to further classify the corrosion performance of both deformed pure enamel-coated and deformed double enamel-coated steel reinforcement.

The following is recommended in order to improve the quality of the information gathered from the three test methods used throughout this study:

1. Loctite's Aquamarine Epoxy (or equivalent) should be used to repair all areas of damage along a protective coating prior to testing.
2. Half-cell potential readings should be conducted after every wet/dry cycle (every 3 weeks) until the specimens have reached the 12^{th} week of testing. Afterwards half-cell potential readings can be carried out on a six week cycle such that the next round of half-cell potential readings will be taken on the 18^{th} week.
3. A minimum of two unreinforced ponding specimens should be cast for each batch of concrete used in the development of the reinforced ponding specimens. The specimens should be used as concrete resistivity control specimens and should remain on the same test schedule as that of the reinforced specimens.
4. A concrete cylinder should be cast for each batch of concrete used in the development of the ponding specimens. This cylinder shall then be used to determine the baseline chloride level within the concrete.
5. Cores taken from ponding specimens for chloride analysis should not border or contain any corrosion induced cracks. If this is not possible, then the concrete powder required for a chloride test should be collected from a side of the core that did not border a corrosion-induced crack.

APPENDIX A

PONDING TEST

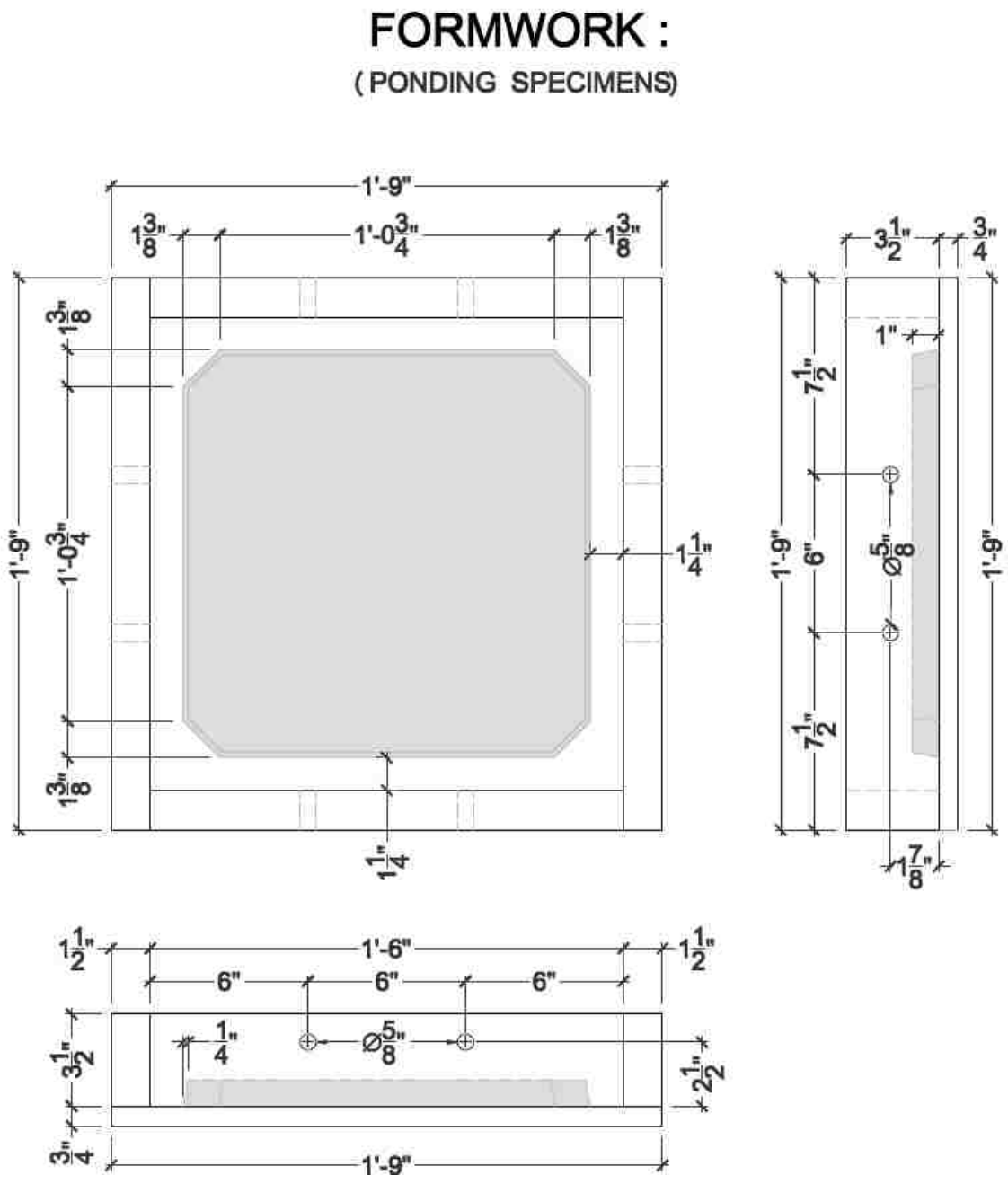

Figure A - 1: Typical ponding specimen form details and dimensions.

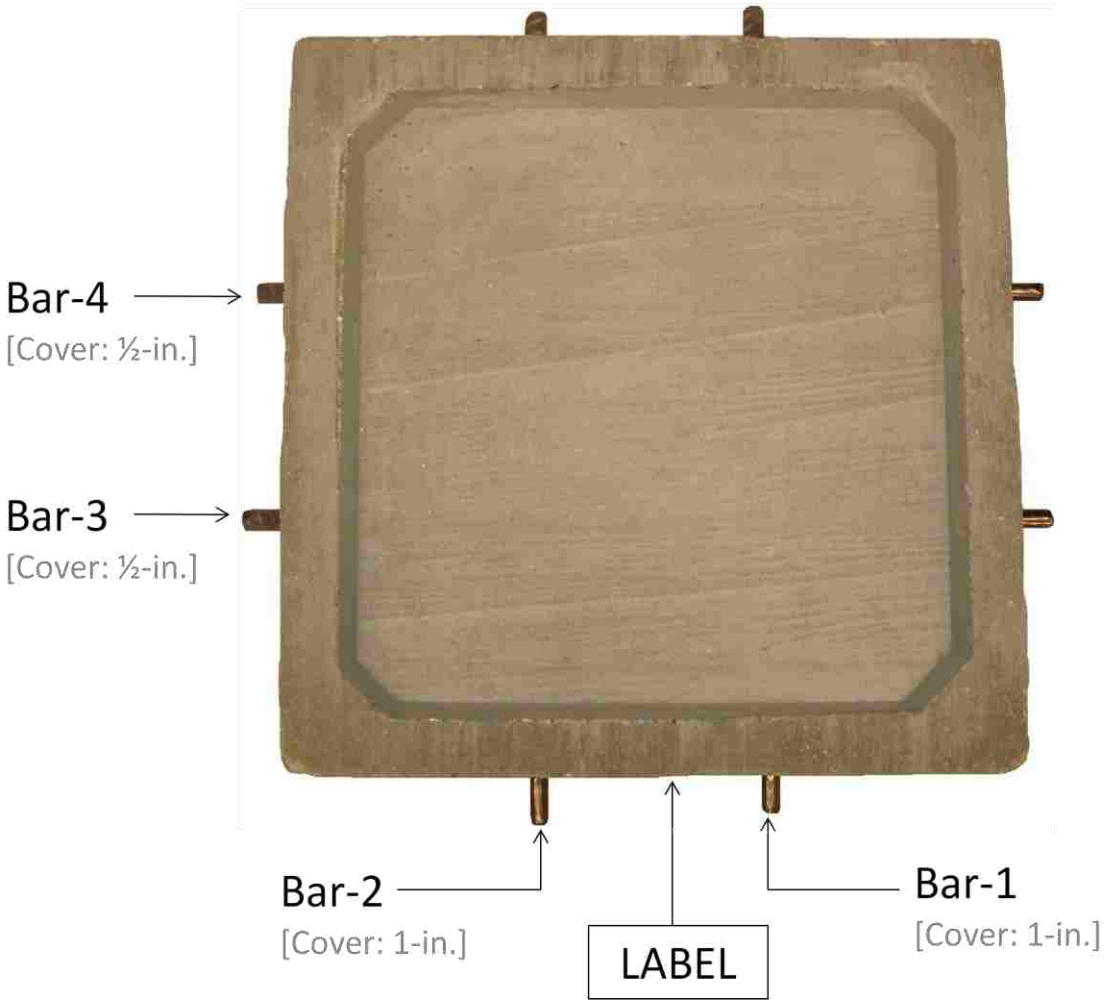

Figure A - 2: Labeling of bars embedded within a ponding specimen with respect to the specimen's label.

Table A - 1: Labels used for ponding specimens.

LABEL	COATING TYPE
M	Uncoated
EP	"Perfect" Epoxy
EP-D	Damaged Epoxy
EN	"Perfect" Enamel
EN-D	Damaged Enamel

MISSOURI S&T University of Science & Technology

Ponding Specimens: Impact Results

Standard: ASTM G14

Tup Wt. (lbs.): 2.0
Drop Height (in.): 36

ENAMEL-COATED (EN) REINFORCEMENT

	Bar	Location	Dimensions (in.)	
EN-D-1	1	1	1/2	1/4
		2	3/8	1/4
		3	1/2	1/2
	2	1	1/8	1/4
		2	3/4	1/2
		3	1/4	3/8
	3	1	3/8	3/4
		2	3/8	3/4
		3	1/2	5/8
	4	1	1/2	5/8
		2	1/8	5/8
		3	1/8	5/8
	Average:		0.38	0.51

	Bar	Location	Dimensions (in.)	
EN-D-2	1	1	1/4	1/2
		2	1/2	3/8
		3	1/2	5/8
	2	1	1 3/8	1/2
		2	1/8	1/2
		3	1/4	3/8
	3	1	1/8	1/8
		2	1/4	1/2
		3	1/8	3/8
	4	1	1/2	1
		2	1/4	1/4
		3	1/8	1/4
	Average:		0.36	0.45

	Bar	Location	Dimensions (in.)	
EN-D-3	1	1	1	3/4
		2	5/8	1/2
		3	13/16	1/2
	2	1	1	3/8
		2	3/16	5/16
		3	9/16	3/8
	3	1	1/2	13/16
		2	1/4	3/4
		3	1/8	1/2
	4	1	3/16	11/16
		2	7/16	9/16
		3	5/32	11/16
	Average:		0.49	0.57

	Bar	Location	Dimensions (in.)	
EN-D-4	1	1	3/16	1/4
		2	1/2	3/8
		3	11/16	3/8
	2	1	15/32	5/8
		2	1/8	3/8
		3	1/32	3/16
	3	1	3/8	5/8
		2	1/4	11/16
		3	3/16	1/4
	4	1	3/32	9/32
		2	1/16	5/32
		3	5/32	7/16
	Average:		0.26	0.39

Overall Average (in.):	0.37	0.48

EPOXY-COATED (EP) REINFORCEMENT

	Bar	Location	Dimensions (in.)	
EP-D-1	1	1	0	0
		2	1/32	1/8
		3	1/64	1/16
	2	1	1/16	3/16
		2	1/16	3/16
		3	1/16	3/16
	3	1	1/32	1/16
		2	1/16	1/8
		3	1/32	5/32
	4	1	1/16	3/16
		2	1/16	3/16
		3	1/32	5/32
	Average:		0.04	0.14

	Bar	Location	Dimensions (in.)	
EP-D-2	1	1	1/16	7/32
		2	1/32	3/16
		3	0	0
	2	1	1/32	5/32
		2	1/16	1/8
		3	1/32	7/32
	3	1	1/32	1/8
		2	1/32	1/8
		3	1/16	3/16
	4	1	1/32	3/16
		2	1/8	1/8
		3	3/32	5/32
	Average:		0.05	0.15

	Bar	Location	Dimensions (in.)	
EP-D-3	1	1	1/16	1/8
		2	1/32	3/16
		3	3/32	5/32
	2	1	1/32	3/16
		2	1/16	3/16
		3	1/32	1/8
	3	1	1/16	3/16
		2	1/16	3/16
		3	1/16	5/32
	4	1	1/16	3/16
		2	1/32	1/8
		3	1/32	1/8
	Average:		0.05	0.16

	Bar	Location	Dimensions (in.)	
EP-D-4	1	1	3/32	7/32
		2	1/16	1/8
		3	1/32	5/32
	2	1	1/32	1/8
		2	1/16	7/32
		3	1/16	1/8
	3	1	1/32	5/32
		2	1/16	7/32
		3	1/16	3/16
	4	1	1/16	1/4
		2	3/32	1/8
		3	1/16	3/16
	Average:		0.06	0.17

Overall Average (in.):	0.05	0.16

Figure A - 3: Dimensions of intentionally damaged areas along both epoxy and 50/50 enamel-coated bars embedded within the ponding specimens.

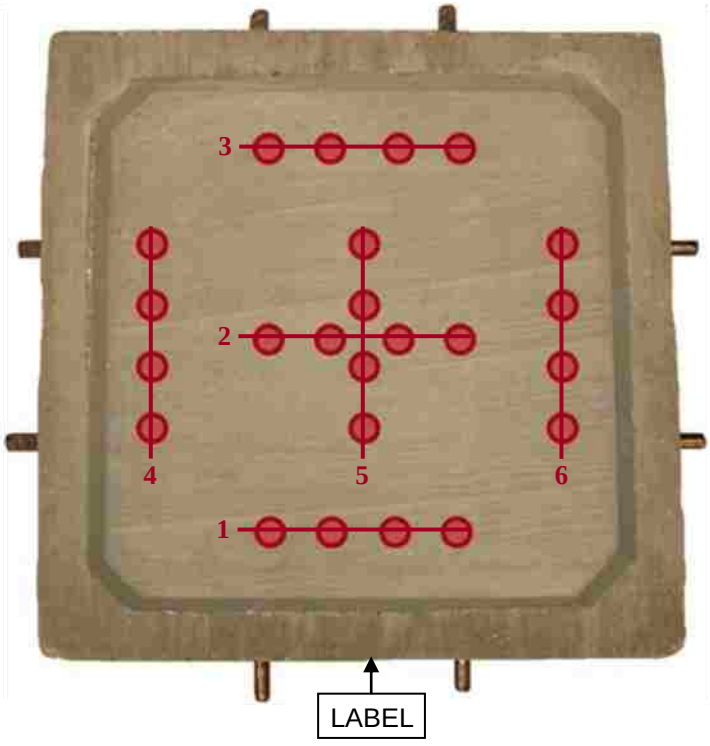

(a)

(b)

Figure A - 4: The locations of the (a) resistivity and (b) corrosion potential measurements with respect to a ponding specimen's label.

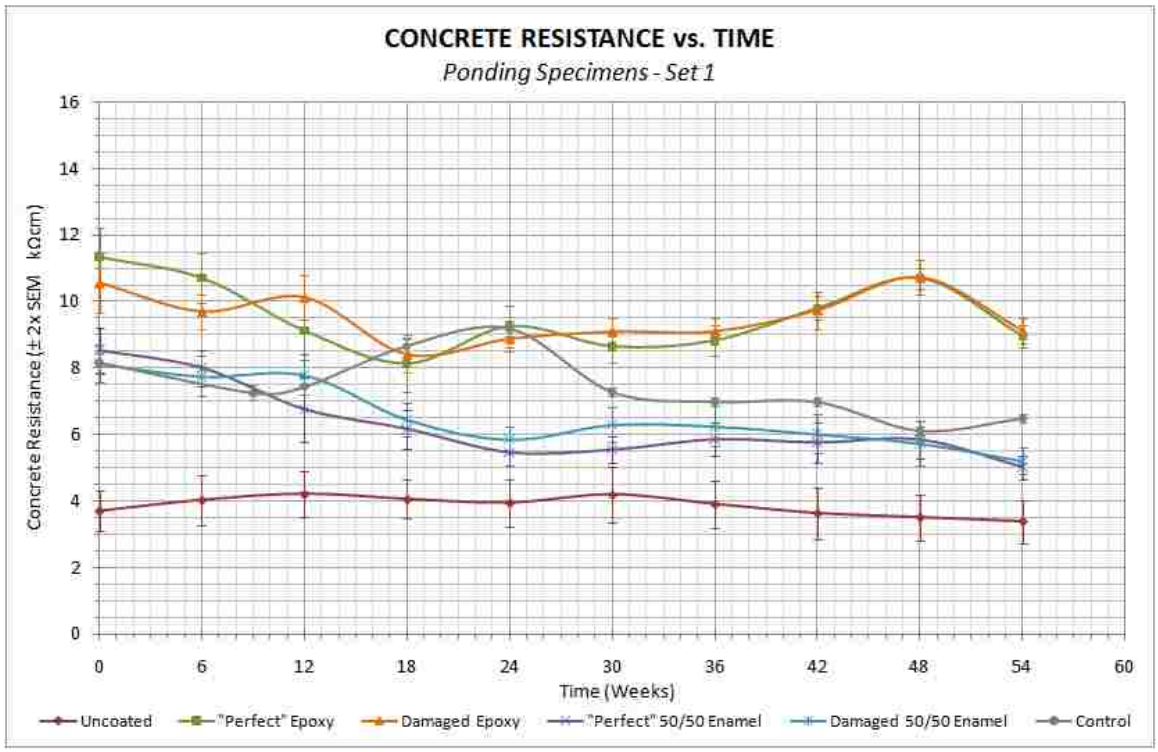

(a)

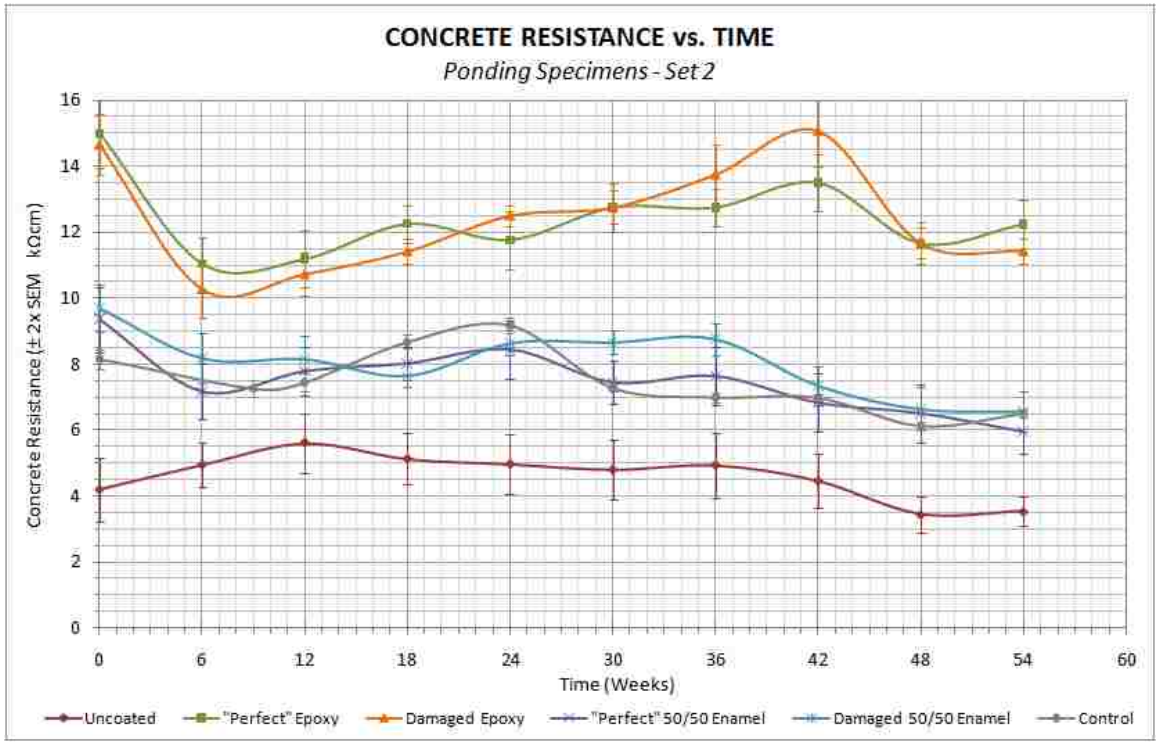

(b)

Figure A - 5: Average concrete resistance for (a) the first and second ponding specimen within each specimen group; (b) third and fourth ponding specimen within each specimen group.

Table A - 2: Resistivity measurements for the first and second uncoated ponding specimen.

Specimen:	Location:	Resistivity Measurements (kΩcm) vs. Time (weeks): 0	6	12	18	24	30	36	42	48	54
M-1	1	4.9	4.8	5.7	5.6	5.5	6.2	5.5	5.3	5.0	4.7
	2	4.9	4.8	4.6	5.4	5.5	5.4	5.4	4.6	4.9	4.7
	3	4.9	5.7	6.4	3.8	5.5	6.3	5.5	5.6	4.7	4.8
	4	3.5	3.9	3.8	3.8	3.8	3.8	2.9	3.3	3.0	3.1
	5	2.9	4.8	3.8	3.2	3.8	3.8	3.8	3.1	2.9	2.9
	6	2.8	3.2	3.2	3.0	3.0	2.9	2.9	2.5	2.4	2.3
M-2	1	5.0	5.6	5.6	5.0	4.6	5.1	4.8	5.6	5.5	5.1
	2	3.9	4.1	3.8	4.6	3.9	3.8	3.8	3.5	3.6	3.1
	3	3.9	5.0	4.6	5.1	4.7	5.4	4.5	3.6	3.4	3.3
	4	3.0	2.3	2.9	3.0	2.1	2.7	2.7	2.7	2.3	2.2
	5	2.3	2.0	2.4	3.0	2.1	2.1	2.2	1.7	2.1	2.1
	6	2.3	2.1	3.7	3.1	2.8	2.8	2.8	2.0	2.2	2.2
M-1 Average:		4.0	4.5	4.6	4.1	4.5	4.7	4.3	4.1	3.8	3.8
M-2 Average:		3.4	3.5	3.8	4.0	3.4	3.7	3.5	3.2	3.2	3.0
Overall Average		3.69	4.03	4.21	4.05	3.94	4.19	3.90	3.63	3.50	3.38
Standard Dev.:		1.04	1.33	1.21	1.03	1.25	1.44	1.21	1.36	1.23	1.15
SEM:		0.30	0.38	0.35	0.30	0.36	0.42	0.35	0.39	0.35	0.33
Maximum:		5.0	5.7	6.4	5.6	5.5	6.3	5.5	5.6	5.5	5.1
Minimum:		2.3	2.0	2.4	3.0	2.1	2.1	2.2	1.7	2.1	2.1

Table A - 3: Resistivity measurements for the third and fourth uncoated ponding specimen.

Specimen:	Location:	Resistivity Measurements (kΩcm) vs. Time (weeks): 0	6	12	18	24	30	36	42	48	54
M-3	1	5.5	6.4	6.3	6.6	6.8	7.2	6.8	5.6	3.7	3.7
	2	4.6	4.5	6.4	6.3	6.0	5.5	5.4	4.8	3.7	3.8
	3	4.9	5.6	7.5	6.4	6.5	6.3	6.3	5.6	3.8	4.1
	4	3.1	4.0	4.6	4.6	4.0	3.8	3.7	3.1	2.3	3.0
	5	2.1	3.8	3.9	3.8	4.1	3.8	3.8	3.1	2.8	2.5
	6	2.1	3.8	3.8	3.8	3.2	2.9	3.0	3.1	2.5	2.4
M-4	1	6.4	6.9	7.3	7.4	7.4	7.1	8.1	7.4	5.4	4.7
	2	5.8	5.6	8.2	5.6	4.6	4.9	5.5	4.8	4.1	4.1
	3	6.8	6.4	6.4	5.5	6.4	5.9	6.3	5.6	4.6	4.7
	4	3.4	3.8	4.3	3.9	3.8	3.6	3.7	3.8	2.9	3.5
	5	3.2	3.8	4.7	3.8	3.8	3.7	3.7	3.7	2.8	3.0
	6	2.5	4.8	3.9	3.8	3.0	2.9	2.9	2.9	2.7	2.9
M-3 Average:		3.7	4.7	5.4	5.3	5.1	4.9	4.8	4.2	3.1	3.3
M-4 Average:		4.7	5.2	5.8	5.0	4.8	4.7	5.0	4.7	3.8	3.8
Overall Average		4.20	4.95	5.61	5.13	4.97	4.80	4.93	4.46	3.44	3.53
Standard Dev.:		1.68	1.18	1.58	1.33	1.55	1.56	1.69	1.41	0.94	0.79
SEM:		0.49	0.34	0.46	0.38	0.45	0.45	0.49	0.41	0.27	0.23
Maximum:		6.8	6.9	8.2	7.4	7.4	7.2	8.1	7.4	5.4	4.7
Minimum:		2.1	3.8	3.8	3.8	3.0	2.9	2.9	2.9	2.3	2.4

Table A - 4: Resistivity measurements for the first and second "perfect" epoxy-coated ponding specimen.

		Resistivity Measurements (kΩcm) vs. Time (weeks):									
	Location:	0	6	12	18	24	30	36	42	48	54
Specimen: EP-1	1	13.0	11.0	7.6	9.0	9.8	9.8	9.8	9.7	9.9	9.0
	2	9.9	9.8	8.4	8.6	11.0	9.8	9.8	9.7	11.0	9.1
	3	12.0	11.0	7.1	5.5	9.4	8.1	9.0	9.8	9.6	8.0
	4	11.0	13.0	12.0	9.0	9.8	8.9	9.1	9.8	11.0	9.1
	5	9.2	9.8	11.0	9.0	10.0	9.0	9.8	11.0	11.0	9.8
	6	12.0	12.0	11.0	11.0	11.0	9.6	9.8	11.0	11.0	9.8
Specimen: EP-2	1	13.0	9.9	9.0	7.5	8.3	7.3	8.0	9.0	11.0	8.6
	2	9.9	9.8	7.3	8.2	8.7	8.1	8.0	9.4	11.0	9.0
	3	13.0	12.0	9.1	5.6	8.1	8.1	8.2	9.1	11.0	9.0
	4	11.0	11.0	8.9	8.1	8.5	8.8	8.1	9.8	11.0	9.1
	5	9.0	8.1	8.9	7.9	8.3	8.1	8.2	9.7	11.0	9.0
	6	13.0	11.0	9.0	8.1	8.1	8.1	8.1	9.6	9.9	8.0
EP-1 Average:		11.2	11.1	9.5	8.7	10.2	9.2	9.6	10.2	10.6	9.1
EP-2 Average:		11.5	10.3	8.7	7.6	8.3	8.1	8.1	9.4	10.8	8.8
Overall Average:		11.33	10.70	9.11	8.13	9.25	8.64	8.83	9.80	10.70	8.96
Standard Dev.:		1.55	1.31	1.53	1.49	1.07	0.80	0.80	0.62	0.55	0.56
SEM:		0.45	0.38	0.44	0.43	0.31	0.23	0.23	0.18	0.16	0.16
Maximum:		13.0	13.0	12.0	11.0	11.0	9.8	9.8	11.0	11.0	9.8
Minimum:		9.0	8.1	7.1	5.5	8.1	7.3	8.0	9.0	9.6	8.0

Table A - 5: Resistivity measurements for the third and fourth "perfect" epoxy-coated ponding specimen.

		Resistivity Measurements (kΩcm) vs. Time (weeks):									
	Location:	0	6	12	18	24	30	36	42	48	54
Specimen: EP-3	1	15.0	11.0	12.0	12.0	12.0	12.0	12.0	14.0	12.0	12.0
	2	13.0	9.8	12.0	12.0	12.0	13.0	12.0	14.0	11.0	11.0
	3	18.0	12.0	12.0	13.0	14.0	14.0	12.0	14.0	9.9	9.9
	4	17.0	12.0	13.0	13.0	12.0	12.0	13.0	14.0	11.0	12.0
	5	14.0	11.0	12.0	13.0	12.0	14.0	13.0	15.0	11.0	11.0
	6	16.0	13.0	13.0	14.0	14.0	14.0	13.0	16.0	12.0	13.0
Specimen: EP-4	1	16.0	11.0	10.0	12.0	12.0	12.0	13.0	13.0	12.0	13.0
	2	12.0	8.9	9.1	11.0	9.2	11.0	12.0	11.0	11.0	12.0
	3	16.0	12.0	12.0	12.0	10.0	13.0	14.0	12.0	13.0	13.0
	4	14.0	9.7	9.1	11.0	11.0	12.0	12.0	12.0	12.0	13.0
	5	13.0	9.1	9.0	11.0	10.0	11.0	12.0	12.0	11.0	12.0
	6	16.0	13.0	11.0	13.0	13.0	15.0	15.0	15.0	14.0	15.0
EP-3 Average:		15.5	11.5	12.3	12.8	12.7	13.2	12.5	14.5	11.2	11.5
EP-4 Average:		14.5	10.6	10.0	11.7	10.9	12.3	13.0	12.5	12.2	13.0
Overall Average:		15.00	11.04	11.18	12.25	11.77	12.75	12.75	13.50	11.66	12.24
Standard Dev.:		1.81	1.42	1.50	0.97	1.51	1.29	0.97	1.51	1.09	1.30
SEM:		0.52	0.41	0.43	0.28	0.44	0.37	0.28	0.44	0.31	0.38
Maximum:		18.0	13.0	13.0	14.0	14.0	15.0	15.0	16.0	14.0	15.0
Minimum:		12.0	8.9	9.0	11.0	9.2	11.0	12.0	11.0	9.9	9.9

Table A - 6: Resistivity measurements for the first and second damaged epoxy-coated ponding specimen.

Specimen:	Location:	Resistivity Measurements (kΩcm) vs. Time (weeks): 0	6	12	18	24	30	36	42	48	54
EP-D-1	1	12.0	11.0	9.8	8.1	9.0	9.8	9.7	11.0	11.0	9.1
	2	7.3	9.2	8.1	8.1	8.7	10.0	9.8	11.0	11.0	9.2
	3	11.0	9.8	9.0	9.0	8.1	8.9	9.8	9.6	10.0	9.0
	4	9.1	9.3	9.9	8.1	8.4	9.1	9.0	11.0	11.0	9.9
	5	9.1	8.9	9.8	8.3	9.1	8.9	9.2	10.0	11.0	9.1
	6	12.0	9.9	11.0	8.0	7.3	7.5	7.4	7.9	9.0	7.5
EP-D-2	1	12.0	8.7	9.9	8.9	9.0	8.2	8.6	8.4	9.8	8.9
	2	9.3	8.9	9.0	8.1	9.0	9.0	8.8	9.4	11.0	9.0
	3	12.0	11.0	11.0	6.4	9.1	9.6	9.0	10.0	12.0	9.8
	4	11.0	10.0	12.0	9.8	9.5	9.8	9.7	10.0	12.0	9.9
	5	10.0	8.7	10.0	8.2	9.5	8.7	8.9	9.3	11.0	9.0
	6	12.0	11.0	12.0	9.8	9.8	9.6	9.3	9.3	10.0	9.1
EP-D-1 Average:		10.1	9.7	9.6	8.3	8.4	9.0	9.2	10.1	10.5	9.0
EP-D-2 Average:		11.1	9.7	10.7	8.5	9.3	9.2	9.1	9.4	11.0	9.3
Overall Average:		10.57	9.70	10.13	8.40	8.88	9.09	9.10	9.74	10.73	9.13
Standard Dev.:		1.58	0.90	1.19	0.91	0.68	0.73	0.68	0.98	0.88	0.63
SEM:		0.46	0.26	0.34	0.26	0.20	0.21	0.20	0.28	0.26	0.18
Maximum:		12.0	11.0	12.0	9.8	9.8	10.0	9.8	11.0	12.0	9.9
Minimum:		7.3	8.7	8.1	6.4	7.3	7.5	7.4	7.9	9.0	7.5

Table A - 7: Resistivity measurements for the third and fourth damaged epoxy-coated ponding specimen.

Specimen:	Location:	Resistivity Measurements (kΩcm) vs. Time (weeks): 0	6	12	18	24	30	36	42	48	54
EP-D-3	1	14.0	12.0	11.0	11.0	12.0	12.0	13.0	14.0	11.0	12.0
	2	13.0	9.8	11.0	11.0	12.0	13.0	16.0	18.0	12.0	12.0
	3	18.0	11.0	12.0	11.0	13.0	13.0	14.0	14.0	12.0	12.0
	4	16.0	11.0	11.0	12.0	13.0	14.0	15.0	17.0	12.0	12.0
	5	14.0	11.0	12.0	11.0	12.0	14.0	16.0	17.0	13.0	12.0
	6	17.0	12.0	12.0	11.0	13.0	14.0	16.0	18.0	13.0	12.0
EP-D-4	1	15.0	9.9	10.0	13.0	13.0	12.0	13.0	15.0	12.0	11.0
	2	13.0	8.4	9.8	11.0	13.0	12.0	12.0	14.0	11.0	11.0
	3	14.0	7.1	8.1	11.0	12.0	12.0	12.0	13.0	11.0	11.0
	4	15.0	11.0	11.0	12.0	13.0	13.0	13.0	15.0	11.0	11.0
	5	13.0	9.0	9.8	11.0	12.0	12.0	13.0	13.0	11.0	10.0
	6	14.0	11.0	11.0	12.0	12.0	12.0	12.0	13.0	11.0	11.0
EP-D-3 Average:		15.3	11.1	11.5	11.2	12.5	13.3	15.0	16.3	12.2	12.0
EP-D-4 Average:		14.0	9.4	10.0	11.7	12.5	12.2	12.5	13.8	11.2	10.8
Overall Average:		14.67	10.27	10.73	11.42	12.50	12.75	13.75	15.08	11.67	11.42
Standard Dev.:		1.61	1.48	1.14	0.67	0.52	0.87	1.60	1.93	0.78	0.67
SEM:		0.47	0.43	0.33	0.19	0.15	0.25	0.46	0.56	0.22	0.19
Maximum:		18.0	12.0	12.0	13.0	13.0	14.0	16.0	18.0	13.0	12.0
Minimum:		13.0	7.1	8.1	11.0	12.0	12.0	12.0	13.0	11.0	10.0

Table A - 8: Resistivity measurements for the first and second "perfect" 50/50 enamel-coated ponding specimen.

		Resistivity Measurements (kΩcm) vs. Time (weeks):									
	Location:	0	6	12	18	24	30	36	42	48	54
Specimen: EN-1	1	9.0	6.3	9.8	7.3	6.3	6.3	6.0	5.8	6.3	4.8
	2	7.6	8.5	5.6	6.4	5.5	5.6	6.3	5.8	6.4	5.5
	3	9.4	9.2	7.2	4.7	4.9	4.7	5.4	5.9	6.3	5.4
	4	9.4	7.9	7.9	5.6	4.5	4.7	5.3	4.7	4.7	4.6
	5	7.4	7.1	3.7	7.3	4.7	4.7	4.7	4.4	4.5	4.2
	6	9.0	7.9	6.3	5.5	4.7	4.6	4.6	4.5	4.4	3.8
Specimen: EN-2	1	9.3	9.1	4.7	4.7	5.5	6.4	7.3	7.8	7.1	5.6
	2	7.0	7.3	5.5	6.4	6.4	6.4	6.3	6.4	6.4	5.6
	3	11.0	8.8	9.0	8.0	6.4	5.9	7.2	7.1	7.2	5.7
	4	8.5	9.1	7.3	6.2	5.5	5.5	5.2	5.1	4.8	4.7
	5	7.4	7.3	6.9	5.5	5.5	5.6	5.6	5.4	5.6	4.9
	6	7.4	7.5	7.2	6.4	5.6	6.1	6.3	6.2	6.4	5.4
EN-1 Average:		8.6	7.8	6.8	6.1	5.1	5.1	5.4	5.2	5.4	4.7
EN-2 Average:		8.4	8.2	6.8	6.2	5.8	6.0	6.3	6.3	6.3	5.3
Overall Average:		8.53	8.00	6.76	6.17	5.46	5.54	5.85	5.76	5.84	5.02
Standard Dev.:		1.19	0.94	1.73	1.03	0.67	0.71	0.88	1.03	1.00	0.61
SEM:		0.34	0.27	0.50	0.30	0.19	0.20	0.25	0.30	0.29	0.18
Maximum:		11.0	9.2	9.8	8.0	6.4	6.4	7.3	7.8	7.2	5.7
Minimum:		7.0	6.3	3.7	4.7	4.5	4.6	4.6	4.4	4.4	3.8

Table A - 9: Resistivity measurements for the third and fourth "perfect" 50/50 enamel-coated ponding specimen.

		Resistivity Measurements (kΩcm) vs. Time (weeks):									
	Location:	0	6	12	18	24	30	36	42	48	54
Specimen: EN-3	1	9.9	6.3	7.3	7.3	6.8	6.4	6.4	5.5	5.3	4.7
	2	7.4	6.3	7.4	8.2	7.8	7.5	8.1	7.2	7.3	6.4
	3	9.3	8.0	7.4	9.0	9.5	9.0	11.0	9.3	9.8	8.2
	4	9.2	7.3	7.2	7.1	6.8	6.3	6.4	5.6	5.5	5.2
	5	7.5	7.2	6.4	7.1	6.7	5.6	5.6	5.5	5.2	4.8
	6	9.1	8.0	5.8	7.3	7.6	6.9	7.2	5.8	5.4	5.5
Specimen: EN-4	1	13.0	3.7	8.8	9.0	9.4	8.9	8.9	8.9	7.3	7.3
	2	7.5	7.2	9.8	8.1	9.3	7.4	8.1	8.0	7.3	6.4
	3	12.0	10.0	10.0	9.8	12.0	9.0	9.1	8.9	8.5	7.3
	4	8.3	7.3	7.1	7.3	8.4	7.2	6.4	5.6	5.5	5.2
	5	9.1	7.2	8.1	8.1	8.5	7.9	7.2	5.7	5.5	4.9
	6	9.9	7.5	8.1	7.9	8.4	7.2	7.2	5.9	5.5	5.5
EN-3 Average:		8.7	7.2	6.9	7.7	7.5	7.0	7.5	6.5	6.4	5.8
EN-4 Average:		10.0	7.2	8.7	8.4	9.3	7.9	7.8	7.2	6.6	6.1
Overall Average:		9.35	7.17	7.78	8.02	8.43	7.44	7.63	6.83	6.51	5.95
Standard Dev.:		1.73	1.45	1.26	0.87	1.51	1.10	1.50	1.54	1.51	1.15
SEM:		0.50	0.42	0.36	0.25	0.44	0.32	0.43	0.44	0.44	0.33
Maximum:		13.0	10.0	10.0	9.8	12.0	9.0	11.0	9.3	9.8	8.2
Minimum:		7.4	3.7	5.8	7.1	6.7	5.6	5.6	5.5	5.2	4.7

Table A - 10: Resistivity measurements for the first and second damaged 50/50 enamel-coated ponding specimen.

		Resistivity Measurements (kΩcm) vs. Time (weeks):									
	Location:	0	6	12	18	24	30	36	42	48	54
Specimen: EN-D-1	1	9.0	7.9	8.9	7.3	5.6	6.4	6.4	6.3	5.7	5.6
	2	7.3	7.4	7.2	6.4	5.5	6.3	6.3	5.6	5.5	5.5
	3	9.4	9.1	8.1	6.8	6.4	7.2	6.9	7.4	6.4	5.8
	4	7.1	7.3	6.3	4.8	4.8	5.4	4.6	4.8	4.7	4.7
	5	8.2	6.6	6.3	5.6	5.5	4.9	4.9	4.3	4.7	4.8
	6	9.4	8.2	7.4	6.5	6.2	6.3	5.5	5.3	5.1	4.8
Specimen: EN-D-2	1	8.5	9.1	8.9	8.1	7.3	8.0	8.1	7.2	8.0	6.5
	2	7.6	7.3	7.2	6.4	5.6	6.4	6.5	6.5	6.4	5.5
	3	9.3	9.1	9.8	7.3	6.5	7.7	7.6	7.3	7.2	5.7
	4	6.7	7.3	7.2	5.5	5.4	5.6	5.7	5.6	5.0	4.7
	5	7.5	5.7	8.1	6.4	5.9	5.6	5.7	5.3	4.0	4.0
	6	7.6	8.0	8.1	6.3	5.6	5.8	6.8	6.6	6.1	4.9
EN-D-1 Average:		8.4	7.8	7.4	6.2	5.7	6.1	5.8	5.6	5.4	5.2
EN-D-2 Average:		7.9	7.8	8.2	6.7	6.1	6.5	6.7	6.4	6.1	5.2
Overall Average:		8.13	7.75	7.79	6.45	5.86	6.30	6.25	6.02	5.73	5.21
Standard Dev.:		0.97	1.04	1.06	0.89	0.65	0.94	1.03	1.02	1.15	0.67
SEM:		0.28	0.30	0.31	0.26	0.19	0.27	0.30	0.29	0.33	0.19
Maximum:		9.4	9.1	9.8	8.1	7.3	8.0	8.1	7.4	8.0	6.5
Minimum:		6.7	5.7	6.3	4.8	4.8	4.9	4.6	4.3	4.0	4.0

Table A - 11: Resistivity measurements for the third and fourth damaged 50/50 enamel-coated ponding specimen.

		Resistivity Measurements (kΩcm) vs. Time (weeks):									
	Location:	0	6	12	18	24	30	36	42	48	54
Specimen: EN-D-3	1	9.9	9.8	9.0	8.1	9.2	8.9	10.0	9.0	8.5	6.4
	2	9.2	7.4	8.1	8.1	9.3	9.0	9.1	7.4	7.3	6.5
	3	11.0	9.2	8.8	8.1	9.6	8.9	9.5	7.8	6.4	6.6
	4	8.1	4.7	4.7	7.3	8.4	8.2	7.9	5.5	5.4	5.5
	5	7.6	8.0	8.1	7.2	8.6	8.9	8.9	6.5	5.6	5.5
	6	9.9	9.0	9.0	8.1	8.6	8.5	8.9	7.3	5.5	5.6
Specimen: EN-D-4	1	11.0	8.1	7.9	7.9	8.4	8.5	9.1	8.9	8.7	8.1
	2	9.8	7.3	9.0	7.5	8.5	9.0	8.9	8.1	7.2	8.1
	3	12.0	9.0	9.0	8.1	9.5	9.9	9.7	7.2	7.2	8.2
	4	9.2	8.6	8.2	7.3	7.5	7.2	7.2	6.3	5.5	5.6
	5	9.1	8.1	8.1	8.1	8.5	8.9	8.0	7.4	6.2	6.4
	6	9.7	9.0	8.0	6.0	7.6	8.1	8.0	6.8	6.2	6.3
EN-D-3 Average:		9.3	8.0	8.0	7.8	9.0	8.7	9.1	7.3	6.5	6.0
EN-D-4 Average:		10.1	8.4	8.4	7.5	8.3	8.6	8.5	7.5	6.8	7.1
Overall Average:		9.71	8.18	8.16	7.65	8.64	8.67	8.77	7.35	6.64	6.57
Standard Dev.:		1.23	1.33	1.18	0.64	0.67	0.65	0.83	1.02	1.15	1.03
SEM:		0.35	0.38	0.34	0.18	0.19	0.19	0.24	0.29	0.33	0.30
Maximum:		12.0	9.8	9.0	8.1	9.6	9.9	10.0	9.0	8.7	8.2
Minimum:		7.6	4.7	4.7	6.0	7.5	7.2	7.2	5.5	5.4	5.5

Table A - 12: Resistivity measurements for the five non-reinforced ponding specimens.

Specimen	Location:	Resistivity Measurements (kΩcm) vs. Time (weeks): 0	9	12	16	24	30	36	42	48	54
C-1	1	9.1	7.4	7.4	8.5	9.2	7.2	7.3	7.0	6.0	6.3
	2	9.1	7.3	7.4	8.7	8.8	7.2	6.4	6.6	6.5	6.4
	3	9.0	8.4	9.0	9.7	9.6	8.0	7.3	7.9	6.6	7.3
	4	9.2	8.4	9.0	9.8	9.8	8.0	7.7	7.9	6.4	7.2
	5	8.3	6.8	6.8	8.2	8.2	7.3	6.8	7.0	6.2	6.4
	6	9.2	7.6	7.5	8.9	9.0	7.2	6.5	7.0	6.7	6.5
C-2	1	8.4	7.5	7.1	7.8	8.5	6.6	6.4	6.5	5.5	6.1
	2	7.5	8.3	8.2	9.0	9.1	7.2	7.2	7.0	6.2	7.1
	3	8.3	7.5	7.1	8.1	9.0	7.3	7.3	7.0	6.2	6.9
	4	9.3	7.8	8.0	9.7	9.8	7.3	7.3	7.0	6.2	6.4
	5	7.8	7.5	7.2	8.6	9.1	7.3	7.2	7.0	6.2	6.4
	6	8.3	7.7	8.1	9.1	9.0	7.3	6.7	6.9	5.6	6.2
C-3	1	8.5	6.8	7.7	9.0	9.0	7.2	7.3	7.1	6.2	6.4
	2	7.5	6.8	8.1	9.0	9.7	7.3	7.3	7.0	6.3	6.4
	3	7.4	7.2	7.4	8.5	8.9	7.1	7.0	7.0	6.5	6.3
	4	8.0	7.4	8.1	9.6	9.9	7.5	7.3	7.1	6.3	6.4
	5	7.0	6.8	8.1	9.1	9.7	7.4	7.2	7.0	6.2	6.7
	6	7.6	7.5	8.0	9.0	8.4	7.3	7.1	7.1	5.4	6.3
C-4	1	8.5	6.8	7.2	8.2	9.7	7.3	7.3	7.0	6.3	6.3
	2	7.1	7.5	7.0	8.1	9.1	7.3	6.8	6.6	6.2	6.4
	3	7.6	8.3	8.0	9.0	11.0	7.3	7.4	7.0	6.6	7.3
	4	9.9	7.4	7.2	9.1	10.0	7.2	7.2	7.0	6.1	5.9
	5	7.4	7.4	7.3	8.2	9.8	7.4	7.3	7.0	6.3	6.4
	6	9.3	7.4	7.3	8.2	9.0	7.3	6.7	7.1	6.2	6.4
C-5	1	7.6	6.2	6.3	8.1	8.1	7.2	6.5	6.3	6.2	6.4
	2	7.0	6.2	6.3	8.1	8.2	6.8	6.6	6.7	6.2	6.4
	3	7.9	6.8	6.7	8.9	9.8	8.1	7.3	6.9	6.2	6.4
	4	8.8	5.9	6.3	8.0	8.5	6.8	6.5	7.0	6.2	6.5
	5	7.0	6.0	6.3	8.1	8.5	7.3	6.8	6.9	6.2	6.4
	6	7.9	7.0	7.2	7.9	8.8	6.6	6.4	6.5	5.5	6.3
C-1 Average:		8.8	7.7	7.9	9.0	9.1	7.5	7.0	7.2	6.2	6.7
C-2 Average:		8.3	7.7	7.6	8.7	9.1	7.2	7.0	7.0	6.0	6.5
C-3 Average:		7.7	7.1	7.9	9.0	9.3	7.3	7.2	7.1	6.0	6.4
C-4 Average:		8.3	7.5	7.3	8.6	9.8	7.3	7.1	7.0	6.3	6.5
C-5 Average:		7.7	6.4	6.5	8.2	8.7	7.1	6.7	6.7	6.1	6.4
Overall Average:		8.16	7.25	7.44	8.67	9.18	7.26	6.99	6.98	6.12	6.49
Standard Dev.:		0.94	0.73	0.61	0.42	0.63	0.29	0.31	0.29	0.23	0.20
SEM:		0.15	0.12	0.13	0.11	0.12	0.06	0.07	0.06	0.06	0.06
Maximum:		9.9	8.3	8.0	9.1	11.0	8.1	7.4	7.1	6.8	7.3
Minimum:		7.0	5.9	6.3	7.9	8.1	6.6	6.4	6.3	5.5	5.9

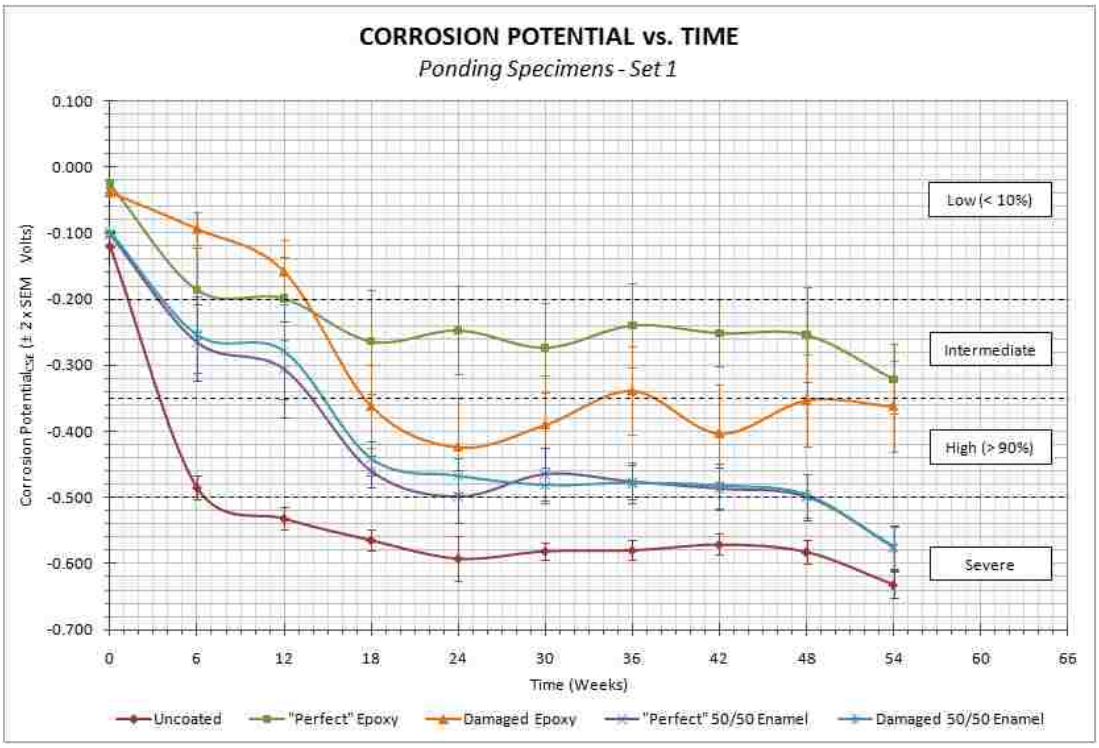

(a)

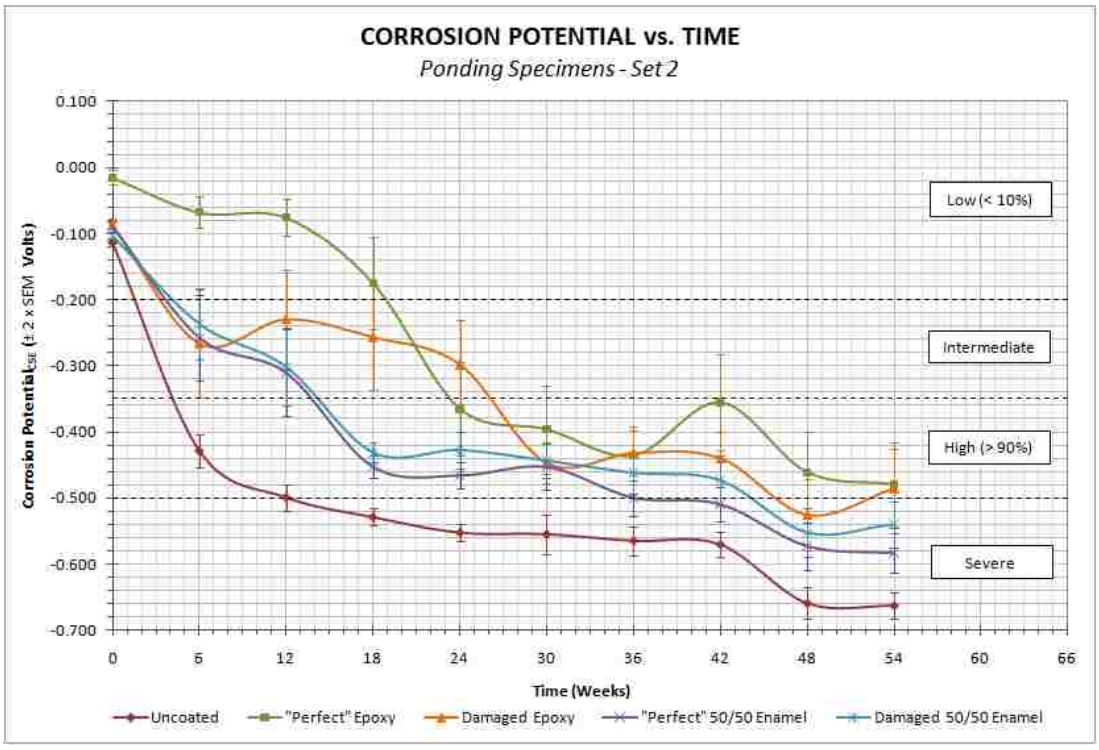

(b)

Figure A - 6: Average corrosion potential for (a) the first and second ponding specimen within each specimen group; (b) third and fourth ponding specimen within each specimen group.

Table A - 13: Corrosion potential measurements for the first and second uncoated ponding specimen.

Specimen:	Location:	Half-Cell Measurements (mV) vs. Time (weeks): 0	6	12	18	24	30	36	42	48	54
M-1	1.1	-128	-440	-511	-535	-554	-575	-564	-542	-556	-600
	1.2	-123	-464	-514	-547	-559	-582	-573	-560	-561	-604
	1.3	-118	-451	-499	-530	-562	-578	-573	-560	-557	-595
	2.1	-124	-457	-533	-568	-516	-537	-519	-504	-513	-583
	2.2	-119	-446	-514	-539	-484	-523	-517	-526	-532	-583
	2.3	-122	-437	-485	-516	-495	-524	-511	-523	-528	-565
	3.1	-121	-490	-569	-606	-629	-617	-599	-581	-595	-627
	3.2	-122	-462	-512	-559	-599	-594	-580	-565	-584	-621
	3.3	-118	-488	-559	-591	-616	-612	-589	-579	-600	-632
	4.1	-115	-425	-485	-504	-558	-576	-562	-549	-560	-594
	4.2	-122	-460	-481	-529	-571	-583	-576	-549	-552	-601
	4.3	-120	-494	-586	-609	-610	-619	-603	-577	-571	-611
M-2	1.1	-119	-456	-491	-535	-563	-534	-529	-511	-537	-585
	1.2	-125	-501	-525	-552	-572	-542	-549	-547	-560	-604
	1.3	-122	-537	-531	-546	-568	-547	-554	-549	-567	-617
	2.1	-116	-462	-500	-540	-546	-573	-585	-580	-618	-676
	2.2	-118	-508	-520	-554	-557	-588	-604	-607	-640	-703
	2.3	-118	-541	-523	-554	-556	-589	-608	-611	-639	-715
	3.1	-119	-485	-523	-563	-592	-617	-613	-597	-584	-632
	3.2	-118	-470	-531	-582	-593	-617	-603	-586	-579	-624
	3.3	-125	-470	-500	-539	-558	-601	-592	-580	-570	-620
	4.1	-124	-575	-619	-654	-796	-618	-639	-643	-662	-722
	4.2	-121	-533	-613	-639	-778	-589	-631	-636	-659	-721
	4.3	-121	-588	-632	-653	-776	-601	-635	-636	-657	-720
M-1 Average:		-121	-460	-521	-553	-563	-577	-564	-551	-558	-601
M-2 Average:		-121	-511	-542	-576	-621	-585	-595	-590	-606	-662
Average:		-121	-485	-532	-564	-592	-581	-580	-571	-582	-631
Standard Dev.:		3	43	43	41	81	31	36	38	43	50
SEM:		1	9	9	8	17	6	7	8	9	10
Maximum:		-115	-425	-481	-504	-484	-523	-511	-504	-513	-565
Minimum:		-128	-588	-632	-654	-796	-619	-639	-643	-662	-722

Table A - 14: Corrosion potential measurements for the third and fourth uncoated ponding specimen.

Specimen:	Location:	Half-Cell Measurements (mV) vs. Time (weeks): 0	6	12	18	24	30	36	42	48	54
M-3	1.1	-111	-438	-525	-505	-503	-449	-472	-497	-608	-632
	1.2	-117	-442	-512	-513	-534	-465	-500	-523	-660	-677
	1.3	-117	-424	-471	-504	-544	-480	-515	-530	-664	-667
	2.1	-116	-415	-492	-514	-509	-464	-509	-516	-587	-614
	2.2	-117	-416	-488	-509	-536	-484	-536	-546	-622	-635
	2.3	-110	-391	-461	-518	-556	-503	-554	-561	-624	-623
	3.1	-113	-436	-491	-532	-547	-573	-591	-622	-714	-695
	3.2	-110	-490	-575	-576	-570	-572	-568	-606	-712	-701
	3.3	-115	-435	-550	-571	-582	-591	-592	-622	-712	-697
	4.1	-109	-402	-467	-513	-582	-702	-670	-659	-674	-679
	4.2	-103	-409	-471	-528	-563	-707	-665	-662	-683	-701
	4.3	-114	-408	-448	-518	-576	-696	-662	-654	-674	-682
M-4	1.1	-117	-464	-502	-517	-520	-529	-545	-540	-567	-590
	1.2	-115	-454	-513	-528	-544	-552	-561	-563	-570	-592
	1.3	-113	-455	-510	-528	-552	-552	-565	-566	-557	-589
	2.1	-122	-294	-395	-453	-469	-464	-473	-490	-616	-629
	2.2	-115	-357	-469	-524	-548	-540	-548	-539	-638	-649
	2.3	-109	-367	-472	-518	-539	-530	-539	-545	-617	-621
	3.1	-120	-410	-456	-512	-536	-539	-552	-578	-699	-647
	3.2	-116	-379	-449	-499	-547	-544	-553	-586	-707	-655
	3.3	-110	-419	-532	-575	-592	-586	-584	-601	-704	-654
	4.1	-106	-617	-616	-607	-614	-603	-611	-564	-736	-758
	4.2	-109	-500	-556	-564	-590	-587	-593	-569	-737	-761
	4.3	-107	-463	-553	-564	-600	-597	-595	-548	-740	-763
M-3 Average:		-113	-426	-496	-525	-550	-557	-570	-583	-661	-667
M-4 Average:		-113	-432	-502	-532	-554	-552	-560	-557	-657	-659
Average:		-113	-429	-499	-529	-552	-555	-565	-570	-659	-663
Standard Dev.:		5	60	49	33	33	73	53	48	57	51
SEM:		1	12	10	7	7	15	11	10	12	10
Maximum:		-103	-294	-395	-453	-469	-449	-472	-490	-557	-589
Minimum:		-122	-617	-616	-607	-614	-707	-670	-662	-740	-763

Table A - 15: Corrosion potential measurements for the first and second "perfect" epoxy-coated ponding specimen.

		Half-Cell Measurements (mV) vs. Time (weeks):									
	Location:	0	6	12	18	24	30	36	42	48	54
Specimen: EP-1	1.1	-38	-75	-62	-43	-77	-127	-101	-335	-350	-354
	1.2	-40	-70	-54	-42	-74	-121	-97	-327	-344	-354
	1.3	-39	-74	-56	-40	-74	-119	-98	-329	-344	-355
	2.1	-13	-21	-62	-19	-104	-105	-107	-255	-94	-149
	2.2	-15	-20	-58	-14	-95	-103	-103	-258	-86	-146
	2.3	-12	-23	-52	-9	-92	-103	-101	-257	-85	-148
	3.1	-29	-474	-360	-405	-298	-399	-326	-320	-298	-358
	3.2	-31	-474	-364	-405	-297	-402	-325	-320	-300	-361
	3.3	-22	-477	-370	-410	-295	-403	-327	-322	-297	-361
	4.1	-47	-227	-231	-324	-380	-319	-415	-327	-345	-444
	4.2	-42	-232	-228	-318	-383	-319	-417	-329	-347	-443
	4.3	-41	-228	-224	-320	-385	-323	-418	-328	-346	-445
Specimen: EP-2	1.1	-40	-73	-75	-513	-243	-431	-193	-134	-111	-326
	1.2	-37	-75	-78	-502	-239	-429	-185	-117	-103	-314
	1.3	-35	-76	-75	-504	-241	-430	-187	-119	-108	-314
	2.1	14	-77	-40	-36	-34	-21	-5	1	-3	-108
	2.2	15	-73	-37	-29	-20	-14	3	7	1	-93
	2.3	12	-75	-38	-28	-23	-16	1	6	1	-92
	3.1	-47	-388	-420	-397	-343	-288	-341	-270	-277	-355
	3.2	-42	-384	-420	-394	-336	-287	-336	-265	-275	-357
	3.3	-47	-374	-419	-394	-332	-287	-335	-261	-274	-349
	4.1	-29	-162	-351	-397	-528	-505	-448	-395	-576	-496
	4.2	-20	-156	-351	-395	-518	-500	-445	-390	-572	-493
	4.3	-18	-162	-350	-398	-517	-506	-445	-387	-567	-490
EP-1 Average:		-31	-200	-177	-196	-213	-237	-236	-309	-270	-327
EP-2 Average:		-23	-173	-221	-332	-281	-310	-243	-194	-239	-316
Average:		-27	-186	-199	-264	-247	-273	-240	-251	-254	-321
Standard Dev.:		19	157	154	192	164	167	157	124	175	129
SEM:		4	32	31	39	33	34	32	25	36	26
Maximum:		15	-20	-37	-9	-20	-14	3	7	1	-92
Minimum:		-47	-477	-420	-513	-528	-506	-448	-395	-576	-496

Table A - 16: Corrosion potential measurements for the third and fourth "perfect" epoxy-coated ponding specimen.

		Half-Cell Measurements (mV) vs. Time (weeks):									
	Location:	0	6	12	18	24	30	36	42	48	54
Specimen: EP-3	1.1	21	5	25	21	-160	-462	-578	-560	-535	-547
	1.2	15	10	30	33	-158	-456	-566	-529	-508	-543
	1.3	30	9	28	37	-158	-461	-579	-537	-515	-543
	2.1	-3	-46	-50	-164	-450	-509	-453	-306	-513	-572
	2.2	-42	-43	-49	-156	-448	-499	-433	-289	-492	-548
	2.3	3	-43	-50	-156	-452	-501	-435	-292	-500	-546
	3.1	20	-124	-143	-385	-455	-543	-559	-582	-655	-662
	3.2	-5	-124	-143	-387	-453	-543	-552	-581	-651	-652
	3.3	-32	-124	-145	-382	-456	-545	-552	-565	-648	-655
	4.1	-2	-63	-63	-58	-52	-76	-350	-87	-427	-582
	4.2	-1	-60	-57	-56	-56	-72	-341	-82	-421	-577
	4.3	0	-65	-56	-54	-46	-71	-342	-78	-419	-572
Specimen: EP-4	1.1	-22	-46	-68	-104	-603	-580	-571	-569	-632	-618
	1.2	-23	-43	-65	-94	-595	-569	-565	-558	-622	-615
	1.3	-25	-34	-65	-97	-594	-568	-567	-553	-618	-610
	2.1	-2	-2	-13	-30	-499	-444	-346	-331	-483	-378
	2.2	-3	-2	-10	-17	-491	-434	-335	-317	-470	-365
	2.3	-5	-1	-9	-18	-491	-436	-337	-317	-479	-368
	3.1	-34	-171	-194	-466	-385	-227	-346	-187	-177	-193
	3.2	-30	-172	-192	-465	-383	-226	-341	-185	-171	-191
	3.3	-36	-163	-191	-469	-383	-226	-341	-179	-171	-186
	4.1	-65	-120	-117	-242	-331	-358	-329	-285	-327	-335
	4.2	-61	-110	-113	-245	-329	-352	-324	-283	-322	-331
	4.3	-59	-96	-108	-246	-328	-356	-322	-280	-320	-327
EP-3 Average:		0	-56	-56	-142	-279	-395	-478	-374	-524	-583
EP-4 Average:		-30	-80	-95	-208	-451	-398	-394	-337	-399	-376
Average:		-15	-68	-76	-175	-365	-396	-436	-356	-462	-480
Standard Dev.:		26	59	68	169	173	164	108	177	150	156
SEM:		5	12	14	35	35	33	22	36	31	32
Maximum:		30	10	30	37	-46	-71	-322	-78	-171	-186
Minimum:		-65	-172	-194	-469	-603	-580	-579	-582	-655	-662

Table A - 17: Corrosion potential measurements for the first and second damaged epoxy-coated ponding specimen.

Specimen	Location:	Half-Cell Measurements (mV) vs. Time (weeks): 0	6	12	18	24	30	36	42	48	54
EP-D-1	1.1	-25	-24	-65	-61	-30	-26	-17	-8	-9	-60
	1.2	-26	-23	-59	-58	-21	-17	-5	-2	-3	-26
	1.3	-30	-20	-56	-54	-19	-15	-7	-2	-3	-21
	2.1	-42	-70	-68	-512	-578	-463	-460	-553	-475	-525
	2.2	-42	-70	-63	-512	-570	-463	-455	-549	-468	-527
	2.3	-38	-69	-63	-515	-571	-464	-452	-542	-462	-518
	3.1	-28	-77	-101	-325	-600	-516	-407	-544	-559	-349
	3.2	-34	-79	-96	-327	-597	-512	-402	-539	-559	-349
	3.3	-32	-78	-95	-325	-595	-512	-400	-541	-549	-343
	4.1	-52	-143	-243	-416	-514	-384	-411	-381	-349	-232
	4.2	-53	-143	-238	-412	-502	-377	-405	-378	-342	-228
	4.3	-49	-141	-237	-413	-505	-379	-406	-375	-339	-226
EP-D-2	1.1	-26	-40	-84	-429	-584	-586	-407	-498	-513	-545
	1.2	-24	-42	-87	-423	-578	-587	-402	-493	-510	-536
	1.3	-24	-42	-82	-421	-577	-588	-390	-490	-508	-531
	2.1	-23	-41	-80	-429	-404	-360	-316	-267	-203	-300
	2.2	-20	-46	-83	-423	-395	-358	-305	-259	-201	-297
	2.3	-15	-42	-76	-422	-401	-362	-305	-262	-193	-295
	3.1	-71	-164	-409	-527	-351	-238	-181	-480	-397	-527
	3.2	-74	-163	-408	-526	-345	-235	-182	-476	-400	-526
	3.3	-70	-160	-409	-534	-351	-235	-180	-476	-392	-524
	4.1	-46	-194	-237	-209	-363	-558	-546	-521	-347	-403
	4.2	-45	-190	-233	-206	-358	-555	-543	-518	-342	-396
	4.3	-41	-193	-232	-206	-357	-558	-543	-515	-340	-397
EP-D-1 Average:		-38	-78	-115	-328	-425	-344	-319	-368	-343	-284
EP-D-2 Average:		-40	-110	-202	-396	-422	-435	-358	-438	-362	-440
Average:		-39	-94	-159	-362	-424	-390	-339	-403	-353	-362
Standard Dev.:		16	60	119	153	182	180	163	179	172	167
SEM:		3	12	24	31	37	37	33	37	35	34
Maximum:		-15	-20	-56	-54	-19	-15	-5	-2	-3	-21
Minimum:		-74	-194	-409	-534	-600	-588	-546	-553	-559	-545

Table A - 18: Corrosion potential measurements for the third and fourth damaged epoxy-coated ponding specimen.

Specimen	Location:	Half-Cell Measurements (mV) vs. Time (weeks): 0	6	12	18	24	30	36	42	48	54
EP-D-3	1.1	-114	-136	-133	-111	-416	-422	-289	-318	-585	-301
	1.2	-125	-128	-122	-102	-412	-415	-280	-313	-582	-298
	1.3	-114	-129	-125	-104	-415	-415	-280	-300	-571	-291
	2.1	-61	-131	-106	-89	-81	-472	-437	-348	-239	-224
	2.2	-53	-129	-95	-85	-76	-472	-430	-333	-246	-224
	2.3	-52	-125	-98	-80	-73	-473	-430	-328	-239	-219
	3.1	-110	-129	-144	-93	-75	-444	-449	-449	-591	-621
	3.2	-108	-126	-134	-92	-71	-432	-441	-450	-583	-619
	3.3	-104	-125	-137	-92	-67	-430	-434	-434	-576	-607
	4.1	-76	-570	-633	-556	-521	-546	-572	-539	-650	-630
	4.2	-64	-562	-627	-549	-520	-536	-555	-530	-639	-627
	4.3	-62	-562	-631	-547	-515	-532	-551	-517	-631	-618
EP-D-4	1.1	-96	-81	-75	-88	-190	-403	-466	-485	-389	-418
	1.2	-92	-80	-66	-77	-183	-397	-456	-478	-381	-414
	1.3	-81	-78	-64	-78	-183	-398	-452	-475	-378	-413
	2.1	-103	-121	-115	-569	-454	-588	-533	-561	-568	-550
	2.2	-91	-112	-104	-556	-450	-582	-525	-544	-556	-548
	2.3	-83	-111	-98	-557	-451	-582	-526	-544	-556	-552
	3.1	-118	-445	-321	-269	-375	-386	-376	-543	-598	-579
	3.2	-108	-441	-321	-270	-373	-381	-375	-535	-580	-577
	3.3	-97	-442	-323	-268	-373	-382	-373	-549	-581	-578
	4.1	-75	-543	-350	-311	-292	-348	-380	-331	-638	-579
	4.2	-74	-542	-347	-310	-292	-348	-377	-320	-629	-582
	4.3	-46	-543	-348	-312	-295	-346	-378	-326	-626	-581
EP-D-3 Average:		-87	-238	-249	-208	-270	-466	-429	-405	-511	-440
EP-D-4 Average:		-89	-295	-211	-305	-326	-428	-435	-474	-540	-531
Average:		-88	-266	-230	-257	-298	-447	-432	-440	-526	-485
Standard Dev.:		23	201	184	195	163	77	85	98	134	148
SEM:		5	41	38	40	33	16	17	20	27	30
Maximum:		-46	-78	-64	-77	-67	-346	-280	-300	-239	-219
Minimum:		-125	-570	-633	-569	-521	-588	-572	-561	-650	-630

Table A - 19: Corrosion potential measurements for the first and second "perfect" 50/50 enamel-coated ponding specimen.

Specimen:	Location:	Half-Cell Measurements (mV) vs. Time (weeks): 0	6	12	18	24	30	36	42	48	54
EN-1	1.1	-106	-125	-210	-390	-416	-438	-430	-411	-430	-517
	1.2	-104	-133	-219	-408	-398	-406	-401	-402	-431	-511
	1.3	-95	-133	-227	-457	-451	-443	-426	-450	-488	-567
	2.1	-96	-124	-114	-383	-460	-435	-466	-423	-430	-515
	2.2	-101	-114	-101	-376	-424	-399	-400	-391	-405	-487
	2.3	-92	-116	-104	-403	-447	-446	-417	-409	-419	-499
	3.1	-112	-412	-491	-534	-534	-541	-548	-583	-569	-632
	3.2	-111	-404	-482	-525	-527	-542	-561	-585	-562	-623
	3.3	-112	-423	-530	-541	-550	-560	-566	-589	-549	-619
	4.1	-106	-366	-430	-477	-717	-590	-499	-530	-629	-696
	4.2	-101	-387	-451	-487	-714	-578	-502	-550	-637	-701
	4.3	-104	-436	-546	-543	-719	-604	-560	-575	-635	-706
EN-2	1.1	-106	-126	-114	-423	-436	-264	-409	-413	-398	-458
	1.2	-106	-126	-108	-407	-409	-251	-389	-388	-385	-469
	1.3	-101	-133	-112	-446	-447	-288	-424	-406	-399	-487
	2.1	-108	-132	-111	-397	-424	-414	-420	-430	-434	-484
	2.2	-104	-128	-108	-386	-396	-395	-405	-406	-425	-497
	2.3	-94	-127	-106	-413	-429	-426	-436	-418	-443	-525
	3.1	-96	-409	-485	-551	-555	-570	-582	-560	-538	-615
	3.2	-97	-374	-441	-492	-507	-528	-536	-537	-517	-604
	3.3	-103	-364	-420	-481	-510	-533	-539	-535	-520	-599
	4.1	-97	-435	-498	-545	-520	-509	-533	-577	-588	-665
	4.2	-97	-411	-471	-497	-493	-505	-502	-564	-585	-667
	4.3	-99	-428	-475	-495	-494	-490	-489	-556	-568	-658
EN-1 Average:		-103	-264	-325	-460	-530	-499	-481	-492	-515	-589
EN-2 Average:		-101	-266	-287	-461	-468	-431	-472	-483	-483	-561
Average:		-102	-265	-306	-461	-499	-465	-477	-487	-499	-575
Standard Dev.:		6	143	179	60	97	100	65	79	84	82
SEM:		1	29	37	12	20	20	13	16	17	17
Maximum:		-92	-114	-101	-376	-396	-251	-389	-388	-385	-458
Minimum:		-112	-436	-546	-551	-719	-604	-582	-589	-637	-706

Table A - 20: Corrosion potential measurements for the third and fourth "perfect" 50/50 enamel-coated ponding specimen.

Specimen:	Location:	Half-Cell Measurements (mV) vs. Time (weeks): 0	6	12	18	24	30	36	42	48	54
EN-3	1.1	-98	-101	-379	-456	-489	-507	-515	-530	-575	-572
	1.2	-104	-105	-377	-413	-424	-427	-430	-459	-515	-526
	1.3	-99	-91	-387	-420	-418	-410	-422	-430	-480	-475
	2.1	-108	-98	-86	-450	-477	-339	-507	-546	-498	-576
	2.2	-108	-103	-94	-412	-445	-268	-446	-478	-420	-513
	2.3	-106	-113	-119	-435	-443	-268	-425	-456	-401	-478
	3.1	-95	-392	-435	-499	-530	-543	-577	-594	-678	-671
	3.2	-99	-433	-517	-532	-563	-557	-564	-585	-672	-669
	3.3	-94	-425	-489	-520	-514	-509	-528	-566	-676	-671
	4.1	-107	-352	-432	-475	-529	-559	-632	-582	-659	-649
	4.2	-109	-354	-437	-463	-494	-542	-609	-566	-654	-651
	4.3	-97	-349	-410	-457	-470	-485	-544	-536	-656	-650
EN-4	1.1	-66	-120	-110	-445	-433	-448	-459	-423	-492	-500
	1.2	-70	-104	-96	-388	-393	-412	-419	-387	-471	-482
	1.3	-86	-95	-91	-388	-408	-447	-455	-402	-493	-496
	2.1	-111	-112	-135	-448	-420	-384	-428	-489	-553	-568
	2.2	-110	-114	-137	-405	-398	-346	-405	-457	-514	-509
	2.3	-103	-133	-150	-432	-442	-387	-449	-463	-543	-524
	3.1	-65	-403	-408	-474	-477	-505	-542	-543	-638	-648
	3.2	-71	-397	-408	-461	-471	-513	-551	-557	-641	-650
	3.3	-61	-447	-482	-553	-550	-557	-559	-562	-636	-645
	4.1	-63	-517	-473	-491	-511	-515	-545	-563	-639	-632
	4.2	-58	-408	-398	-414	-432	-464	-499	-535	-625	-626
	4.3	-59	-414	-405	-438	-451	-480	-482	-516	-618	-622
EN-3 Average:		-102	-243	-347	-461	-483	-451	-517	-527	-574	-592
EN-4 Average:		-77	-272	-274	-445	-449	-455	-483	-491	-572	-575
Average:		-89	-258	-311	-453	-466	-453	-500	-509	-573	-583
Standard Dev.:		19	157	160	43	48	87	66	62	87	72
SEM:		4	32	33	9	10	18	13	13	18	15
Maximum:		-58	-91	-86	-388	-393	-268	-405	-387	-401	-475
Minimum:		-111	-517	-517	-553	-563	-559	-632	-594	-676	-671

Table A - 21: Corrosion potential measurements for the first and second damaged 50/50 enamel-coated ponding specimen.

Specimen	Location:	Half-Cell Measurements (mV) vs. Time (weeks): 0	6	12	18	24	30	36	42	48	54
EN-D-1	1.1	-97	-110	-104	-385	-434	-488	-421	-404	-399	-463
	1.2	-92	-115	-96	-375	-400	-437	-393	-380	-394	-467
	1.3	-86	-116	-103	-402	-421	-438	-410	-409	-423	-502
	2.1	-95	-111	-107	-414	-454	-462	-453	-432	-443	-539
	2.2	-103	-123	-104	-392	-425	-425	-429	-429	-465	-564
	2.3	-98	-124	-103	-401	-437	-416	-418	-445	-460	-554
	3.1	-99	-481	-484	-531	-537	-569	-573	-590	-578	-644
	3.2	-97	-409	-436	-475	-492	-519	-524	-572	-568	-636
	3.3	-96	-387	-420	-464	-495	-500	-490	-567	-563	-626
	4.1	-97	-450	-511	-569	-602	-610	-614	-607	-590	-653
	4.2	-103	-388	-455	-512	-549	-569	-584	-584	-583	-654
	4.3	-102	-374	-451	-510	-546	-555	-559	-575	-571	-646
EN-D-2	1.1	-102	-123	-114	-380	-410	-427	-383	-400	-411	-465
	1.2	-101	-123	-112	-377	-394	-415	-376	-380	-395	-461
	1.3	-109	-127	-121	-404	-420	-457	-431	-426	-429	-510
	2.1	-104	-123	-108	-361	-389	-394	-404	-387	-410	-483
	2.2	-97	-124	-109	-362	-377	-376	-394	-378	-404	-513
	2.3	-96	-123	-113	-379	-399	-393	-429	-402	-420	-541
	3.1	-104	-419	-490	-541	-562	-572	-573	-556	-593	-674
	3.2	-102	-374	-422	-455	-483	-496	-507	-522	-590	-672
	3.3	-105	-368	-411	-452	-491	-487	-473	-461	-525	-669
	4.1	-85	-351	-457	-516	-532	-542	-571	-578	-583	-646
	4.2	-87	-330	-453	-478	-494	-516	-548	-560	-576	-641
	4.3	-92	-319	-412	-465	-479	-494	-521	-533	-548	-627
EN-D-1 Average:		-97	-266	-281	-453	-483	-499	-489	-500	-503	-579
EN-D-2 Average:		-99	-242	-277	-431	-453	-464	-468	-465	-490	-575
Average:		-98	-254	-279	-442	-468	-482	-478	-482	-497	-577
Standard Dev.:		6	140	176	64	63	66	76	84	80	79
SEM:		1	29	36	13	13	13	15	17	16	16
Maximum:		-85	-110	-96	-361	-377	-376	-376	-378	-394	-461
Minimum:		-109	-481	-511	-569	-602	-610	-614	-607	-593	-674

Table A - 22: Corrosion potential measurements for the third and fourth damaged 50/50 enamel-coated ponding specimen.

Specimen	Location:	Half-Cell Measurements (mV) vs. Time (weeks): 0	6	12	18	24	30	36	42	48	54
EN-D-3	1.1	-111	-102	-84	-369	-341	-404	-333	-374	-490	-477
	1.2	-109	-110	-93	-387	-358	-387	-339	-363	-507	-496
	1.3	-107	-111	-109	-443	-402	-403	-354	-366	-556	-561
	2.1	-115	-120	-194	-370	-310	-408	-427	-376	-524	-513
	2.2	-121	-115	-183	-373	-297	-368	-396	-346	-545	-540
	2.3	-117	-114	-183	-411	-323	-370	-390	-331	-532	-512
	3.1	-104	-320	-447	-470	-449	-488	-526	-563	-630	-634
	3.2	-103	-316	-408	-422	-420	-426	-455	-527	-607	-609
	3.3	-105	-326	-406	-423	-441	-433	-452	-493	-594	-594
	4.1	-101	-355	-416	-482	-492	-522	-522	-570	-622	-613
	4.2	-108	-360	-411	-444	-470	-499	-531	-573	-637	-620
	4.3	-98	-395	-470	-488	-525	-541	-545	-571	-634	-618
EN-D-4	1.1	-101	-96	-312	-415	-408	-377	-427	-409	-414	-416
	1.2	-88	-107	-325	-417	-399	-374	-394	-397	-394	-401
	1.3	-96	-104	-343	-451	-440	-415	-416	-399	-404	-408
	2.1	-97	-113	-110	-421	-434	-407	-449	-455	-481	-448
	2.2	-99	-107	-102	-398	-407	-385	-425	-443	-469	-443
	2.3	-101	-102	-99	-422	-428	-397	-451	-436	-469	-435
	3.1	-104	-433	-471	-509	-566	-566	-559	-559	-597	-590
	3.2	-107	-381	-410	-426	-476	-481	-486	-500	-555	-554
	3.3	-105	-370	-400	-424	-474	-481	-487	-481	-526	-523
	4.1	-88	-382	-425	-465	-477	-499	-581	-624	-706	-662
	4.2	-99	-377	-428	-462	-458	-488	-565	-606	-693	-651
	4.3	-95	-364	-416	-459	-472	-532	-583	-607	-681	-644
EN-D-3 Average:		-108	-229	-284	-424	-402	-437	-439	-454	-573	-566
EN-D-4 Average:		-98	-245	-320	-439	-453	-450	-485	-493	-532	-515
Average:		-103	-237	-302	-431	-428	-444	-462	-474	-553	-540
Standard Dev.:		8	133	144	37	67	62	76	94	90	85
SEM:		2	27	29	8	14	13	16	19	18	17
Maximum:		-88	-96	-84	-369	-297	-368	-333	-331	-394	-401
Minimum:		-121	-433	-471	-509	-566	-568	-583	-624	-706	-662

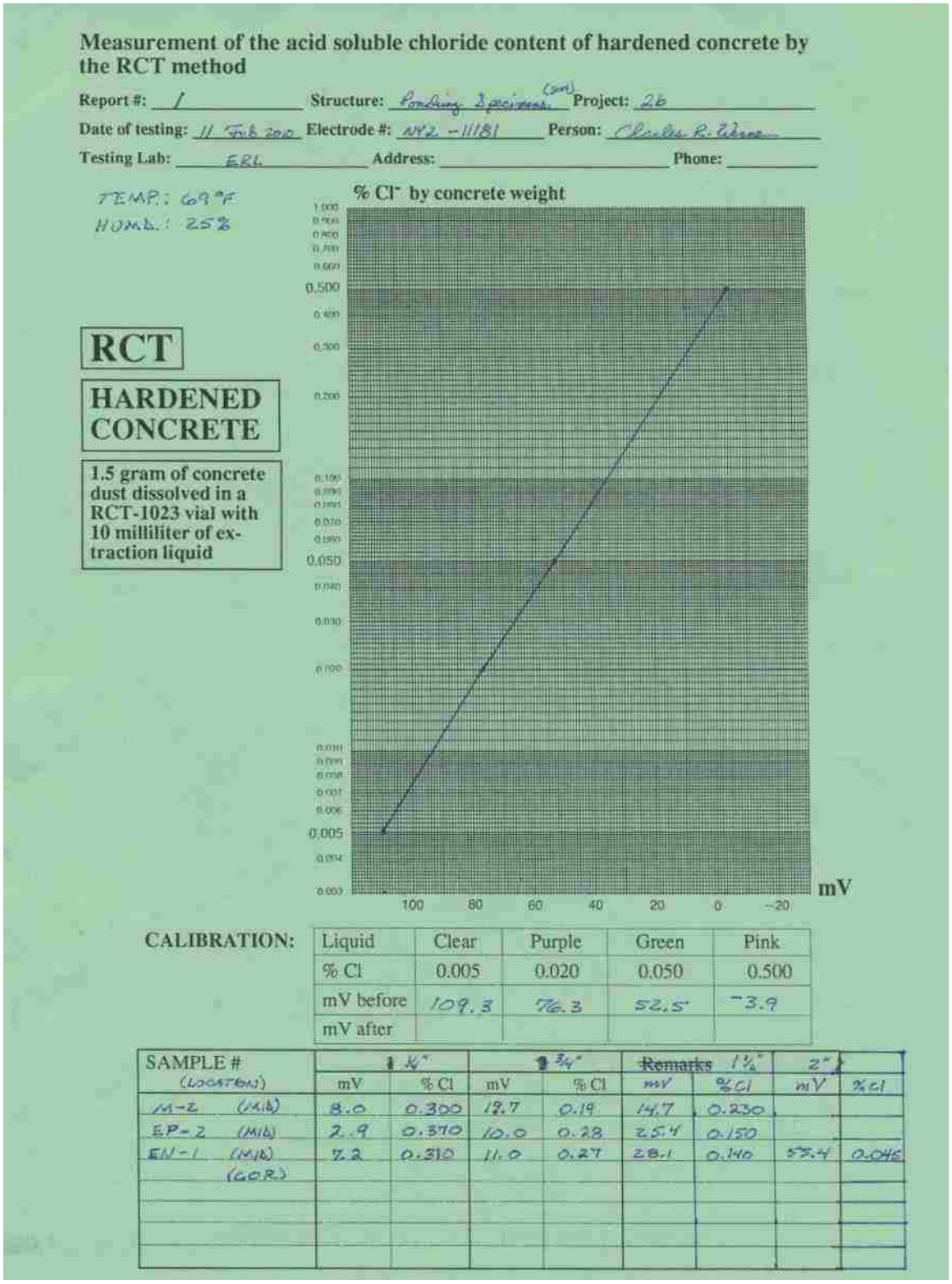

Measurement of the acid soluble chloride content of hardened concrete by the RCT method

Report #: 1 Structure: Ponding Specimens (SM) Project: 26

Date of testing: 11 Feb 200 Electrode #: NN2 -11181 Person: Charles R. Hare

Testing Lab: ERL Address: _____ Phone: _____

TEMP.: 69°F
HUMD.: 25%

% Cl⁻ by concrete weight

0.500
0.050
0.005

100 80 60 40 20 0 −20 mV

RCT

HARDENED CONCRETE

1.5 gram of concrete dust dissolved in a RCT-1023 vial with 10 milliliter of extraction liquid

CALIBRATION:

Liquid	Clear	Purple	Green	Pink
% Cl	0.005	0.020	0.050	0.500
mV before	109.3	76.3	52.5	-3.9
mV after				

SAMPLE # (LOCATION)	¼" mV	¼" % Cl	¾" mV	¾" % Cl	Remarks 1½" mV	1½" % Cl	2" mV	2" % Cl
M-2 (MAB)	8.0	0.300	12.7	0.19	14.7	0.230		
EP-2 (MAB)	2.9	0.370	10.0	0.28	25.4	0.150		
EN-1 (MAB) (COR.)	7.2	0.310	11.0	0.27	28.1	0.140	55.4	0.045

Figure A - 7: Typical data sheet used while conducting a chloride analysis upon a set of ponding specimens.

Figure A - 8: A series of images showing the progression of the removal of a ponding specimen's reinforcement.

(a)

(b)

Figure A - 9: The (a) front and (b) back view of the four bars that were embedded within the first uncoated ponding specimen (M-1) which reported a final corrosion potential of -601 mV and an overall resistance of 4.2 kΩcm.

(a)

(b)

Figure A - 10: The (a) front and (b) back view of the four bars that were embedded within the second uncoated ponding specimen (M-2) which reported a final corrosion potential of -662 mV and an overall resistance of 3.5 kΩcm.

(a)

(b)

Figure A - 11: The (a) front and (b) back view of the four bars that were embedded within the third uncoated ponding specimen (M-3) which reported a final corrosion potential of -667 mV and an overall resistance of 4.5 kΩcm.

(a)

(b)

Figure A - 12: The (a) front and (b) back view of the four bars that were embedded within the fourth uncoated ponding specimen (M-4) which reported a final corrosion potential of -659 mV and an overall resistance of 4.8 kΩcm.

(a)

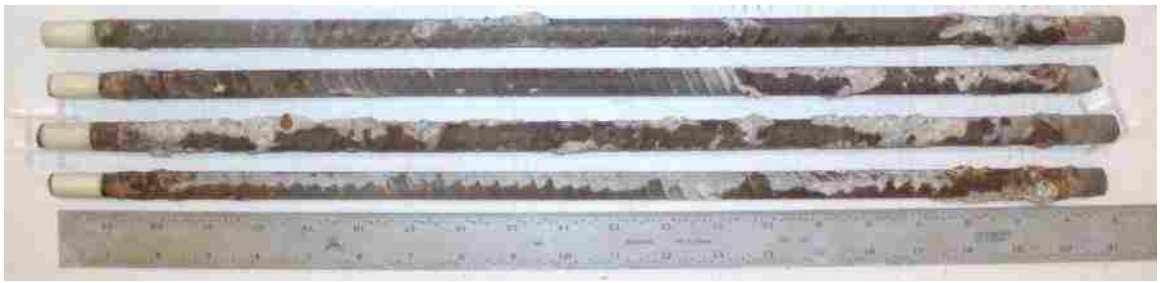

(b)

Figure A - 13: The (a) front and (b) back view of the four bars that were embedded within the first "perfect" 50/50 enamel-coated ponding specimen (EN-1) which reported a final corrosion potential of -589 mV and an overall resistance of 6.0 kΩcm.

(a)

(b)

Figure A - 14: The (a) front and (b) back view of the four bars that were embedded within the second "perfect" 50/50 enamel-coated ponding specimen (EN-2) which reported a final corrosion potential of -561 mV and an overall resistance of 6.6 kΩcm.

(a)

(b)

Figure A - 15: The (a) front and (b) back view of the four bars that were embedded within the third "perfect" 50/50 enamel-coated ponding specimen (EN-3) which reported a final corrosion potential of -592 mV and an overall resistance of 7.1 kΩcm.

(a)

(b)

Figure A - 16: The (a) front and (b) back view of the four bars that were embedded within the fourth "perfect" 50/50 enamel-coated ponding specimen (EN-4) which reported a final corrosion potential of -575 mV and an overall resistance of 7.9 kΩcm.

(a)

(b)

Figure A - 17: The (a) front and (b) back view of the four bars that were embedded within the first damaged 50/50 enamel-coated ponding specimen (EN-D-1) which reported a final corrosion potential of -579 mV and an overall resistance of 6.3 kΩcm.

(a)

(b)

Figure A - 18: The (a) front and (b) back view of the four bars that were embedded within the second damaged 50/50 enamel-coated ponding specimen (EN-D-2) which reported a final corrosion potential of -575 mV and an overall resistance of 6.8 kΩcm.

(a)

(b)

Figure A - 19: The (a) front and (b) back view of the four bars that were embedded within the third damaged 50/50 enamel-coated ponding specimen (EN-D-3) which reported a final corrosion potential of -555 mV and an overall resistance of 4.8 kΩcm.

(a)

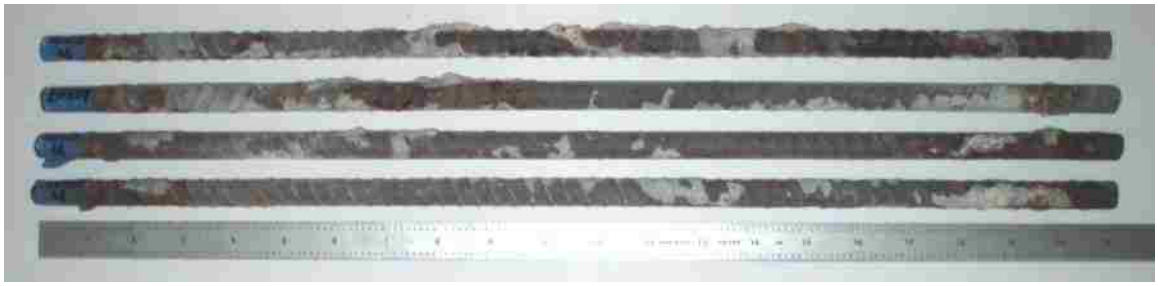

(b)

Figure A - 20: The (a) front and (b) back view of the four bars that were embedded within the fourth damaged 50/50 enamel-coated ponding specimen (EN-D-4) which reported a final corrosion potential of -555 mV and an overall resistance of 4.8 kΩcm.

(a)

(b)

Figure A - 21: The (a) front and (b) back view of the four bars that were embedded within the first "perfect" epoxy-coated ponding specimen (EP-1) which reported a final corrosion potential of -327 mV and an overall resistance of 9.9 kΩcm.

(a)

(b)

Figure A - 22: The (a) front and (b) back view of the four bars that were embedded within the second "perfect" epoxy-coated ponding specimen (EP-2) which reported a final corrosion potential of -316 mV and an overall resistance of 9.2 kΩcm.

(a)

(b)

Figure A - 23: The (a) front and (b) back view of the four bars that were embedded within the third "perfect" epoxy-coated ponding specimen (EP-3) which reported a final corrosion potential of -583 mV and an overall resistance of 12.8 kΩcm.

(a)

(b)

Figure A - 24: The (a) front and (b) back view of the four bars that were embedded within the fourth "perfect" epoxy-coated ponding specimen (EP-4) which reported a final corrosion potential of -376 mV and an overall resistance of 12.1 kΩcm.

(a)

(b)

Figure A - 25: The (a) front and (b) back view of the four bars that were embedded within the first damaged epoxy-coated ponding specimen (EP-D-1) which reported a final corrosion potential of -284 mV and an overall resistance of 9.4 kΩcm.

(a)

(b)

Figure A - 26: The (a) front and (b) back view of the four bars that were embedded within the second damaged epoxy-coated ponding specimen (EP-D-2) which reported a final corrosion potential of -440 mV and an overall resistance of 9.7 kΩcm.

(a)

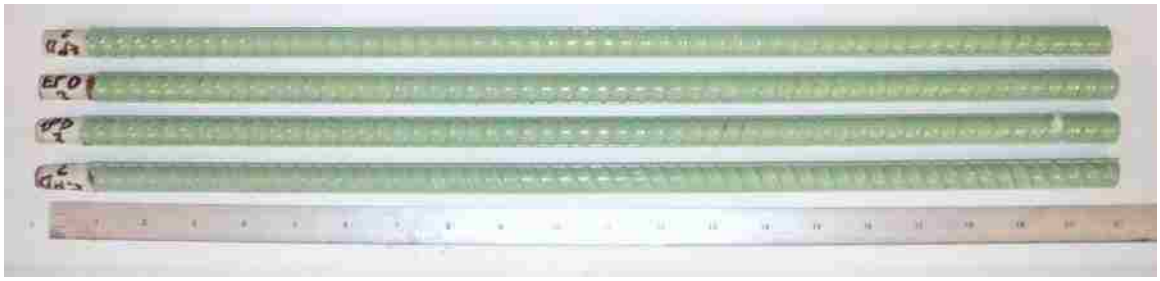

(b)

Figure A - 27: The (a) front and (b) back view of the four bars that were embedded within the third damaged epoxy-coated ponding specimen (EP-D-3) which reported a final corrosion potential of -440 mV and an overall resistance of 13.0 kΩcm.

(a)

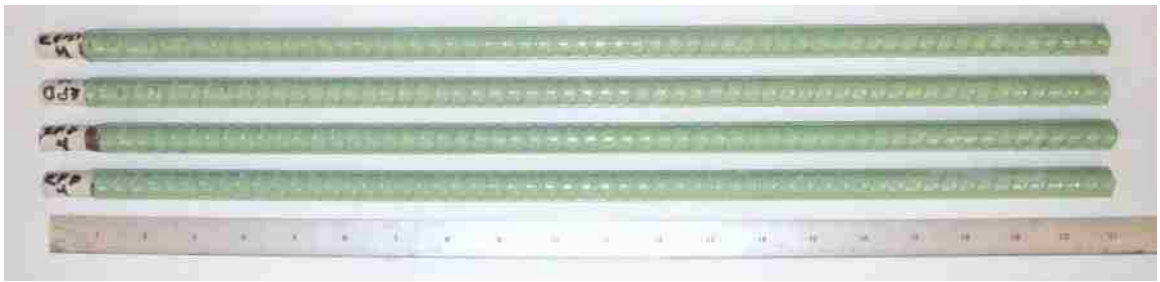

(b)

Figure A - 28: The (a) front and (b) back view of the four bars that were embedded within the fourth damaged epoxy-coated ponding specimen (EP-D-4) which reported a final corrosion potential of -531 mV and an overall resistance of 11.8 kΩcm.

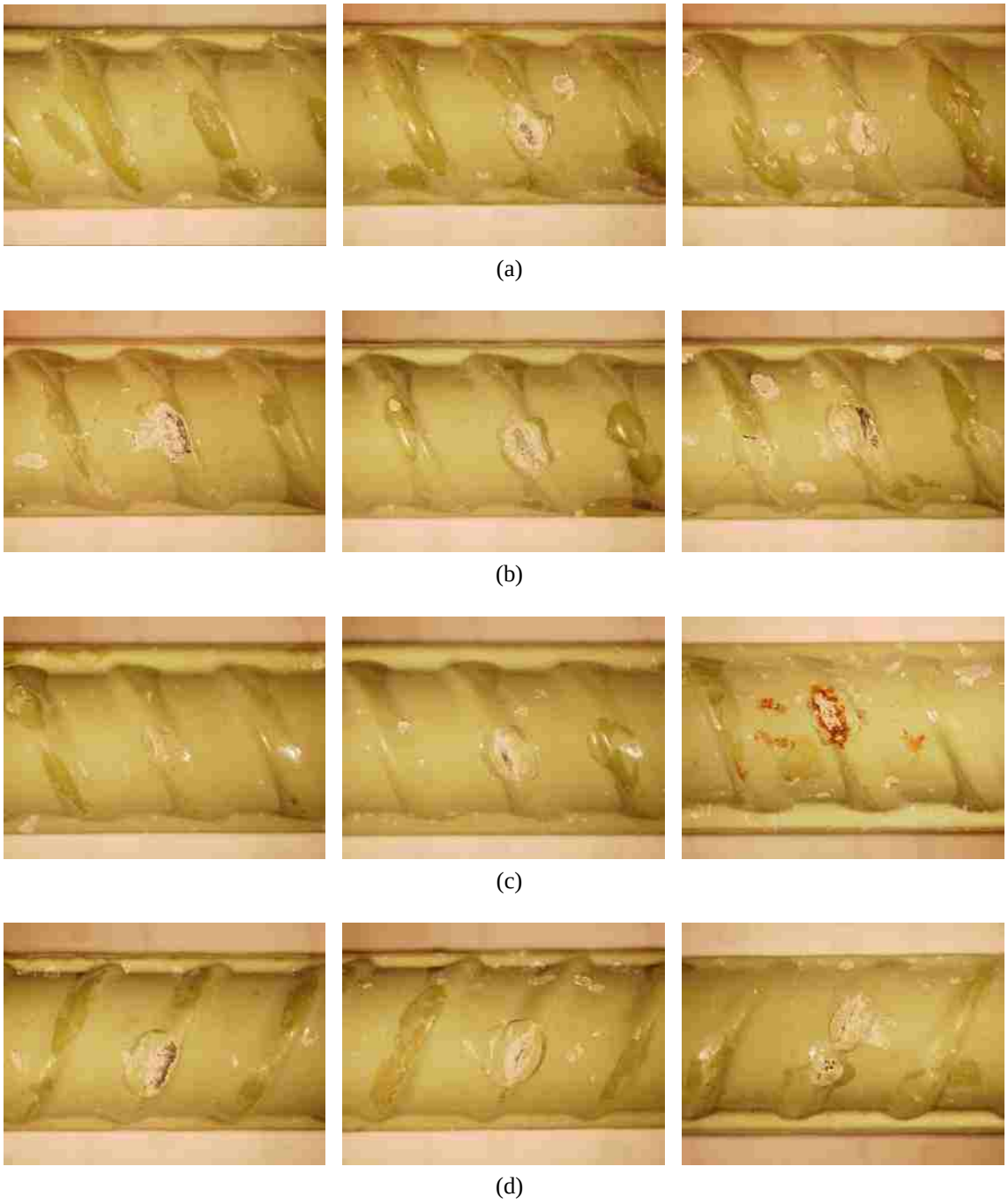

Figure A - 29: The three intentionally damaged areas along (a) bar-1; (b) bar-2; (c) bar-3; and (d) bar-4 of ponding specimen EP-D-1.

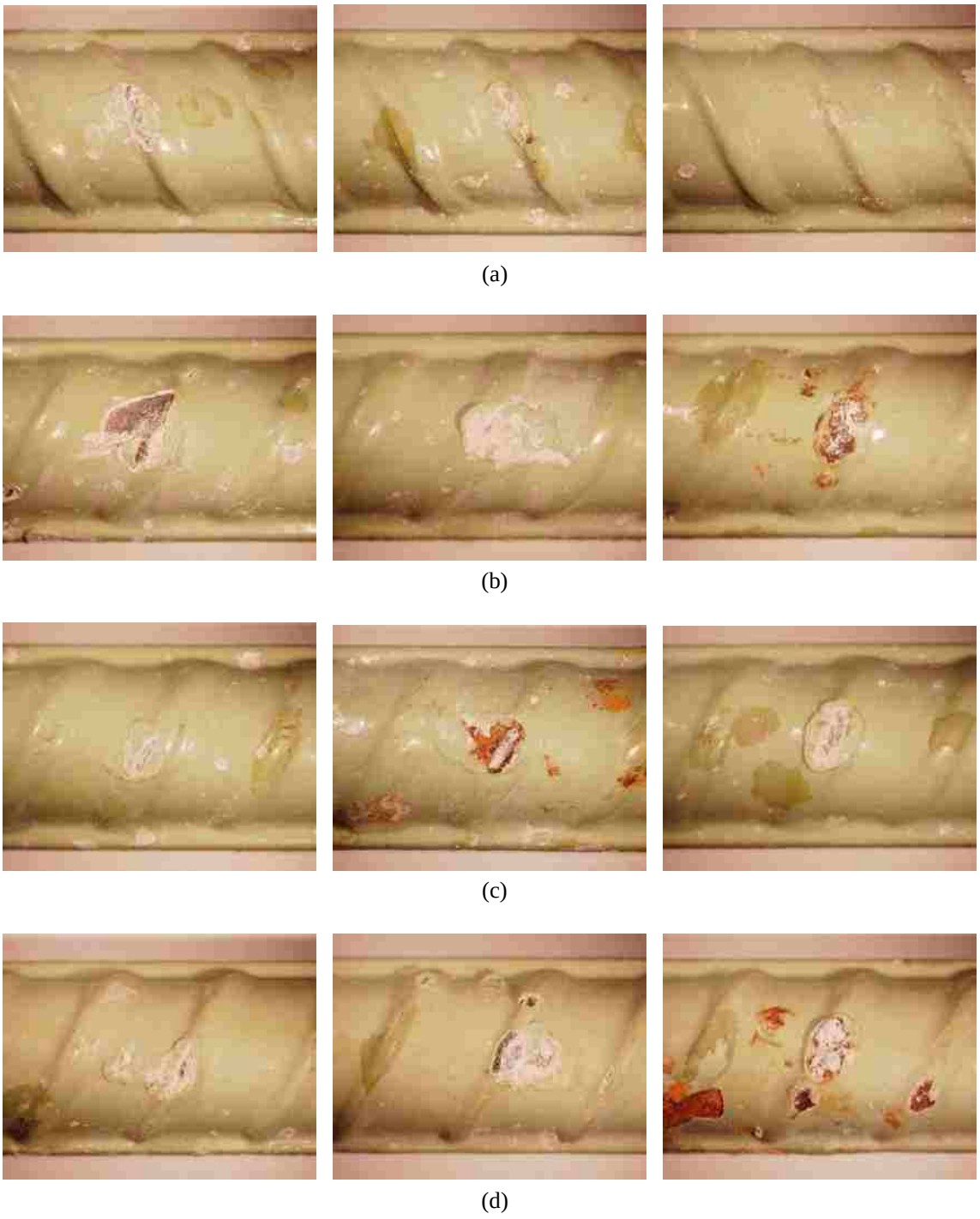

Figure A - 30: The three intentionally damaged areas along (a) bar-1; (b) bar-2; (c) bar-3; and (d) bar-4 of ponding specimen EP-D-2.

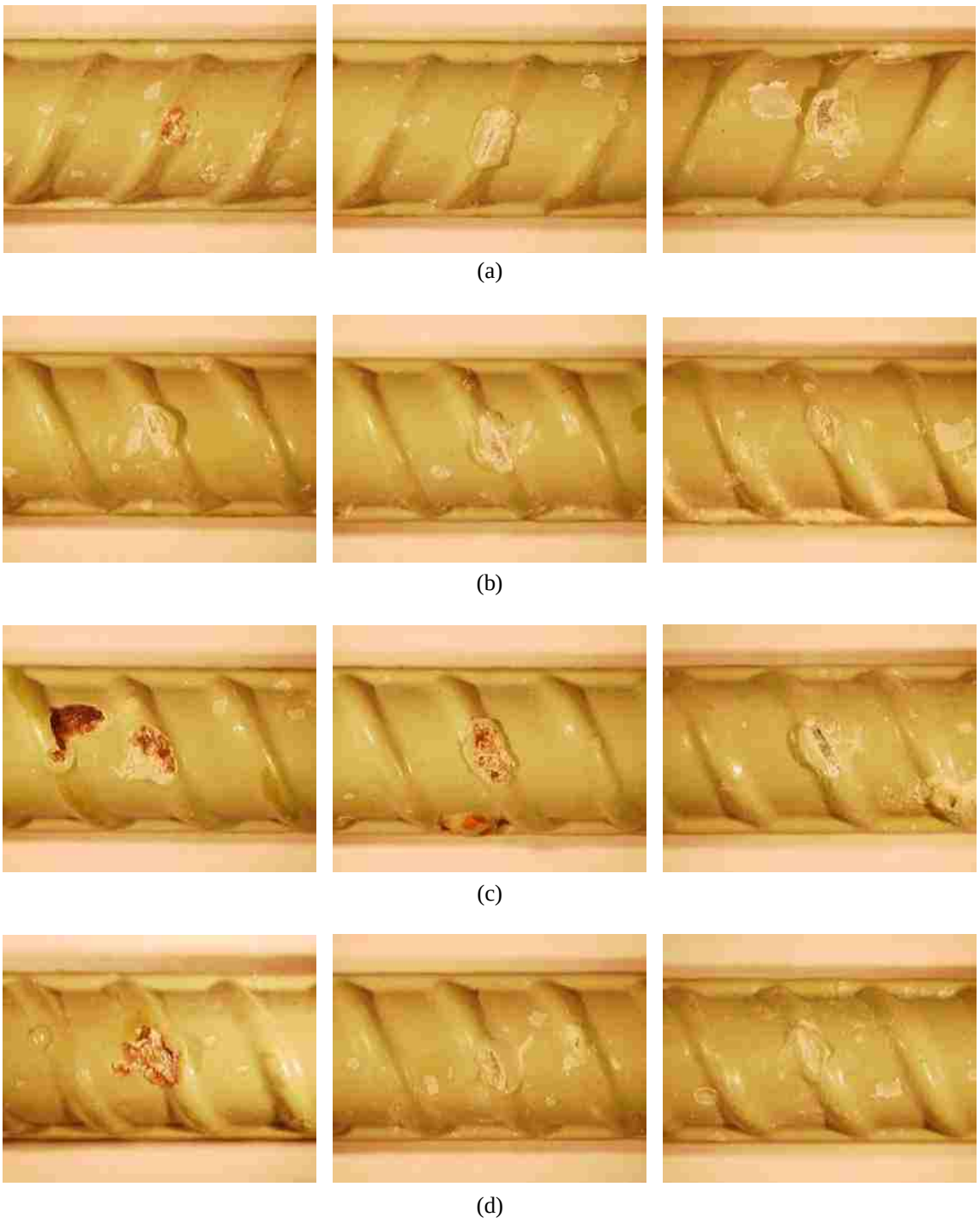

Figure A - 31: The three intentionally damaged areas along (a) bar-1; (b) bar-2; (c) bar-3; and (d) bar-4 of ponding specimen EP-D-3.

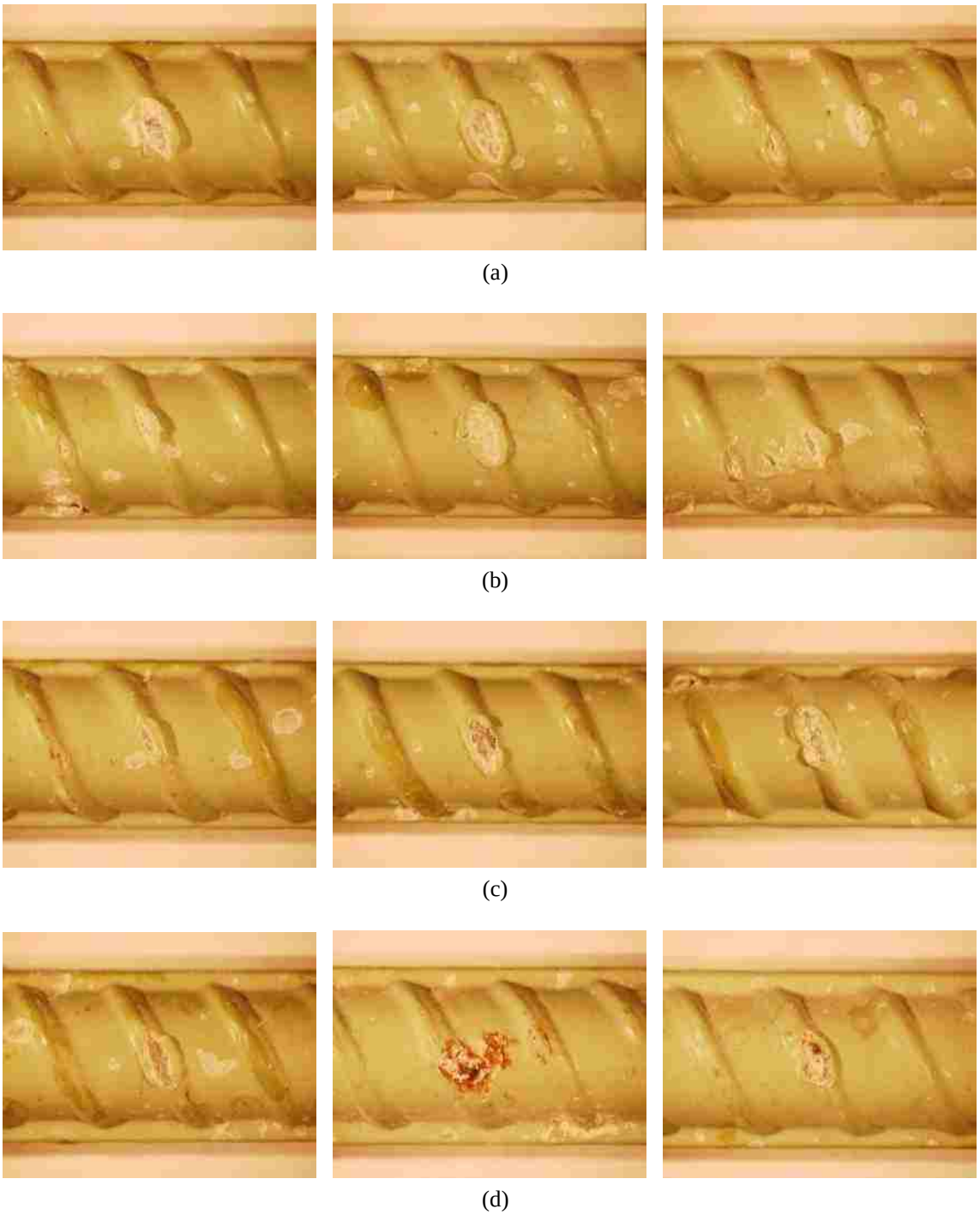

Figure A - 32: The three intentionally damaged areas along (a) bar-1; (b) bar-2; (c) bar-3; and (d) bar-4 of ponding specimen EP-D-4.

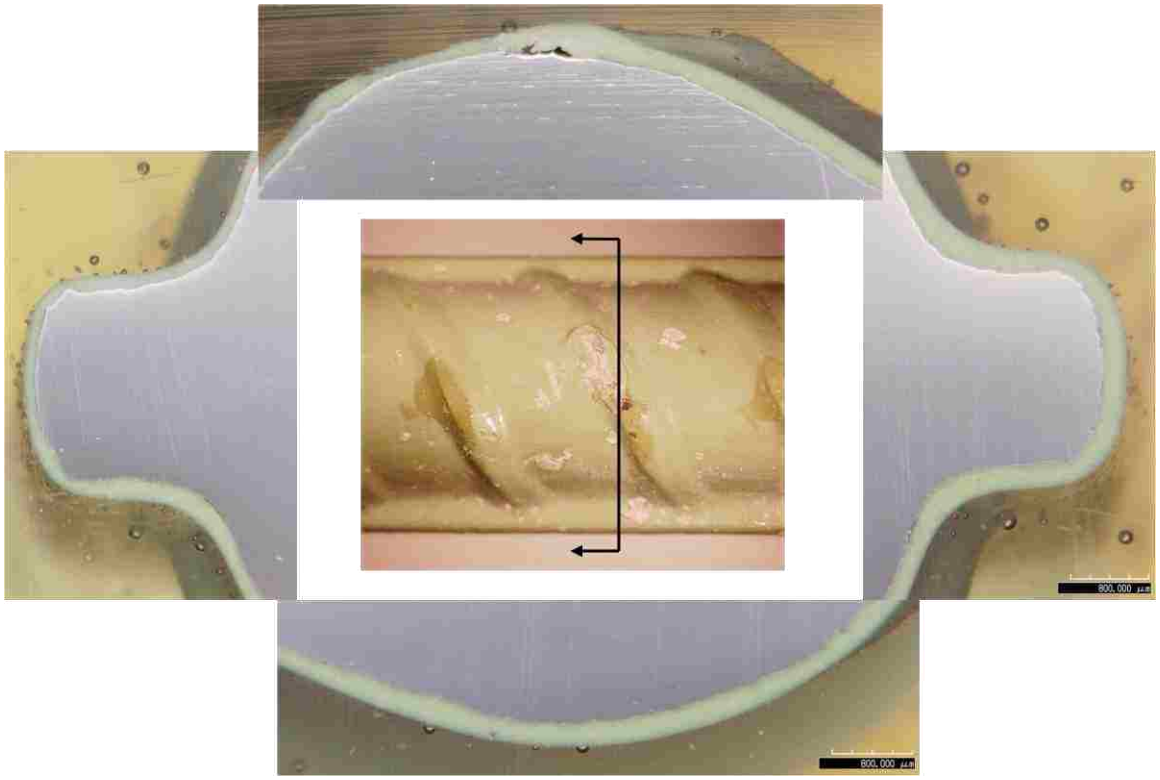

Figure A - 33: A cross-section through an intentionally damaged area along bar-1 of specimen EP-D-2.

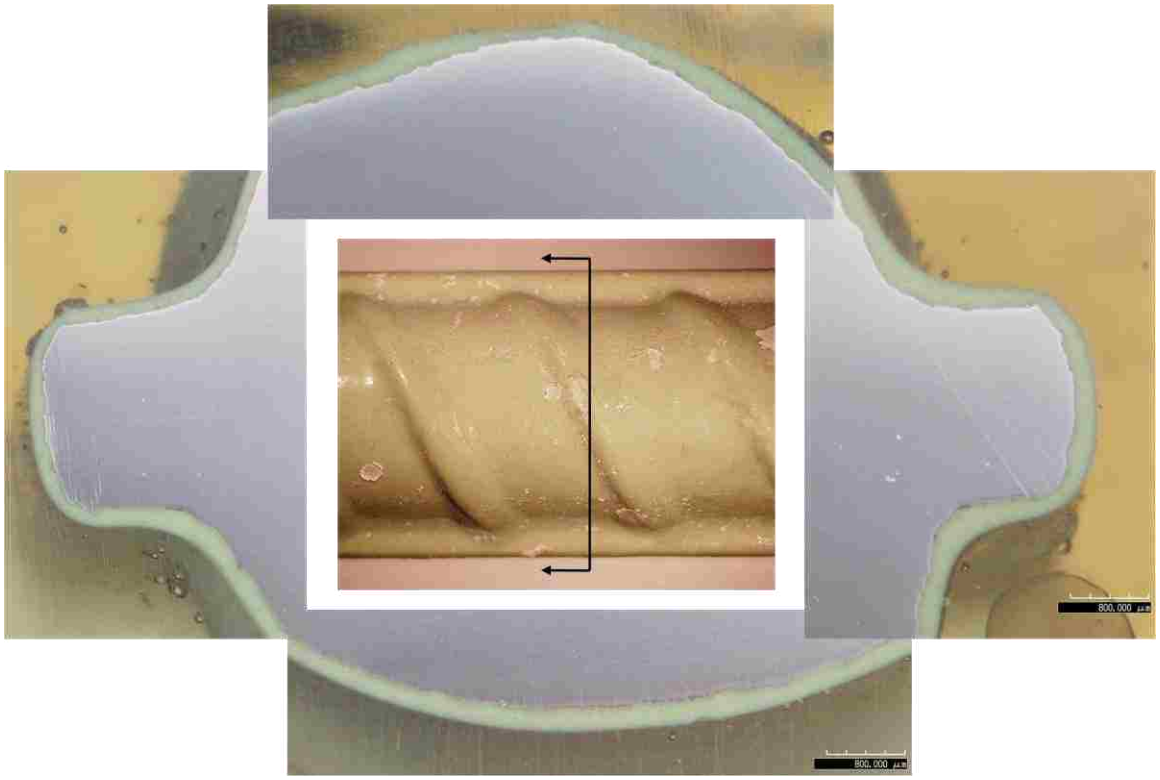

Figure A - 34: A cross-section through an intentionally damaged area along bar-1 of specimen EP-D-2.

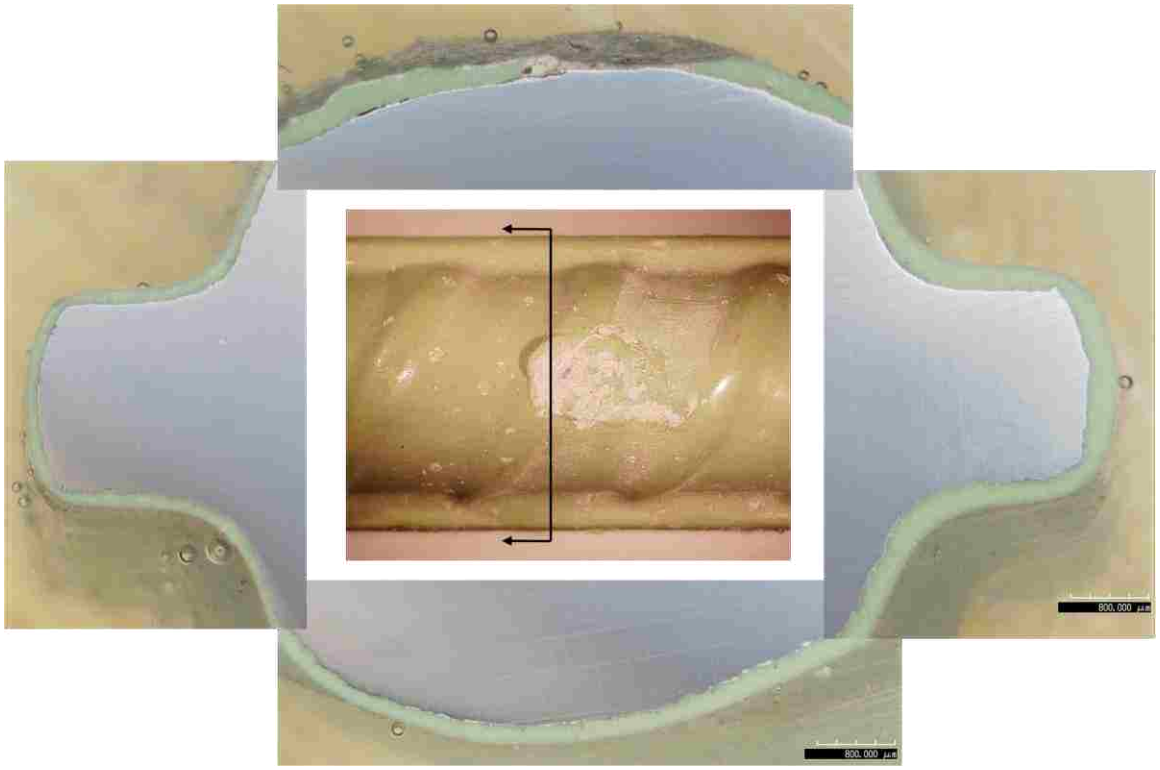

Figure A - 35: A cross-section through an intentionally damaged area along bar-2 of specimen EP-D-2.

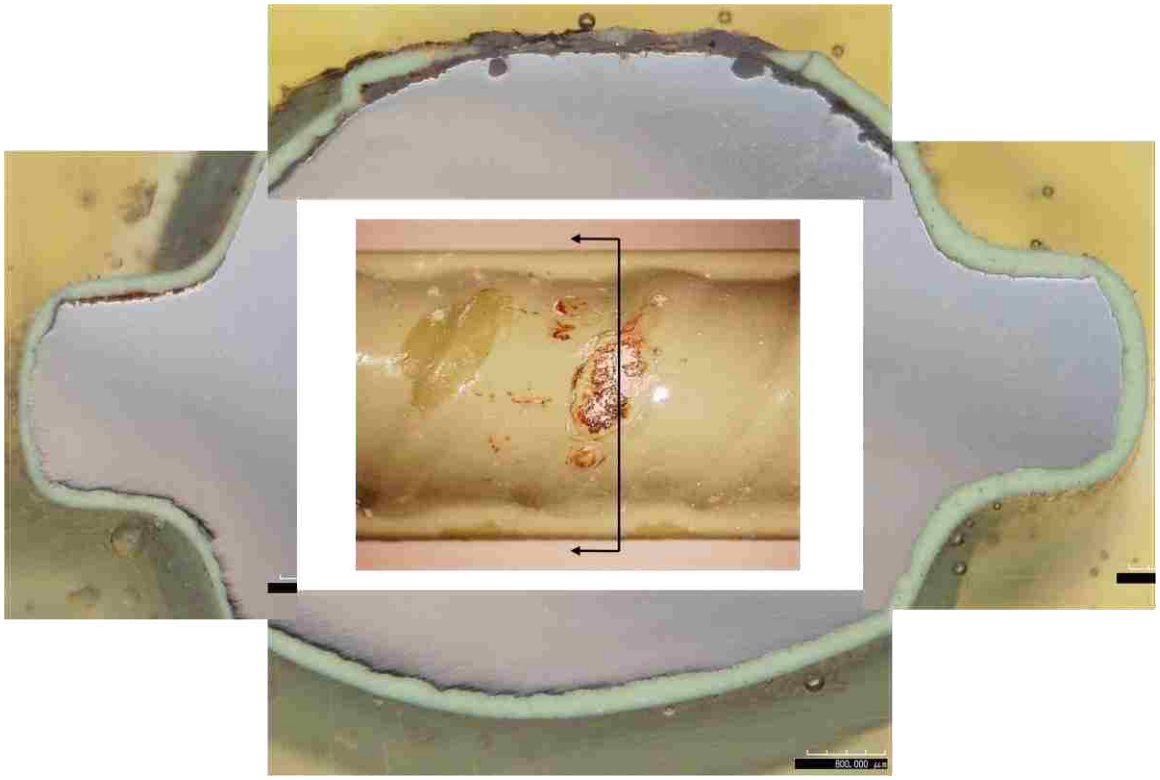

Figure A - 36: A cross-section through an intentionally damaged area along bar-2 of specimen EP-D-2.

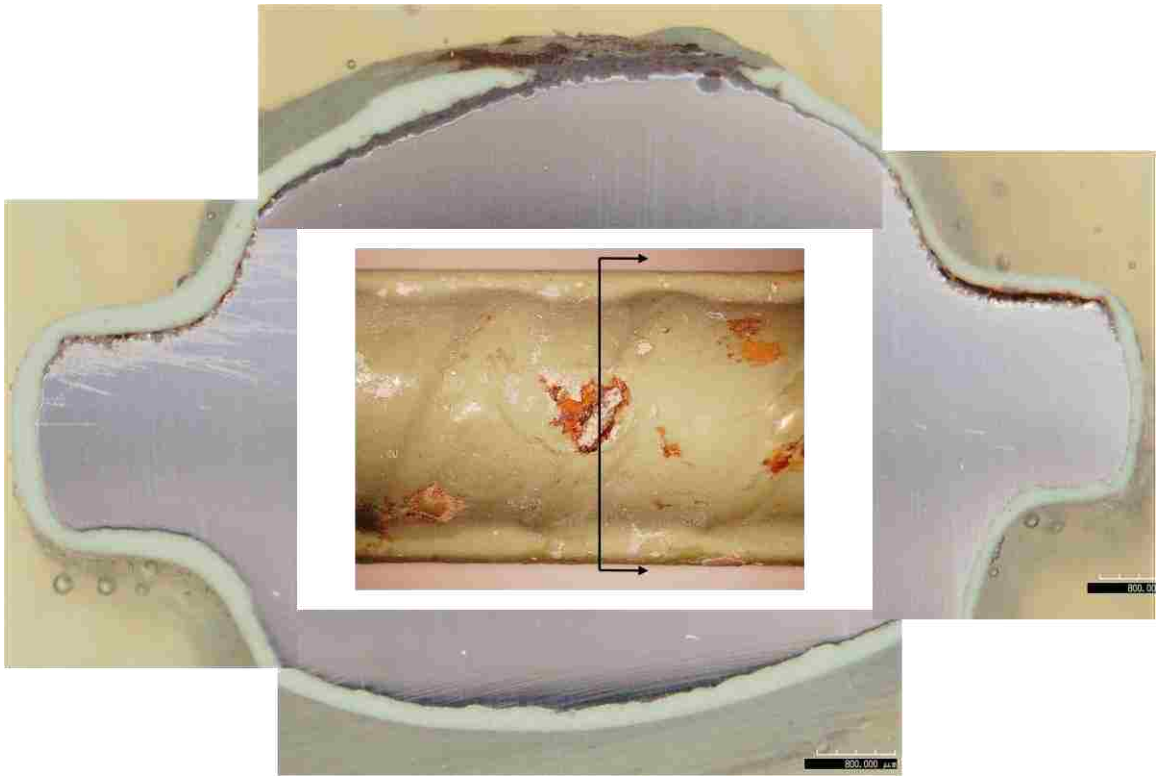

Figure A - 37: A cross-section through an intentionally damaged area along bar-3 of specimen EP-D-2.

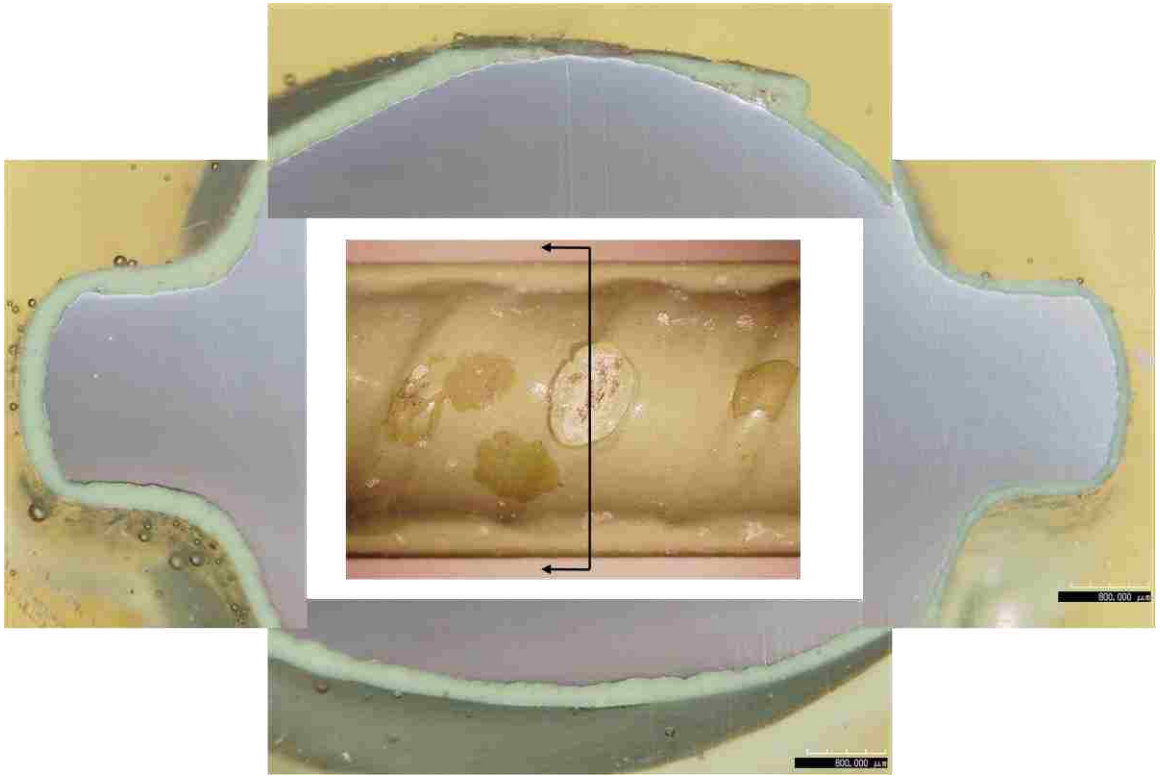

Figure A - 38: A cross-section through an intentionally damaged area along bar-3 of specimen EP-D-2.

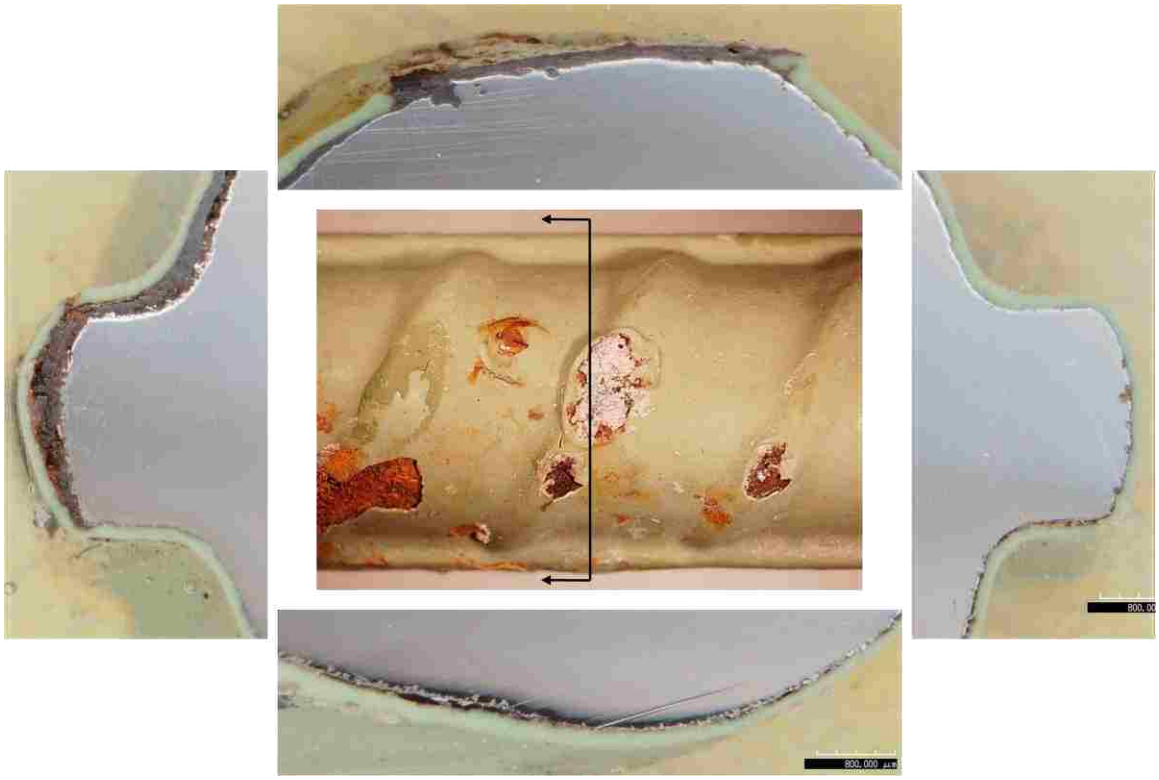

Figure A - 39: A cross-section through an intentionally damaged area along bar-4 of specimen EP-D-2.

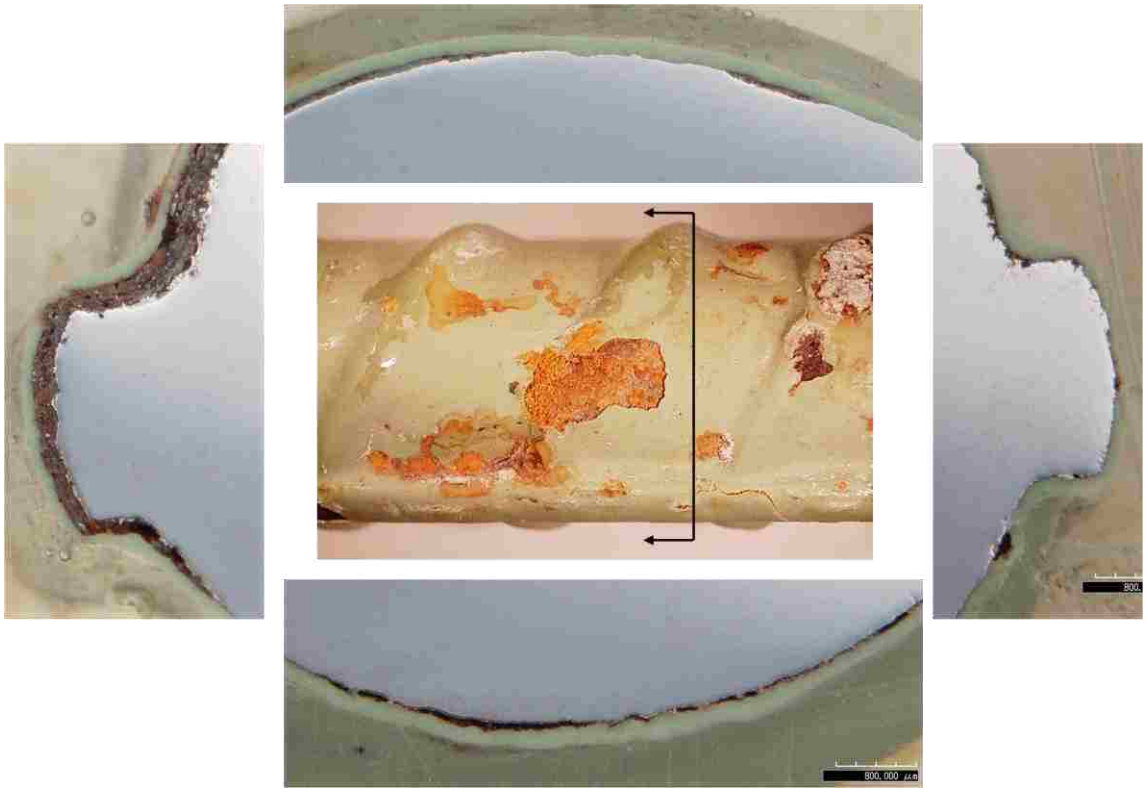

Figure A - 40: A cross-section through an unexplained area of damaged along bar-4 of specimen EP-D-2.

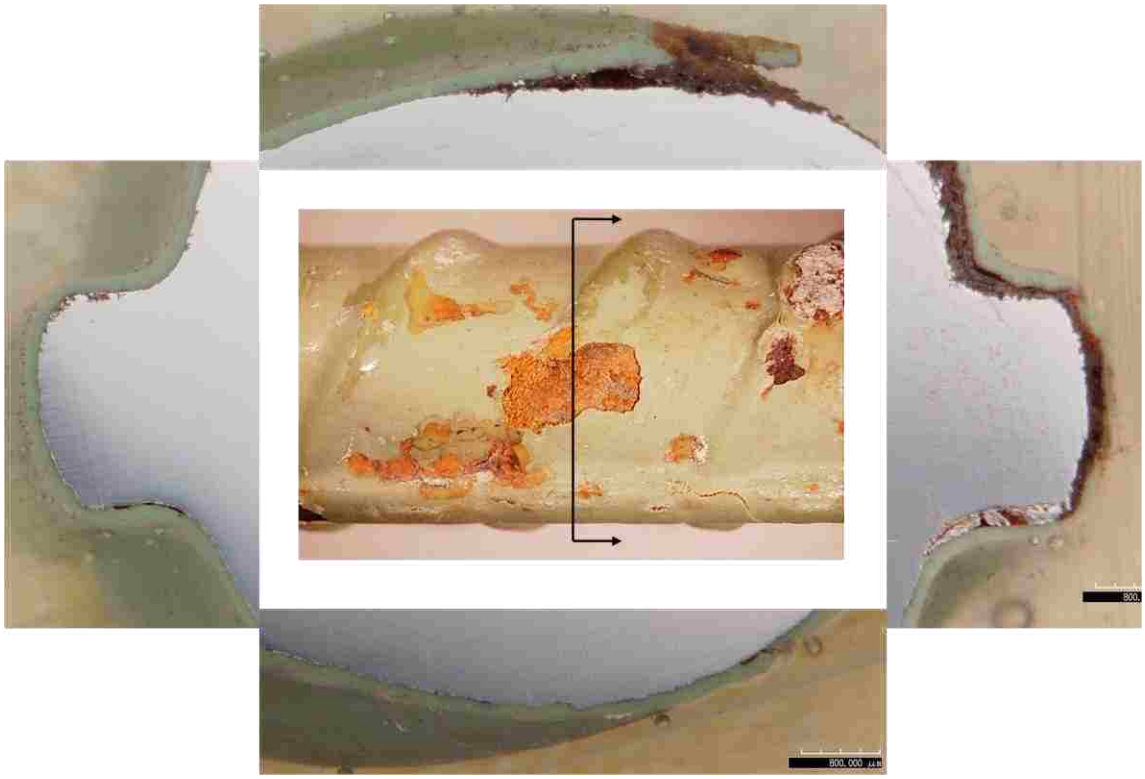

Figure A - 41: A cross-section through an unexplained area of damaged along bar-4 of specimen EP-D-2.

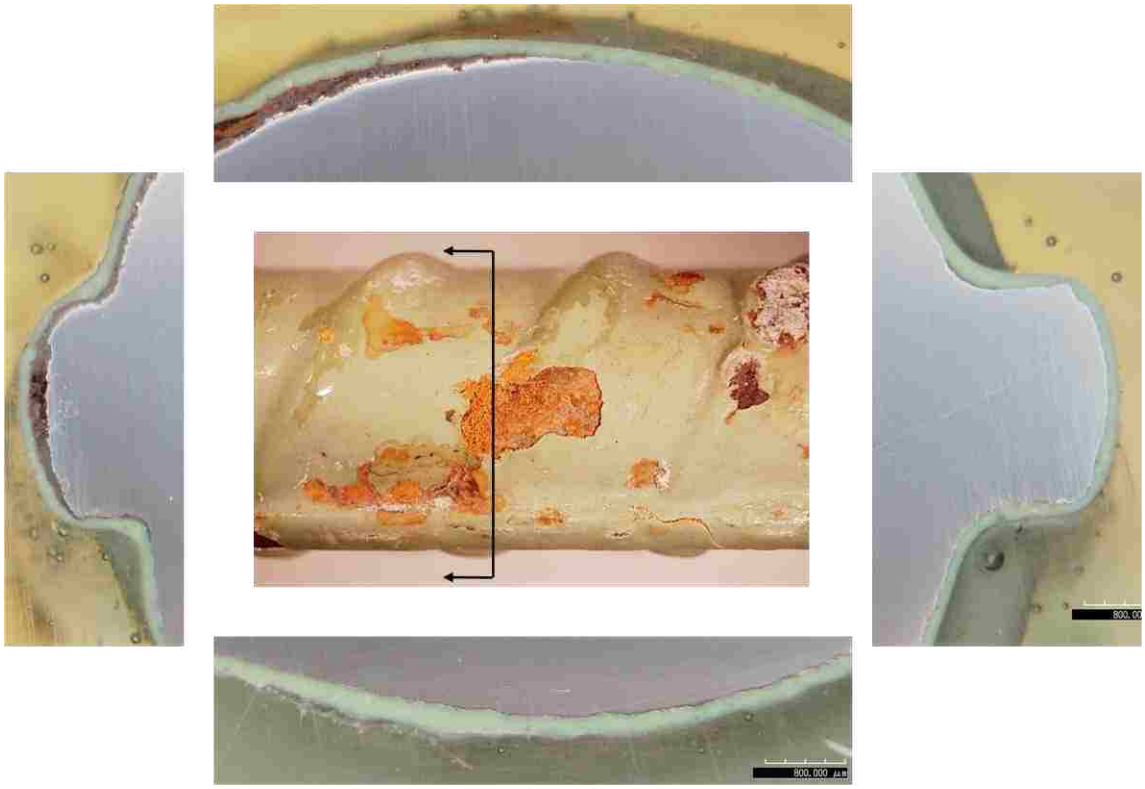

Figure A - 42: A cross-section through an unexplained area of damaged along bar-4 of specimen EP-D-2.

APPENDIX B

SALT SPRAY TEST

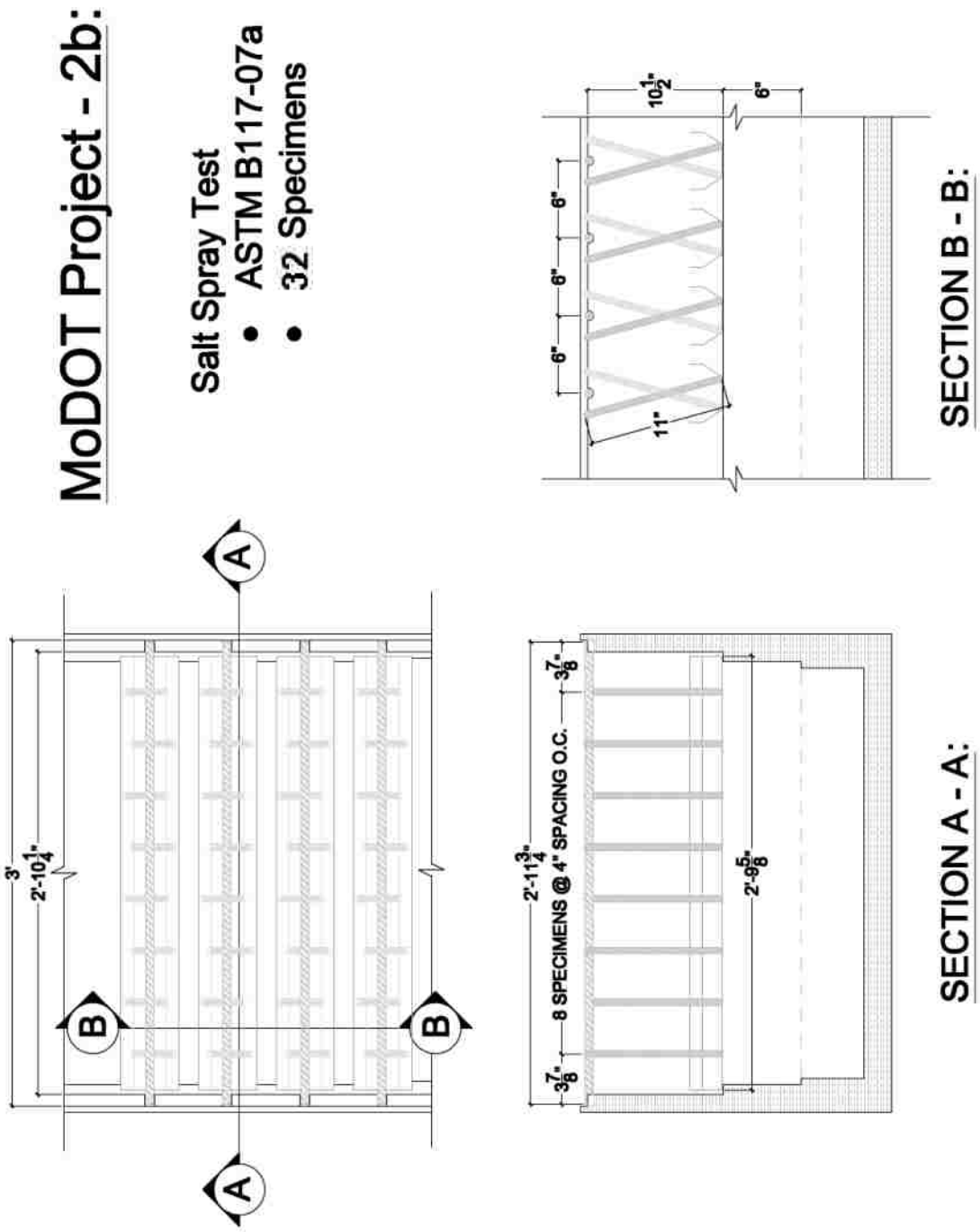

Figure B - 1: Salt spray pecimen layout within the salt spray chamber.

Figure B - 2: Front side of the smooth 50/50 enamel-coated salt spray specimens after testing.

Figure B - 3: Backside of the smooth 50/50 enamel-coated salt spray specimens after testing.

Figure B - 4: Front side of the deformed 50/50 enamel-coated salt spray specimens after testing.

Figure B - 5: Backside of the deformed 50/50 enamel-coated salt spray specimens after testing.

Figure B - 6: Right side of the deformed 50/50 enamel-coated salt spray specimens after testing.

Figure B - 7: Left side of the deformed 50/50 enamel-coated salt spray specimens after testing.

Figure B - 8: Front side of the smooth double enamel-coated salt spray specimens after testing.

Figure B - 9: Backside of the smooth double enamel-coated salt spray specimens after testing.

Figure B - 10: Front side of the deformed double enamel-coated salt spray specimens after testing.

Figure B - 11: Backside of the deformed double enamel-coated salt spray specimens after testing.

Figure B - 12: Right side of the deformed double enamel-coated salt spray specimens after testing.

Figure B - 13: Left side of the deformed double enamel-coated salt spray specimens after testing.

Figure B - 14: Front side of the smooth pure enamel-coated salt spray specimens after testing.

Figure B - 15: Backside of the smooth pure enamel-coated salt spray specimens after testing.

Figure B - 16: Front side of the deformed pure enamel-coated salt spray specimens after testing.

Figure B - 17: Backside of the deformed pure enamel-coated salt spray specimens after testing.

Figure B - 18: Right side of the deformed pure enamel-coated salt spray specimens after testing.

Figure B - 19: Left side of the deformed pure enamel-coated salt spray specimens after testing.

Figure B - 20: Front side of the smooth epoxy-coated salt spray specimens after testing.

Figure B - 21: Backside of the smooth epoxy-coated salt spray specimens after testing.

Figure B - 22: Front side of the deformed epoxy-coated salt spray specimens after testing.

Figure B - 23: Backside of the deformed epoxy-coated salt spray specimens after testing.

Figure B - 24: Right side of the deformed epoxy-coated salt spray specimens after testing.

Figure B - 25: Left side of the deformed epoxy-coated salt spray specimens after testing.

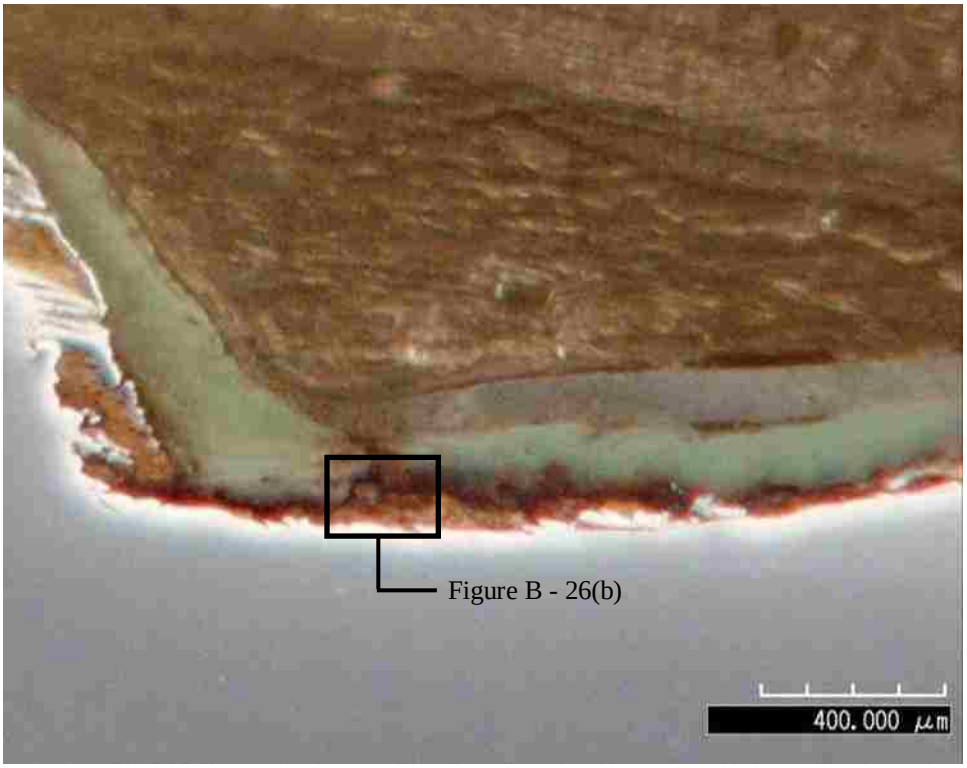

(a)

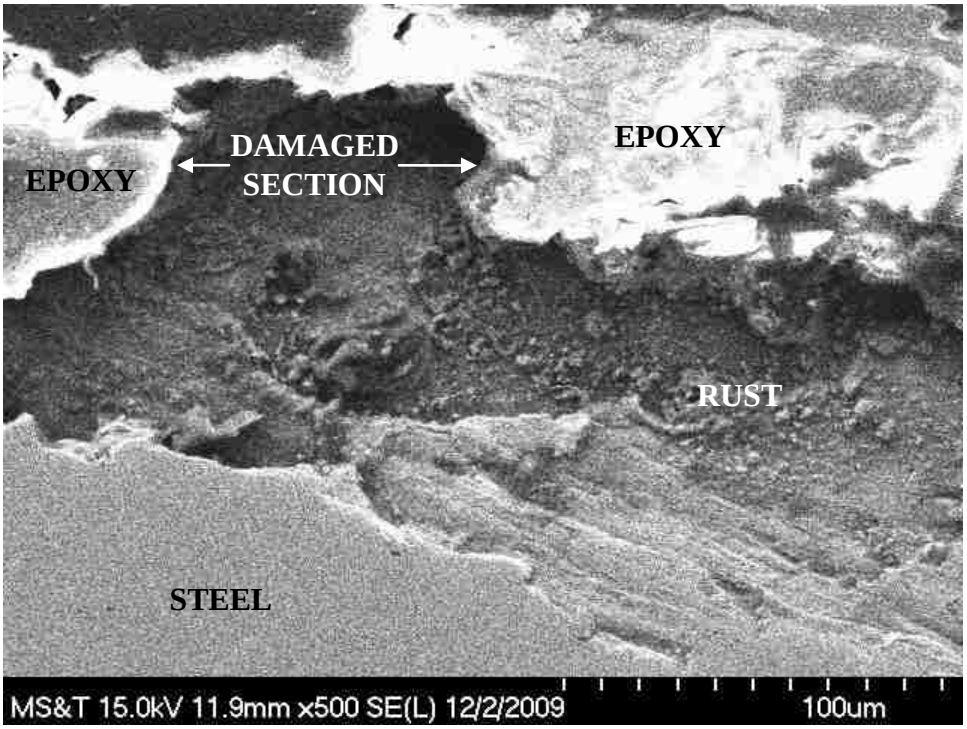

(b)

Figure B - 26: (a) Rust undercutting the epoxy coating near an unintentionally damaged section along salt spray specimen. (b) A close-up of the damaged section within the epoxy coating.

APPENDIX C

ACCELERATED CORROSION TEST (ACT)

Table C - 1: T_{corr} values for the non-grouted smooth 50/50 enamel-coated ACT specimens.

Specimen No.	t_{corr} (hrs.)
1	0
2	0
3	0
4	0
5	0
6	0
7	0
8	0
Average t_{corr}:	0
Standard Deviation:	0
Standard Error:	0
COV:	- - - - -

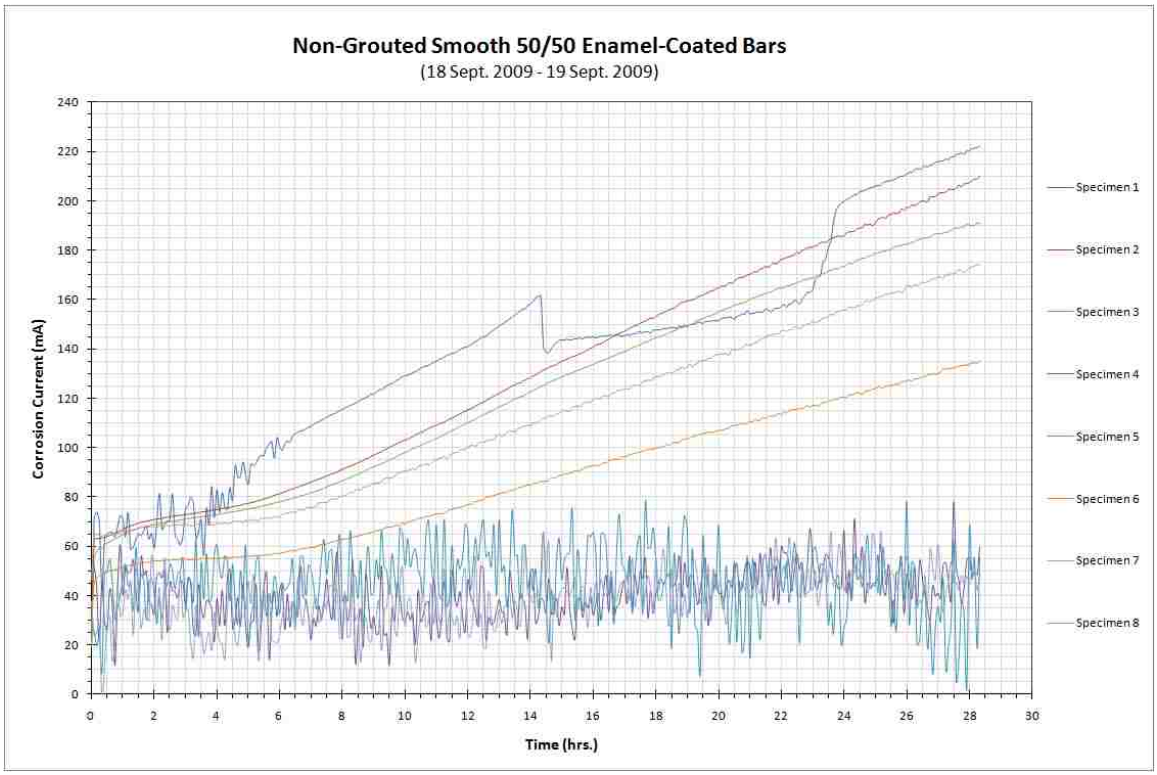

Figure C - 1: Corrosion current versus time plot for the non-grouted smooth 50/50 enamel-coated ACT specimens.

Table C - 2: T_{corr} values for the non-grouted deformed 50/50 enamel-coated ACT specimens.

Specimen No.	t_{corr} (hrs.)
1	0
2	0
3	0
4	OMITTED
5	0
6	0
7	0
8	0
Average t_{corr}:	0
Standard Deviation:	0
Standard Error:	0
COV:	- - - - -

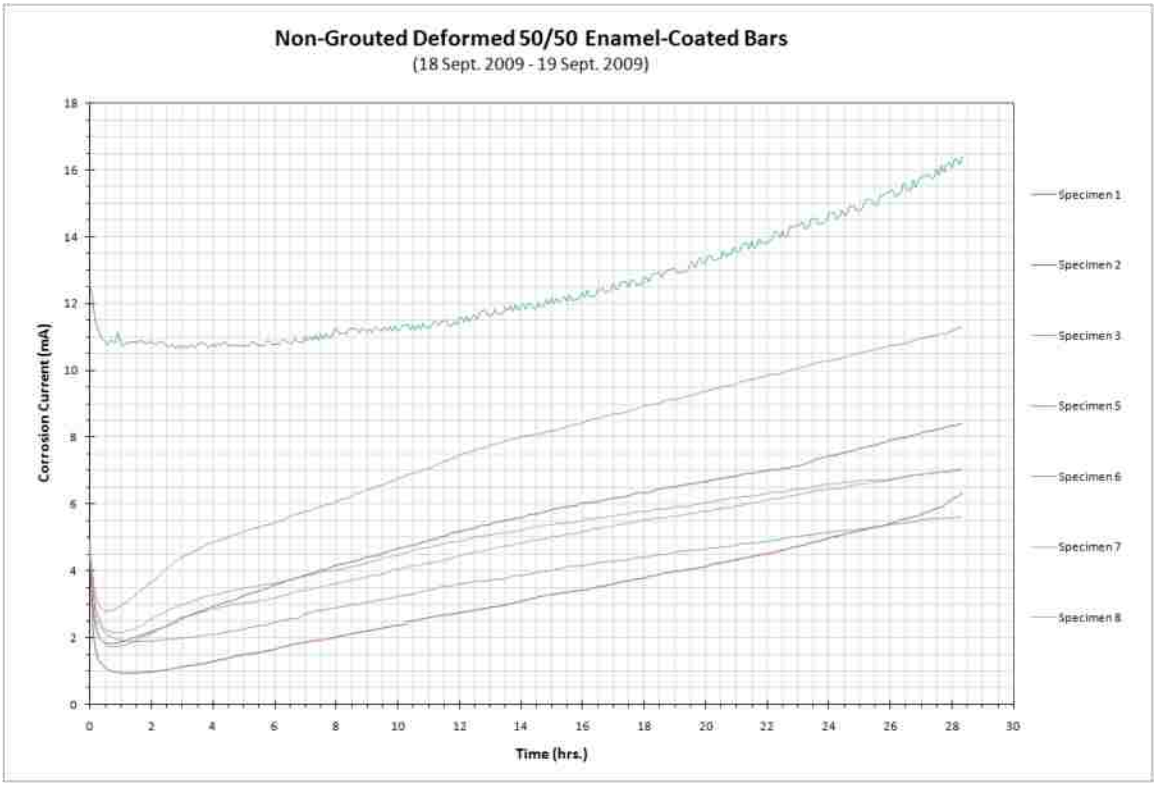

Figure C - 2: Corrosion current versus time plot for the non-grouted deformed 50/50 enamel-coated ACT specimens.

Table C - 3: T_{corr} values for the non-grouted smooth pure enamel-coated ACT specimens.

Specimen No.	t_{corr} (hrs.)
1	0
2	0
3	0
4	0
5	0
6	0
7	0
8	0
Average t_{corr}:	0
Standard Deviation:	0
Standard Error:	0
COV:	- - - - -

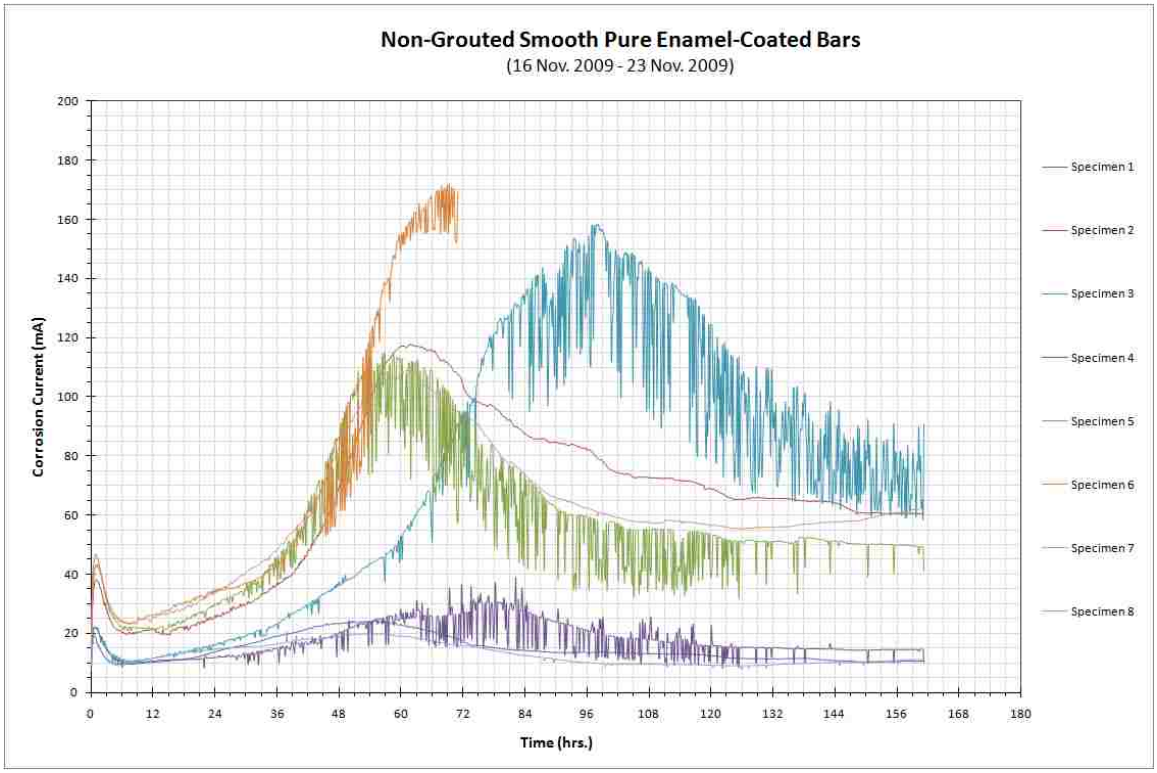

Figure C - 3: Corrosion current versus time plot for the non-grouted smooth pure enamel-coated ACT specimens.

Table C - 4: T_{corr} values for the non-grouted deformed pure enamel-coated ACT specimens.

Specimen No.	t_{corr} (hrs.)
1	68
2	175
3	99
4	151
5	66
6	131
7	66
8	90
Average t_{corr}:	106
Standard Deviation:	42
Standard Error:	15
COV:	39.7%

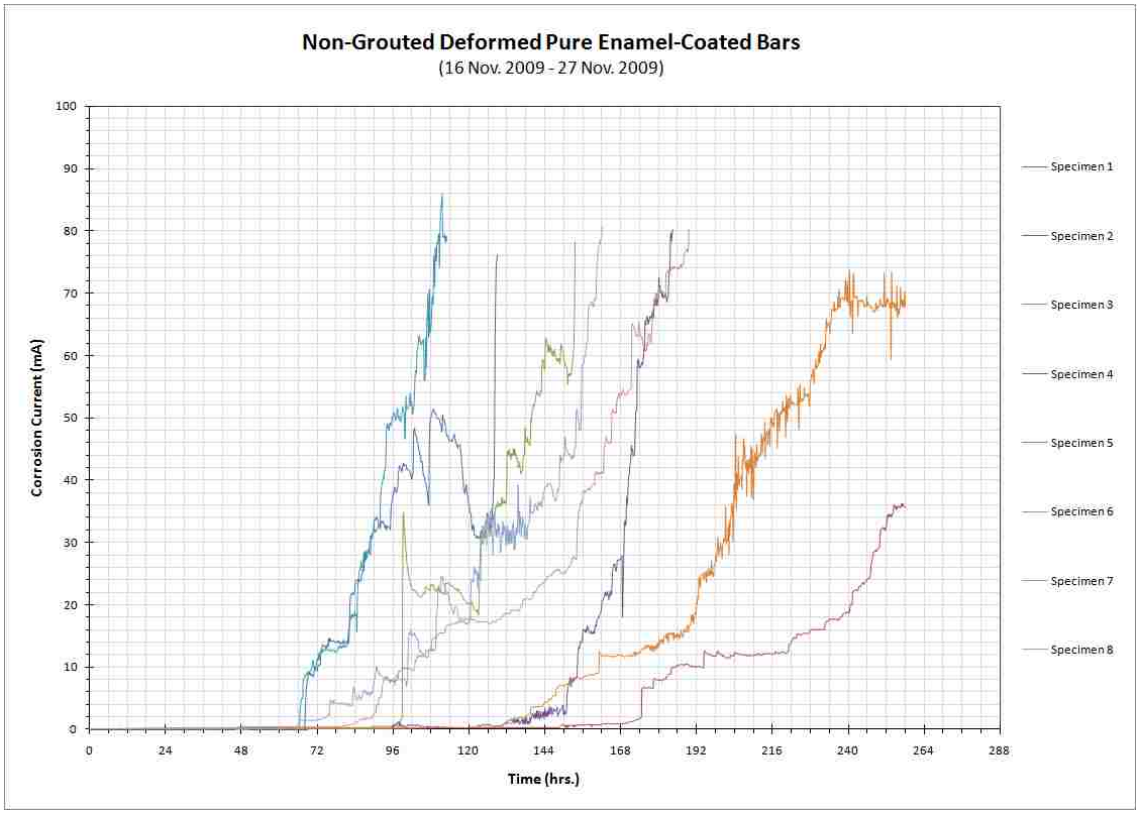

Figure C - 4: Corrosion current versus time plot for the non-grouted deformed pure enamel-coated ACT specimens.

Table C - 5: T_{corr} values for the non-grouted smooth double enamel-coated ACT specimens.

Specimen No.	t_{corr} (hrs.)
1	0
2	0
3	0
4	0
5	0
6	0
7	0
8	0
Average:	0
Standard Deviation:	0
Standard Error:	0
COV:	- - - - -

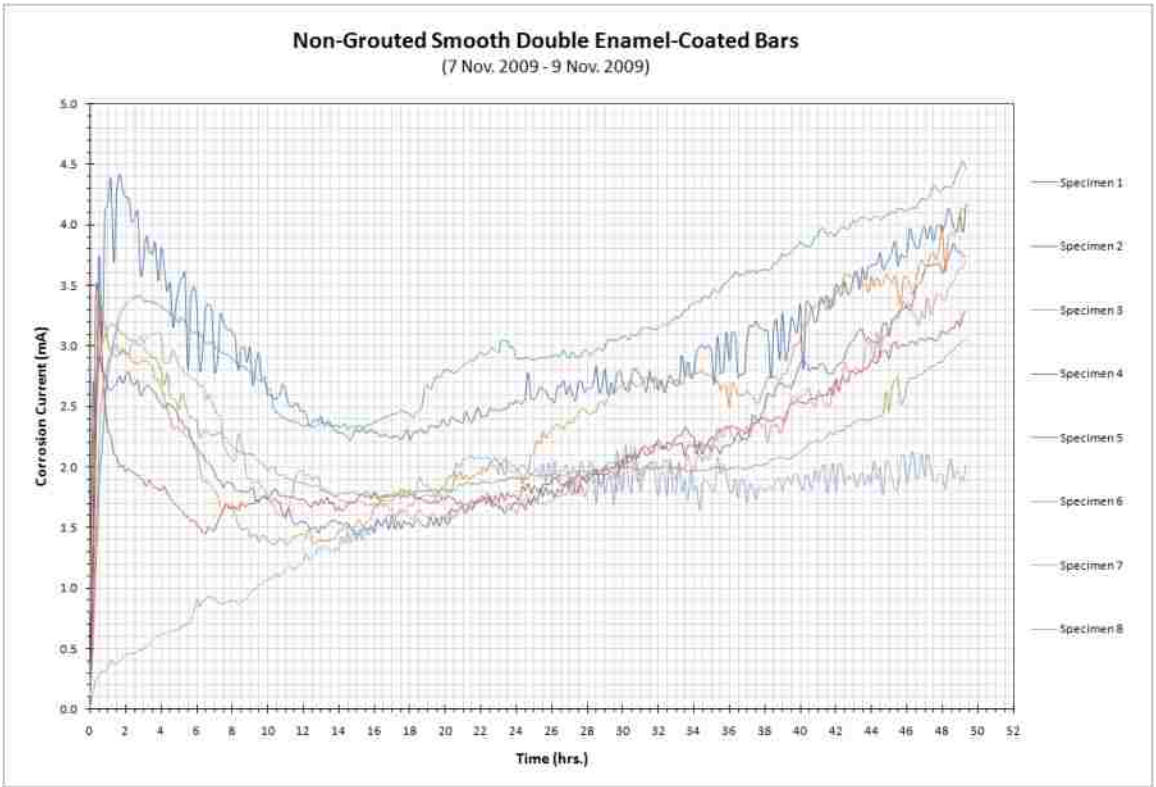

Figure C - 5: Corrosion current versus time plot for the non-grouted smooth double enamel-coated ACT specimens.

Table C - 6: T_{corr} values for the non-grouted deformed double enamel-coated ACT specimens.

Specimen No.	t_{corr} (hrs.)
1	0
2	0
3	0
4	0
5	0
6	0
7	0
8	0
Average:	0
Standard Deviation:	0
Standard Error:	0
COV:	- - - - -

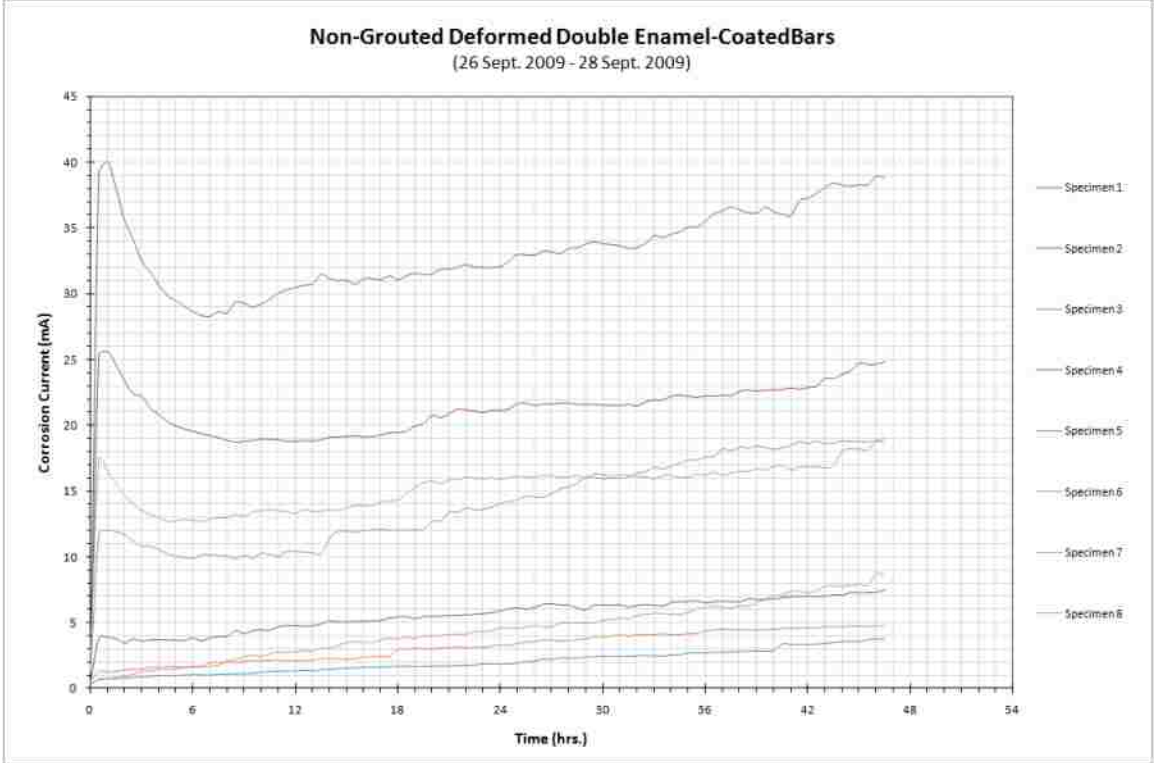

Figure C - 6: Corrosion current versus time plot for the non-grouted deformed double enamel-coated ACT specimens.

Table C - 7: T_{corr} values for the non-grouted smooth epoxy-coated ACT specimens.

Specimen No.	t_{corr} (hrs.)
1	> 668
2	> 668
3	> 668
4	> 668
5	> 668
6	> 668
7	> 668
8	> 668
Average:	> 668
Standard Deviation:	0
Standard Error:	0
COV:	-----

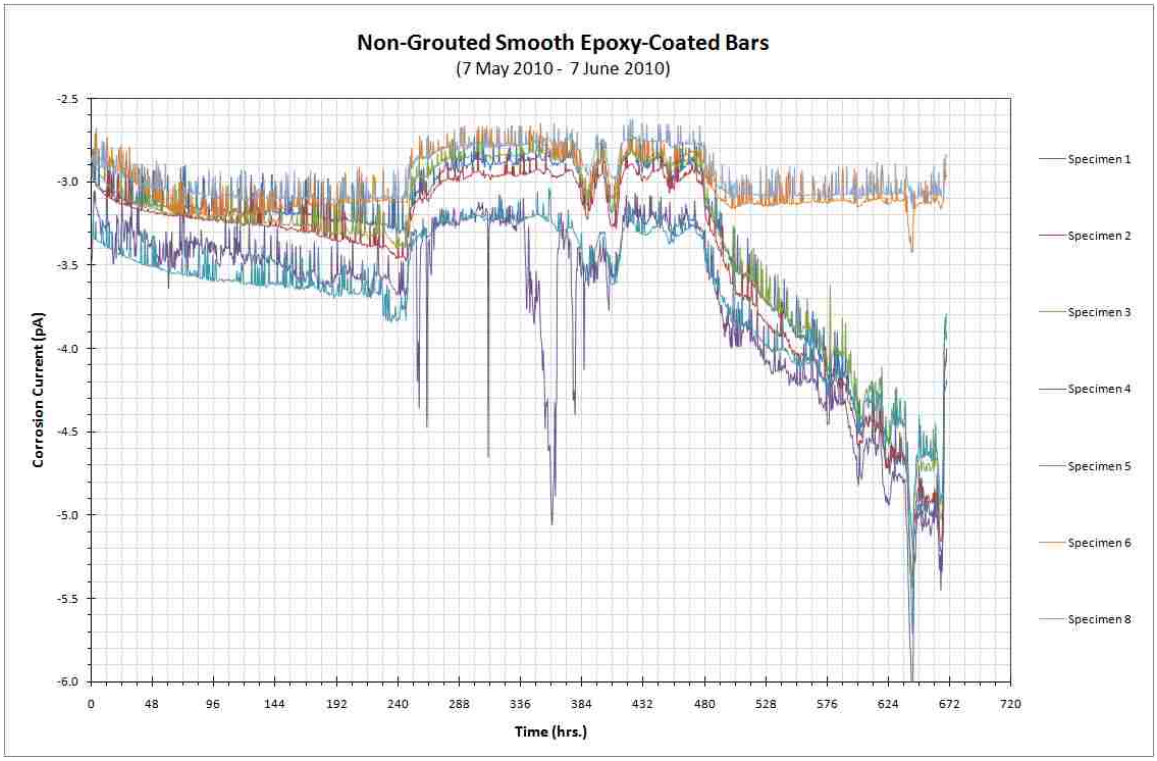

Figure C - 7: Corrosion current versus time plot for the non-grouted smooth epoxy-coated ACT specimens.

Table C - 8: T_{corr} values for the non-grouted deformed epoxy-coated ACT specimens.

Specimen No.	t_{corr} (hrs.)
1	> 746
2	> 746
3	> 746
4	> 746
5	> 746
6	> 746
7	> 746
8	> 746
Average:	> 746
Standard Deviation:	0
Standard Error:	0
COV:	------

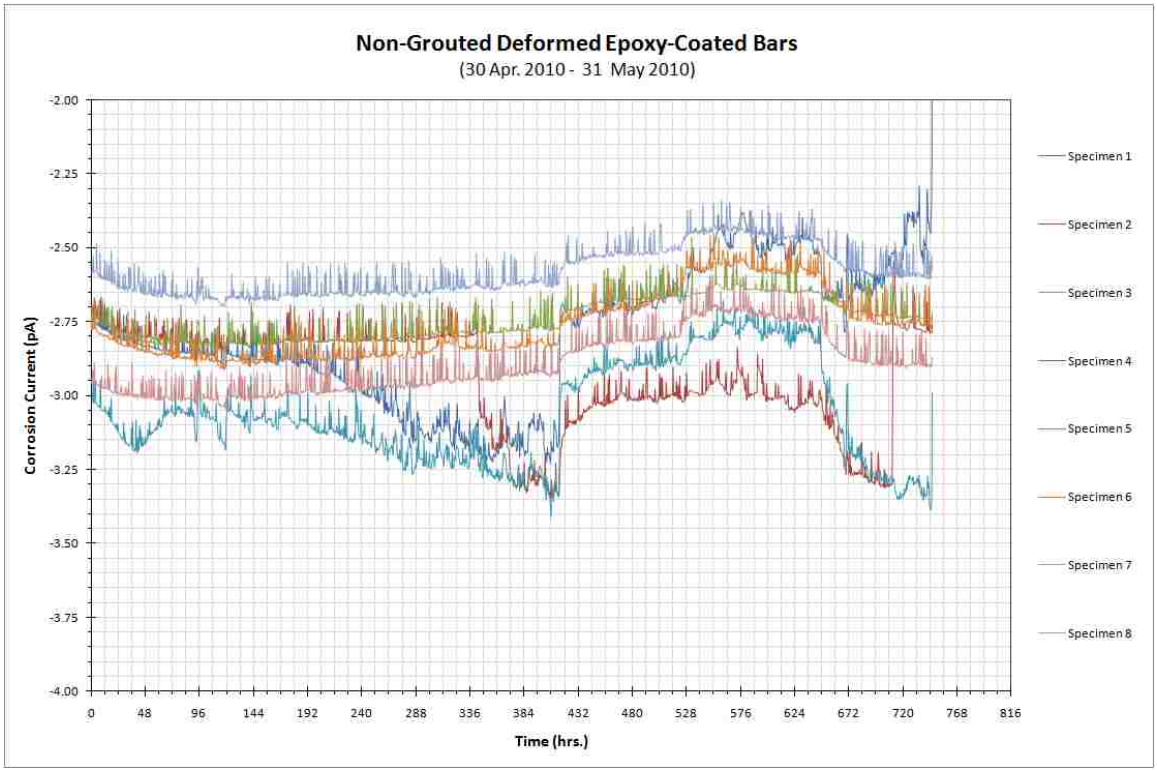

Figure C - 8: Corrosion current versus time plot for the non-grouted deformed epoxy-coated ACT specimens.

Table C - 9: T_{corr} values for the grouted smooth uncoated ACT specimens.

Specimen No.	t_{corr} (hrs.)
1	238
2	221
3	180
4	199
5	213
6	215
7	212
8	186
Average:	208
Standard Deviation:	19
Standard Error:	7
COV:	9.1%

Figure C - 9: Corrosion current versus time plot for the grouted smooth uncoated ACT specimens.

Table C - 10: T_{corr} values for the grouted deformed uncoated ACT specimens.

Specimen No.	t_{corr} (hrs.)
1	198
2	148
3	195
4	168
5	196
6	128
7	187
8	OMITTED
Average:	174
Standard Deviation:	27
Standard Error:	10
COV:	15.7%

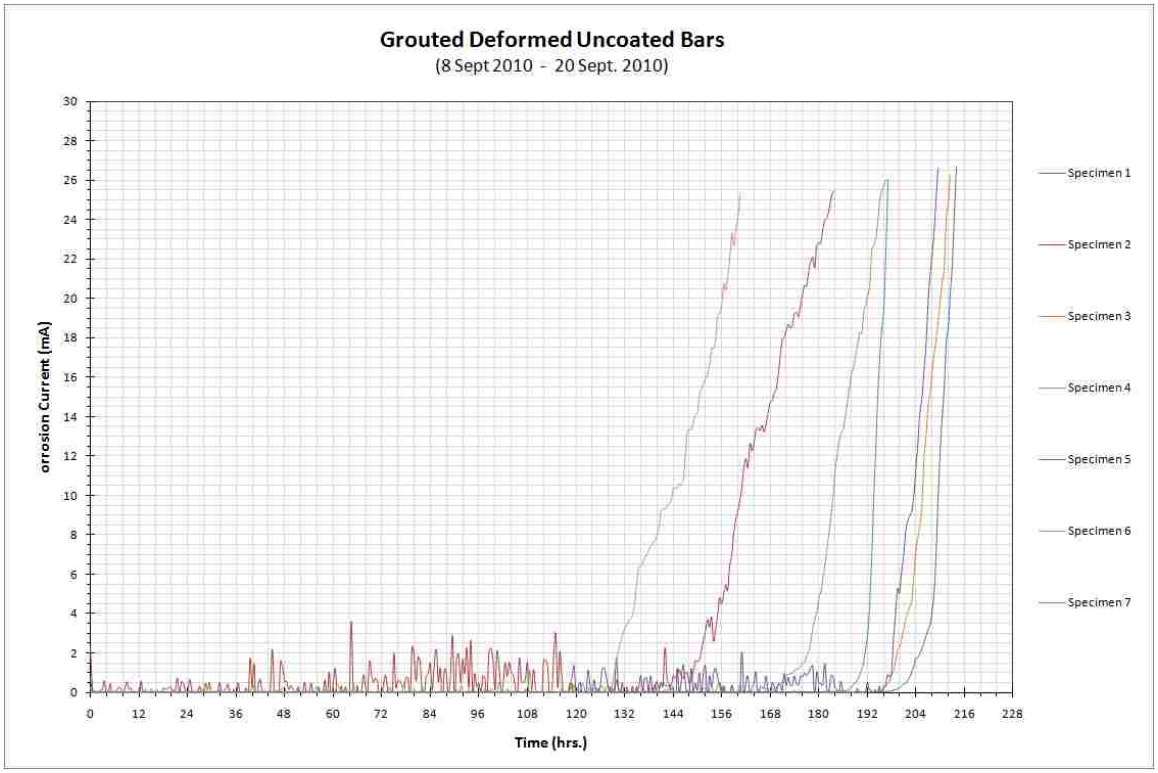

Figure C - 10: Corrosion current versus time plot for the grouted deformed uncoated ACT specimens.

Table C - 11: T_{corr} values for the grouted smooth 50/50 enamel-coated ACT specimens.

Specimen No.	t_{corr} (hrs.)
1	175
2	241
3	213
4	258
5	174
6	253
7	195
8	270
Average:	222
Standard Deviation:	38
Standard Error:	14
COV:	17.2%

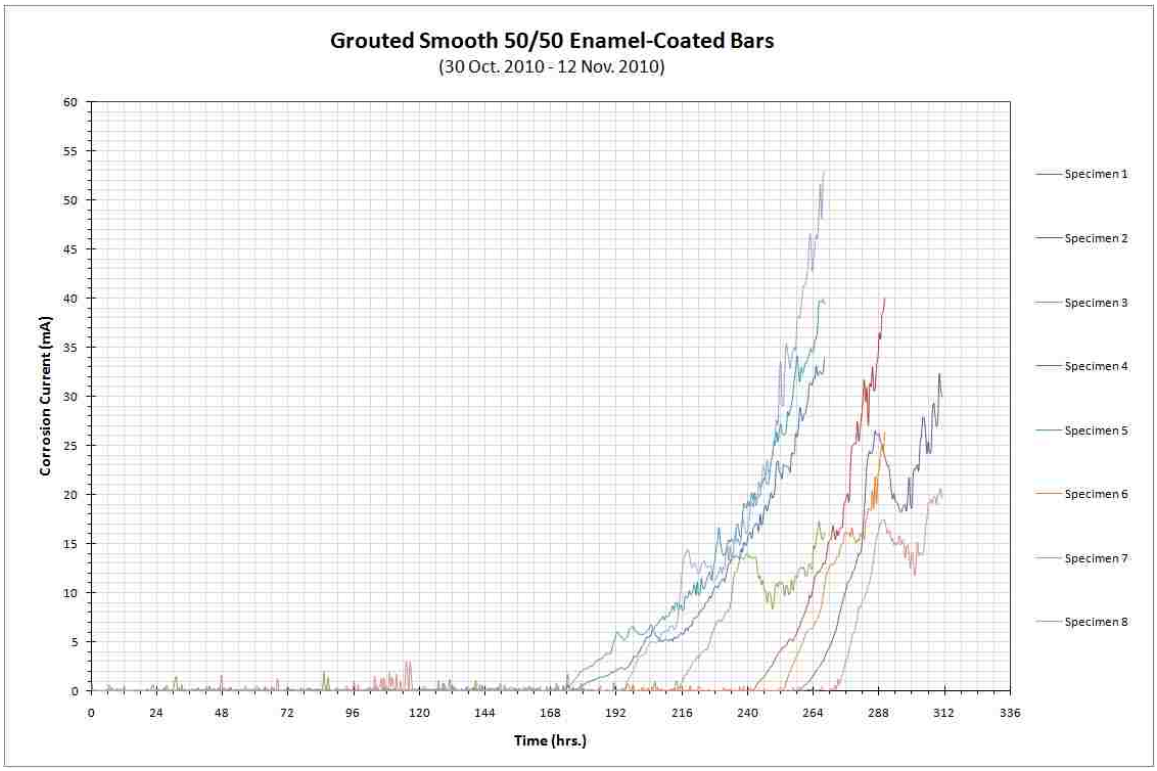

Figure C - 11: Corrosion current versus time plot for the grouted smooth 50/50 enamel-coated ACT specimens.

Table C - 12: T_{corr} values for the grouted deformed 50/50 enamel-coated ACT specimens.

Specimen No.	t_{corr} (hrs.)
1	228
2	216
3	102
4	252
5	198
6	204
7	126
8	OMITTED
Average:	189
Standard Deviation:	55
Standard Error:	21
COV:	29.0%

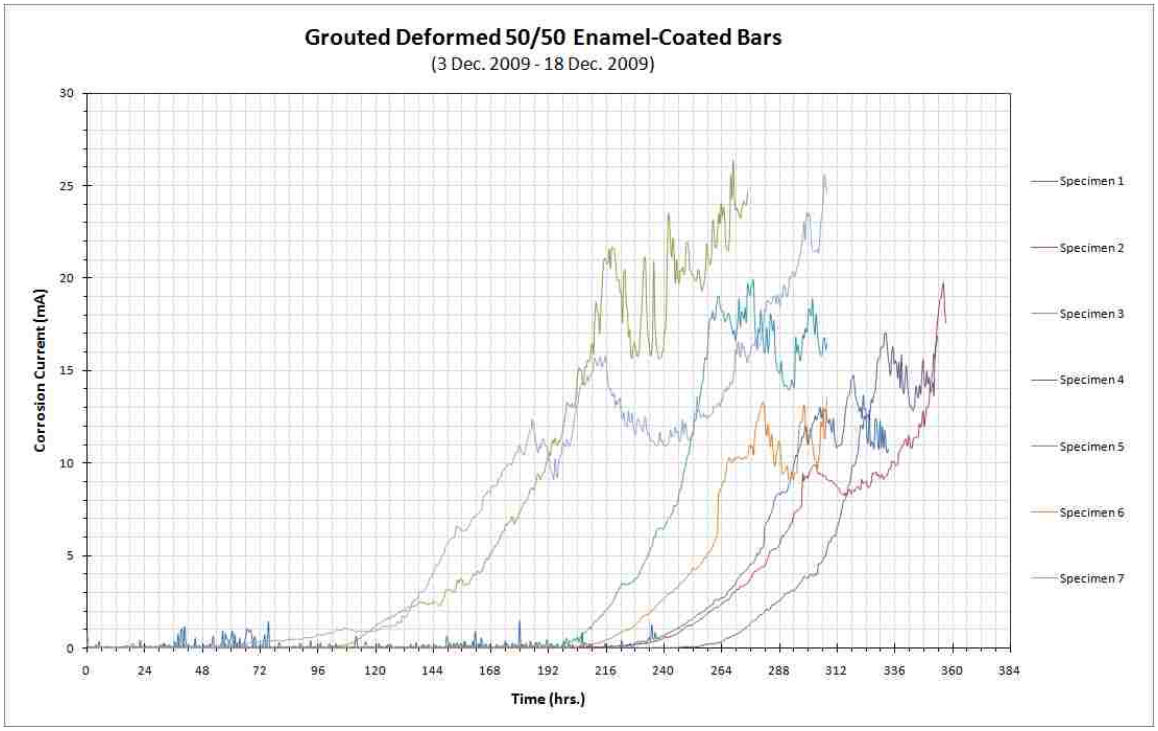

Figure C - 12: Corrosion current versus time plot for the grouted deformed 50/50 enamel-coated ACT specimens.

Table C - 13: T_{corr} values for the grouted smooth pure enamel-coated ACT specimens.

Specimen No.	t_{corr} (hrs.)
1	624
2	672
3	660
4	456
5	540
6	624
7	576
8	528
Average:	585
Standard Deviation:	74
Standard Error:	26
COV:	12.6%

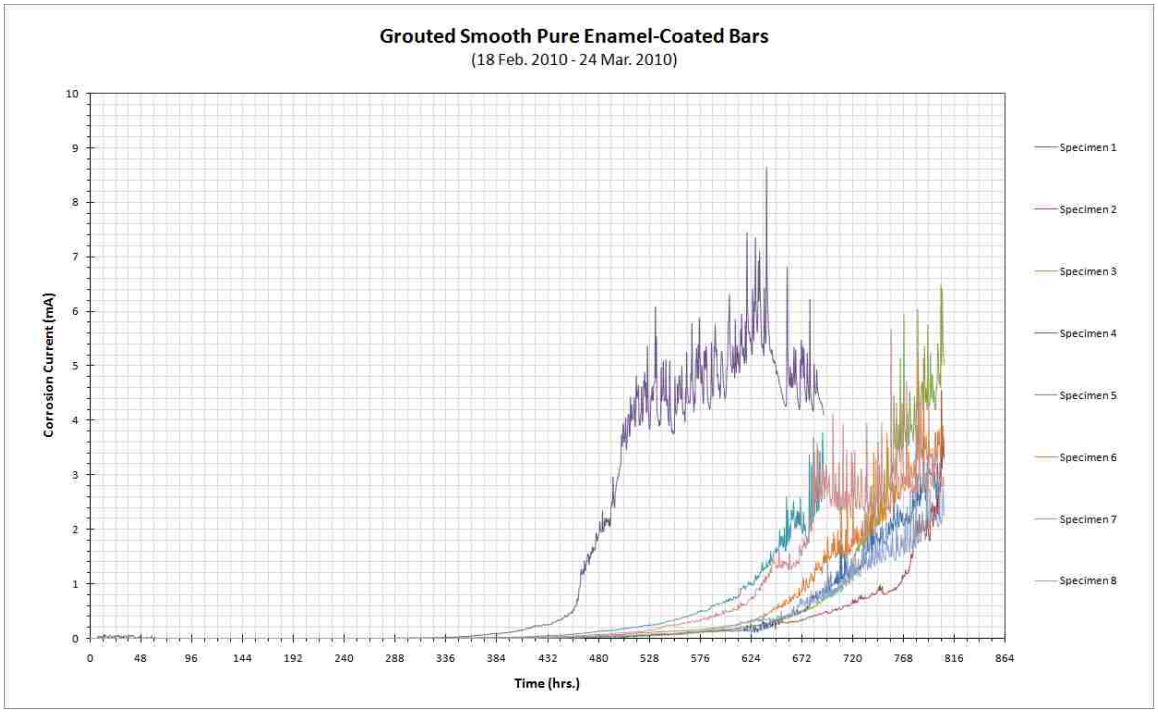

Figure C - 13: Corrosion current versus time plot for the grouted smooth pure enamel-coated ACT specimens.

Table C - 14: T_{corr} values for the grouted deformed pure enamel-coated ACT specimens.

Specimen No.	t_{corr} (hrs.)
1	588
2	439
3	408
4	412
5	620
6	260
7	238
8	303
Average:	409
Standard Deviation:	141
Standard Error:	50
COV:	34.6%

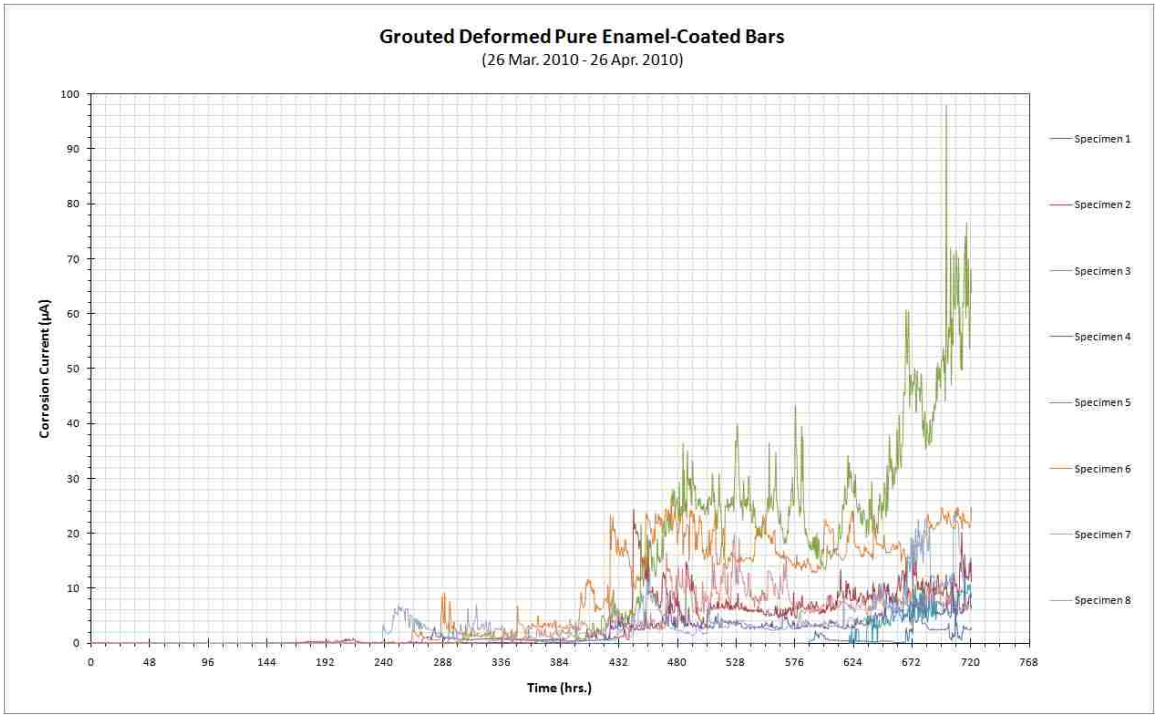

Figure C - 14: Corrosion current versus time plot for the grouted deformed pure enamel-coated ACT specimens.

Table C - 15: T_{corr} values for the grouted smooth double enamel-coated ACT specimens.

Specimen No.	t_{corr} (hrs.)
1	825
2	636
3	1080
4	912
5	694
6	1372
7	1154
8	1032
Average:	963
Standard Deviation:	246
Standard Error:	87
COV:	25.5%

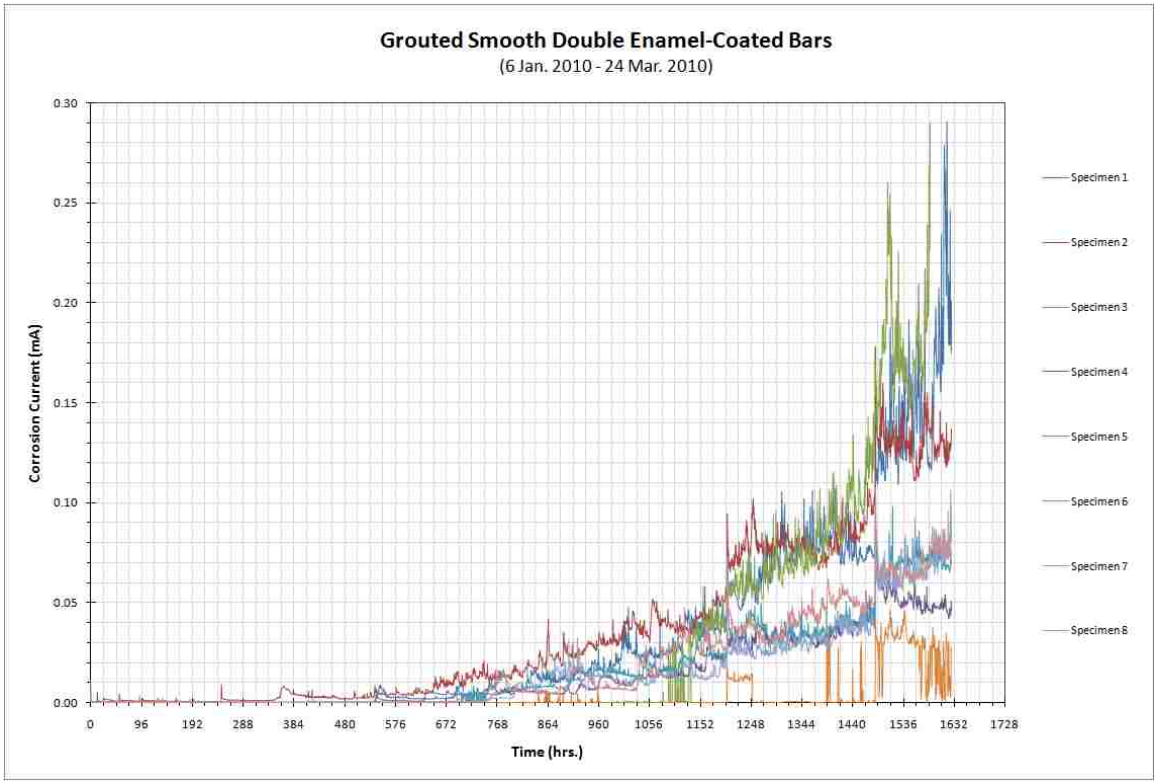

Figure C - 15: Corrosion current versus time plot for the grouted smooth double enamel-coated ACT specimens.

Table C - 16: T_{corr} values for the grouted deformed double enamel-coated ACT specimens.

Specimen No.	t_{corr} (hrs.)
1	824
2	720
3	624
4	594
5	471
6	648
7	738
8	690
Average:	664
Standard Deviation:	106
Standard Error:	38
COV:	16.0%

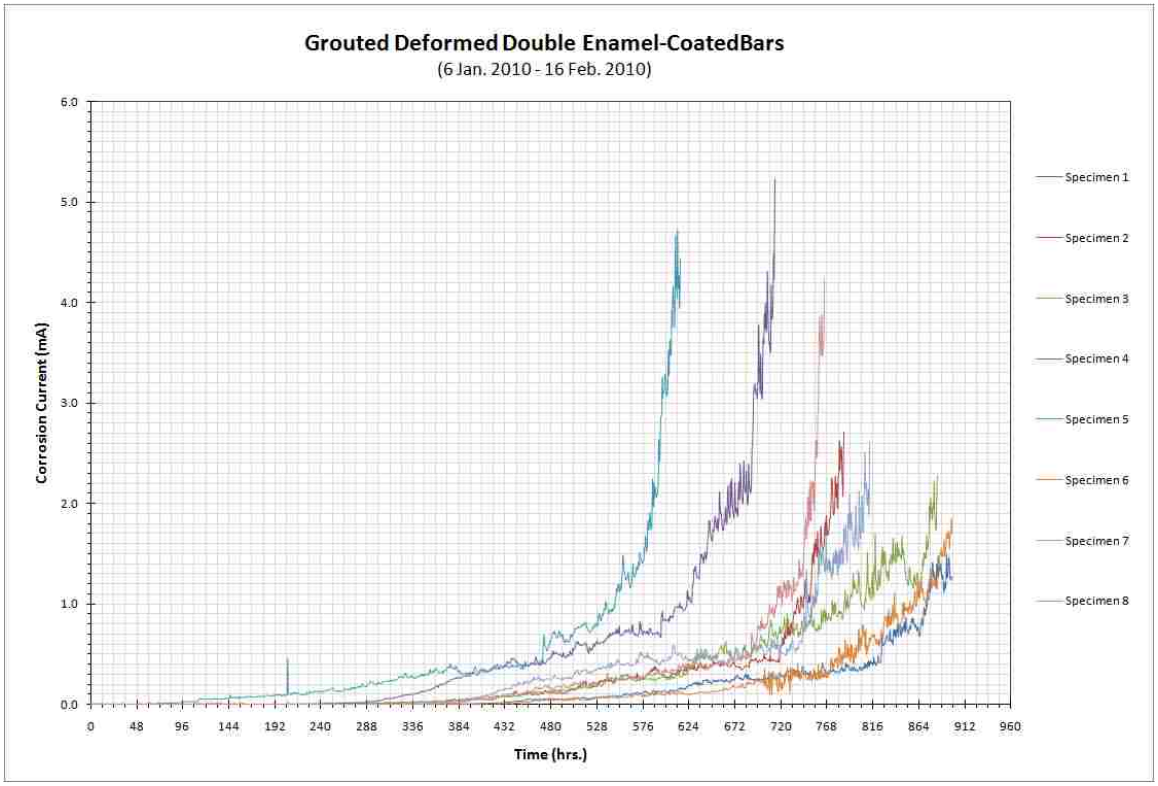

Figure C - 16: Corrosion current versus time plot for the grouted deformed double enamel-coated ACT specimens.

Table C - 17: T_{corr} values for the grouted smooth epoxy-coated ACT specimens.

Specimen No.	t_{corr} (hrs.)
1	> 2000
2	> 2000
3	> 2000
4	> 2000
5	> 2000
6	> 2000
7	> 2000
8	> 2000
Average:	> 2000
Standard Deviation:	0
Standard Error:	0
COV:	- - - - -

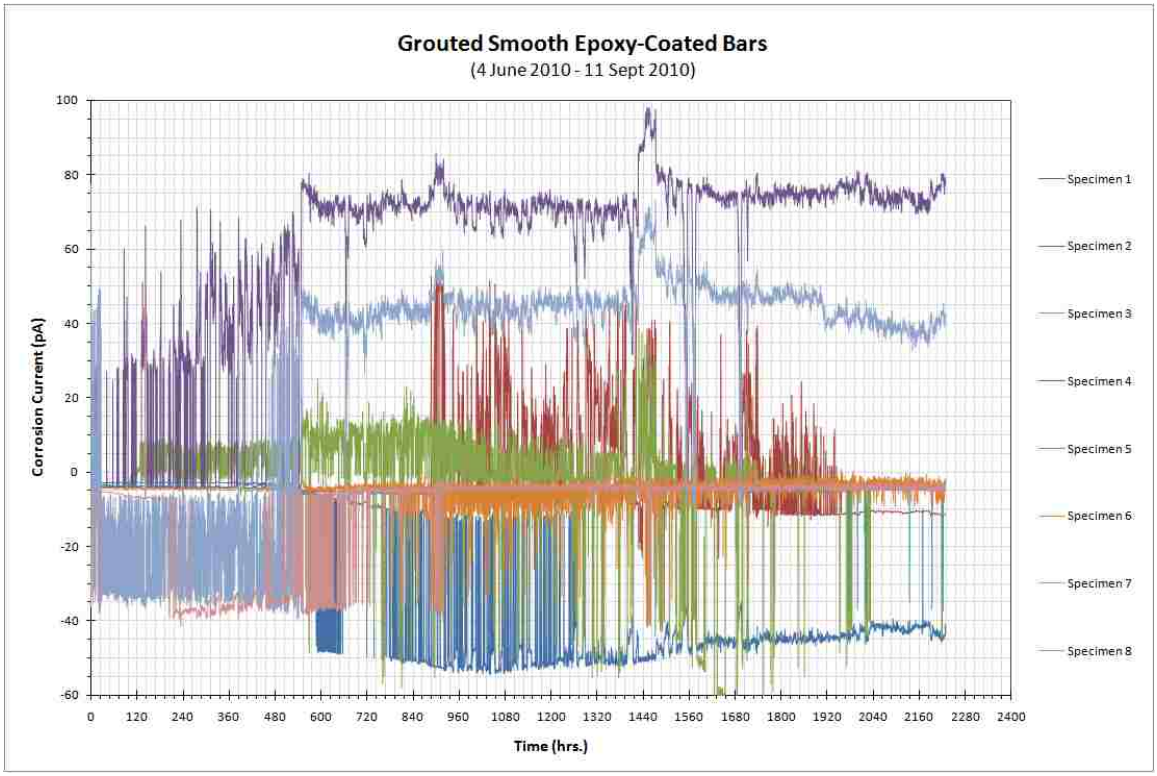

Figure C - 17: Corrosion current versus time plot for the grouted smooth epoxy-coated ACT specimens.

Table C - 18: T_{corr} values for the grouted deformed epoxy-coated ACT specimens.

Specimen No.	t_{corr} (hrs.)
1	> 2000
2	> 2000
3	> 2000
4	> 2000
5	> 2000
6	> 2000
7	> 2000
8	> 2000
Average:	> 2000
Standard Deviation:	0
Standard Error:	0
COV:	- - - - -

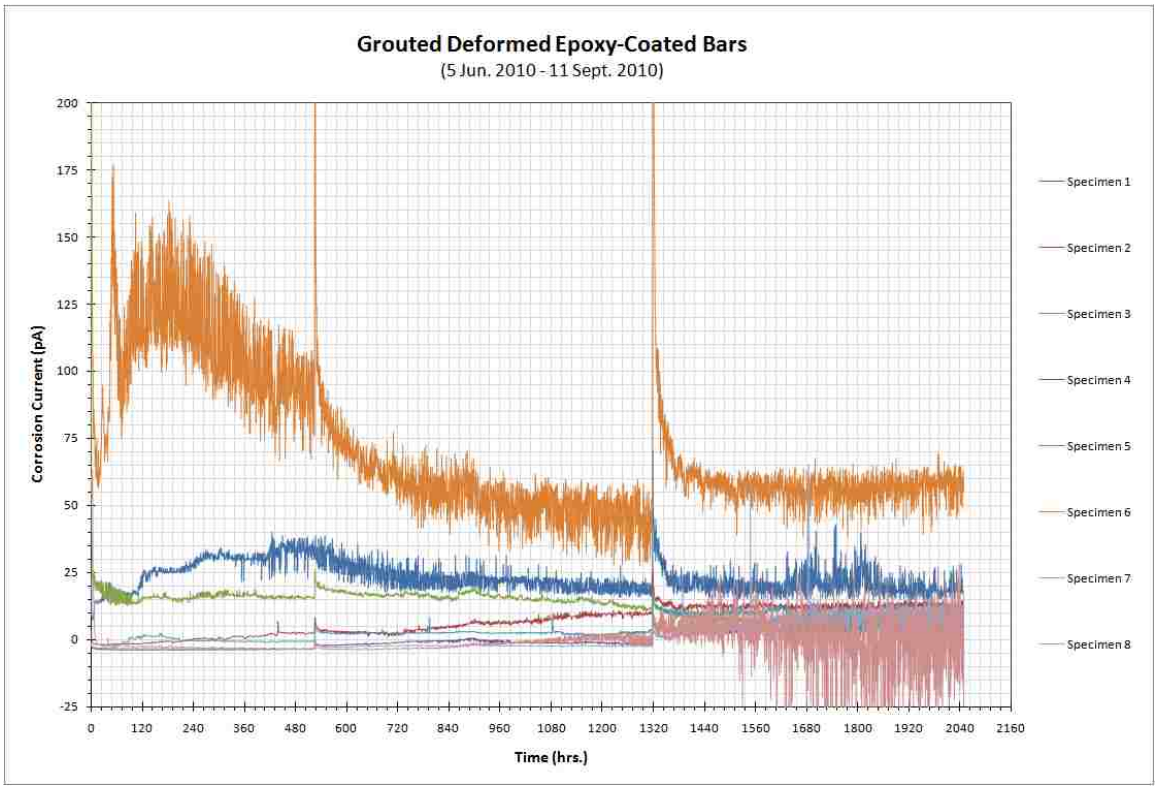

Figure C - 18: Corrosion current versus time plot for the grouted deformed epoxy-coated ACT specimens.

BIBLIOGRAPHY

AASHTO T 259 (2002). Resistance of Concrete to Chloride Ion Penetration. *American Association of State Highway and Transportation Officials*, Washington D.C..

ACI 222R (2001). Protection of Metals in Concrete Against Corrosion. *American Concrete Institute*, Farmington Hills, MI.

Arcelor Mittal (2008). Steel for Enamelling and Enamelled Steels - User Manual. <http://www.arcelormittal.com/fce/repository/Brochures/Steelforenamelling_usermanual_EN.pdf>

Andrews, Andrew I. (1961). *Porcelain Enamels: The Preparation, Application, and Properties of Enamels.* The Garrard Press (Second Edition).

ASTM A 615 (2009), *Standard Specification for Deformed and Plain Carbon-Steel Bars for Concrete Reinforcement*, American Society of Testing and Materials, West Conshohocken, PA.

ASTM A 775 (2007). Standard Specification for Epoxy-Coated Steel Reinforcing Bars. *American Society of Testing and Materials*, West Conshohocken, PA.

ASTM B 117 (2009). Standard Practice for Operating Salt Spray (Fog) Apparatus. *American Society of Testing and Materials*, West Conshohocken, PA.

ASTM C 39 (2009). Standard Test Method for Compressive Strength of Cylindrical Concrete Specimens. *American Society of Testing and Materials*, West Conshohocken, PA.

ASTM C 617 (2009). Standard Practice for Capping Cylindrical Concrete Specimens. *American Society of Testing and Materials*, West Conshohocken, PA.

ASTM C 876 (2009). Standard Test Method for Corrosion Potentials of Uncoated Reinforcing Steel in Concrete. *American Society of Testing and Matierals*, West Conshohocken, PA.

ASTM A 934 (2007). Standard Specification for Epoxy-Coated Prefabricated Steel Reinforcing Bars. *American Society of Testing and Materials*, West Conshohocken, PA.

ASTM C 1543 (2009). Standard Test Method for Determining the Penetration of Chloride Ion into Concrete by Ponding. *American Society of Testing and Materials*, West Conshohocken, PA.

ASTM D 3963 (2007). Standard Specification for Fabrication and Jobsite Handling of Epoxy-Coated Reinforcing Bars. *American Society of Testing and Materials*, West Conshohocken, PA.

ASTM G 14 (2004). Standard Test Method for Impact Resistance of Pipeline Coatings (Falling Weight Test). *American Society of Testing and Materials*, West Conshohocken, PA.

ASTM G 16 (2010). Standard Guide for Applying Statistics to Analysis of Corrosion Data. *American Society of Testing and Materials*, West Conshohocken, PA.

Broomfield, John P. (2007). *Corrosion of Steel in Concrete: Understanding, Investigation and Repair*. Taylor & Francis (Second Edition).

Carino, Nicholas J. (1999). Nondestructive Techniques to Investigate Corrosion Status in Concrete Structures. *Journal of Performance of Constructed Facilities, 13(3),* 96-106.

Doppke, T. and Bryant, A. (1983). "The Salt Spray Test: Past, Present, and Future." *Proc. of the 2nd Automotive Corrosion Prevention Conference,* 57-72.

Griffith, A. and Laylor, M. H. (1999). "Epoxy Coated Reinforcment Study," *Report No. 527*. Oregon Department of Transportation, Salem, Oregon.

Gu, P. and Beaudoin, J. (1998). Obtaining Effective Half-Cell Potential Measurements in Reinforced Concrete Structures. *Institute for Research in Construction, No. 18,* 1-4.

Gustafson, David P. (1999). Epoxy-Coated Reinforcing Bars: An Effective Corrosion-Protection System for Reinforced Concrete Structures. *Concrete Reinforcing Steel Institute*, Schaumburg, Illinois.

Hartt, W.H., Powers, R.G., Leroux, V., and Lysogorski, D.K. (2004). "Critical Literature Review of High-Performance Corrosion Reinforcements in Concrete Bridge Applications," *Report No. FHWA-RD-04-093*. Federal Highway Administration, McLean, Virginia.

Hausmann, D.A. (1967). Steel Corrosion in Concrete: How Does it Occur? *Materials Protection, 6,* 19-23.

Koch, G.H., Brongers, M.P., Thompson, N.G., Virmani, Y.P., and Payer, J.H. (2001). "Corrosion Cost and Preventive Strategies in the United States," *Report No. FHWA-RD-01-156*. Federal Highway Administration, McLean, Virginia.

Langford, P. and Broomfield, J. (1987). Monitoring the Corrosion of Reinforcing Steel. *Construction Repair, 1(2),* 32-36.

Lee, S. and Krauss P. (2004). "Long-Term Performance of Epoxy-Coated Reinforcing Steel in Heavy Salt-Contaminated Concrete," *Report No. FHWA-HRT-04-090.* Federal Highway Administration, McLean, Virginia.

Pacheco, Alexandre R. (2003). *Evaluating the Corrosion Protection of Post-Tensioning Grouts: Standardization of an Accelerated Corrosion Test.* PhD Dissertation, The Pennsylvania State University.

Pyć, Wioleta A. (1998). *Field Performance of Epoxy-Coated Reinforcing Steel In Virginia Bridge Decks.* PhD Dissertation, Viginia Polytechnic Institute and State University.

Pyć, W. A., Weyers, R. E., Weyers, R. M., Mokarem, D. W., Zemajtis, J., Sprinkel, M. M., and Dillard, J. G. (2000). "Field Performance of Epoxy-Coated Reinforcing Steel In Viginia Bridge Decks," *Report No. VTRC 00-R16.* Virginia Transportation Research Council, Charlottesville, Virginia.

Sagüé, A., Lee, J., Chang, X., Pickering, H., Nystrom, E., Carpenter, W., Kranc, S., Simmons, T., Boucher, B., and Hierholzer, S. (1994). "Corrosion of Epoxy Coated Rebar in Florida Bridges," *Final Report WPI No. 0510603.* Florida Department of Transportation.

Sengul, O. and Gjørv, O. (2009). Effect of Embedded Steel on Electrical Resistivity Measurements on Concrete Structures. *ACI Materials Journal, 106(1),* 11-18.

Smith, Charles O. (1977). *The Science of Engineering Materials*. Prentice-Hall (Second Edition).

Sohanghpurwaia, Ali A. (2005). "Condition and Performance of Epoxy-Coated Rebars in Bridge Decks of the State of Pennsylvania and New York." *Metropolis and Beyond Proceedings of the 2005 Structures Congress and the 2005 Forensic Engineering Symposium,* American Society of Civil Engineers.

Song, H., Jung, M., Lee, C., Kim, S., and Ann K. (2010). Influence of Chemistry of Chloride Ions in Cement Matrix on Corrosion of Steel. *ACI Materials Journal, 107(4),* 332-339.

Thompson, N.G., Lankard, D. and Sprinkel, M. (1992). "Improved grouts for bonded tendons in post-tensioned bridge structures," *Report No. FHWA-RD-91-092*. Federal Highway Administration, Cortest Columbus Technologies.

Volz, J.S., Schokker, A.J., and Pacheco, A.R. (2008). "Linear polarization resistance for acceptance testing of post-tensioning grouts." *Proc. Concrete Bridge Conference*, St. Louis, Missouri, May.

Weiss, C., Morefield, S., Malone, P., and Koenigstein, M. (2009). "Use of Vitreous-Ceramic Coatings on Reinforcing Steel for Pavements." *Proc. National Conference on Preservation Repair and Rehabilitation of Concrete Pavements*, Washington D.C.

Whiting, D.A. and Nagi, M.A. (2003). *Electrical Resistivity of Concrete - A Literature Review,* R&D Serial No. 2457. Portland Cement Association, Skokie, Illinois.

Zemajtis, J., Weyers, R.E., Sprinkel, M.M., and McKell, W.T. Jr. (1996). "Epoxy-Coated Reinforcement - A Historical Performance Review," *Report No. VTRC 97-IR1*. Virginia Transportation Research Council, Charlottesville, Virginia.

VITA

Charles Robert Werner was born on May 3, 1984 in Scranton, Pennsylvania. He was named after his two grandfathers, Charles Ferdinand Werner and Robert Martin Mahon; however, throughout his life he was better known as "Chip."

Chip grew up in Clarks Summit, Pennsylvania and later graduated from Abington Height in May 2003. Later that same year, he attended The Pennsylvania State University where he graduated within a Bachelor's of Science degree in Civil Engineering in May 2008. Currently, Chip is attending the Missouri University of Science and Technology where he hopes to attain a Master's of Science degree in Civil Engineering in December 2010.